

**THE CHEMISTRY OF SOME
DI- AND TRI-PHENYLMETHANE
DYES**

by

Stephen Anthony GORMAN
B.Sc. (Hons)

being a thesis submitted to the University of Central Lancashire
in partial fulfilment of the requirement for the degree of

DOCTOR OF PHILOSOPHY

November 1998

Department of Environmental Management
University of Central Lancashire
Preston

ACKNOWLEDGEMENTS

I would like to express my sincere gratitude to Dr. Don Mason, my Director of Studies, and to Professor John D. Hepworth, Second Supervisor, for their constant interest, support and guidance throughout the course of my work and during the writing of my thesis.

My thanks are also due to Dr. B. M. Heron and Dr. C. D. Gabbutt for their interest and help.

I am also indebted to my employer, William Blythe Ltd., for allowing the time for my studies.

S. A. G.

DECLARATION

I declare that, whilst registered with the University of Central Lancashire for the degree of Doctor of Philosophy, I have not been a registered candidate or enrolled student for another award of any other academic or professional institution during the research programme. No portion of the work referred to in this thesis has been submitted in support of any application for another degree or qualification of any other University or Institution of learning.

Signed

Stephen A. Gorman

A NOTE ON REFERENCES

Throughout this work, a reference system based on that introduced by A. R. Katritzky and J. M. Lagowski in the monograph "Chemistry of the Heterocyclic *N*-Oxides", Academic press, New York, 1971, will be employed. This system has been used for the highly acclaimed "Comprehensive Heterocyclic Chemistry" series, edited by A. R. Katritzky and C. W. Rees, Pergamon Press, 1984 and is currently used for the series "Advances in Heterocyclic Chemistry", edited by A. R. Katritzky, academic press, New York from volume 40, 1986, onwards.

The references are designated by a number-letter coding of which the first two numbers denote the year of publication, the next one to six letters denote the journal, and the final numbers denote the page. A more detailed explanation may be found in the aforementioned publications.

ABSTRACT

The chemistry of some di- and tri-phenylmethane dyes.

Stephen A. Gorman

Two series of dyes have been prepared: a comprehensive series of novel, unsymmetrical Malachite Green type dyes containing different amino substituents in the 4-positions of the phenyl rings and a series of symmetrical Michler's Hydrol Blue type dyes. Both series of dyes have been synthesised from the relevant carbinols or hydrols. The amino substituents used were dimethylamino, diethylamino, pyrrolidino, piperidino, morpholino, thiomorpholino and *N*-methylpiperazino.

The rates of alkaline hydrolysis of the dyes at various hydroxide ion concentrations and temperatures have been investigated with a view to elucidating the reaction mechanism and the nature of substituent effects. The rate data obtained for each dye studied have been used to obtain thermodynamic activation parameters and to test the applicability of an isokinetic relationship in the dye systems. The various methods of computation and their results have been compared and discussed in relation to literature data for similar dyes. A stopped-flow technique was used for the kinetic investigation of the fast reactions associated with the unstable dyes studied. The analysis of kinetic data using single substituent parameter regression techniques has enabled substituent constants for piperidine, thiomorpholine and *N*-methylpiperazine to be interpolated.

The steric and electronic effects of the terminal amino substituents on the visible absorption spectra of the dyes have been examined in solvents of varying acidity. The steric and electronic symmetry of the Malachite Green type dyes has been investigated and is discussed.

The results from the spectral investigation and the kinetic study indicate that diphenylmethane dyes are considerably less stable than the corresponding triphenylmethane dyes and the reasons for this behaviour are discussed. In addition, piperidino, morpholino, thiomorpholino and *N*-methylpiperazino are less able to stabilise a dye by electron donation than dimethylamino, diethylamino and pyrrolidino and the reasons for this behaviour are also discussed.

The ^1H and ^{13}C nmr spectra of the dyes and carbinols have been recorded. Certain chemical shifts have been used to determine the relative electron donor ability of the terminal amino groups. The results from the ^1H and ^{13}C nmr spectra are discussed in relation to the steric and electronic effects of the heterocyclic moieties.

CONTENTS

Page

1. <u>INTRODUCTION</u>	1
1.1 Brief history of dyes	1
1.2 Hydrolysis of TPM/DPM dyes	6
1.3 Kinetics	7
1.3.1 The dependence of rate of reaction on temperature	9
1.3.2 The dependence of rate of reaction on ionic strength	16
1.3.3 The influence of solvent	17
1.3.4 The influence of substituents in the benzene ring on the rate of reaction	18
1.4 Basic theory of colour	26
1.5 Electronic absorption spectroscopy	29
1.6 Colour and constitution	33
1.6.1 Early colour theories	33
1.6.2 Valence bond theory	34
1.6.3 Molecular orbital models	35
1.6.4 The Free-Electron Molecular Orbital method	41
1.6.5 The Hückel Molecular Orbital method	44
1.6.6 The Pariser-Parr-Pople Molecular Orbital method	46
1.6.7 Configuration Interaction	47
1.6.8 The Perturbational Molecular Orbital method	48
1.6.9 The Hammett equation	54
1.7 Electronic absorption spectra of TPM/DPM dyes	57
1.7.1 Introduction	57
1.7.2 The effect of terminal groups on the absorption spectra of TPM/DPM dyes	59
1.7.3 The effect of substitution at the 2-position of the phenyl rings on the absorption spectra of TPM/DPM dyes	64
1.7.4 The effect of substitution at the 3-position of the phenyl rings on the absorption spectra of TPM/DPM dyes	68
1.7.5 TPM/DPM dyes with extended chromophoric systems	72

2.	<u>RESULTS AND DISCUSSION</u>	86
2.1	Synthetic work	89
2.1.1	Preparation of leuco bases	90
2.1.2	Preparation of intermediates and precursors	93
2.1.3	Preparation of benzophenones	97
2.1.4	Preparation of diarylcarbinols	101
2.1.5	Preparation of triarylcarbinols	104
2.1.6	Preparation of perchlorate salts	121
2.2	Absorption spectra	132
2.2.1	The absorption spectra of the diphenylcarbinols	133
2.2.2	The absorption spectra of some unsymmetrical analogues of MG	137
2.2.2.1	The effects of increased acidity	155
2.2.2.2	Electronic and structural symmetry	165
2.3	Kinetic investigations	172
2.3.1	General	172
2.3.2	Unsymmetrical MGs	178
2.3.3	Analogues of Michler's Hydrol Blue	227
3.	<u>EXPERIMENTAL</u>	235
3.1	Organic synthesis	236
3.1.1	Preparation of disubstituted benzophenones	236
3.1.2	Preparation of monosubstituted benzophenones	237
3.1.3	Preparation of diarylhydrols	239
3.1.4	Preparation of intermediates	241
3.1.5	Preparation of aryllithium compounds	243
3.1.6	Preparation of the unsymmetrical derivatives of Malachite Green	244
3.1.7	Preparation of the perchlorate salts	251
3.2	Kinetic studies	260
3.2.1	Chemicals	260
3.2.2	Apparatus	260
3.2.3	Instrumentation	261

3.2.4	Experimental methods	263
4.	<u>CONCLUSIONS</u>	266
5.	<u>REFERENCES</u>	270

APPENDICES

FIGURES

Page

1A	Conformational changes accompanying the hydrolysis of a TPM dye and the ionisation of its dye base	6
1B	The proportion of molecules having energy in excess of E_{act}	10
1C	The concentrations of reactants (A), products (C) and intermediates (B) for a first order reaction as postulated in the Transition State Theory	12
1D	A potential energy curve for a reaction	13
1E	The proportionality of ΔG and ΔH arising from the temperature invariance of σ	23
1F	The non-proportionality of ΔG and ΔH leading to a breakdown of the Hammett equation	24
1G	The absorption spectra of the classes of cones	28
1H	The wavelength and type of electromagnetic radiation	29
1I	Apparatus used in the constant-flow technique	32
1J	Apparatus used in the stopped-flow technique	32
1K	Postulated resonance forms of MHB	34
1L	Molecular and atomic orbitals	37
1M	A Jablonski scheme	40
1N	FEMO wave functions for a linear, conjugated molecule	43
1O	π MOs for a linear, conjugated molecule in (a) the FEMO model and (b) the HMO model	45
1P	Some examples of alternant and non-alternant systems	49
1Q	The effect on the energies of the orbitals and the first electronic transition by replacing a carbon atom of an odd-alternant with an atom of differing electronegativity	51
2A	The relationship between a univalent cationic dye and its immediate precursors	89
2B	A plot of 1H chemical shift for the proton adjacent to the amino-bearing carbon atom against σ^+ substituent constants	119
2C	Enantiomers for the unsymmetrical MGs	120
2D	Nitrogen-phenyl ring resonance interaction for <i>N</i> -phenylpyrrolidine	146
2E	Nitrogen-phenyl ring resonance interaction for <i>N</i> -phenylpiperidine	146

2F	Transition state formed during reaction of enamines with electrophile	150
2G	The formation of protonated Pyrrolidine Green	159
2H	Visible absorption spectrum of Pyrrolidine Green, PG^+ , (A) and protonated Pyrrolidine Green, PGH^{2+} , (B)	160
2I	Two extreme resonance configurations for the structurally unsymmetrical dye Mo-Pi	166
2J	A plot of $\epsilon_{\max}(x)$ against $\lambda_{\max}(x)$ deviation for twelve unsymmetrical MG type dyes	170
2K	Plot of \ln absorbance against time for varying concentrations of EtDPM at 293.8K; (\blacklozenge) 4.67×10^{-4} , (\blacksquare) 2.52×10^{-4} and (\blacktriangle) 1.12×10^{-4} mol dm ⁻³ $10^3 [OH^-] = 0.5$ mol dm ⁻³ , $I = 0.01$ mol dm ⁻³	175
2L	Isokinetic relationship in the co-ordinates $\log k_2$ versus $\log k_{293}$ with k_2 at 303 K (\blacksquare), 318 K (\bullet) and 333 K (\blacktriangle)	207
3A	Schematic diagram of the Hi-Tech Scientific SFA-11 Rapid Kinetics Accessory	262

TABLES

Page

1.1	Table of complementary colours	27
1.2	The visible absorption spectra in 98% acetic acid of some derivatives of Michler's Hydrol Blue	59
1.3	The visible absorption spectra in 98% acetic acid of some derivatives of Crystal Violet	60
1.4	The visible absorption spectra in 98% acetic acid of some derivatives of Malachite Green	61
1.5	The visible absorption spectra in 100% acetic acid of some unsymmetrical derivatives of Crystal Violet	63
1.6	The visible absorption spectra in 98% acetic acid of some <i>ortho</i> -substituted derivatives of Crystal Violet	65
1.7	The visible absorption spectra in 98% acetic acid of some <i>ortho</i> -substituted derivatives of Michler's Hydrol Blue	66
1.8	The visible absorption spectra in 98% acetic acid of some <i>ortho</i> -substituted derivatives of Malachite Green	67
1.9	The visible absorption spectra in 98% acetic acid of some <i>meta</i> -substituted derivatives of Crystal Violet, Malachite Green and Michler's Hydrol Blue	69
1.10	Relative shifts of λ_{\max} for analogous derivatives of Crystal Violet, Malachite Green and Michler's Hydrol Blue	70
1.11	The visible absorption spectra in 98% acetic acid of some <i>meta</i> - and <i>para</i> -substituted derivatives of Malachite Green	72
1.12	The visible absorption spectra in 98% acetic acid of some biphenyl and 9,9-dimethylfluorenyl analogues of Crystal Violet and Malachite Green	74
1.13	The visible absorption spectra in 98% acetic acid of some longitudinally conjugated naphthalene analogues of Crystal Violet, Malachite Green and Michler's Hydrol Blue	77
1.14	The visible absorption spectra in 98% acetic acid of some transversely conjugated naphthalene analogues of Crystal Violet, Malachite Green and Michler's Hydrol Blue	79
1.15	The visible absorption spectra in 98% acetic acid of some phenanthryl analogues of Malachite Green and Crystal Violet	81

1.16	The visible absorption spectra in 98% acetic acid of some ethynologues and vinylogues of Crystal Violet and Malachite Green	83
2.1	Summary of abbreviations used for the Michler's Hydrol Blue analogues studied in this investigation	86
2.2	Summary of abbreviations used for the unsymmetrical Malachite Green analogues studied in this investigation	88
2.3	Preparative data for some 4,4'-diaminobenzophenones	98
2.4	Preparative data for some 4-aminobenzophenones	100
2.5	Preparative data for the reduction of some 4,4'-diaminobenzophenones	103
2.6	¹³ C chemical shifts (ppm) for the carbinols (2.1-5)	110
2.7	¹³ C chemical shifts (ppm) for the carbinols (2.1-5)	111
2.8	¹ H chemical shifts (ppm) for the carbinols (2.1-6)	113
2.9	¹ H chemical shifts (ppm) for the carbinols (2.1-6)	114
2.10	¹³ C chemical shifts (ppm) for the dye cations (2.1-7)	124
2.11	¹³ C chemical shifts (ppm) for the dye cations (2.1-7)	125
2.12	¹ H chemical shifts (ppm) for the dye cations (2.1-8)	127
2.13	¹ H chemical shifts (ppm) for the dye cations (2.1-8)	128
2.14	Absorption bands of some symmetrical MHB analogues in 98% acetic acid	133
2.15	Absorption spectra of some symmetrical MG analogues in 98% acetic acid	136
2.16	Absorption spectra of some unsymmetrical MGs in 98% acetic acid	137
2.17	Absorption spectra of some unsymmetrical MGs containing a dimethylamino group in 98% acetic acid	139
2.18	Absorption spectra of some unsymmetrical MGs containing a diethylamino group in 98% acetic acid	140
2.19	Absorption spectra of some unsymmetrical MGs containing a pyrrolidino group in 98% acetic acid	141
2.20	Absorption spectra of some unsymmetrical MGs containing a piperidino group in 98% acetic acid	142
2.21	Dissociation constants for some amino compounds	143

2.22	Comparison of spectral shifts for some unsymmetrical MGs bearing terminal dimethylamino and diethylamino groups in 98% acetic acid	145
2.23	Comparison of spectral shifts for some unsymmetrical MGs bearing terminal pyrrolidino and piperidino groups in 98% acetic acid	148
2.24	Pauling electronegativity values	153
2.25	Base strengths for a series of some 3-aminocyclohex-2-enones	154
2.26	Absorption spectra of symmetrical Violet dyes in 98% and 10% acetic acid	157
2.27	Relationship between basicity of the terminal group and the observed shift in the main absorption band following an increase in the solvent acidity	158
2.28	Absorption spectra of some unsymmetrical MGs in 100% acetic acid	161
2.29	Absorption spectra of some unsymmetrical MGs in 50% acetic acid	162
2.30	Absorption spectra of some unsymmetrical MGs in 10% acetic acid	163
2.31	Deviations in the electronic absorption spectra of some unsymmetrical MGs	167
2.32	The effect of hydroxide ion and acetone concentration on k' for Brilliant Green using different experimental techniques	173
2.33	Rate constant k_2 for the reaction between Brilliant Green and hydroxide ion using different experimental techniques	173
2.34	The effect of temperature and hydroxide ion concentration on k' for 4'-dimethylamino-4"-diethylaminotriphenylmethyl perchlorate	178
2.35	The effect of temperature and hydroxide ion concentration on k' for 4'-pyrrolidino-4"-diethylaminotriphenylmethyl perchlorate	179
2.36	The effect of temperature and hydroxide ion concentration on k' for 4'-piperidino-4"-diethylaminotriphenylmethyl perchlorate	180
2.37	The effect of temperature and hydroxide ion concentration on k' for 4'-morpholino-4"-diethylaminotriphenylmethyl perchlorate	181
2.38	The effect of temperature and hydroxide ion concentration on k' for 4'-dimethylamino-4"-pyrrolidinotriphenylmethyl perchlorate	182

2.39	The effect of temperature and hydroxide ion concentration on k' for 4'-piperidino-4"-pyrrolidinotriphenylmethyl perchlorate	183
2.40	The effect of temperature and hydroxide ion concentration on k' for 4'-morpholino-4"-pyrrolidinotriphenylmethyl perchlorate	184
2.41	The effect of temperature and hydroxide ion concentration on k' for 4'-dimethylamino-4"-piperidinotriphenylmethyl perchlorate	185
2.42	The effect of temperature and hydroxide ion concentration on k' for 4'-morpholino-4"-piperidinotriphenylmethyl perchlorate	186
2.43	The effect of temperature and hydroxide ion concentration on k' for 4'-dimethylamino-4"-morpholinotriphenylmethyl perchlorate	187
2.44	The effect of temperature and hydroxide ion concentration on k' for 4'- <i>N</i> -methylpiperazino-4"-diethylaminotriphenylmethyl perchlorate	188
2.45	The effect of temperature and hydroxide ion concentration on k' for 4'- <i>N</i> -methylpiperazino-4"-dimethylaminotriphenylmethyl perchlorate	189
2.46	The effect of temperature and hydroxide ion concentration on k' for 4'- <i>N</i> -methylpiperazino-4"-pyrrolidinotriphenylmethyl perchlorate	190
2.47	The effect of temperature and hydroxide ion concentration on k' for 4'- <i>N</i> -methylpiperazino-4"-piperidinotriphenylmethyl perchlorate	191
2.48	The effect of temperature and hydroxide ion concentration on k' for 4'- <i>N</i> -methylpiperazino-4"-morpholinotriphenylmethyl perchlorate	192
2.49	The effect of temperature and hydroxide ion concentration on k' for 4'-thiomorpholino-4"-dimethylaminotriphenylmethyl perchlorate	193
2.50	The effect of temperature on the rate constant k_2 for the hydrolysis of the 4'-dimethylamino-4"-diethylaminotriphenylmethyl cation	194
2.51	The effect of temperature on the rate constant k_2 for the hydrolysis of the 4'-pyrrolidino-4"-diethylaminotriphenylmethyl cation	194
2.52	The effect of temperature on the rate constant k_2 for the hydrolysis of the 4'-piperidino-4"-diethylaminotriphenylmethyl cation	194
2.53	The effect of temperature on the rate constant k_2 for the hydrolysis of the 4'-morpholino-4"-diethylaminotriphenylmethyl cation	195
2.54	The effect of temperature on the rate constant k_2 for the hydrolysis of the 4'-dimethylamino-4"-pyrrolidinotriphenylmethyl cation	195
2.55	The effect of temperature on the rate constant k_2 for the hydrolysis of the 4'-piperidino-4"-pyrrolidinotriphenylmethyl cation	195

2.56	The effect of temperature on the rate constant k_2 for the hydrolysis of the 4'-morpholino-4"-pyrrolidinotriphenylmethyl cation	196
2.57	The effect of temperature on the rate constant k_2 for the hydrolysis of the 4'-dimethylamino-4"-piperidinotriphenylmethyl cation	196
2.58	The effect of temperature on the rate constant k_2 for the hydrolysis of the 4'-morpholino-4"-piperidinotriphenylmethyl cation	196
2.59	The effect of temperature on the rate constant k_2 for the hydrolysis of the 4'-dimethylamino-4"-morpholinotriphenylmethyl cation	197
2.60	The effect of temperature on the rate constant k_2 for the hydrolysis of the 4'- <i>N</i> -methylpiperazino-4"-diethylaminotriphenylmethyl cation	197
2.61	The effect of temperature on the rate constant k_2 for the hydrolysis of the 4'- <i>N</i> -methylpiperazino-4"-dimethylaminotriphenylmethyl cation	197
2.62	The effect of temperature on the rate constant k_2 for the hydrolysis of the 4'- <i>N</i> -methylpiperazino-4"-pyrrolidinotriphenylmethyl cation	198
2.63	The effect of temperature on the rate constant k_2 for the hydrolysis of the 4'- <i>N</i> -methylpiperazino-4"-piperidinotriphenylmethyl cation	198
2.64	The effect of temperature on the rate constant k_2 for the hydrolysis of the 4'- <i>N</i> -methylpiperazino-4"-morpholinotriphenylmethyl cation	198
2.65	The effect of temperature on the rate constant k_2 for the hydrolysis of the 4'-thiomorpholino-4"-dimethylaminotriphenylmethyl cation	199
2.66	Thermodynamic activation parameters for the reaction between some unsymmetrical MG type dyes and hydroxide ion (298.2 K)	200
2.67	Interpolated kinetic data for the unsymmetrical MGs	202
2.68	Kinetic data for the parent dyes at 298.2 K and ionic strength 0.01 mol dm ⁻³	202
2.69	Isokinetic temperature determined from log k_2 versus log k_{293} with k_2 at 333 K, 318 K and 303 K	208
2.70	The σ^+ values used for the determination of the temperature dependence of the reaction constant, ρ	210
2.71	Reaction constants determined from log k_2 versus σ^+ for some unsymmetrical MGs (2.3-1; R ¹ = NMe ₂)	212
2.72	Reaction constants determined from log k_2 versus σ^+ for some unsymmetrical MGs (2.3-1; R ¹ = NEt ₂)	213

2.73	Reaction constants determined from $\log k_2$ versus σ^+ for some unsymmetrical MGs (2.3-1; $R^1 =$ Pyrrolidine)	213
2.74	Reaction constants determined from $\log k_2$ versus σ^+ for some unsymmetrical MGs (2.3-1; $R^1 =$ Piperidine)	214
2.75	Reaction constants determined from $\log k_2$ versus σ^+ for some unsymmetrical MGs (2.3-1; $R^1 =$ Morpholine)	214
2.76	Reaction constants determined from $\log k_2$ versus σ^+ for some unsymmetrical MGs (2.3-1; $R^1 =$ <i>N</i> -Methylpiperazine)	215
2.77	Values of β determined from the temperature dependence of the reaction constant for a series of unsymmetrical MGs	215
2.78	Reaction constant values for parent Green dyes	216
2.79	Values of β determined from Arrhenius plots for some unsymmetrical MG type dye series	219
2.80	σ_p^+ Substituent constants calculated for <i>N</i> -methylpiperazine	223
2.81	σ_p^+ Substituent constants calculated for piperidine	223
2.82	σ_p^+ Substituent constants calculated for thiomorpholine	224
2.83	Summary of σ_p^+ substituent constants for the terminal amino-groups used in the present investigation	224
2.84	Comparison of σ_p^+ constants	226
2.85	The effect of temperature and hydroxide ion concentration on k' for 4,4'-bis(dimethylamino)diphenylmethyl perchlorate	227
2.86	The effect of temperature and hydroxide ion concentration on k' for 4,4'-bis(diethylamino)diphenylmethyl perchlorate	228
2.87	The effect of temperature and hydroxide ion concentration on k' for 4,4'-dipyrrolidinodiphenylmethyl perchlorate	229
2.88	The effect of temperature on the rate constant k_2 for the hydrolysis of the 4,4'-bis(dimethylamino)diphenylmethyl cation	230
2.89	The effect of temperature on the rate constant k_2 for the hydrolysis of the 4,4'-bis(diethylamino)diphenylmethyl cation	230
2.90	The effect of temperature on the rate constant k_2 for the hydrolysis of the 4,4'-dipyrrolidinodiphenylmethyl cation	230
2.91	Thermodynamic activation parameters for the reaction between some MHB analogues and hydroxide ion (298.2 K)	231

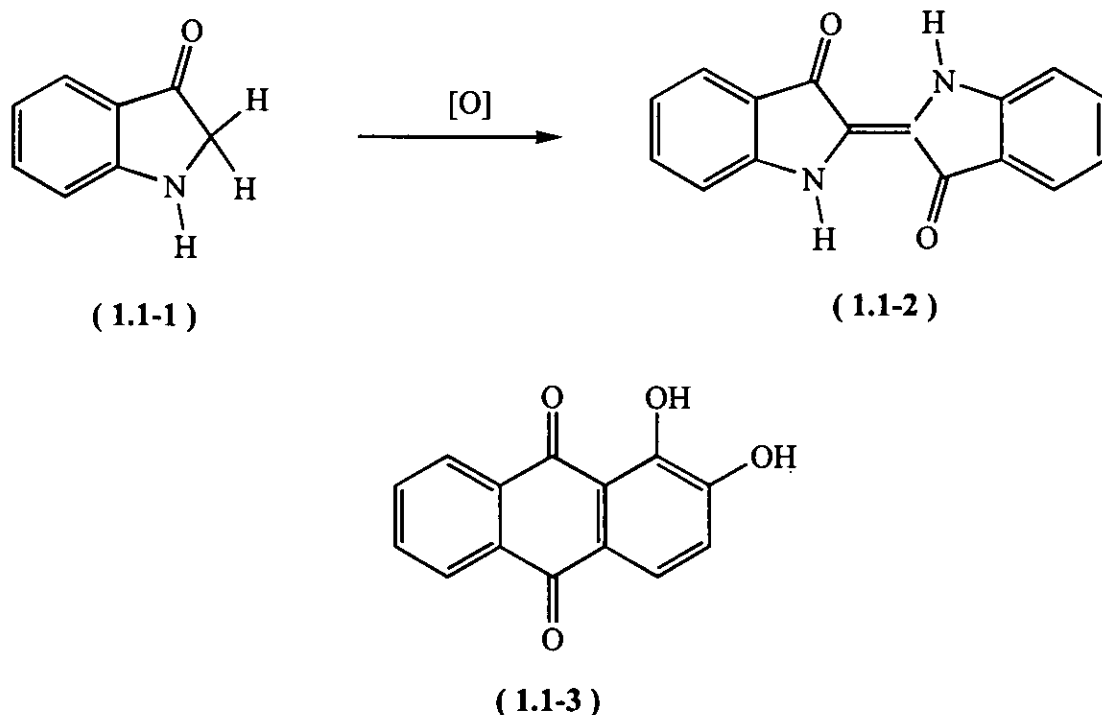
2.92	Comparison of k_2 values for related dye systems	232
2.93	Interpolated values of $\log k_2$ used for the computation of the isokinetic relationship	233

1.

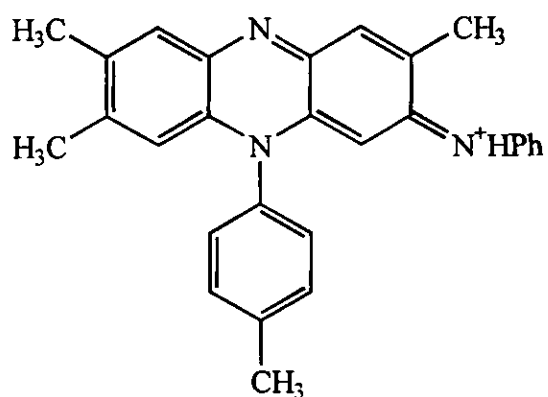
INTRODUCTION

1.1 Brief history of dyes

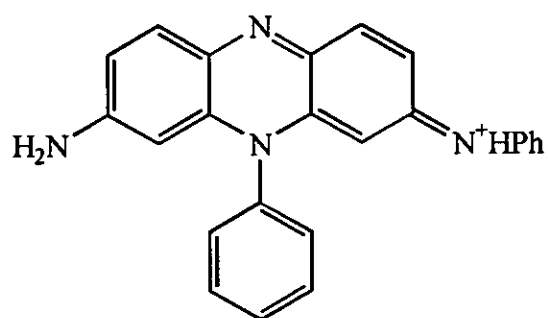
Prior to the 1860s, all textiles and other materials were dyed using natural products from sources as bizarre as a snail to the more conservational plant extracts (90MI1, 95CIB547). Two of the most common dyes were indigo (1.1-2), obtained from *Indigofera tinctoria* - a native plant of Asia - whose active colouring component was the air oxidation product of indoxyl (1.1-1), and madder, obtained from *Rubia tinctorium*, whose active colouring component was alizarin (1.1-3).



Reports of the preparation of the first synthetic dye are understandably patchy, but without doubt the first commercial process for synthetic dye manufacturing is attributed to William Henry Perkin with the process coming on-line in 1864 (90MI1). The dye manufactured was called Aniline Purple and was actually a mix of two dyes (1.1-4; 1.1-5).



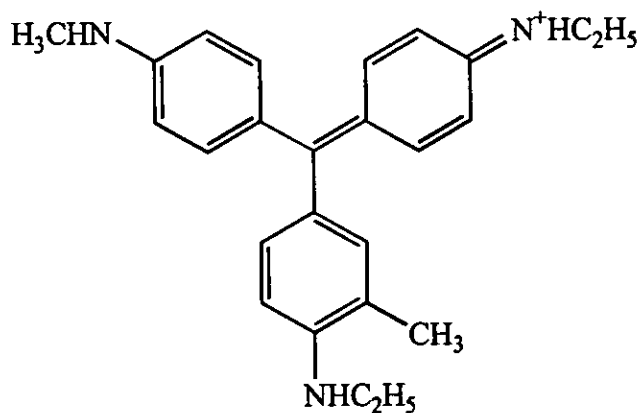
(1.1-4)



(1.1-5)

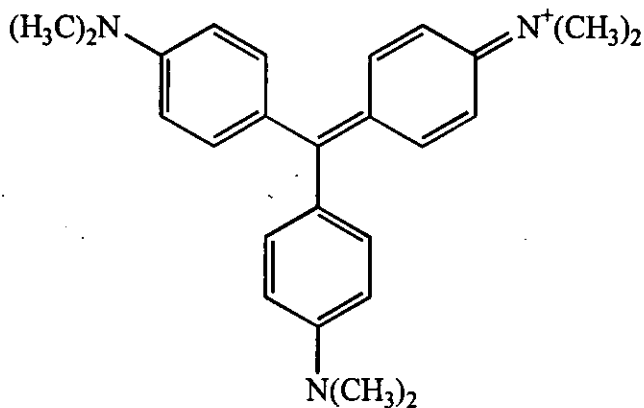
With the obvious commercial rewards of dye manufacturing, the amount of interest shown in synthetic dyes at that time was not surprising. However, the first attempts at the synthesis of new dyes were hampered by the lack of knowledge in structural organic chemistry which, even at the virtual infancy of chemistry itself, already lagged behind the other chemistry disciplines. One of the major achievements of the field of dyes is its awakening of structural organic chemistry. With the rapid advances in structural organic chemistry came the discovery of a new class of synthetic dyes: the azo dye. The azo dye contains at least one azo group and whilst being slow to take off commercially, is now the largest class of commercial dyes.

Many of the earliest dyes were of the triphenylmethane type (TPM), such as Hofmann's Violet (1.1-6).

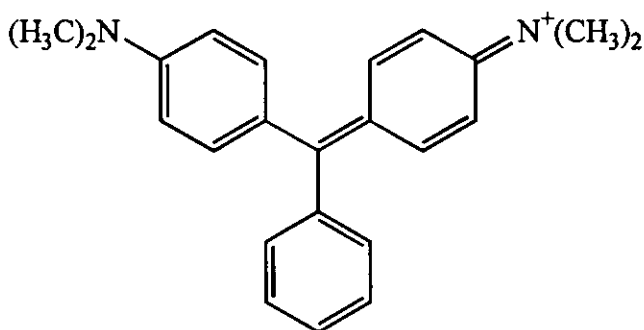


(1.1-6)

Since their discovery, TPM dyes have been extensively studied. Two of the oldest and most studied examples are Crystal Violet (CV) (1.1-7) and Malachite Green (MG) (1.1-8).



(1.1-7)

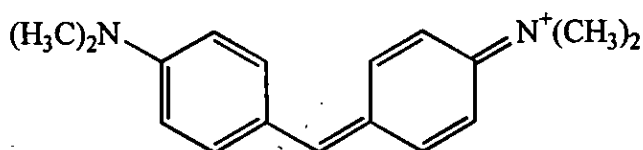


(1.1-8)

Recent TPM dyes that have been synthesised and studied have contained substituents in the various positions of the phenyl rings (71JSDC187, 89JCS(P2)1087) as well as employing heteroatoms to bridge the 2,2'-positions of adjacent phenyl rings to produce new classes of compounds (76MI1). In addition, the preparation of the vinylogues and ethynologues of TPM dyes has been undertaken in order to develop compounds with novel properties (81CL311, 87JCSCC710, 88JCS(P1)3157, 94Th1).

The compounds prepared and studied in this investigation are unsymmetrical derivatives of MG containing modified terminal amino groups. The unsymmetrical nature was achieved by substituting two different groups at the terminal positions of the MG system.

A branch of dyes similar to the TPM dyes are the diphenylmethane (DPM) dyes, in which the unsubstituted phenyl ring of MG is absent, being replaced by a hydrogen atom or other non-aromatic moiety. One of the simplest DPM dyes - the analogues of which are being studied as part of this project - is Michler's Hydrol Blue (MHB) (1.1-9).



(1.1-9)

The symmetrical analogues of MHB prepared and studied in this investigation contained different amino groups at the terminal positions of the phenyl rings.

Today, TPMs are still used in textiles but are also finding applications in pharmacology (79ML111, 86AB242), biology (79ML111) and as photoconductive materials for use in electrophotography (85PP78) and jet printing (87P24756). Applications in chemistry are in areas such as surface and analytical chemistry (93CR381), where their ability to complex with metal ions and their highly coloured nature make them invaluable for both research and routine operations. TPMs are also finding applications in the photographic (86JIS9), food and cosmetic industries (82MI2). As a result of their many applications, and the possible health hazards associated with certain members of this class of compounds, research has been directed towards an assessment of their impact on the aquatic environment and possible waste-water treatments (93CR183). More recently, investigations have been conducted into the photochromism of certain TPM dyes (94CM412, 95CM945, 97JA2062).

The central carbon atom of a TPM or DPM carbocation is sp^2 hybridised. Maximum resonance stabilisation of the TPM ion would be achieved if all three benzene rings and the central carbon atom were coplanar. Molecular models suggest that interference between the *ortho* hydrogens of adjacent benzene rings forces the rings out of the plane defined by the central carbon atom and its three sp^2 hybrid bonds. Spectroscopic and X-ray crystallographic measurements of the perchlorate salt of triphenylmethane

(61PRFR14 65AC437) have shown that the rings are twisted more than 30° out of this plane. In fact, the structure of the ion has been described as a symmetrical propeller-like conformation (59JCS3957) with an unsymmetrical conformation also existing and, where free rotation is allowed, possibly an equilibrium existing between the two (42JA1774, 54JOC155, 93CR381).

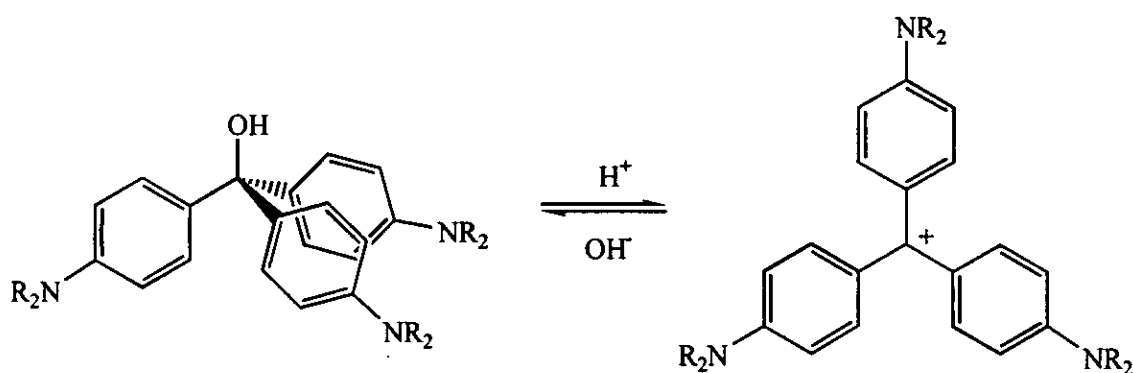
In DPM dyes, however, the benzene rings may be more nearly coplanar because any overlap of the *ortho* hydrogens can be compensated for by an increase in the phenyl-carbon-phenyl bond angle (59JCS3957).

1.2 Hydrolysis of TPM/DPM dyes

In the presence of hydroxyl ions, TPM/DPM dyes are known to decolourise because of the conformational changes accompanying the attack on the carbocation (49JCS1724). The central carbon atom changes from the near planar conformation of its sp^2 hybridised state whilst ionised to the tetrahedral structure associated with its sp^3 hybridised state as the carbinol (Figure 1A). The intervention of a saturated (sp^3) carbon atom prevents delocalisation and hence destroys the extended conjugation of the system.

Figure 1A

Conformational changes accompanying the hydrolysis of a TPM dye
and the ionisation of its dye base



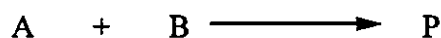
The hydrolysis of TPM dyes has been extensively studied but the hydrolysis of DPM dyes has received little attention. The rate of hydrolysis of TPM and DPM dyes can be monitored spectrophotometrically by studying the fading of the highly coloured dye solution and kinetic studies have investigated the effect of concentration, temperature, ionic strength, pressure, solvent medium and structural modifications on the rate of hydrolysis (52JA5988, 61JCS861, 70BCSJ601, 70JPC1382, 70TFS2305, 80JCTB317, 83JA6782).

1.3 Kinetics

Most reactions can be defined by a sequence of steps involving either a unimolecular reaction, where a single molecule decomposes or reconfigures by initiation of a non-chemical nature, or a bimolecular reaction in which two molecules combine to exchange energy or atoms thereby bringing about a chemical change.

Through the study of the kinetics of a reaction, a rate equation can be constructed. This equation provides valuable information on the reaction studied. The rate of a chemical reaction is expressed in terms of the rate of change of concentration of a reactant or product.

For example, for the reaction:



the rate equation can be written

$$\text{Rate} = k [A]^m [B]^n \quad 1.1$$

where k = rate constant (a constant at constant temperature)

m = the order of reaction with respect to A

n = the order of reaction with respect to B

$m + n$ = the overall order of the reaction

The order can only be obtained experimentally. A reaction may have a relatively slow step, called the rate determining step. Molecularity describes the number of species taking part in a reaction step and is not necessarily the same as the order.

The experimental determination of m and n in equation 1.1 can be simplified using the isolation method, where one of the reactants is kept in a large excess so that its concentration remains effectively constant. Equation 1.1 can be simplified, if B is in large excess

$$\text{Rate} = k_{\text{obs}} [\text{A}]^m \quad 1.2$$

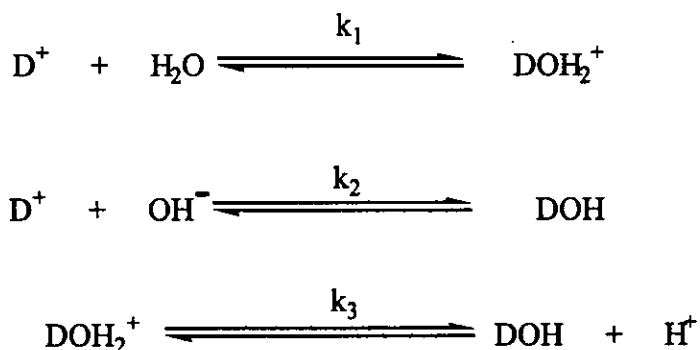
k_{obs} is the observed rate constant. It is related to the true constant by

$$k_{\text{obs}} = k [\text{B}]^n \quad 1.3$$

The reaction is said to be exhibiting pseudo "mth" order kinetics. The order with respect to B can be then determined by carrying out a series of experiments where [B] is varied but always in a large excess. k_{obs} is calculated each time and from the application of equation 1.3, both k and n can be obtained.

Rate equations are used to give information on reaction mechanisms. Sometimes a reaction involves several steps. If one of these steps is a particularly slow, rate determining step the rate equation reflects this. Otherwise the rate equations may be more complex and involve terms for each step.

Previous studies on Brilliant Green (BG) and Pyrrolidine Green (PG) (80JCTB317, 83JCS(P2)975, 85JCS(P2)107) resulted in the following reaction sequence being proposed for TPM dyes. It would seem reasonable to assume DPM dyes react by a similar pathway.



From extended work on Malachite Green (MG) derivatives, a whole series of equilibria can be predicted involving mono- and di-protonated species depending upon the conditions (62ACS2251, 62JA2349, 63ACS2083, 64ACS447, 66ACS444). Under the

experimental conditions used in this study, the back reactions are negligible and the rate equation was shown to be

$$\text{Rate} = -d[\text{Dye}^+]/dt = k_1[\text{Dye}^+][\text{H}_2\text{O}] + k_2[\text{Dye}^+][\text{OH}^-] \quad 1.4$$

$$= k'[\text{Dye}^+] \quad 1.5$$

where

$$k' = k_1 [\text{H}_2\text{O}] + k_2 [\text{OH}^-] \quad 1.6$$

The hydroxide ion is a much stronger nucleophile than water and so $k_2 \gg k_1$.

1.3.1 The dependence of rate of reaction on temperature

Chemical reactions are generally sensitive to temperature change and as a rough estimate it can be expected that, in most cases, the rate will double for every 10 K rise in temperature. The relationship between the rate constant, k , of a chemical reaction and the temperature is expressed in the Arrhenius equation 1.7.

$$\ln k = \ln A - E_{\text{act}}/RT \quad 1.7$$

where k = rate constant

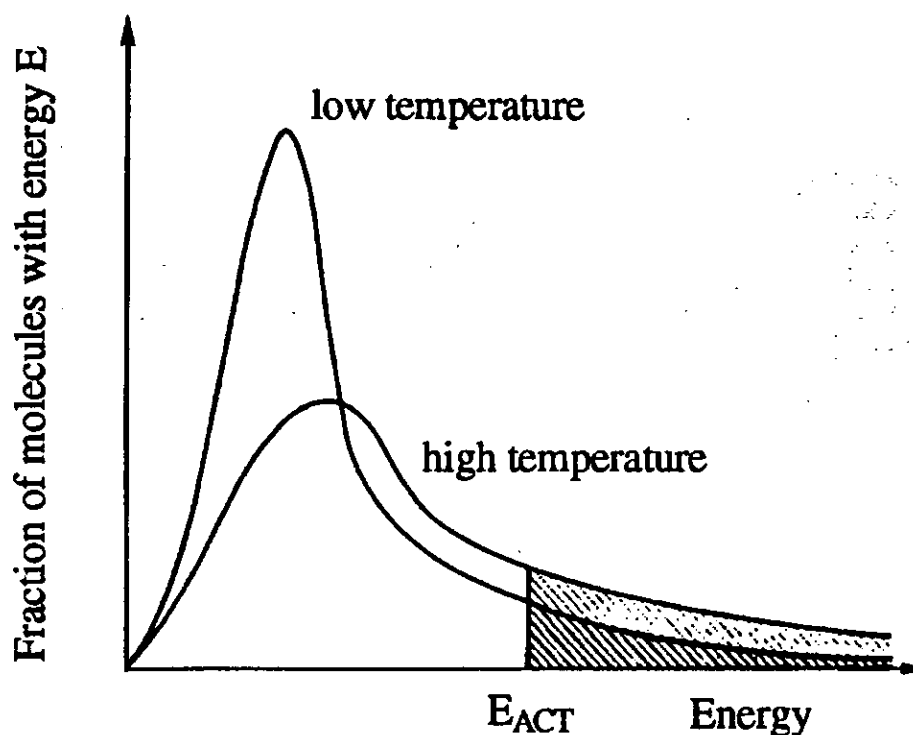
A = frequency or pre-exponential factor and is related to the frequency of collisions between reactant molecules

E_{act} = energy of activation and is the minimum amount of energy that must be acquired by molecules before they react

The Boltzmann factor, $\exp(-E_{\text{act}}/RT)$, gives the fraction of molecules possessing at least E_{act} at temperature T . The fraction of molecules with energy greater than E_{act} is the area beyond E_{act} expressed as a fraction of the total area of the curve as illustrated in Figure 1B. It can be seen that as the temperature increases, the fraction of molecules possessing energy greater than E_{act} increases.

Figure 1B

The proportion of molecules having an energy in excess of E_{act}



It follows from equation 1.7, that if values of the rate constant are obtained at various temperatures a plot of $\ln k$ against the reciprocal of the temperature will produce a linear plot of gradient $-E_{act}/R$ and intercept $\ln A$.

For gases, the simple collision theory requires that two molecules in a bimolecular reaction must collide and have energies equal to or greater than the activation energy in order to react. Hence, the greater the E_{ACT} the fewer molecules possess sufficient energy to react and so the slower the rate of reaction.

For gases, the frequency of collisions is given by Z , the bimolecular collision frequency. In theory, the pre-exponential factor, A , should equal Z , if the collision theory is applicable to the system under investigation and equation 1.7 can then be rewritten

$$k = Z \exp.(-E_{act}/RT)$$

1.8

where Z = collision number

However, there is only good agreement between the experimental rate constant and the value calculated from the collision theory in a very few cases and these usually involve simple molecules in the gas phase. This is because as well as colliding molecules requiring energies greater than E_{act} , they must also have a particular distribution of energy between the bonds - a feature of increasing importance for reactants other than simple molecules. As a result, a steric or probability factor, P , is introduced into equation 1.8 which is a measure of the discrepancy between the theoretical and experimental rate constants. The closer P is to unity, the more applicable is the collision theory to the reaction under investigation.

$$k = PZ \exp.(-E_{act}/RT)$$

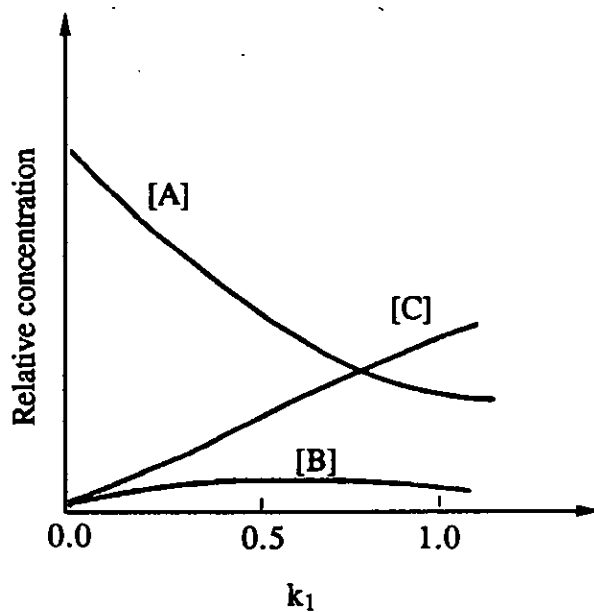
1.9

The collision theory, obtained from the kinetic theory of gases, assumes that molecules are hard spheres possessing only translational energy and fails to consider the rotational and vibrational energy also possessed by molecules. As a result, the collision theory works reasonably well for simple bimolecular gas phase reactions but is inadequate for uni- and ter-molecular reactions and for reactions in solutions.

The Transition State Theory postulates that chemical reactions proceed through the formation of a transition state complex that acts as an intermediate. Both reactants (A) and products (C) are in equilibrium with the transition state complex (B) whose concentration remains small but constant throughout a reaction. This is illustrated in Figure 1C.

Figure 1C

The concentrations of reactants (A), products (C) and intermediates (B)
for a first order reaction as postulated in the Transition State Theory



For example, the energy diagram shown in Figure 1D can be drawn for the reaction

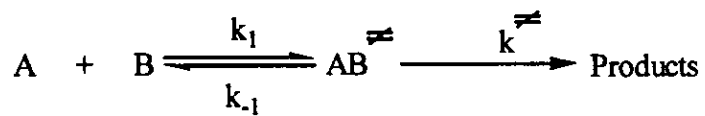
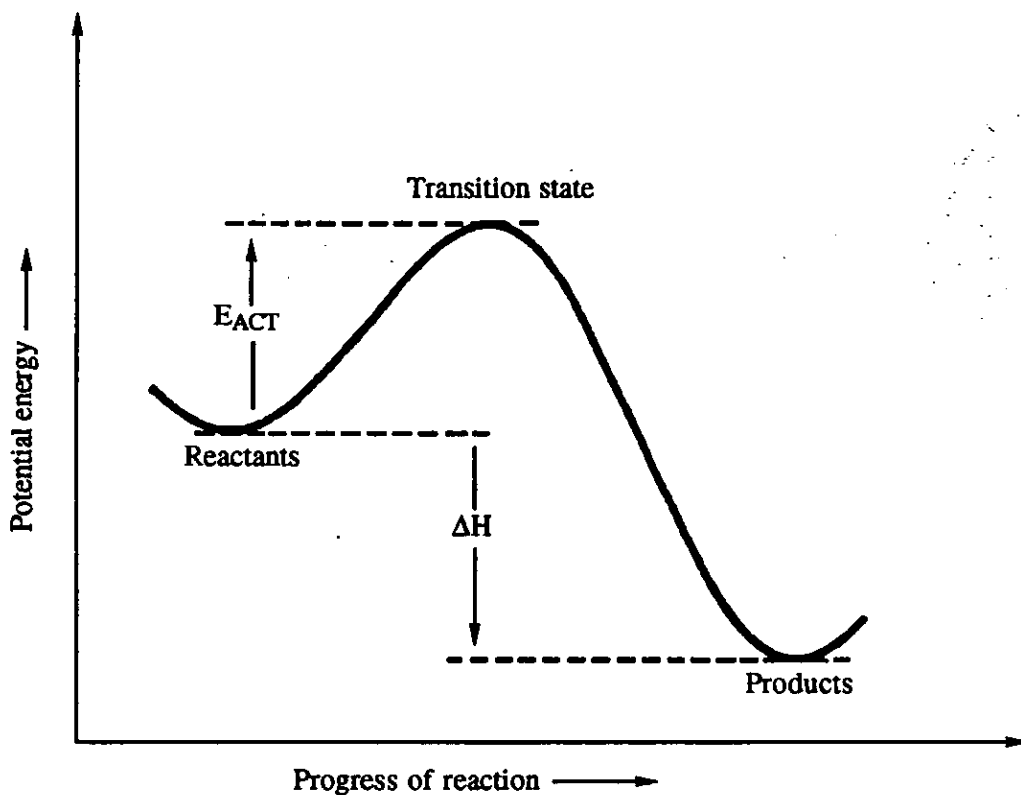


Figure 1D

A potential energy curve for a reaction



k^* is the rate constant for the formation of the products by the breakdown of the activated complex AB^* . This rate is controlled by the frequency of the loose vibrational mode, ν . The associated energy, $h\nu$, is approximately equal to $K_B T$.

$$h\nu = K_B T \quad 2.0$$

where h = Planck's constant

K_B = Boltzmann's constant

Therefore

$$k^* = \nu = K_B T / h \quad 2.1$$

Rate of reaction = Rate of removal of AB^{\ddagger}

$$-d[A]/dt = -d[AB^{\ddagger}]/dt = k^{\ddagger}[AB^{\ddagger}] \quad 2.2$$

Rate of formation of $AB^{\ddagger} = k_1 [A][B] - k_{-1} [AB^{\ddagger}] - k^{\ddagger}[AB^{\ddagger}]$

Consideration of these equations leads to equation 2.3.

$$k = (K_B T/h) \exp.(-\Delta G^{\ddagger}/RT) \quad 2.3$$

Substituting

$$\Delta G^{\ddagger} = \Delta H^{\ddagger} - T\Delta S^{\ddagger} \quad 2.4$$

into 2.3 gives

$$k = (K_B T/h) \exp.(\Delta S^{\ddagger}/R) \exp.(-\Delta H^{\ddagger}/RT) \quad 2.5$$

where ΔS^{\ddagger} = the entropy of activation

ΔH^{\ddagger} = the enthalpy of activation

At a given temperature the term $K_B T/h$ is constant and the rate constant is determined by ΔG^{\ddagger} (equation 2.3). The activation energy E^{\ddagger} is related to the enthalpy of activation by

$$\Delta H^{\ddagger} = E^{\ddagger} - nRT \quad 2.6$$

$n = 1$ for all liquid phase reactions (74MII1).

Combining 2.5 and 2.6 gives

$$k = (K_B T/h) \exp.(\Delta S^*/R) \exp.([-E^*/ RT] + n) \quad 2.7$$

The simple collision theory equation 1.9 combined with equation 2.7 gives

$$PZ = (K_B T/h) \exp.([\Delta S^*/ R] + n) \quad 2.8$$

From equation 2.8 it can be seen that the probability factor, P, is related to the entropy of activation, ΔS^* , that is, the difference in entropy between the activated state and the reactants. For reactions involving simple molecules there is relatively little rearrangement in the degrees of freedom when going from the reactants to the activated state. In these cases, ΔS^* will only be small - either negative or positive - and the collision theory and the transition state theory will give similar results.

For reactions involving more complex molecules there will be a significant rearrangement of energy among the degrees of freedom and a large change in the value of the entropy of formation for the activated complex. The reaction rate will be significantly different from that calculated by the simple collision theory. The frequency factor, A, is related to the entropy of activation by

$$A = (K_B T/h) \exp.([\Delta S^*/R] + n) \quad 2.9$$

For a reaction in solution $n = 1$ and equation 2.9 can be written as

$$\ln A = \ln K_B T/h + 1 + \Delta S^*/R \quad 3.0$$

Thus ΔS^* can be determined from a plot of $\ln k$ against the reciprocal of the temperature. A negative entropy of activation results through an increase in order or loss of freedom when the transition state complex is formed from the reactants and vice versa.

1.3.2 The dependence of rate of reaction on ionic strength

It has been shown that the rate of an ionic reaction depends on the ionic strength, I , of the solution (32CR229) which is affected by the addition of an inert salt to the reaction medium. This is known as the primary salt effect. The effective concentration or activity of an ion is given by the equation

$$a = c f$$

3.1

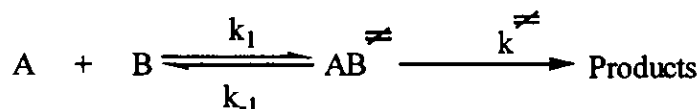
where a = the activity of the ion

c = the concentration of the ion

f = the activity coefficient of the ion which for dilute solutions

is <1 and at infinite dilution approaches unity.

From the transition state theory



Application of the Debye-Huckel Theory to the Transition State Theory gives

$$\log k = \log k_0 + 2AZ_A Z_B \sqrt{I} \quad 3.2$$

$Z_A Z_B$ is the product of the respective charges carried by the reactant ions. From equation 3.2, it can be seen that a plot of $\log k$ against \sqrt{I} would give a linear slope of gradient $2AZ_A Z_B$ and intercept of $\log k_0$. Linear slopes are only obtained at relatively low concentrations ($I < 0.01 \text{ mol dm}^{-3}$) (66MI1, 78MI1).

It can be seen that an increase in the salt concentration increases the rate constant of a reaction between ions of like sign but decreases the rate of reaction between ions of opposite sign. Reactions between an ion and a neutral molecule do not exhibit primary salt effects. Oppositely charged ions react more slowly in solutions of high ionic

concentration because the formation of the uncharged complex is disfavoured because of its reduced interaction with the ionic medium. The opposite is true for ions of like charge. The rate of hydrolysis of TPM dyes has been shown to decrease with increasing ionic strength ($Z_A Z_B \approx 1$), indicating a reaction between oppositely singly charged ions in the rate determining step (61JICS861, 70BCSJ601, 70JCS(TFS)2305, 81Th1, 82JCS(P2)987, 82Th1, 85JCS(P2)107).

1.3.3 The influence of solvent

For reactions involving ions, both the nature of the ions and the nature of the solvent and hence the degree of solvation of the reactants and activated complex have a pronounced influence on the rate of a reaction. However, as the solvent is nearly always present in a vast excess it is often not included in the rate equation (50MI1). If the reactants or activated complex are solvated, then there will be a decrease in the potential energy of the species by an amount equal to the energy of solvation. Thus, if the activated complex is solvated to a greater degree than the reactants, the decrease in potential energy of the activated complex will result in a reduced enthalpy of activation and hence a faster rate of reaction. However, if the reactants are solvated to a greater degree than the activated complex, the decrease in their potential energy will result in an increased enthalpy of activation and hence a slower rate of reaction. If both reactants and activated complex are solvated to a similar extent the net effect on the rate of reaction may well be small. Even for solvents with similar polarities there may be a difference between protic and aprotic solvents where deviations may occur when hydrogen bonding plays an important role in the solute - solvent interactions (77MI1).

The degree of solvation can also effect the entropy of activation of a reaction. For reactions involving oppositely charged ions, this effect may be negligible as a result of mutually opposing effects. However, for reactions involving similarly charged ions, there can be a significant decrease in the entropy of activation. This is known as electrostriction. It occurs because the doubly charged activated complex electrostatically attracts nearby solvent molecules to a greater extent than would a neutral activated complex. As a result, the solvent molecules are less free to move and a decrease in the entropy of activation results.

Solvent effects on the rate of hydrolysis of TPM dyes have been studied and in general an increase in the rate of reaction is observed when the polarity of the solvent is decreased (70JPC1382, 83Th1). This indicates a reaction between oppositely charged reactants resulting in a disappearance of charge in the transition state.

1.3.4 The influence of substituents in the benzene ring on the rate of reaction

The rate of reaction or position of equilibrium for reactions involving a side chain attached to a benzene nucleus can be influenced by the nature and position of a substituent on the ring. When the substituents are in the *meta* or *para* positions of the ring their influence on the rate of reaction or equilibria of the side chain has been quantitatively stated in the Hammett equation. For the purpose of this study, only reaction rates will be considered but any conclusions may be equally applicable to equilibria. The Hammett equation relates the electronic effects - both inductive and mesomeric (resonance) - of the substituent on the ring to the rate of the side chain reaction. Where steric interferences are negligible the effect of the substituent is effectively consistent. The Hammett equation does not apply to substituents in the *ortho* positions of the ring because their steric effects on the side chain reaction are so much more pronounced. Equally, the Hammett equation cannot be applied to aliphatic compounds because of the conformations that exist as a result of free rotation about the single bonds. The Hammett equation for a side chain reaction is

$$\log k/k_0 = \sigma \rho \quad 3.3$$

where k is the rate constant for the side reaction of a *meta*- or *para*-substituted benzene derivative

k_0 is the rate constant for the unsubstituted compound

σ is the substituent constant

ρ is the reaction constant

The reaction constant, ρ , is a measure of the susceptibility of the reaction to substituent effects. It is a measure of the sensitivity of the reaction to electronic substituent effects.

The dissociation of benzoic acids in water at 25°C was chosen as the standard reaction for which ρ was assigned a value of 1.0. If ρ is positive, then that reaction is accelerated by electron withdrawing substituents and slowed down by electron donating substituents. For a ρ of negative value, the opposite is true. When the transition state of the side reaction involves electron capture, the process is accelerated by electron accepting substituents and ρ is positive. When the transition state of the side reaction involves electron donation, the process is accelerated by electron donating substituents and ρ is negative. The magnitude of ρ is a measure of the extent of charge development on the atom of the side chain adjacent to the ring in passing from the ground state to the transition state. The greater the extent of charge development, the greater the magnitude of ρ . The nature of the solvent can have a pronounced effect on ρ . If the degree of solvation and hence charge stabilisation alter, then the susceptibility of the ring will also alter and so will ρ .

σ is the characteristic substituent constant which reflects the ability of the group to attract or repel electrons. Hydrogen is assigned a value of zero and a positive value of σ represents a substituent that attracts electrons to a greater degree than hydrogen and a negative value of σ represents a substituent that donates electrons to a greater degree than hydrogen. Unlike ρ , σ values are not affected to any important extent by the nature of the solvent.

There are two electronic components of σ : the inductive effect from the σ bond bonding the substituent to the ring and the resonance effect from the overlap of the π orbitals of the substituent with those of the aromatic ring.

The inductive effect is due to the effective electron repelling or attracting property of the substituent. The σ bond is strong and therefore the inductive effect is not polarisable and as a consequence the inductive effect is constant, not being affected by changes in the electronic environment of the ring.

The resonance effect on the other hand is highly polarisable, being affected by changes in the electronic environment of the ring. Since resonance effects occur on alternate atoms of the ring, any resonance from the *meta* substituent would have little influence on the side chain reaction. As a consequence of this, the Hammett constants can then be rewritten as (56M11, 58JA2436, 59JA5343)

$$\sigma_m = \sigma_I + a\sigma_R \quad 3.4$$

$$\sigma_p = \sigma_I + \sigma_R \quad 3.5$$

- where σ_m = substituent constant in the *meta* position
 σ_p = substituent constant in the *para* position
 σ_I = that proportion of σ due to the inductive effect
 σ_R = that proportion of σ due to the resonance effect
 a = extent of communication of resonance effect to *meta* position

Hence, it can be deduced that the difference in σ_p and σ_m for the same substituent in the same ring system will be a measure of the resonance effect of that substituent

$$\sigma_R = \sigma_p - \sigma_m \quad 3.6$$

Resonance between the side chain and the substituent is known as through conjugation. This through conjugation or rather the change of through conjugation will affect the σ values for that substituent. As a result, modified σ values for certain substituents have been derived which are symbolised as σ^o .

Since deviations are due to resonance effects and *meta* substituents display little resonance, for *meta* substituents σ and σ^o values are equivalent, as they are for *para* substituents except where the resonance is strong. The extent of through conjugation can be written as $(\sigma_p - \sigma_p^o)$.

Resonance donor substituent constants are designated σ^+ and include substituents such as NMe_2 , OMe , Me , OH , Hal . etc.

Resonance acceptor substituent constants are designated σ^- and include substituents such as NO_2 , CN , COOH etc.

It can be considered that σ^+ and σ^- are not fixed values but vary with the electronic demand of the reaction centre (59RTC815).

This leads to equations proposed by Yukawa, Tsuno and Sawada (66BCJ2274) to account for the enhanced resonance

$$\log k/k_0 = \rho \{ \sigma + r(\sigma^+ - \sigma) \} \quad 3.7$$

and later by Humffray and Ryan (69JCS1138)

$$\log k/k_0 = \rho \{ \sigma + r(\sigma^- - \sigma) \} \quad 3.8$$

If r is zero the above equations simplify to the Hammett equation. When r is unity, correlation with σ^+ or σ^- is indicated and a modified form of the Hammett equation can be written

$$\log k = \log k_0 + \rho \sigma^+ \text{ (or } \sigma^-) \quad 3.9$$

It has been shown previously that the thermodynamics of both equilibria and reactions may be treated in a similar manner. It should be remembered, however, that the parameters for equilibria are based on the ground state and under standard conditions and as such are more reliable than for reactions where an activated complex is assumed to be generated that is then in equilibrium with the reactant molecules.

The Gibb's Free Energy change for an equilibrium is

$$\Delta G = -RT \ln K = -2.303 RT \log K \quad 4.0$$

and for a reaction correlated by the Hammett equation

$$\log k_X/k_Y = \rho \log K_X/K_Y \quad 4.1$$

where k_X and k_Y are the rate constants for the side chain of a benzene nucleus bearing substituent X and Y in a *meta* or *para* position

K_X and K_Y are the ionisation constants of the equivalently substituted benzoic acids in water at 25°C

The Hammett equation is therefore an example of a linear free energy relationship.

Since

$$\Delta G = \Delta H - T\Delta S \quad 4.2$$

It follows that

$$\delta_x \Delta G = \delta_x \Delta H - T\delta_x \Delta S \quad 4.3$$

Reaction series tend to fall into one of three classes all of which can be related to equation 4.3.

i) Isokinetic relationship

ΔH is linearly related to ΔS for a reaction series. For a reaction or equilibrium series

$$\delta_x \Delta H = \beta \delta_x \Delta S \quad 4.4$$

where β is the proportionality constant

Substituting into equation 4.3 gives

$$\delta_x \Delta G = \delta_x \Delta H - T/\beta(\delta_x \Delta H) \quad 4.5$$

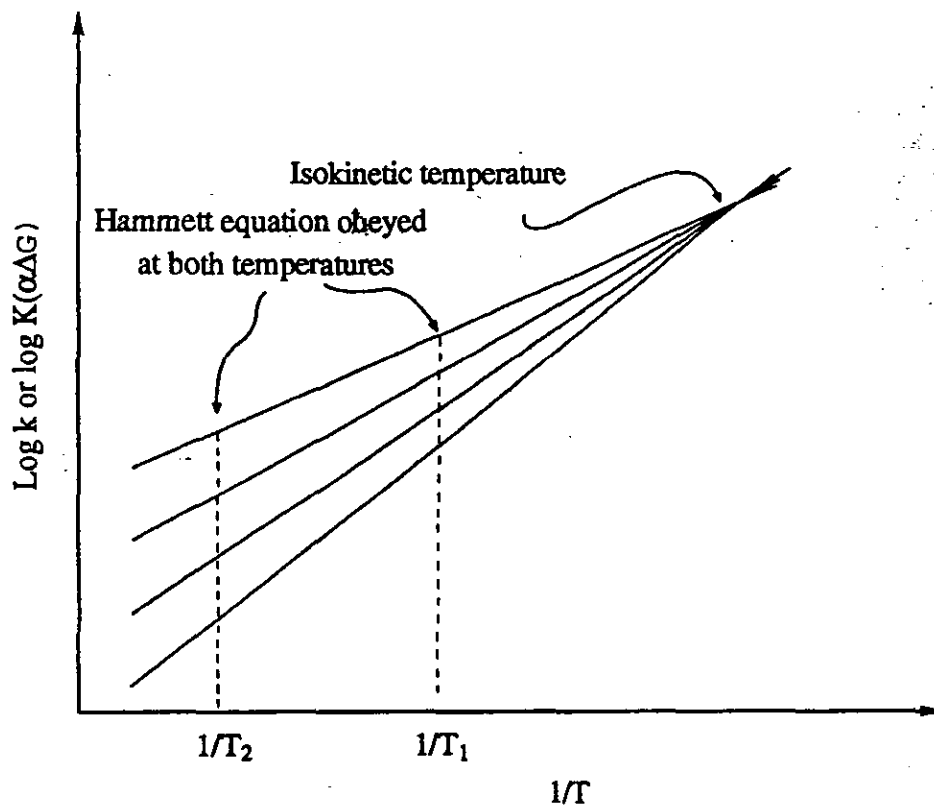
so

$$\delta_x \Delta G = \delta_x \Delta H (1 - T/\beta) \quad 4.6$$

The constant, β , has the dimensions of temperature and when the temperature of the experiment is the same as β then, in theory, all the reactions in the set will proceed at the same rate since $\delta_x \Delta G$ will be zero. This is illustrated in Figure 1E. In this case, β is known as the isokinetic temperature.

Figure 1E

The proportionality of ΔG and ΔH arising from the temperature invariance of σ

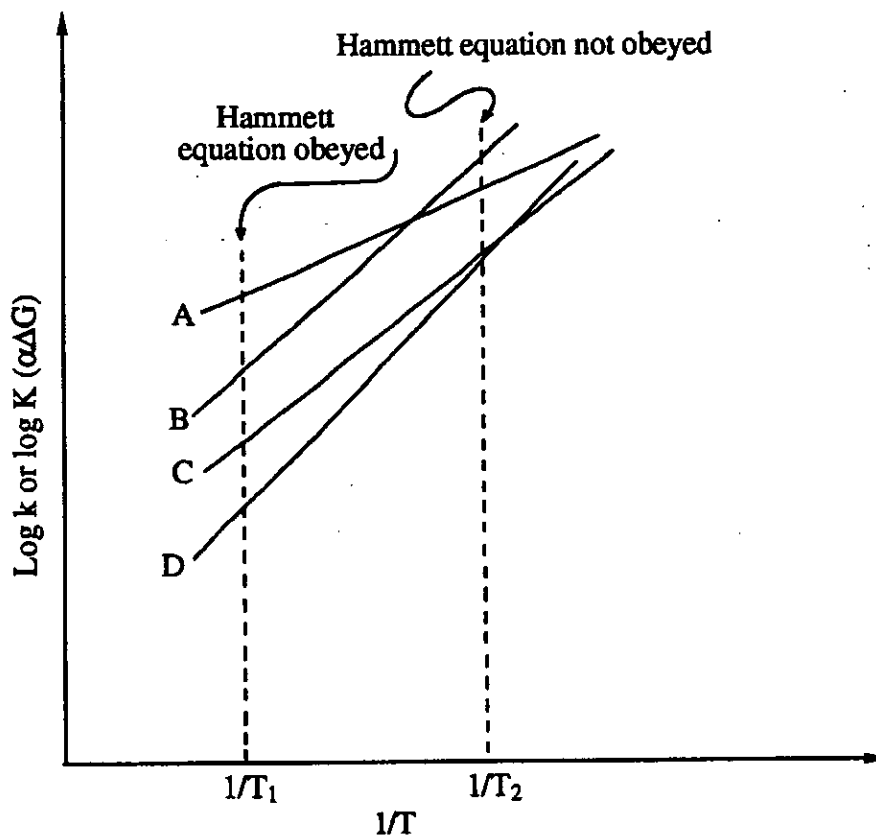


On passing through this point, the reactivity of substituents is reversed; a rate accelerating substituent becomes a rate retarding substituent and a rate retarding substituent becomes rate accelerating.

If $\delta_x \Delta G$ was not proportional to $\delta_x \Delta H$ at any temperature then the results as illustrated in Figure 1F would be obtained.

Figure 1F

The non-proportionality of ΔG and ΔH leading to a breakdown of the Hammett equation



Large numbers of reactions exist for which ΔH , ΔS plots are linear, but there also exist large numbers of reactions for which neither ΔH , ΔS nor ΔG , ΔH plots are linear. In practice, the range of temperature variation of ΔG that can be experimentally determined is only small and so predicted deviations from the equation are difficult or impossible to detect. Only for small temperature ranges can ΔH be assumed constant and, as the thermal capacity change ΔC_p ($\delta \Delta H / \delta T$) is not usually zero over large ranges, ΔH may vary producing slight curvature in the ΔG versus $1/T$ plots.

ii) Isoentropic relationship

ΔS is constant for a reaction series.

when $\delta_x \Delta S = 0$

$$\delta_x \Delta G = \delta_x \Delta H \quad 4.7$$

Here $\beta = \text{infinity}$ and it is termed the isoentropic relationship. A plot of $\log k$ (or $\log K$) versus $1/T$ for a reaction set produces lines that intersect at a point on the y-axis.

iii) Isoenthalpic relationship

ΔH is constant for a reaction series.

when $\delta_x \Delta H = 0$

$$\delta_x \Delta G = \delta_x \Delta S \quad 4.8$$

Here $\beta = 0$ and it is termed the isoenthalpic relationship. A plot of $\log k$ (or $\log K$) versus $1/T$ for a reaction set produces lines that are parallel.

The last two cases are seldom observed for reactions in solution.

1.4 Basic theory of colour

Visible light is that part of the electromagnetic spectrum with wavelengths in the range 380 - 750 nm. As with all other wavelengths of radiation in the electromagnetic spectrum, light has been described as having dual characteristics. That is, it exhibits the properties associated with both wave and particle theory.

In wave theory, radiation can be characterised by either its wavelength, λ , or its frequency, ν . The velocity of light is given by

$$c = \lambda \nu \qquad 4.9$$

where c = the velocity of the wave
 ν = the frequency of the wave
 λ = the wavelength of the wave

In particle theory, radiation can be characterised by the energy of a photon. The energy of a photon is given by the Einstein-Planck equation

$$E = h \nu \qquad 5.0$$

where E = the energy of the photon
 h = Planck's constant
 ν = the frequency of the radiation

When the radiation is spread fairly evenly over the visible region the sensation of white is seen, but white light may be split into several colours by the use of a prism or diffraction grating. Of most interest to colour chemists is the ability of certain species to selectively absorb wavelengths of visible radiation. Once a species has absorbed, and hence removed, radiation of a particular wavelength from the visible region, it is the remaining radiation that is transmitted or reflected and which is perceived as colour. The relationship between the colour of light absorbed and that seen is shown in Table 1.1.

Table 1.1

Table of complementary colours

Light absorbed		Complementary colour seen
Wavelength/nm	Colour	
400 - 435	Violet	Green-yellow
435 - 480	Blue	Yellow
480 - 490	Green-blue	Orange
490 - 500	Blue-green	Red
500 - 560	Green	Purple
560 - 580	Yellow-green	Violet
580 - 595	Yellow	Blue
595 - 605	Orange	Green-blue
605 - 750	Red	Blue-green

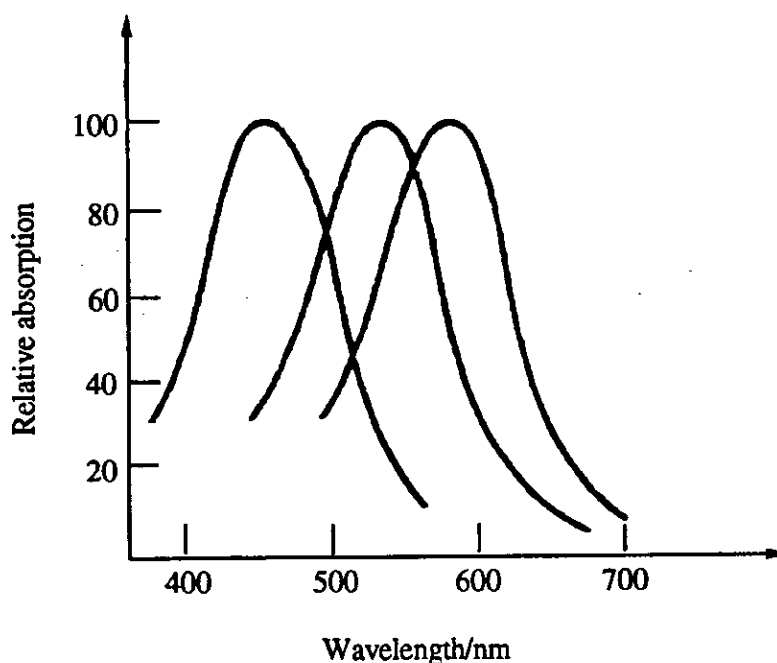
Mixing any of the complementary colours produces the sensation of white. The most familiar detector for visible radiation is the human eye. Colour is the result of a stimulus received by the eye and then interpreted by the brain. Within the eye, light falls upon the retina which contains two main type of structures: rods and cones.

Rods function under conditions of low intensity illumination and provide vision in shades of black, white and grey.

Cones function under conditions of high intensity illumination and are the colour sensitive receptors. There are three types of cones, each of which contains one of three light sensitive pigments. Each pigment has a particular spectral sensitivity and the colour of a particular stimulus is a ratio of activity of the three kinds of receptors. This is the component theory of colour (or trichromatic theory) which was first proposed by Young in 1802, refined by Helmholtz in 1852 and finally confirmed in the early 1960's with the development of microspectrophotometry (93MI1). The spectral response of each pigment is shown in Figure 1G.

Figure 1G

The absorption spectra of the classes of cones



When all three receptors are simultaneously stimulated, the colour white is registered as all responses to a specific colour in the brain are neutralised by each other. Mixing complementary colours produces the sensation of white because if, for example, the complementary colours blue (450 nm) and yellow (590 nm) are incident on the retina it can be seen, from Figure 1G, that all three receptors are stimulated and hence white is once again seen through neutralisation of individual responses in the brain (71MI1, 76MI1).

Non-spectral colours, for example brown, are a result of a fairly even spread of absorption over the entire spectrum and black results from complete absorption throughout the spectrum.

Not only is colour dependent on the species illuminated and the eye/brain perceiving the optical stimulus but also on the nature of the illuminating light. A blue species in monochromatic blue light would appear black due to the complete absorption of the incident radiation, resulting in zero reflection or transmission of any wavelengths of visible radiation. This apparent change in colour due to the nature of the illuminating light source is one form of dichroism.

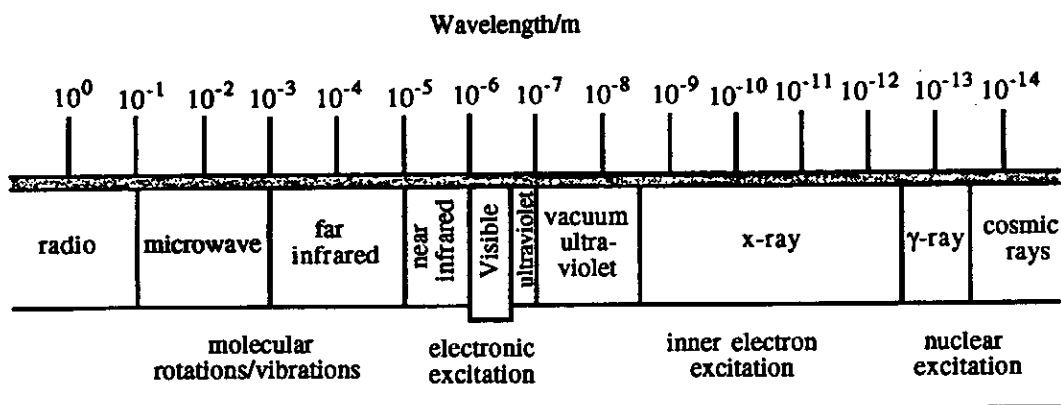
The colour of a species can also be affected by its physical form e.g. crystal form, lattice defects, particle size and shape, its refractive index and also the environmental conditions when it is viewed e.g. temperature, solvent or dispersing medium. Colour may also be characterised by its hue, strength or brightness.

1.5 Electronic absorption spectroscopy

The principle of quantum mechanics states that only discrete energy levels exist for an object and that there are well defined transition energies between the various states that an object can exhibit. For the purpose of this study, only the effects of the interaction between electromagnetic radiation and the object's electronic environment will be considered in any depth. In the absence of radiation, all the electrons in a molecule are in their lowest energy levels and the molecule is in its ground state. When radiation interacts with a molecule, only those wavelengths whose energies correspond exactly to the energy level differences in the molecule will be absorbed. Transitions of the components of the nucleus are of very high energy and so for nuclear excitation, γ -rays are required. For inner electrons bound in large atoms, high energy X-ray radiation is required. For the electronic excitation of molecules, energy in the visible and UV is required, whereas for molecular vibrations and rotations energy from the IR and microwave regions is sufficient. This is illustrated in Figure 1H.

Figure 1H

The wavelength and type of electromagnetic radiation



Materials which exhibit colour have transition energies between electronic levels of no less than ≈ 1.7 eV (750 nm) and no more than ≈ 3.2 eV (380 nm), that is, they absorb radiation in the visible region of the electromagnetic spectrum. Vibrational and rotational energy levels are superimposed on the electronic levels in a molecule and photons on either side of the principle absorption band are also absorbed, producing the familiar broad absorption bands that are observed in UV and visible spectra. Several processes in materials produce colour by selective absorption. These are:

- 1) Transitions in conjugated organic compounds
- 2) Intermolecular charge transfer transitions
- 3) Intramolecular charge transfer transitions
- 4) Crystal field transitions
- 5) Band transitions

Only the transitions in conjugated organic compounds will be discussed in detail in this study. UV and visible spectra are measured using automatic spectrophotometers that produce a spectrum of the amount of radiation absorbed as a function of the wavelength, λ , or wavenumber, $\nu = 1/\lambda$, of the incident radiation.

Transition energies may be quoted in any one of several ways. In SI units, the kilojoule per mole (kJ mol^{-1}) is used and is, in fact, the energy possessed by one 'mole' of photons. In quantum mechanics, another term is used to quantify the transition energies, the eV, where $1 \text{ eV} = 96.55 \text{ kJ mol}^{-1}$.

If we consider a beam of light of intensity, I , passing through a thickness, dL , of a solution of molar concentration, c , then the reduction in intensity due to absorption will be

$$-dI/I = k c dL \quad 5.1$$

where k is a constant

For a cell of thickness, L , the reduction in intensity will be given by the integration of equation 5.1

$$-\ln I = k c L + \text{constant} \quad 5.2$$

when $L = 0$, $I = I_0$ then

$$-\ln I = k c l - \ln I_0 \quad 5.3$$

or

$$\ln I_0/I = k c l \quad 5.4$$

When c is expressed in mol dm^{-3} and L in cm , k is known as the molar absorptivity or molar extinction coefficient, ϵ , and the familiar Beer-Lambert equation, 5.5, is obtained

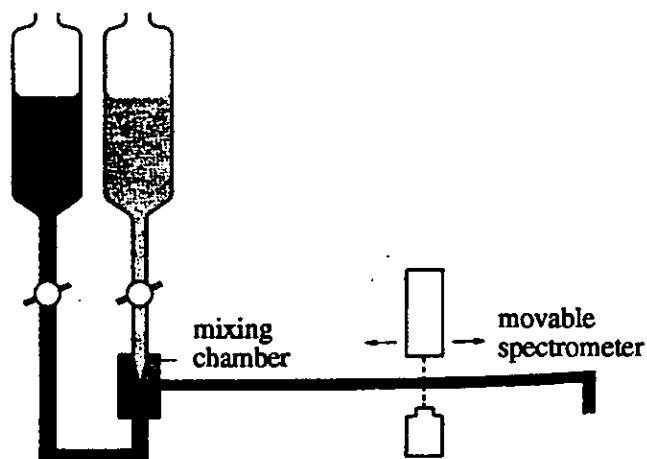
$$\ln I_0/I = \epsilon c L \quad 5.5$$

ϵ is a measure of the intensity of absorption of radiation of a particular wavelength by the solute. The term, $\log I_0/I$, is equivalent to the absorbance and for a solute to obey Beer's Law a plot of absorbance against concentration should be linear.

The rate of hydrolysis of TPM/DPM dyes is followed by monitoring the rate of decolourisation of a solution of the dye. The conventional method for the spectrophotometric determination of rate constants involves mixing the reactants, filling the cell and bringing the cell contents to the correct temperature. This is only practical for reactions with half-life times of the order of minutes. For reactions with half-life times of 60s or less, two other techniques are available: the constant-flow method and the stopped-flow method. In the constant-flow method, the reactants are thoroughly mixed as they flow along a tube. Observing the absorption at various positions along the tube is equivalent to measuring the absorption at different time intervals after mixing. The major drawback with this method is that large volumes of reactants are required.

Figure 1I

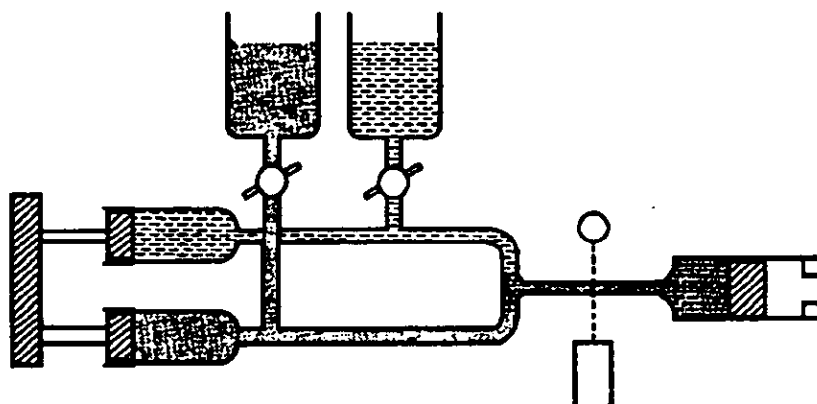
Apparatus used in the constant-flow technique



The stopped-flow method involves mixing the reactants thoroughly and injecting them into a cell. The cell is fitted with a plunger that moves as the cell fills. The flow into the cell is halted when the plunger reaches a pre-determined stop position. The reaction then continues in the cell and is monitored as a function of time. For this method, only small volumes of reactants are required.

Figure 1J

Apparatus used in the stopped-flow technique



1.6 Colour and constitution

From the earliest days of dyes and pigments, researchers and workers in the field of colour chemistry have tried to rationalise, both quantitatively and qualitatively, the relationship between colour and constitution. There will now follow a brief review of some of these treatments, as applicable to TPM/DPM dyes (69MI1, 71MI1, 76MI1, 90MI1, 91MI1).

1.6.1 Early colour theories

The first real attempt to rationalise colour and constitution was conducted by Witt (1876BER522), who developed the idea of Graebe and Liebermann (1868BER106) - that organic dyes became colourless on reduction and hence that there is a link between colour and unsaturation - by stating that the colour of organic dyes is associated with the presence of certain unsaturated groups of atoms, for example, azo, ethylene, carbonyl and nitroso groups, which he called chromophores. Witt called species containing these groups chromogens. It was also observed that the presence of basic or weakly acidic groups intensified the colour of the chromogens. These groups were called auxochromes.

The next major development was by Armstrong (1888PCS27), who proposed that the presence of a quinonoid structure in the organic species was essential if the compound was to be a dye.

It was not until some time later that it was realised that auxochromes were electron donors, or groups with a non-bonding pair of electrons, which could conjugate with any aromatic group present in the chromogen, if spatial constrictions allowed. As the area of colour chemistry developed, specific terminology was introduced to convey ideas and information. As a result, certain phrases are now well established in the field of colour chemistry. Some common examples are:

Bathochromic shift - the displacement of an absorption band to longer wavelengths

Hypsochromic shift - the displacement of an absorption band to shorter wavelengths

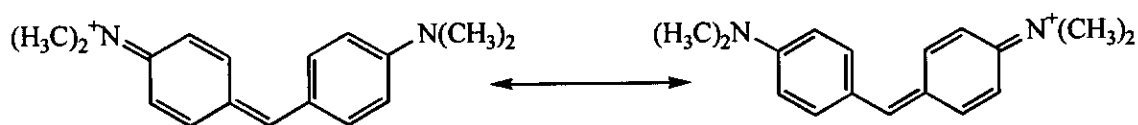
Hyperchromic effect - an increase in the intensity of an absorption band

Hypochromic effect - a decrease in the intensity of an absorption band

1.6.2 Valence bond theory

Before the developments of quantum theory, molecules that absorbed in the visible region of the spectrum were considered to exist as resonance forms of the parent molecule; colour was a result of the energy difference between the resonance forms that the molecule displayed. These resonance forms were the classical or Kekulé structures predicted for the molecule. This was the principle of the resonance theory. As quantum mechanics developed, its influence on resonance theory produced the valence bond theory. In this theory, the molecule was considered to exist as resonance hybrids of the parent molecule, and that the wave functions of the hybrids combined to produce new molecular wave functions of different energy. Albeit incorrectly, it was often the case that only the low energy hybrids were considered. The lowest energy molecular wave function was considered to be the ground state of the molecule and the higher molecular wave functions to be the first excited state. The energy difference between the two wave functions was then the energy of the first absorption band of the molecule. For a chromogen such as MHB, the resonance forms that were predicted to exist are shown in Figure 1K.

Figure 1K
Postulated resonance forms of MHB



Each resonance form is of equal energy, leading to degenerate atomic wave functions. The resulting molecular wave function energy difference, ΔE_1 , would produce an absorption band at a particular wavelength in the visible region of the electromagnetic spectrum. If one of the terminal amino groups of MHB was replaced by a different group this would alter the molecular wave function energy levels and produce a new absorption band. For example, if one of the terminal amino groups in MHB was replaced by a methoxy group, one of the resulting resonance hybrids would be of higher

energy than the other; the oxygen atom of the methoxy group would not bear the positive charge as well as the nitrogen atom of the remaining amino group. This would create non-degenerate atomic wave functions, resulting in an increased splitting of the molecular wave functions, ΔE_2 , relative to that in MHB. As $\Delta E_2 > \Delta E_1$, greater energy would be required for the transition from the ground state to the first excited state. Therefore, valence bond theory would predict a hypsochromic shift of the absorption band when one of the terminal amino groups of MHB is replaced by a methoxy group.

The valence bond theory, with its weak theoretical foundations, is essentially a qualitative, semi-intuitive technique for the prediction of absorption bands. As such, in recent times, it has been superseded by other, more quantitative techniques. Despite this, however, the valence bond theory is surprisingly successful at the prediction of the wavelengths of absorption bands.

1.6.3 Molecular orbital models

Equation 7.1 is the Schrödinger equation.

$$\mathbf{H}\Psi_i = E_i\Psi_i \quad 5.6$$

where

H is the Hamiltonian operator which is a function of the momenta and co-ordinates of all the particles in the system

E is the energy of the possible states of the system

Ψ is the wave function describing each of the possible states of the system

If it was possible to calculate the solutions to the Schrödinger wave equation for a molecule, then the energies of all the possible electronic transitions for that molecule would be known, but this has only been possible for the simplest systems. To compensate for the complexity of the solutions to the Schrödinger wave equation, approximations are introduced, which limit the parameters of the treatment.

When considering electronic excitation only, the vibrational motion of the particles in the atom is ignored and the wave function of the system corresponds to a function of the co-ordinates of the electrons only. This electronic wave function can be represented by a

series of simpler wave functions, each of which describes the behaviour of one electron only. These simpler wave functions are the atomic orbitals from which the molecular orbitals are created.

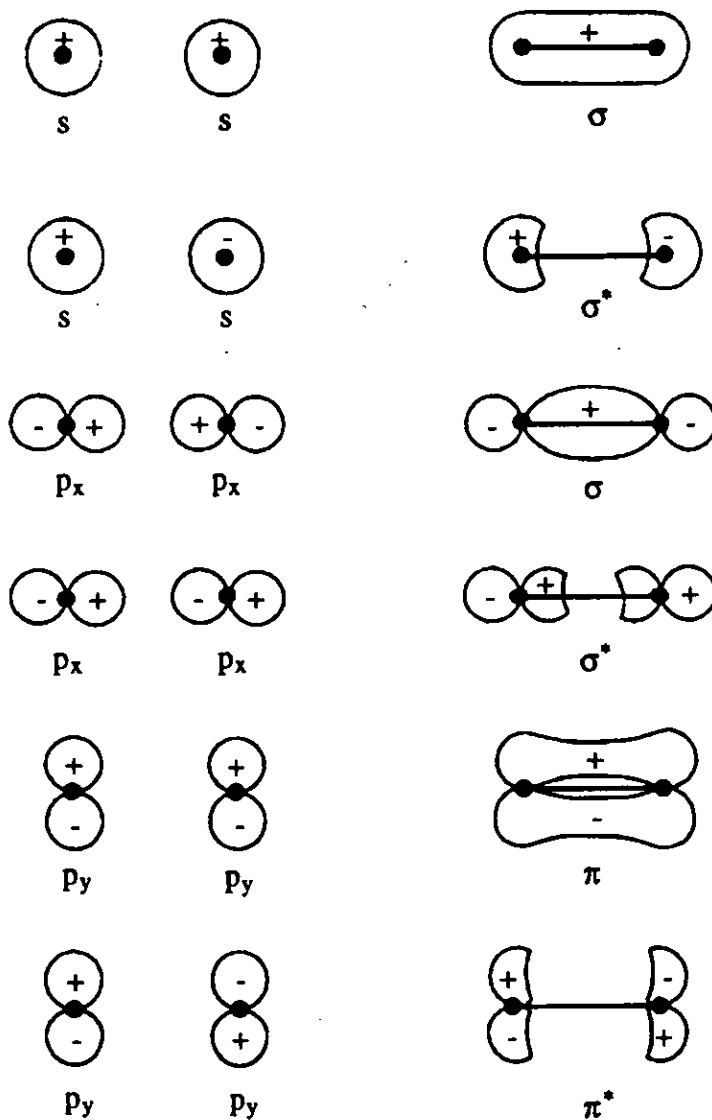
Molecular orbitals (molecular wave functions) are generated by the overlap of two or more atomic orbitals (atomic wave functions). The type of molecular orbital (MO) created depends on the nature of the overlap of the atomic orbitals (AO's). For simplicity, only the linear combination of atomic orbitals (LCAO) is considered.

Because the orbitals are wave functions, they have the property of phase which is given a symbol either + or -. If the overlapping atomic wave functions are in phase (either ++ or --), the resulting molecular wave function is reinforced, and the MO is termed bonding. However, if the overlapping atomic wave functions are out of phase (+-), the resulting molecular wave function is cancelled and the MO is termed anti-bonding (the * superscript denotes an anti-bonding orbital).

The nature of the overlap of AOs is determined by their relative orientation to each other. The overlap of s orbitals can only be end on to produce a σ bond. As a result of this direct overlap, the σ bond is a strong, low energy bond. However, p orbitals can take part in end on overlap to produce a σ bond but because of their directional properties they can also take part in sideways overlap to produce a π bond. The combination of wave function phase and orientation of AO overlap produces the types of MOs commonly postulated in modern chemistry. These MOs are shown in Figure 1L. The p_z orbitals will be perpendicular to the plane of the paper.

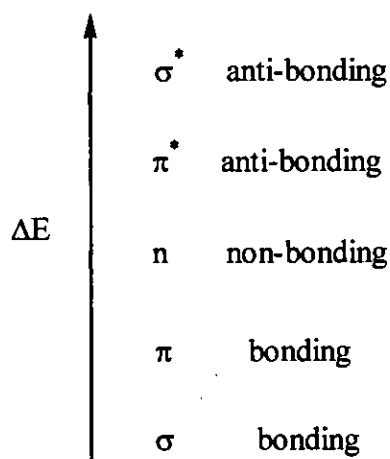
Figure 1L

Molecular and atomic orbitals



MOs generally have the following order of energy, $\sigma^* > \pi^* > \pi > \sigma$. Electrons are fed into the MOs in order of increasing energy. Each MO can accommodate two electrons of opposite spin, in accord with the Pauli exclusion principle.

There are three types of valence electrons that give rise to electronic transitions in organic molecules. These are those associated with σ bonds, π bonds and non-bonded (n) electrons associated with heteroatoms. The relative energies of these valence electrons are



Once a ground state molecule absorbs a photon of energy, an electron is promoted into a higher energy orbital, producing an excited state. There are rules relating to the type of electronic transition that can occur and transitions are described as being spin allowed or spin forbidden. For spin allowed transitions, the spin multiplicity of the ground state and excited state must be the same. Spin forbidden transitions occur where there is a change in the multiplicity of the atom in going from the ground state to an excited state. As electrons of like spin tend to avoid occupying the same region of space, triplet states are of a slightly lower energy than singlet states because of the absence of any repulsive forces. Spin forbidden transitions occur far less frequently than spin allowed transitions and as a result only produce very weak absorption bands.

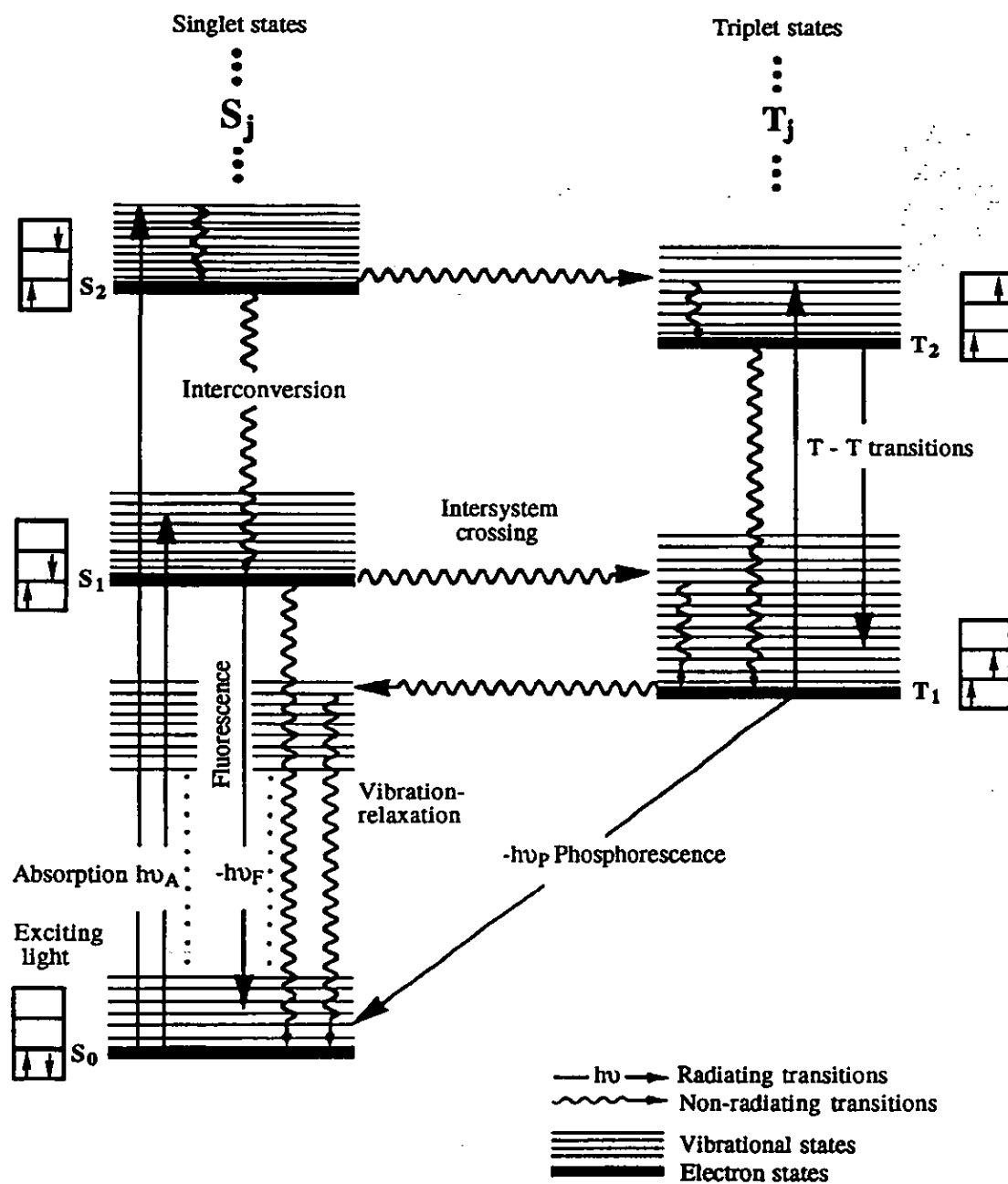
Once an electron has been electronically excited, the energy it has gained can be lost in one or more of the following ways.

- 1) Radiationless transitions, where the excess energy is lost either by thermal degradation *via* vibration or rotation (known as internal conversion) or by a change in multiplicity of the atom (known as intersystem crossing).
- 2) Radiative decay, where the excess energy is lost by the emission of a photon of radiation. Fluorescence is the radiation emitted by a spin allowed process i.e. no change in the multiplicity of the atom. Phosphorescence is the radiation emitted by a spin forbidden process.
- 3) Photochemical reactions, where the excess energy is lost *via* a chemical reaction. Photochemical reactions, in general, only occur for triplet states which have lifetimes

sufficiently long enough (100 ns - 10 s) to allow a reaction to proceed. Singlet states, on the other hand, tend to be very short lived states (1 - 100 ns), which are too short to enable chemical reactions to occur.

These processes are summarised in Figure 1M which is known as a Jablonski diagram.

Figure 1M
A Jablonski scheme



The difference in energy between the electronic transitions occurring in the species determines the energy of the photons required for the transitions and therefore at what wavelength radiation from the electromagnetic spectrum is absorbed.

Saturated molecules can only undergo $\sigma \rightarrow \sigma^*$ transitions. This is the highest energy transition and requires large excitation energies; these transitions generally occur in the far UV region. Non-bonded electrons are less tightly held and so require lower excitation energies. The $n \rightarrow \pi^*$ and $\pi \rightarrow n$ transitions generally occur in the visible region. $\pi \rightarrow \pi^*$ transitions are intermediate in excitation energy terms to $\sigma \rightarrow \sigma^*$ and $n \rightarrow \pi^*$ transitions and generally occur in the near UV and visible regions. The lowest energy band in an absorption spectrum is usually a result of the transition of an electron from the highest occupied MO (HOMO) to the lowest unoccupied MO (LUMO).

1.6.4 The Free-Electron Molecular Orbital method

The Free-Electron Molecular Orbital (FEMO) method is probably the simplest molecular orbital treatment for the calculation of transition energies for conjugated molecules. The fundamental approximation in the FEMO method is that the σ and π electrons can be considered independent of each other. Interelectronic repulsion energies between electrons are also negated. For a planar molecule possessing several conjugated double bonds, the π orbitals will extend over the entire molecular framework and any π electrons present will therefore be delocalised over the whole system. The energies of the π orbitals present in the molecule can then be calculated by considering the motion of one electron in each orbital only, and a total for the system can be obtained by feeding in the necessary number of electrons into each π orbital system. The energy of each electron is the potential energy of that electron due to the attractive forces of the positive nuclear centre of the molecule. This potential energy representation is simplified by assuming that the potential energy over the length of the molecule is arbitrarily zero, being infinite at the end of the molecule to effectively keep the motion of the electron within the framework of the system. The situation is now analogous to the quantum mechanical model of a particle in a box. As such, the motion of the electron within the molecule can be described as a wave that has nodes at each end of the molecule. There must therefore be an integral number of half wavelengths within the system to describe the motion of the electron. The wavelength of the wave describing the motion of the electron across the molecule is given by the de Broglie relationship (equation 5.7).

$$\lambda = h / mv \quad 5.7$$

where λ is the wavelength of the wave

h is Planck's constant

m is the mass of an electron

v is the velocity of an electron

The stationary states then set up can be described as standing waves, mathematically, by

$$L = n\lambda / 2 \quad 5.8$$

where L is the length of the box (system)

n is an integer

Combining equations 5.7 and 5.8 to calculate the velocity of the electron gives

$$v = nh / 2mL \quad 5.9$$

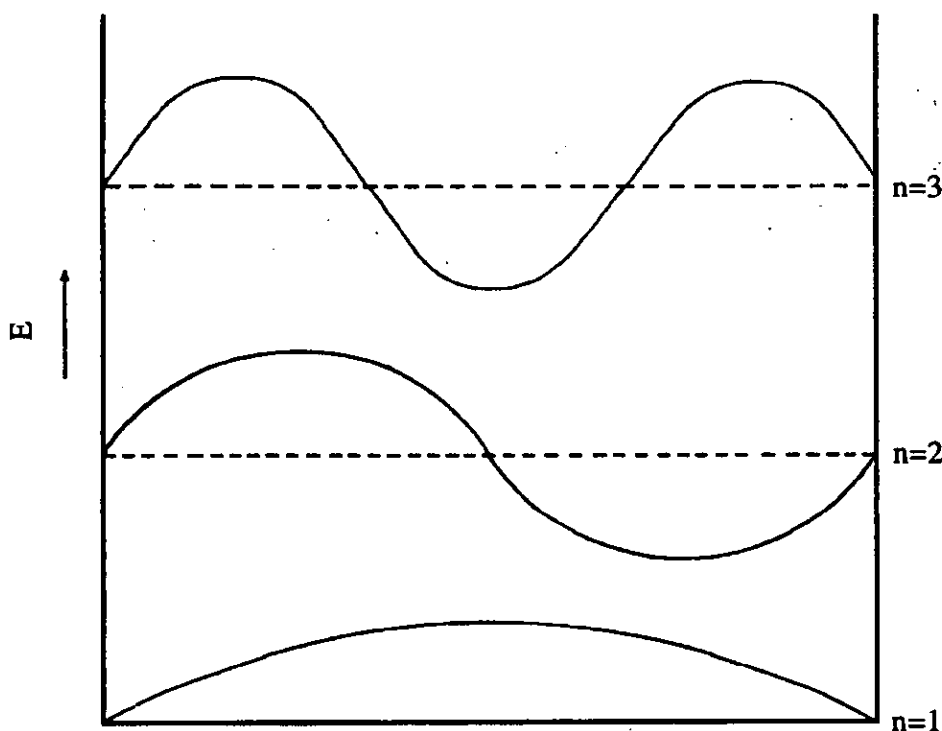
The total energy of the electron is the sum of its kinetic energy and potential energy, which will be equal to the energy of the orbital the electron occupies. As the potential energy is arbitrarily zero, the situation simplifies to consideration of the electron's kinetic energy only.

$$E_n = mv^2 / 2 = n^2 h^2 / 8mL^2 \quad 6.0$$

where E_n is the energy of the MO

The energy of the MOs increases with increasing n as does the number of nodes in the system as shown in Figure 1N.

Figure 1N
FEMO wave functions for a linear, conjugated molecule



The value of L is usually equated to the length of the molecule plus one additional bond at each end of the molecule. For cyclic conjugated systems, the diameter of the ring is equated to the length of the molecule. For more complex π systems, modified FEMO treatments are used involving two- and three-dimensional models, resulting in more complex computations. As a method of transition energy calculation, considering the assumptions made, the FEMO method is reasonably accurate, and has been reasonably successful for the calculation of absorption maxima for a range of cyanine dyes (60JCS3812). However, other later MO treatments do take into account electron-electron interactions and so have superseded the FEMO method as a predictive technique.

1.6.5 The Hückel Molecular orbital method

The Hückel molecular orbital method (HMO), like the FEMO method, assumes σ and π electrons can be treated independently and that electronic interactions can be ignored. Unlike the FEMO method, the HMO method uses the LCAO procedure to calculate the one electron orbital function and energies. The assumption is that the molecular orbital wave function is the sum of the individual atomic orbital wave functions. Thus, for a system of n overlapping p orbitals, the MO wave function can be written as

$$\psi = c_1\Phi_1 + c_2\Phi_2 + \dots + c_n\Phi_n \quad 6.1$$

where ψ is the MO wave function

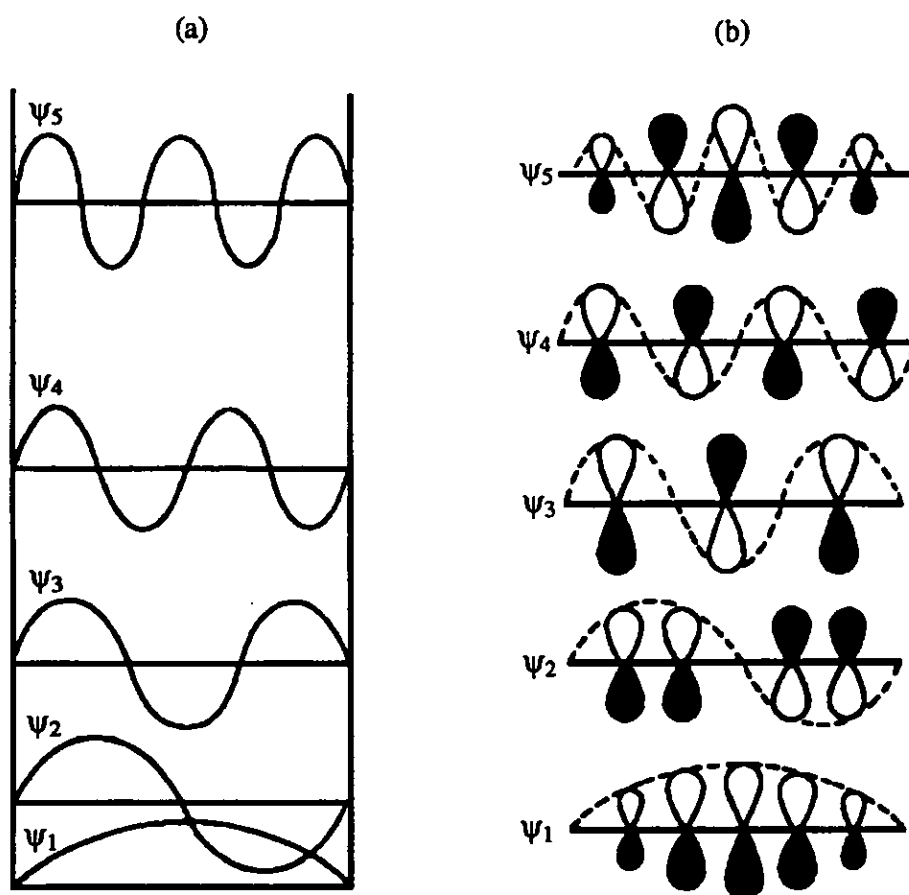
Φ is the AO wave function

c is the mixing coefficient

The mixing coefficients, c_n , are a measure of the contributions of each AO to the MO, and have values between ± 1 . A positive coefficient represents an in-phase overlap of AOs and a negative coefficient represents an out-of-phase overlap of AOs. The energy of an atom is equated to the total orbital energy of its electrons, that is, the sum of the energy possessed by each electron by virtue of its occupancy of a particular orbital. Instead of solving the Schrödinger wave equation, an approximation is made that, if an equation relating to the energy of the system contains adjustable parameters, the best solution for the energy term is that with the parameters adjusted so as to produce the lowest value for the energy. This is known as the variation method. Combining equations 5.6 and 6.1 and integrating over space produces an equation relating the energy of the system to the AO wave functions, the LCAO mixing coefficients and the dynamic operator, H . It can then be shown that the energy of the system is defined by a series of integral equations, known as secular equations, that relate the energy of the system to the degree of overlap of AOs (overlap integrals), the energy of the electron when it occupies a particular AO (Coulomb integral, α) and also to the energy of the electron when it occupies the region of overlap between two AOs (resonance integral, β). The overlap integrals are then equated to zero, to simplify the treatment, since their influence on the solution to the problem is negligible. All integrals are assumed to be of equal value for each atom. The secular equations can then be simplified further,

producing an energy equation in terms of α and β only. α and β are empirical parameters and are not derived mathematically. The MOs can be described in terms of the mixing coefficients and the atomic wave functions both mathematically and diagrammatically (Figure 10). The similarity with the molecular wave function profile derived using the FEMO method can be seen.

Figure 10
 π MOs for a linear, conjugated molecule in (a) the FEMO model and
(b) the HMO model



Values for the bond order of a given bond can also be derived, with some degree of accuracy, using the HMO treatment. The stabilisation obtained by delocalisation in conjugated hydrocarbons can also be determined. This extra stability is known as the

resonance energy of the molecule. The energy for an electronic transition can be obtained as the energy difference between the two orbitals under study. As a result of the assumptions made in the HMO method it has many limitations, but it has been successfully applied to symmetrical cyanines (50JCS2329).

The HMO method was principally derived for application to hydrocarbons, where the assumptions that all the Coulomb integrals and resonance integrals are equivalent has some justification. However, this is clearly not the case for systems containing heteroatoms, and a modified α term must be implemented. This can only be done once the original α term has been used to calculate electron densities. These electron densities are then used to determine the modified α terms. New modified α terms are then calculated until a consistent set of values is obtained. This technique is known as self-consistency and allows the HMO method to be applied to heteroatom bearing systems.

1.6.6 The Pariser-Parr-Pople molecular orbital method

The Pariser-Parr-Pople molecular orbital (PPP-MO) method is, to date, the most successful treatment for the calculation of the transition energies of dyes. It was developed independently by Pariser and Parr (53JCP466) and Pople (53TFS1375) and supersedes other treatments, such as the FEMO and HMO methods, because, although it still considers σ and π electrons to be independent of each other, it does take into account interelectronic repulsion effects. The treatment can analyse systems containing heteroatoms, singlet and triplet states can be differentiated and, because molecular geometry is considered, *cis*- and *trans*-isomers can be distinguished.

The PPP-MO method uses the LCAO approach to obtain a series of secular equations, as in the HMO method, but with the PPP-MO method, the α and β terms are not considered equivalent with other α and β terms. The α and β terms now take into account interelectronic repulsion effects and the extent of electron occupation in the π orbitals of the molecule. Taking these α and β integrals, equations can be derived whereby if the interatomic distances, bond angles, valence state ionisation potentials, electron affinities of all atoms, the sum of the attractive forces on the electron by virtue of its position relative to the positive nuclear structure of the molecule, all π electron densities and π bond orders are known, then the transition energy for any given transition can be derived.

The PPP-MO method is another example of a self-consistent field technique, whereby an initial calculation is carried out to obtain α and β terms, which are then modified by repeated calculations until consistent values are obtained.

This method has proved to be valuable in the calculation and interpretation of the visible spectra of many dyes (86CIB997). The calculations involved in a PPP-MO treatment of a dye are ideally suited to computers, making the PPP-MO method routinely applicable to many systems.

1.6.7 Configuration interaction

The PPP-MO method considers closed-shell systems, that is, systems in which the lower π orbitals are doubly occupied. For open-shell systems, that is, excited states, the PPP-MO method is not as successful as it is for the ground state molecule. An excited electron, $\pi \rightarrow \pi^*$ transition, experiences interactions that are not considered by the PPP-MO method or any other closed-shell system method.

In configuration interaction (CI), it is approximated that the electronic configuration of any state can be represented as a series of one-electron MO wave functions, and that the total wave function of a particular electronic configuration is the sum of the products of individually occupied MO wave functions. Secular equations can once again be derived using the Schrödinger equation and the LCAO treatment of MO wave functions. This CI treatment leads to improved electronic transition energy values. The main drawback for a CI treatment is the number of possible excited states that can exist from a set of MO wave functions. This situation is made slightly simpler because firstly, singlet and triplet configurations, on the whole, do not interact and secondly, the interaction between configurations is at a minimum when the energy separation between the configurations is large. This reduces the interactions to be considered because any singly excited configurations will not be affected by any doubly or triply excited configurations. For electronic calculations, only singly excited configurations need be considered. As a result, CI has been successful at predicting transition energies in systems for which other treatments have proved less than adequate.

More involved treatments have been developed to aid the characterisation of transition energies. These include treatments such as the extended HMO (EHMO) method (62JCP2179, 62JCP2872, 62JCP3489, 63JCP1397). $\pi \rightarrow \pi^*$ transitions are influenced by

the proximity of σ electrons and may also be affected by $\sigma \rightarrow \sigma^*$ transitions. In taking these influences into account, other treatments have been developed. These 'all valence electron' methods include the complete neglect of differential overlap (CNDO) method (66JCP3289), the partial neglect of differential overlap (PNDO) (67JA3089), the intermediate neglect of differential overlap (INDO) (67MP83) and the modified INDO (MINDO) (69JCP1262, 70JA590, 75JA1285). All these methods are more sophisticated than the PPP-MO method, requiring more involved computations which result in them only being applied to large molecular systems, where simpler treatments provide less than adequate results.

1.6.8 The perturbational molecular orbital theory

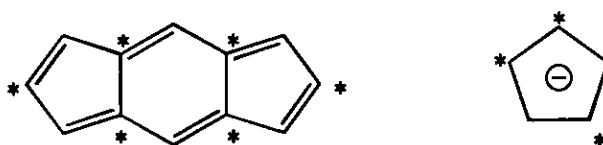
The HMO method was originally devised for unsaturated hydrocarbons for which, in the HMO treatment, there are two theoretically distinct types: the alternant hydrocarbons (AH) which contain open chains with an odd or even number of carbon atoms and/or rings containing an even number of carbon atoms and the non-alternant (NAH) hydrocarbons which contain at least one ring possessing an odd number of carbon atoms. To characterise a hydrocarbon by this treatment, the complete molecular structure is drawn out and alternate atoms are starred, always ensuring the maximum number of starred atoms. If two adjacent atoms are of the same type, starred or unstarred, the molecule is considered to be a non-alternant system. Examples are shown in Figure 1P.

Figure 1P

Some examples of alternant and non-alternant systems



Alternant systems



Non-alternant systems

AH with an even number of atoms will have an even number of MOs and so orbital pairing will occur; there will be a symmetrical distribution of orbital energy about the non-bonding level, α .

Paired orbitals have LCAO mixing coefficients of the same magnitude but not necessarily the same sign. At unstarred positions, the LCAO mixing coefficients are zero. Each atom in an uncharged AH has a π electron density of unity, which is why the HMO method applies so well to these cases. The assumption in the HMO method that all the Coulomb integrals, α , are equivalent is then applicable. However, in charged AHs (anionic or cationic) and neutral NAHs the π electron density for each atom is not equivalent and so the HMO method does not apply to these cases. NAH do not display orbital pairing. For AH with an odd number of atoms, if orbital pairing occurs there will be an extra, unpaired orbital remaining; this orbital is described as a non-bonding MO (NBMO), whose energy is given as α and which lies at the line of symmetry about which the paired orbitals are resolved. In AH systems, there will be a NBMO for every starred position in excess of unstarred positions. As a result, some systems may have several

NBMOs. The π bond orders of NBMOs are zero since they have neither bonding nor anti-bonding properties.

The perturbational molecular orbital (PMO) theory is an extension of the HMO method, whereby the energy difference between two states under investigation can be readily calculated (50JCP265, 50JCP275, 50JCP283, 52JA3341, 52JA3345, 52JA3350, 52JA3353, 52JA3357). Firstly, the chromogen under investigation is related to the corresponding iso- π -electronic hydrocarbon by substituting any heteroatoms present with carbon atoms. If the system is AH, then PMO theory can be applied. The perturbations are then the various structural changes that must be applied to the hydrocarbon in order to generate the chromogen. These perturbations can then be related to the absorption spectrum of the chromogen by implementing the following characteristics of AHs.

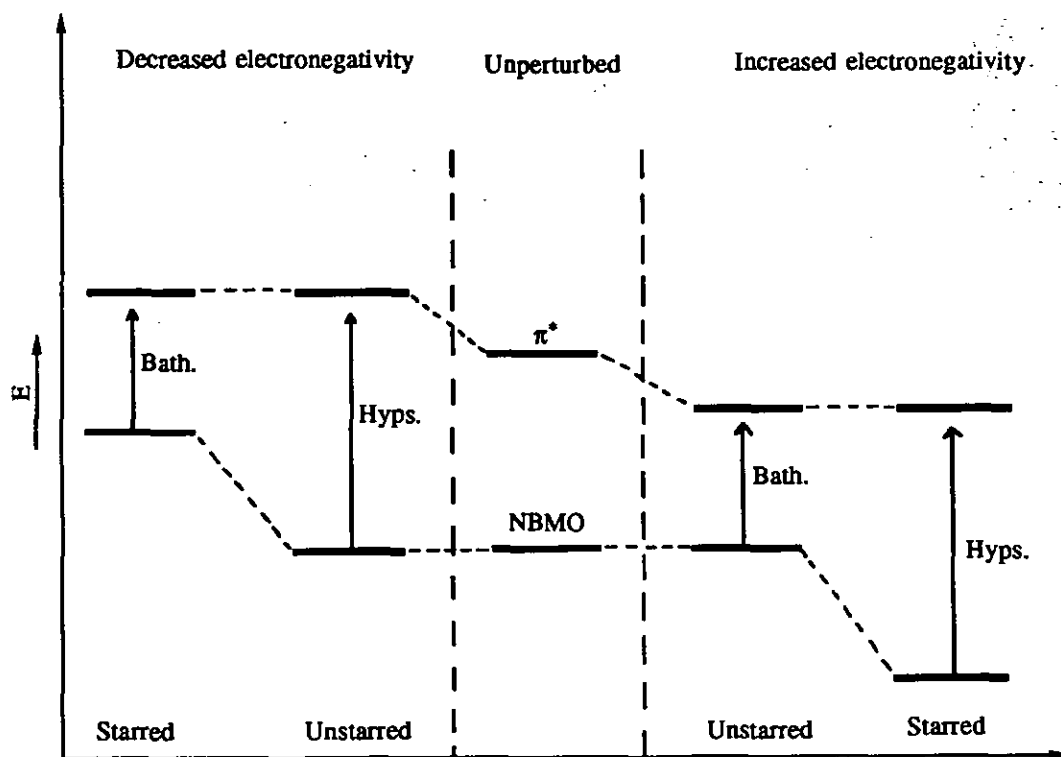
- 1) In even alternants, the first absorption band corresponds to a transition between the HOMO and the LUMO.
- 2) In odd alternants, the first absorption band corresponds to a transition between the NBMO and the LUMO.

In an even alternant system, PMO predicts that any change in the electronegativity of a position in the system will have a minimal effect on the position of the first absorption band in the spectrum of that compound.

This is not the case for an odd alternant system, where the effect on the position of the first absorption band in the spectrum of the compound depends on the nature of the group introduced and the position at which it is introduced into the chromogen. At an unstarred position, the NBMO's coefficient is zero and, as a result, its energy is unaffected by a change in the electron density of its environment. However, the LUMO will be affected and the degree to which its energy is altered determines whether an electronic transition is hypsochromic or bathochromic relative to the unsubstituted molecule. For NBMOs at a starred position, the change in electronic density of its environment will affect the energy of the orbital and to a greater degree than for the LUMO. The extent of the effect will once again determine whether an electronic transition is hypsochromic or bathochromic relative to the unsubstituted molecule. This is illustrated in Figure 1Q.

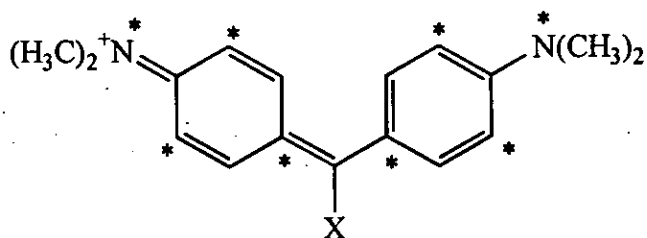
Figure 1Q

The effect on the energies of the orbitals and the first electronic transition
by replacing a carbon atom of an odd-alternant with an atom of differing
electronegativity

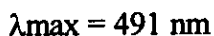
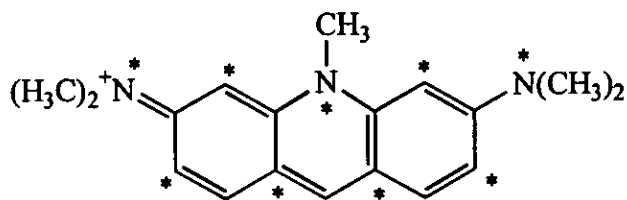
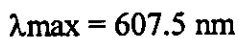
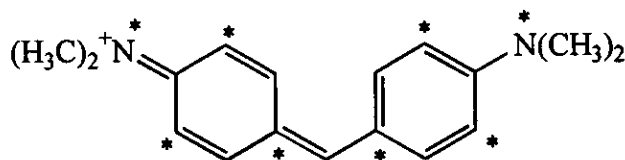


General rules enable the effect on the position of the first absorption band of introducing a group into a chromogen relative to the unsubstituted compound to be predicted.

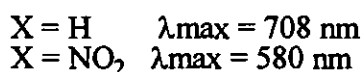
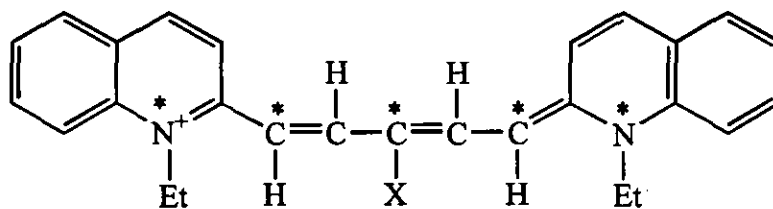
- 1) Attaching an electron withdrawing substituent at an unstarred position produces a bathochromic shift in the first absorption band relative to the unsubstituted molecule.



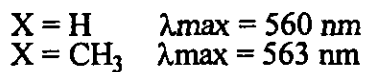
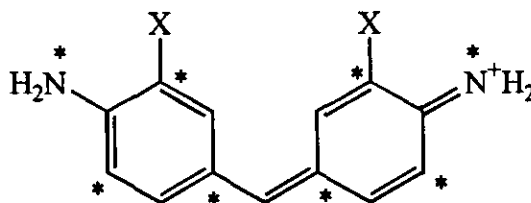
- 2) Attaching an electron donating substituent at an unstarred position produces a hypsochromic shift of the first absorption band relative to the unsubstituted molecule.



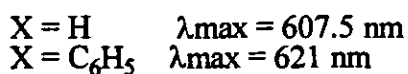
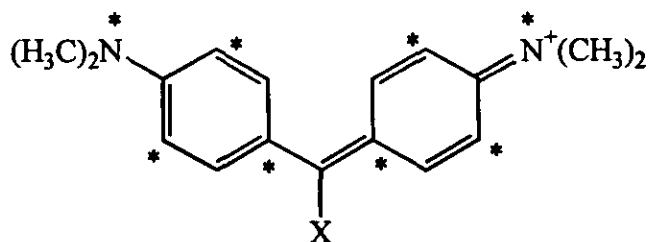
- 3) Attaching an electron withdrawing substituent at a starred position produces a hypsochromic shift of the first absorption band relative to the unsubstituted molecule.



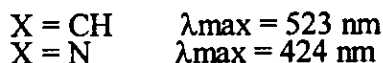
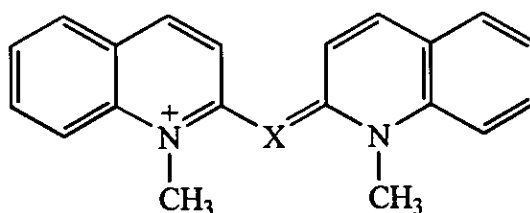
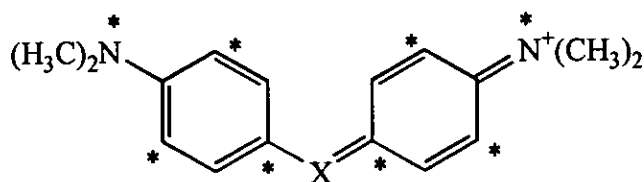
- 4) Attaching an electron donating substituent at a starred position produces a bathochromic shift of the first transition band relative to the unsubstituted molecule.



- 5) If the conjugation of a system is extended by the introduction of a neutral unsaturated group, a bathochromic shift of the first absorption band is produced and this is irrespective of the point of attachment.



- 6) Replacing a carbon atom with a more electronegative heteroatom has the same effect as attaching an electron withdrawing substituent at that position.



TPM dyes deviate from these rules. In the case of TPM dyes, an even alternant side chain is attached to an unstarred position of the parent odd alternant chromogen. Substituents in the even alternant side chain must always be considered as attached to an unstarred position. Since the side chain is a phenyl ring, the 2-, 3- and 4-positions are all considered to be inactive.

1.6.9 The Hammett equation

The foundations and principles behind the Hammett equation have already been discussed and it is therefore unnecessary to include such a treatment here. By analogy to the change in the rate of a side chain reaction or equilibrium of a benzene derivative as a result of the electronic properties of a substituent on the benzene ring, the change in the wavelength of the absorption maxima of a chromogen can be related to the electronic properties of a substituent on a neutral benzene ring attached to the chromogen. If a

substituted benzene ring is attached to a chromogen, then provided that neither the benzene ring nor the substituent is involved with the electronic excitation process, the substituent will effect the position of the absorption maxima of the chromogen as a result of its electron donating/withdrawing properties. The influence of the substituent will cause a change in electron density at the point of attachment of the substituted benzene ring with the chromogen that is then transmitted over the entire molecular framework. The modified electron density will result in modified orbital energies which will result in modified transition energies.

The ability of a substituent to act as an electron donor/acceptor is reflected in its Hammett substituent constant, σ . Correlation between the transition energy of an electronic excitation process and the Hammett σ constant of a substituent is summarised in equation 6.2.

$$\Delta\nu = \nu_x - \nu_h = \rho \sigma_x \quad 6.2$$

where ν_x is the absorption frequency of the substituted chromogen

ν_h is the absorption frequency of the unsubstituted chromogen

σ_x is the Hammett substituent constant for substituent x

ρ is a measure of the sensitivity of an absorption band to substituent effects

If ρ is positive, then the absorption band is displaced to longer wavelengths with an increase in the electron donating strength of the substituent. For MG, the central carbon atom is an unstarred position and therefore any carbon atoms in the phenyl ring attached at this point cannot be classed as active or inactive because the π electron density in the phenyl ring is uniform and the NBMO coefficient at each position is zero. Therefore, a substituent placed at any of these positions will not modify the energy of the NBMO. Thus, only the energy of the π^* MO is altered. This allows a relationship between the response of the x-band to substitution in the phenyl ring and the appropriate Hammett substituent constant to be established. A linear correlation between first absorption bands and Hammett substituent constants has been established for 3- and 4-substituted MGs (61JCS1285, 71JSDC187, 77JSDC451, 82JSDC10). Such correlations exist because only electronic effects need be considered. Strongly conjugating groups, such as OH and OCH₃, deviate from this relationship (61JCS1285). For 2-substituted TPM dyes there

will be a significant steric influence, which results in a loss of the qualitative relationship between absorption band position and electronic properties of a substituent (71JSDC187, 77JSDC451, 82JSDC10).

1.7 Electronic absorption spectra of TPM/DPM dyes

1.7.1 Introduction

The interpretation of electronic absorption spectra for the rationalisation of organic structures has been an accepted practice in chemistry for many years. When the organic molecule to be studied is a highly coloured organic dye that, by definition, absorbs strongly in the visible region of the electromagnetic spectrum, then the spectra can provide valuable information on the structure of the dye. In fact, the consequences of structural modifications to a dye may be visually perceptible.

It was first suggested by Lewis and Calvin (39CR273) that a planar or nearly planar TPM dye molecule should exhibit two separate absorption bands. These two bands arise as a result of polarisation along the two mutually perpendicular x and y axes of the molecule. Unsymmetrical dyes display both bands, but symmetrical dyes display only one band. Studies have shown that there is also a contribution to the absorption bands from polarisation along the third, z, axis of the molecule (79BCJ2244, 80JPC1361).

The first band - the x-band - corresponds to the electronic excitation from the $n \rightarrow \pi^*$ transition. This excited state produces a high electron density on the central carbon atom. The resulting charge migration involves the central carbon atom and the phenyl rings bearing an auxochromic group, with the charge being mainly located on the terminal nitrogen atoms.

The second band - the y-band - corresponds to the electronic excitation from the $\pi \rightarrow \pi^*$ orbital. This transition is of lower intensity than the x-band transition. The greater the optical asymmetry of the molecule, the greater the separation between the x- and y-bands.

Arylmethane dyes are typified by MHB (1.1-9), MG (1.1-8) and CV (1.1-7). MHB is a symmetrical diphenylmethane dye which absorbs at 607.5 nm ($\epsilon_{\max} = 147,500 \text{ dm}^3 \text{ mol}^{-1} \text{ cm}^{-1}$) in 98% acetic acid (89JCS(P2)1087). Replacing the hydrogen of the central carbon atom of MHB by a phenyl ring produces the unsymmetrical TPM dye, MG, which exhibits two absorption bands as predicted. For MG, in 98% acetic acid, the x-band at 621 nm ($\epsilon_{\max} = 104,000 \text{ dm}^3 \text{ mol}^{-1} \text{ cm}^{-1}$) displays the expected bathochromic shift resulting from the extended conjugation relative to MHB. The y-band of MG is at 427.5

nm ($\epsilon_{\max} = 20000 \text{ dm}^3 \text{ mol}^{-1} \text{ cm}^{-1}$). Introduction of a third dimethylamino group at the 4-position of the phenyl ring of MG produces the symmetrical TPM dye, CV, which displays a single absorption band at 589 nm ($\epsilon_{\max} = 117,000 \text{ dm}^3 \text{ mol}^{-1} \text{ cm}^{-1}$) in 98% acetic acid. In certain solvents (e.g. toluene), there is a pronounced splitting of the x- and y-bands for CV producing a shoulder on the main absorption band. There is much debate as to the cause of this phenomenon (93CR381).

Substituents can be introduced into the parent dye molecules and the resulting modifications to the absorption spectrum of the dye can be explained by reference to the steric and electronic effects of the substituent on the dye system.

Electronically symmetrical dyes such as CV possess two more starred sites than non-starred positions and therefore contain two NBMOs whereas unsymmetrical dyes, such as MG, possess only one extra starred position and therefore contain only one NBMO. The two NBMOs of CV are necessarily degenerate and the main absorption band arises as a result of the electronic transition from the two degenerate NBMOs to the LUMO. This accounts for the sometimes different behaviour of MG and CV to steric and electronic perturbations.

As the y-band transition involves a certain degree of charge migration from the phenyl ring into the molecular framework, prediction of the effects of substitution in the phenyl ring on the absorption band of the chromogen is more difficult and is not always consistent with the electronic nature of the substituent. However, in general, the presence of an electron withdrawing group produces a hypsochromic shift in λ_{\max} for the y-band and a decrease in $\epsilon_{\max}(y)$, whilst an electron donating group produces a bathochromic shift in λ_{\max} and an increase in ϵ_{\max} for the y-band.

When a substituent is introduced into a chromogen, depending on the position of substitution and the nature of the substituent, the parent chromogen may experience steric strain. To compensate for this extra instability, the molecule may rotate about particular bonds. This enforced rotation can have a pronounced effect on the absorption of the chromogen which will be reflected in the spectrum of the dye. For DPM/TPM dyes, a near planar molecule is essential for efficient charge delocalisation throughout the system. However, if the induced rotation is sufficient to render this charge delocalisation ineffective, drastic changes in the spectrum of the dye will be observed. By far the greatest steric strain is observed if substitution occurs at the *ortho* position of the phenyl ring in TPM dyes and at the central carbon atom in DPM dyes.

1.7.2 The effect of terminal groups on the absorption spectra of TPM/DPM dyes

The terminal positions of MHB, CV and MG are starred or active sites. PMO theory (50JCS2329) predicts that any increase in the electron density at these positions will result in a bathochromic shift of λ_{\max} of the main absorption band. The magnitude of the shift will be related to the extent of electron donation by the alkyl group attached to the terminal nitrogen atom. Some data are provided in Tables 1.2 – 1.4 (82Th1, 83Th1, 89JCS(P2)1087).

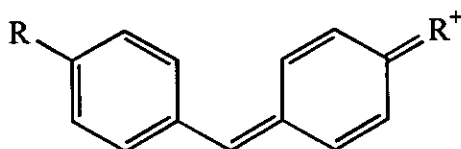


Table 1.2
The visible absorption spectra in 98% acetic acid of some derivatives of Michler's Hydrol Blue

R	λ_{\max}/nm	$10^{-4}\epsilon_{\max}/\text{dm}^3 \text{mol}^{-1} \text{cm}^{-1}$
NMe ₂	607.5	14.75
NEt ₂	613	17.6
Pyrrolidino	613	15.7
Piperidino	619	0.23
Morpholino	613	3.1

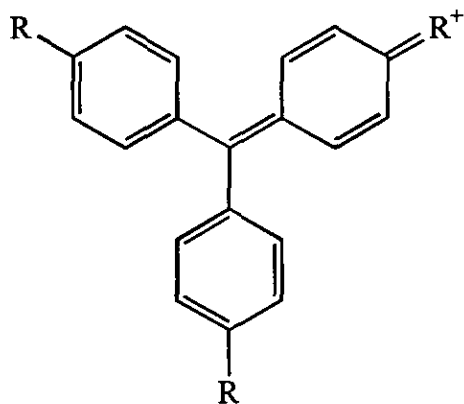


Table 1.3

The visible absorption spectra in 98% acetic acid of some derivatives of Crystal Violet

R	λ_{\max}/nm	$10^{-4}\epsilon_{\max}/\text{dm}^3 \text{mol}^{-1} \text{cm}^{-1}$
NMe ₂	589	11.7
NEt ₂	592.5	13.0
Pyrrolidino	591	12.1
Piperidino	602	11.5
Morpholino	596	10.6

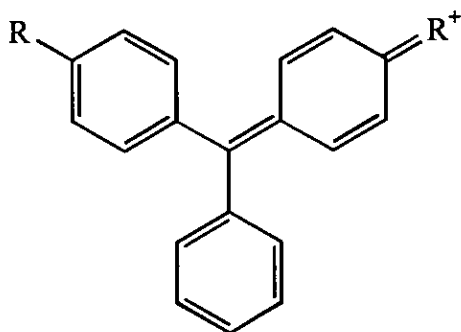


Table 1.4

The visible absorption spectra in 98% acetic acid of some derivatives of Malachite Green

R	x-band		y-band	
	λ_{\max}/nm	$10^4 \epsilon_{\max} / \text{dm}^3 \text{ mol}^{-1} \text{ cm}^{-1}$	λ_{\max}/nm	$10^4 \epsilon_{\max} / \text{dm}^3 \text{ mol}^{-1} \text{ cm}^{-1}$
NMe ₂	621	10.4	427.5	2.0
NEt ₂	629.5	11.9	430	1.8
Pyrrolidino	630	11.6	429	1.8
Piperidino	634	10.4	431	1.7
Morpholino	623	9.0	433	1.9

A study of Tables 1.2 - 1.4 allows the electron donating nature of the substituents to be described. Increasing the length of the alkyl chain increases the electron donating ability of the terminal group which is reflected in the availability of the nitrogen lone pair of electrons to confer stability on the central carbocation. The diethylamino and pyrrolidino groups have a similar electron donating ability as indicated by their $\lambda_{\max}(x)$ values but, in every series, the $\epsilon_{\max}(x)$ value of the pyrrolidino derivative is lower than that of the diethylamino derivative. This has been ascribed to partial deconjugation of the 5-membered heterocyclic ring arising from a clash between the pyrrolidino α -methylene protons and the *ortho* protons of the phenyl ring (84JCS(P2)149, 89JCS(P2)1087).

When the terminal group is the 6-membered piperidine moiety, $\lambda_{\max}(x)$ is the most bathochromic of the series indicating the greater donating power of the piperidino group. There is a further reduction in $\epsilon_{\max}(x)$ which has been attributed to the greater steric hindrance suffered by the 6-membered ring than for the 5-membered ring (89JCS(P2)1087). This reduction in $\epsilon_{\max}(x)$ is most pronounced in the DPM derivative, and is probably associated with the lower stability of the MHB system compared to MG or CV.

With the introduction of morpholine, the presence of the oxygen, with its inductive electron withdrawing effect, results in an overall reduction in electron donation into the chromogen relative to the piperidino derivative.

When the terminal groups in CV are replaced by other amino groups, bathochromic and hypsochromic shifts in λ_{\max} are observed. Whilst the resulting dyes are structurally unsymmetrical they are apparently electronically symmetrical (89JCS(P2)1087).

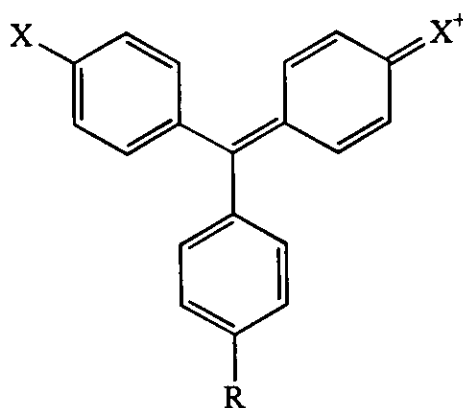
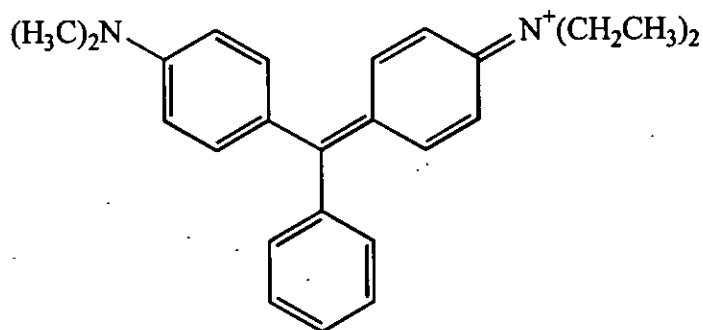


Table 1.5

The visible absorption spectra in 100% acetic acid of some unsymmetrical derivatives of Crystal Violet

R	X	λ_{\max}/nm	$10^4 \epsilon_{\max} / \text{dm}^3 \text{mol}^{-1} \text{cm}^{-1}$
NMe ₂	NEt ₂	591	11.8
NEt ₂	NMe ₂	592	12.2
NMe ₂	Pyrrolidino	588	12.0
NEt ₂	Pyrrolidino	589.5	13.2
NMe ₂	Piperidino	591.5	11.9
NEt ₂	Piperidino	597	12.1
NMe ₂	Morpholino	592.5	10.7
NEt ₂	Morpholino	597.5	10.9
Pyrrolidino	NMe ₂	594.5	9.4
Pyrrolidino	NEt ₂	594	12.0
Piperidino	NMe ₂	597	11.9
Piperidino	NEt ₂	598.5	10.4
Morpholino	NMe ₂	594.5	10.8
Morpholino	NEt ₂	597.5	10.4
Pyrrolidino	Piperidino	597.5	12.7
Pyrrolidino	Morpholino	602.5	10.5
Piperidino	Pyrrolidino	601.5	10.4
Piperidino	Morpholino	606.5	10.8
Morpholino	Pyrrolidino	601.5	3.1
Morpholino	Piperidino	604	6.5

For MG, when one of the dimethylamino groups is replaced by a diethylamino group the structurally unsymmetrical dye (1.7-1) is generated which absorbs at an intermediate wavelength (626 nm) between those of MG and Brilliant Green (BG) (86JSDC15).



(1.7-1)

Both BG (82JSDC10) and this hybrid Green (86JSDC15) show the same responses in $\lambda_{\text{max}}(x)$ and $\epsilon_{\text{max}}(x)$ as MG to substitution in the phenyl ring.

1.7.3 The effect of substitution at the 2-position of the phenyl rings on the absorption spectra of TPM/DPM dyes

The absorption spectra of DPM/TPM dyes are dependent upon the molecular conformation of the dye. Of the available sites for substitution on the phenyl rings of DPM/TPM dyes, substitution at the 2-position will be the most influential. The effects will be a combination of both steric and electronic effects and as such, a quantitative relationship between the Hammett substitution constant and λ_{max} of the substituted dye is unlikely.

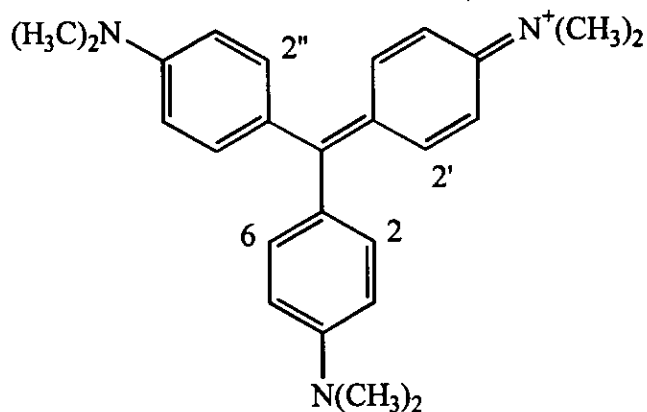


Table 1.6

The visible absorption spectra in 98% acetic acid of some *ortho*-substituted derivatives of Crystal Violet

Substituent in CV	λ_{\max}/nm	$10^{-4} \epsilon_{\max}/\text{dm}^3 \text{ mol}^{-1} \text{ cm}^{-1}$
None	589	11.7
2-CH ₃	597	11.0
2,2'-diCH ₃	605	10.3
2,2',2''-triCH ₃	614	10.0
2,6-diCH ₃	616	11.2

Introduction of an *ortho* substituent results in a further deviation from molecular coplanarity. An *ortho* substituent will influence the parent molecule through steric and electronic considerations. The simplest case to study involves the introduction of methyl groups at the *ortho* positions of the phenyl rings. Purely on steric considerations, for CV this should result in a bathochromic shift of the main absorption band and a reduction in its intensity. Electronically though, the methyl groups should produce a hypsochromic shift. In practice, it has been found that steric effects predominate (59JCS3957). Introduction of additional *ortho* methyl groups gives a progressive and uniform bathochromic shift and a consistent decrease in absorption intensity, which would suggest that the steric strain produces uniform axial rotation between all the phenyl rings and that symmetry is conserved (59JCS3957).

For the 2,6-dimethyl derivative it is postulated that the steric strain is relieved by rotation of only the di-substituted ring. This results in greater charge localisation on the two other dimethylamino groups, producing the bathochromic shift observed and the increase in the intensity of the absorption band.

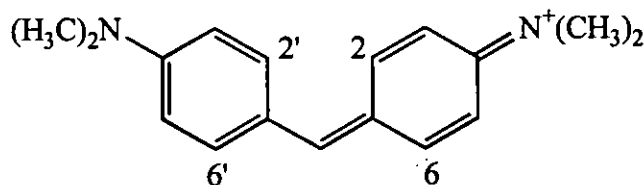


Table 1.7

The visible absorption spectra in 98% acetic acid of some *ortho*-substituted derivatives of Michler's Hydrol Blue

Substituent in MHB	λ_{\max}/nm	$10^{-4}\epsilon_{\max}/\text{dm}^3 \text{mol}^{-1} \text{cm}^{-1}$
None	607.5	14.75
2-CH ₃	614.5	13.0
2,2'-diCH ₃	623	12.1
2,2',6,6'-tetraCH ₃	649	5.5

For MHB, the *ortho* positions are not identical and bulky substituents are expected to take up the 'outside' positions, so minimising steric strain. It might be expected that an *ortho* methyl group would produce a hypsochromic shift of the main absorption band through its electronic influence. However, this is not the case, indicating the importance of steric factors on the dye spectrum. This effect is replicated in the 2,2'-dimethyl derivative.

The overlap of the *ortho* hydrogens in MHB may be reduced by a slight increase in the phenyl-carbon-phenyl bond angle. This would bring the two 'outside' *ortho* carbon atoms closer together and may be the method by which MHB derivatives approach uniplanarity (59JCS3957). For the 2,2',6,6'-tetramethyl derivative, the main absorption band is significantly shifted to the red suggesting interaction between the two 'inside' methyl groups which may result in an increased phenyl-carbon-phenyl bond angle. This would accentuate the reduction in peak intensity.

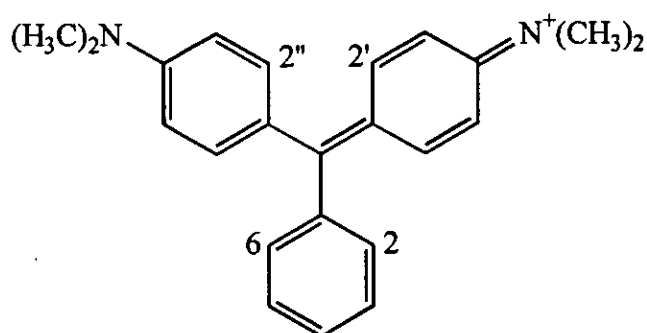


Table 1.8
The visible absorption spectra in 98% acetic acid of some *ortho*-
substituted derivatives of Malachite Green

R	x-band		y-band	
	λ_{\max}/nm	$10^{-4}\epsilon_{\max} / \text{dm}^3 \text{mol}^{-1} \text{cm}^{-1}$	λ_{\max}/nm	$10^{-4}\epsilon_{\max} / \text{dm}^3 \text{mol}^{-1} \text{cm}^{-1}$
None	621	10.4	427.5	2.0
2-CH ₃	622.5	12.3	420	1.5
2'-CH ₃	635	7.5	437.5	2.0
2,2'-diCH ₃	634	8.4	431	1.8
2',2''-diCH ₃	648	6.7	445	1.8
2,6-diCH ₃	624	13.2	410	1.2

The study of steric effects in MG is complicated by its lower molecular symmetry. On steric considerations, substitution at the *ortho* position of the phenyl ring of MG should result in a bathochromic shift of the x-band and a hypsochromic shift of the y-band with a reduction in intensity for both bands. In practice, there is a reduction in both $\lambda_{\max}(\text{y})$ and $\epsilon_{\max}(\text{y})$ consistent with the loss of planarity. This is accentuated in the 2,6-dimethyl analogue. However, whilst $\lambda_{\max}(\text{x})$ responds as expected, $\epsilon_{\max}(\text{x})$ increases with the enforced bond rotation (67JSDC368). This has been attributed to twisting of the *meta*-xylyl group such that it becomes orthogonal to the dimethylamino bearing rings thus enabling them to become more planar and hence facilitating conjugation.

The effects of a given substituent in the *ortho* position of the phenyl ring of MG are directly related to its Van der Waals radius unless the substituent is particularly large (61JCS1285) or it is able to rotate to reduce its steric influence (71JSDC187, 77JSDC451).

Introduction of a methyl group into the *ortho* position of the dimethylaminophenyl rings of MG produces a bathochromic shift of $\lambda_{\max}(x)$ and a reduction in $\epsilon_{\max}(x)$ indicating the increased axial rotation in these rings. A hypsochromic shift would be expected purely on electronic considerations. The observations suggest that whilst the phenyl ring is in a more crowded environment, it takes a more active role in the charge delocalisation process and $\lambda_{\max}(y)$ is shifted to the red.

1.7.4 The effect of substitution at the 3-position of the phenyl rings on the absorption spectra of TPM/DPM dyes

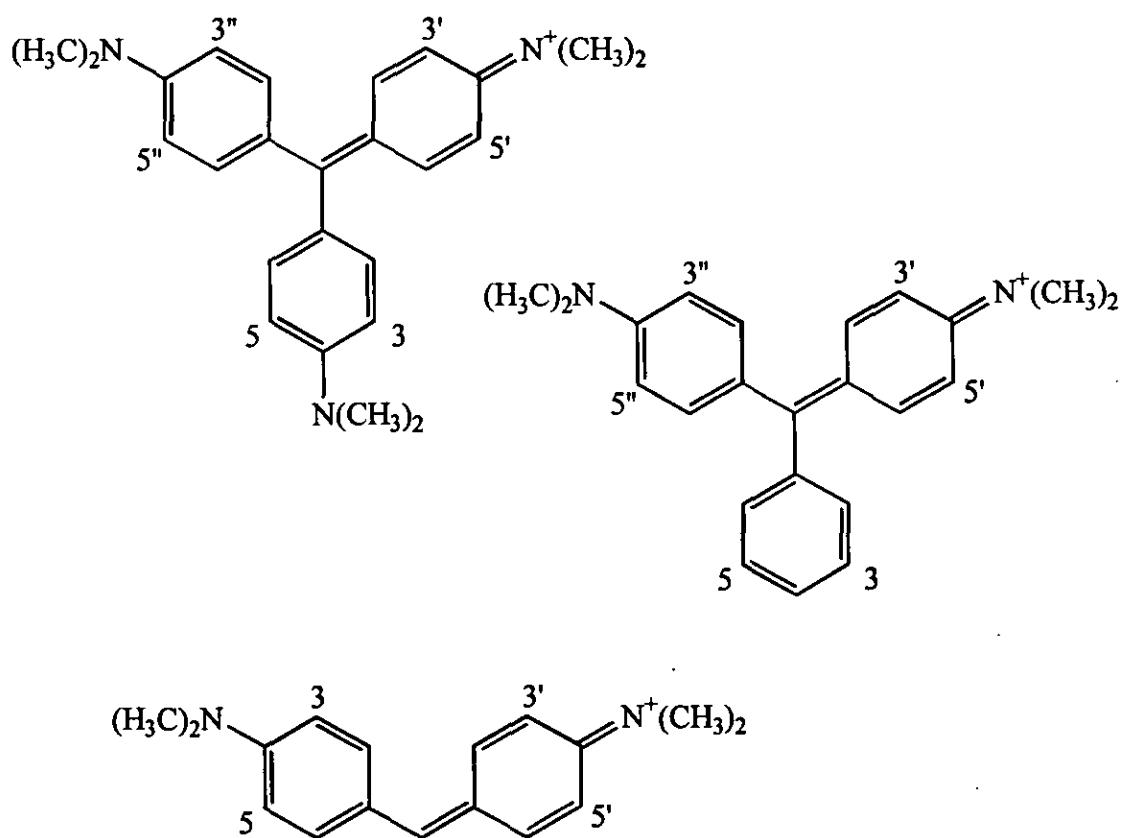


Table 1.9

The visible absorption spectra in 98% acetic acid of some *meta*-substituted derivatives of Crystal Violet, Malachite

Green and Michler's Hydrol Blue

R	x-band		y-band	
	λ_{\max}/nm	$10^4 \epsilon_{\max} / \text{dm}^3 \text{mol}^{-1} \text{cm}^{-1}$	λ_{\max}/nm	$10^4 \epsilon_{\max} / \text{dm}^3 \text{mol}^{-1} \text{cm}^{-1}$
CV	589	11.7	-	-
3-CH ₃	599.5	9.5	-	-
3,3'-di CH ₃	607.5	7.8	-	-
3,3',3"-tri CH ₃	615	1.3	-	-
3,5-di CH ₃	610.5	9.6	(430)	(0.8)
3,3',5,5'-tetra CH ₃	618	4.9	-	-
MG	621	10.4	427.5	2.0
3'- CH ₃	627.5	6.3	436	1.6
3',5'-di CH ₃	630	1.8	452.5	1.2
3',3"-di CH ₃	617	1.1	430	0.4
3',3'',5',5"-tetra CH ₃	616	0.015	446	0.011
MHB	607.5	14.75	-	-
3- CH ₃	602.5	0.06	-	-
3,3'-di CH ₃	584	0.03	-	-

A substituent at the *meta* position in MHB, MG and CV twists the adjacent dimethylamino group, reducing its mesomeric interaction with the chromophoric system. This has a marked effect on the visible absorption spectrum of the dye. Each dye system displays a reduction in $\epsilon_{\max}(x)$ as a result of the reduced conjugation but the response of $\lambda_{\max}(x)$ appears to be different for each dye with both bathochromic and hypsochromic shifts being observed relative to the parent dye. This, however, is not the case and the apparently contradictory response of $\lambda_{\max}(x)$ does, in fact, follow a distinct pattern.

If a conjugated carbon chain is to be deformed out of coplanarity, energy must be provided. The degree to which a bond will be deformed is a function of its bond order which will determine the amount of energy required to promote the deformation. Weak bonds will deform more easily and require less energy. For symmetrical cyanines, all bonds will have the same bond order and so will rotate to the same extent, maintaining some degree of symmetry. If pH_n is the contribution to the bond order of a bond by an electron occupying the HOMO and pL_n is the contribution to the bond order of a bond by an electron occupying the LUMO, then it can be shown that for symmetrical cyanine dyes pL_n is negative for the central and terminal bonds. Therefore, rotation of these bonds would decrease the energy of the LUMO which would produce a bathochromic shift of $\lambda_{\max}(x)$. However, it can also be shown that the effect of terminal heteroatoms is to render pH_n negative. As a result, rotation about the terminal bonds decreases the energy of the HOMO and a hypsochromic shift of $\lambda_{\max}(x)$ is predicted. As a consequence, the effects of *meta* substitution in MHB, MG and CV cannot be unambiguously defined without detailed calculations. A general trend relating the effect of inducing non-coplanarity on planar symmetrical dyes compared to planar unsymmetrical dyes is that non-coplanarity will have an increasingly bathochromic effect along the series MHB < MG < CV. This is clearly illustrated in Table 1.10.

Table 1.10
Relative shifts of λ_{\max} for analogous derivatives of Crystal Violet,
Malachite Green and Michler's Hydrol Blue

Substituent	$\Delta \lambda_{\max}(x)$ (nm) relative to parent dye		
	MHB	MG	CV
3'-CH ₃	-5	6.5	10.5
3',3''-diCH ₃	-23.5	-4	18.5
3'-5'-diCH ₃	-	9	21.5
3',3'',5',5''-tetraCH ₃	-	-5	29

For MG, the 3',3"-dimethyl and 3',3",5',5"-tetramethyl derivatives show small hypsochromic shifts of λ_{\max} relative to the parent dye, whereas the 3'-methyl and 3',5'-dimethyl derivatives show bathochromic shifts of λ_{\max} . This has been attributed to the electronically unsymmetrical nature of the last two dyes with the charge tending to be localised on the unhindered dimethylamino group (60JCS3790). The spectral shifts brought about by crowding substituents causing heterocyclic cyanines to depart from coplanarity varies with the degree of electronic symmetry of the heterocyclic cyanine (60JCS3790).

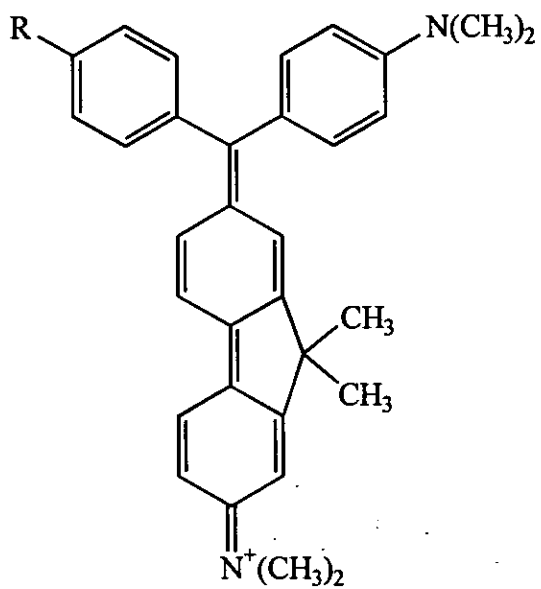
For *meta* and *para* substitution in the phenyl ring of MG there will be no additional departure from coplanarity and the effects of such substitution on $\lambda_{\max}(x)$ will be solely a result of the electronic influence of the substituent. An electron donating substituent will produce a hypsochromic shift in $\lambda_{\max}(x)$ and an electron withdrawing substituent a bathochromic shift. In general, the y-band responds to an electron donating substituent by a bathochromic shift and to an electron withdrawing substituent by a hypsochromic shift although these effects are by no means consistent. The response of the x-band to *meta* and *para* substitution is linearly related to the appropriate Hammett substituent constant as discussed earlier. Examples of such responses are shown in Table 1.11 for the MG system (61JCS1285, 70JSDC200, 71JSDC187).

Table 1.11
The visible absorption spectra in 98% acetic acid of some *meta*-
and *para*-substituted derivatives of Malachite Green

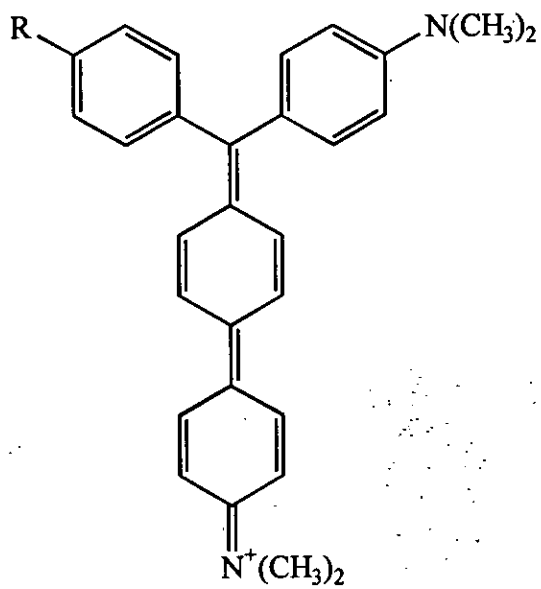
Substituent	x-band		y-band	
	λ_{\max}/nm	$10^4 \epsilon_{\max} / \text{dm}^3 \text{ mol}^{-1} \text{ cm}^{-1}$	λ_{\max}/nm	$10^4 \epsilon_{\max} / \text{dm}^3 \text{ mol}^{-1} \text{ cm}^{-1}$
None	621	10.4	427.5	2.0
3-CH ₃	618.5	10.6	433	2.2
4-CH ₃	616.5	10.6	437.5	2.5
4- <i>t</i> -Bu	616	10.4	440	2.6
3-F	630	10.4	426.5	2.2
4-F	620	10.6	430.5	2.1
3-Cl	630	10.3	426	1.7
3-OCH ₃	622.5	10.7	435	1.8
4-OCH ₃	608	10.6	465	3.4
4-OH	602.5	10.6	470	3.6
3-NO ₂	637.5	8.7	425	1.4
4-NO ₂	645	8.3	425	1.7

1.7.5 TPM/DPM dyes with extended chromophoric systems

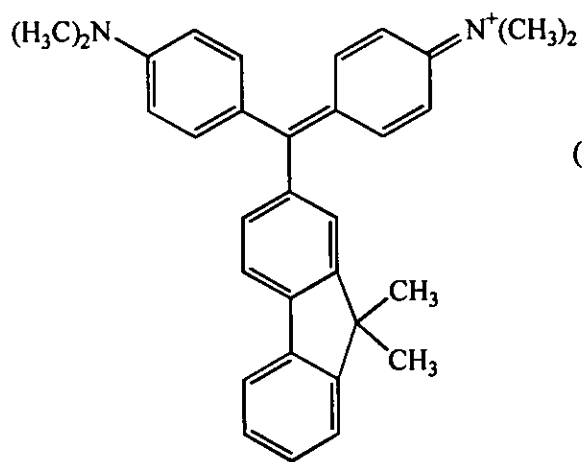
To further our knowledge of the chemistry of TPM/DPM dyes and to develop new dyes for novel purposes, the effects of extending the chromophoric system of existing dyes have been studied. The most extensively studied systems have contained the 9,9-dimethylfluorene, biphenyl, naphthalene and phenanthrene moieties. A brief review will be made of the effects on MHB, MG and CV of extending their chromophoric system by the introduction of these groups.



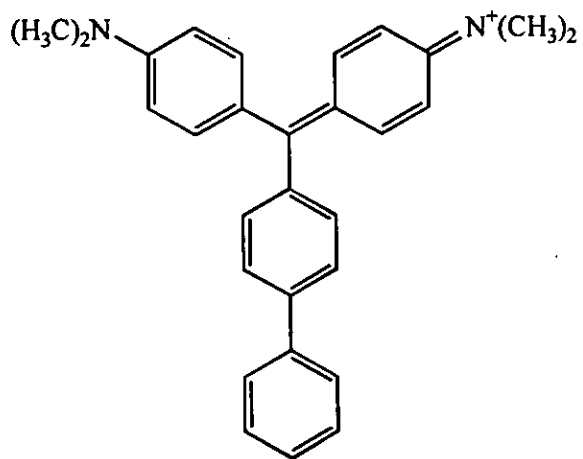
(1.7-2)



(1.7-3)



(1.7-4)



(1.7-5)

Table 1.12

**The visible absorption spectra in 98% acetic acid of some biphenyl
and 9,9-dimethylfluorenyl analogues of Crystal Violet and
Malachite Green**

Dye	Solvent	x-band		y-band	
		λ_{\max}/nm	$10^4 \epsilon_{\max} / \text{dm}^3 \text{ mol}^{-1} \text{ cm}^{-1}$	λ_{\max}/nm	$10^4 \epsilon_{\max} / \text{dm}^3 \text{ mol}^{-1} \text{ cm}^{-1}$
CV	a	589	11.6	-	-
1.7-2; R=NMe ₂	a	621	9.5	474	1.3
	b	628.5	9.2	464	3.0
	c	614	10.8	418	0.5
1.7-3; R=NMe ₂	c	617.5	9.4	415	0.8
MG	a	621	10.4	427.5	2.0
1.7-2; R=H	c	675	1.25	468	0.72
1.7-3; R=H	c	625	0.4	463	0.3*
1.7-4	a	623	9.7	484	3.9
1.7-5	a	625.5	10.2	454	3.1

a: 98% acetic acid; b: 90% acetic acid; c: Ethanol containing one molar equivalent of hydrogen chloride; * Bands fade rapidly

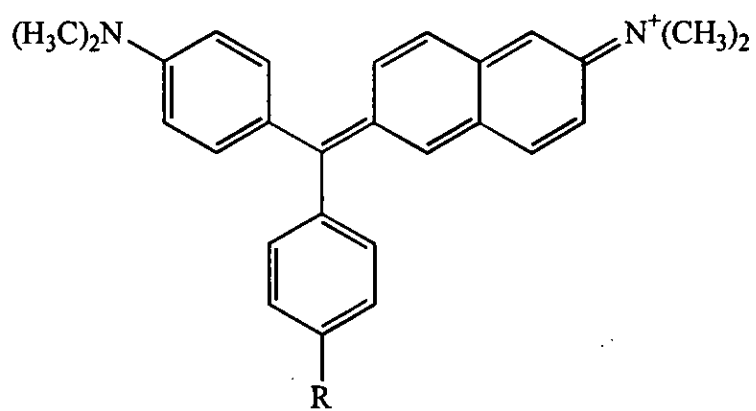
It can be seen from Table 1.12 that the introduction of the 9,9-dimethylfluorenyl and biphenyl groups into CV and MG extends the conjugation of the systems, resulting in a bathochromic shift of the main absorption band. If the terminal nitrogen atom present on the extended groups of CV was effectively conjugated then only one band would be observed in the visible absorption spectrum. However, in 98% acetic acid, a second band is observed for the 9,9-dimethylfluorenyl derivative. This second band is attributed to a bivalent ion rather than to a loss of symmetry in the CV cation because an increase in the acidity of the solvent results in a reduction in the intensity of the first absorption band and an increase in the intensity of the second band (82JCS(P2)1037). The larger bathochromic shift of $\lambda_{\max}(x)$ brought about by the introduction of the biphenyl group

into CV is also a result of the presence of the bivalent ion (70JCS(B)975) - the bathochromic shift of the first band coupled with a decrease in its intensity plus the hypsochromic shift of the second absorption band coupled with an increase in its intensity are consistent with the presence of an electron withdrawing group such as a protonated dimethylamino group.

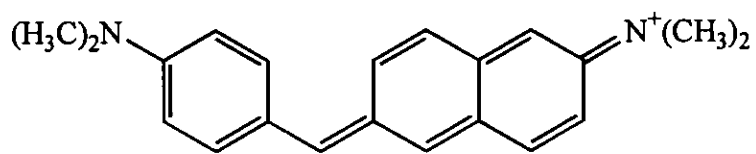
For compounds 1.7-4 and 1.7-5, the red shifts in $\lambda_{\max}(y)$ indicate the enhanced conjugation along the y-axis of the molecule. The slight hypsochromic shift of the x-band of 1.7-4 is consistent with the electron donating effect of a substituent in the 3-position of MG. The 9,9-dimethylfluorenyl and biphenyl derivatives of MG show less tendency to form the univalent cation than their CV analogues reflecting the greater stability of the CV system. The nearest approximation to the univalent cation for MG is in ethanolic hydrogen chloride but even in this medium the biphenyl derivative has a tendency to fade, indicating incomplete conversion of the dye base into the cation.

The 9,9-dimethylfluorenyl derivative of MG displays a red shift of $\lambda_{\max}(x)$ of 54 nm compared to only 4 nm for the biphenyl derivative, which reflects the increased planarity and hence greater conjugation along the x-axis brought about by the bridging isopropyl unit.

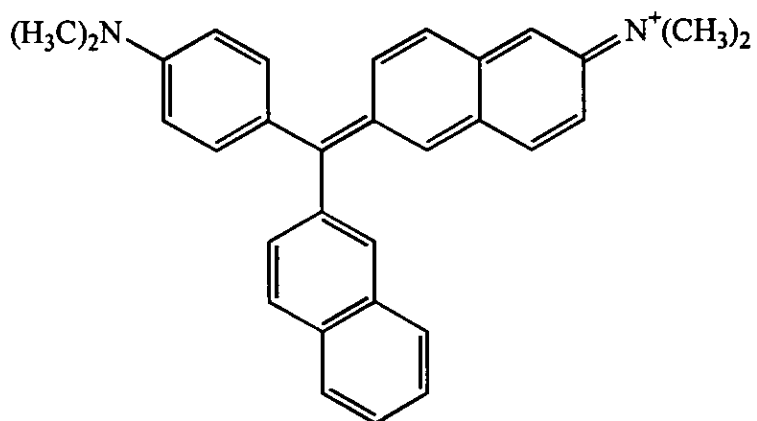
Overall, 9,9-dimethylfluorenyl stabilises the univalent ion to a greater degree than biphenyl but it is with some difficulty that any mesomeric effect is transmitted through the 9,9-dimethylfluorenyl system. The poor transmission of mesomeric effect by the biphenyl system has been ascribed to rotation of the molecule about the phenyl-phenyl bond. The enforced planarity of the biphenyl moiety of 9,9-dimethylfluorenyl results in a moderate improvement in conjugation across the system.



(1.7-6)



(1.7-7)



(1.7-8)

Table 1.13

The visible absorption spectra in 98% acetic acid of some longitudinally conjugated naphthalene analogues of Crystal Violet, Malachite Green and Michler's Hydrol Blue

Dye	Solvent	x-band		y-band	
		λ_{\max}/nm	$10^4 \epsilon_{\max} / \text{dm}^3 \text{ mol}^{-1} \text{ cm}^{-1}$	λ_{\max}/nm	$10^4 \epsilon_{\max} / \text{dm}^3 \text{ mol}^{-1} \text{ cm}^{-1}$
CV	a	589	11.6	-	-
1.7-6; R=NMe ₂	a	613	10.3	-	-
	b	629	8.6	442	1.9
	c	613.5	10.9	-	-
MG	a	621	10.4	427.5	2.0
1.7-6; R=H	a	690	5.0	474	1.8
1.7-8	a	626.5	10.5	458	3.2
MHB	a	607.5	14.8	-	-
1.7-7	a	673	0.29	-	-

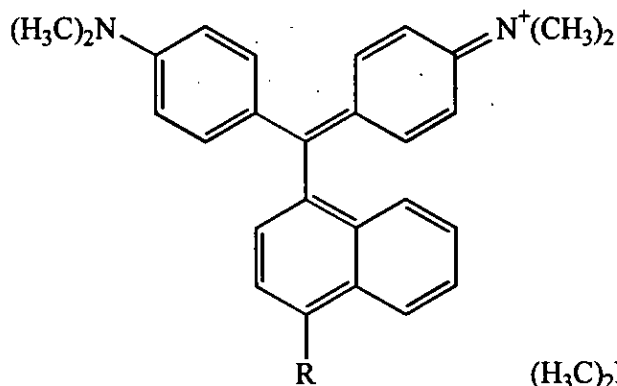
a: 98% acetic acid; b: 70% acetic acid, c: Ethanol containing one molar equivalent of hydrogen chloride

With the longitudinally conjugated naphthalene derivative of CV, only one band is observed in ethanol containing one molar equivalent of hydrogen chloride indicating an even distribution of charge throughout the system. The bathochromic shift of $\lambda_{\max}(x)$ relative to CV is attributed to the more extended conjugation of the naphthalene system. One band is also observed in 98% acetic acid, but increasing the acidity of the solvent results in the formation of the bivalent ion.

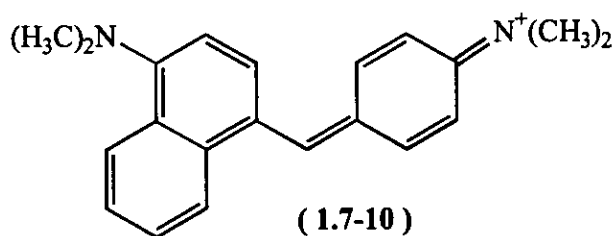
The naphthalene analogue of MG (1.7-6; R = H) shows less tendency to form the univalent cation and conversion of dye base to dye is incomplete. The pronounced bathochromic shift of $\lambda_{\max}(x)$ relative to MG is ascribed to the extended conjugation along the x-axis of the system.

The naphthalene analogue of MHB displays a significant bathochromic shift relative to the parent compound as expected from the extended conjugation, but conversion to the dye in 98% acetic acid is only slight at room temperature.

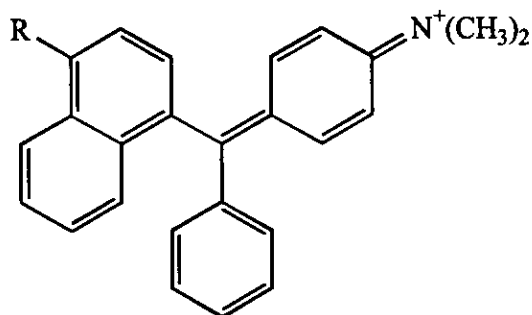
It is apparent that the terminal nitrogen atom in a longitudinally conjugated naphthalene moiety has a greater tendency to conjugate with the central carbon atom of a TPM/DPM dye than for the corresponding 9,9-dimethylfluorenyl and biphenyl analogues.



(1.7-9)



(1.7-10)



(1.7-11)

Table 1.14

The visible absorption spectra in 98% acetic acid of some transversely conjugated naphthalene analogues of Crystal Violet, Malachite Green and Michler's Hydrol Blue

Dye	Solvent	x-band		y-band	
		λ_{\max}/nm	$10^4 \epsilon_{\max} / \text{dm}^3 \text{mol}^{-1} \text{cm}^{-1}$	λ_{\max}/nm	$10^4 \epsilon_{\max} / \text{dm}^3 \text{mol}^{-1} \text{cm}^{-1}$
CV	a	589	11.7	-	-
1.7-9; R=NMe ₂	a	623.5	9.4	-	-
	b	638.5	10.2	426	0.9
MG	a	621	10.4	427.5	2.0
1.7-9; R=H	a	630	12.0	460	1.1
1.7-11; R=NMe ₂	c	666	5.0	446	1.6
MHB	a	607.5	14.8	-	-
1.7-10	a	651	1.6	-	-

a: 98% acetic acid; b: 50% acetic acid, c: 100% acetic acid

Introduction of a transversely conjugated naphthalene ring into the TPM/DPM system creates steric hindrance at both the central carbon and the terminal nitrogen atom. For the CV derivative (1.7-9; R = NMe₂), only one band is displayed in the visible absorption spectrum both in 98% acetic acid and ethanolic hydrogen chloride indicating effective conjugation of the terminal nitrogen atom on the naphthalene moiety (72JCS(P2)2281). The bathochromic shift of $\lambda_{\max}(x)$ is due in part to the extended conjugation but also to the steric crowding of the central carbon and the terminal nitrogen atoms. Increasing the acidity of the solvent results in protonation of the *peri*-hindered dimethylamino group as indicated by the presence of a second absorption band.

The transversely conjugated naphthalene derivative of MG (1.7-11; R = NMe₂) is similar in many respects to the corresponding longitudinally conjugated analogue in that there is less tendency to form the univalent ion than with the analogous CV derivative. A pronounced bathochromic shift of the x-band is observed relative to MG as a consequence of both the electronic and steric effects of the naphthalene system. It has been shown for MG that crowding at the central carbon and hindrance of the terminal dimethylamino function lead to an increase in $\lambda_{\max}(x)$ (60JCS3790, 61JCS1529). Progressive protonation of the *peri*-hindered dimethylamino group occurs in an increasingly acidic solvent.

For MHB, the transversely conjugated naphthalene derivative (1.7-10) shows a pronounced red shift relative to the parent compound, but conversion of the dye base to the cation is low in 98% acetic acid at room temperature. A reduction in the intensity of the main absorption band on increasing the acidity of the system indicates the ease of protonation of the *peri*-hindered dimethylamino group (72JCS(P2)2281).

It can be concluded, therefore, that despite the crowding associated with the transversely conjugated naphthalene system, the terminal nitrogen atoms in this system are better able to conjugate with the central carbon atom of the dye than those of the corresponding longitudinally conjugated naphthalene system.

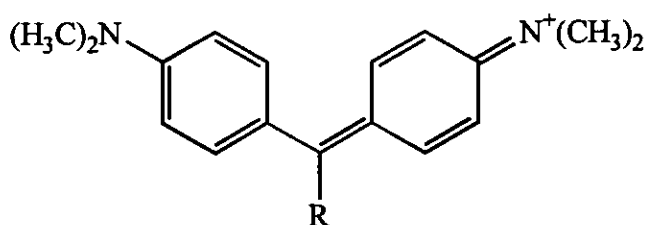
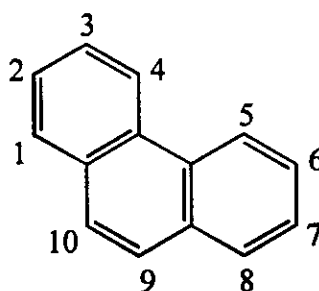


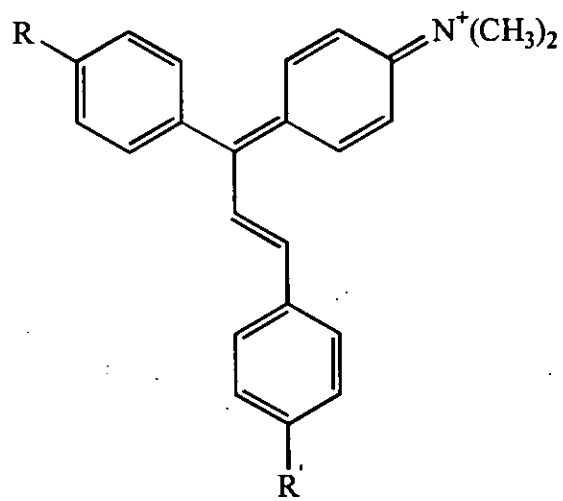
Table 1.15**The visible absorption spectra in 98% acetic acid of some phenanthryl analogues of Malachite Green and Crystal Violet**

R	x-band		y-band	
	λ_{\max}/nm	$10^4 \epsilon_{\max} / \text{dm}^3 \text{mol}^{-1} \text{cm}^{-1}$	λ_{\max}/nm	$10^4 \epsilon_{\max} / \text{dm}^3 \text{mol}^{-1} \text{cm}^{-1}$
Phenyl	621	10.4	427.5	2.0
2-Phenanthryl	626	10.4	462	3.6
3-Phenanthryl	627.5	10.4	474	2.6
1-Phenanthryl	630.5	12.3	455	1.1
9-Phenanthryl	632.5	12.4	470	1.4
4-Phenanthryl	634	12.7	450	1.0
3-(6-NMe ₂ -Phenanthryl)	635	8.7	-	-

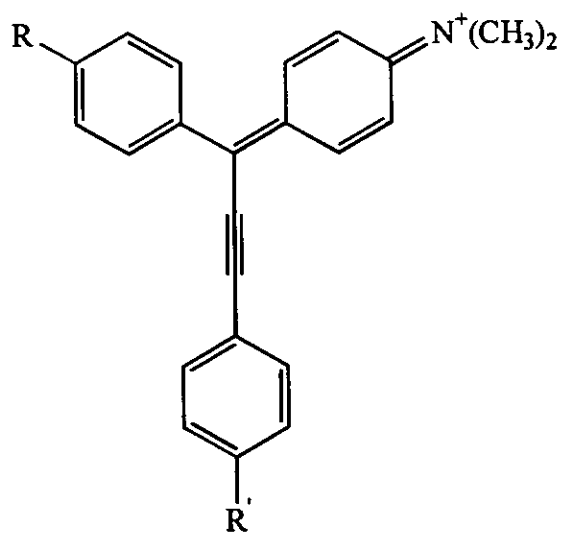
The phenanthrene derivatives of MG behave in a similar manner to their 1- or 2-naphthyl analogues depending on whether steric or electronic effects predominate (74JCS(P2)59). It has been established (71JCS(B)319) that an increase in $\epsilon_{\max}(x)$ and a reduction in $\epsilon_{\max}(y)$ is indicative of steric hindrance in the MG system where a further loss of molecular planarity occurs. This is illustrated in Table 1.15 with the 4-phenanthryl derivative displaying the greatest steric effect. However, this effect is less than expected, a feature which has been ascribed to the release of overcrowding by a slight deformation of the phenanthrene ring system (74JCS(P2)59).

For the 2- and 3-phenanthryl analogues, an increase in $\epsilon_{\max}(y)$ and no change in $\epsilon_{\max}(x)$ suggests that the absence of steric effects and that the electronic effects of the phenanthrene system extends the conjugation along the y-axis of the molecule. This is further supported by the bathochromic shift of $\lambda_{\max}(y)$.

The 3-(6-dimethylaminophenanthryl) derivative of CV shows a single band of reduced intensity suggesting a decreased ability of the dimethylamino group to stabilise the cation through the larger ring system.



(1.7-12)



(1.7-13)

Table 1.16

**The visible absorption spectra in 98% acetic acid of some ethynologues
and vinylogues of Crystal Violet and Malachite Green**

Dye	Solvent	x-band		y-band	
		λ_{\max}/nm	$10^{-4}\epsilon_{\max} / \text{dm}^3 \text{mol}^{-1} \text{cm}^{-1}$	λ_{\max}/nm	$10^{-4}\epsilon_{\max} / \text{dm}^3 \text{mol}^{-1} \text{cm}^{-1}$
CV	c	589	11.6	-	-
	b	584	12.0	-	-
1.7-12a; R=R'=NMe ₂	a	690	10.2	-	-
1.7-13a; R=R'=NMe ₂	a	670	10.3	-	-
	b	663	13.1	-	-
1.7-12b; R=H; R'=NMe ₂	a	715	10.0	462	1.3
1.7-13b; R=H; R'=NMe ₂	a	736	6.3	477.5	1.8
1.7-12c; R=NMe ₂ ; R'=H	a	656	4.7	490	2.9
1.7-13c; R=NMe ₂ ; R'=H	a	690	11.3	489	5.5
	b	688	10.1	493	3.6
1.7-13d; R=NMe ₂ ; R'=NO ₂	b	713	8.2	494	3.0
1.7-13e; R=NMe ₂ ; R'=Cl	b	695	9.0	498	3.4
1.7-13f; R=NMe ₂ ; R'=OMe	b	680	10.3	530	4.3

a: Probably acetic acid (estimated ϵ value); b: dye perchlorate in CH₂Cl₂, c: 98% acetic acid

A further method of extending the conjugation in MG and CV is to introduce a vinyl or ethynyl unit between one of the phenyl rings and the central carbon atom, thus producing a series of vinylogues (1.7-12) and ethynologues (1.7-13), several of which were investigated some years ago (51CR1043, 51CR1977). However, recent interest in dyes absorbing beyond 700 nm in the near infra-red for laser and optical storage technologies and for medicinal purposes has meant a resurgence of interest in this branch of TPM/DPM dyes with novel dyes being synthesised and studied (86CL329, 88JCS(P1)3155, 94Th1).

Data for the extinction coefficients from earlier reports vary significantly and, coupled with the tendency in more recent reports to study the dye perchlorate in dichloromethane, means that comparisons between data must be treated with care.

It can be seen that introduction of the vinyl (1.7-12a) and ethynyl (1.7-13a) units into CV produces a large bathochromic shift of $\lambda_{\max}(x)$ as a result of the extended conjugation. The presence of a single band indicates effective conjugation between the terminal nitrogen atom on the extended branch of the dye and the central carbon atom and illustrates the importance of the allene-quinonoid form to the overall structure of the molecule.

For the unsymmetrical vinyl (1.7-12b) and ethynyl (1.7-13b) derivatives of MG, $\lambda_{\max}(x)$ shows similar large red shifts because of the extended conjugation along the x-axis, and $\lambda_{\max}(y)$ behaves in a like manner as a result of the reduction in overcrowding along the y-axis. The symmetrical vinyl (1.7-12c) and ethynyl (1.7-13c) derivatives of MG display a bathochromic shift of $\lambda_{\max}(x)$, though not as great as that for the unsymmetrical analogues. $\lambda_{\max}(y)$ for the symmetrical derivatives of MG displays a large bathochromic shift as a result of the extended conjugation along the y-axis of the molecule.

It can be seen from the data in Table 1.16 that the symmetrical ethynologues of MG (1.7-13) respond to *para* substitution in the phenyl ring in the same manner as the parent compound. An electron donating substituent produces a hypsochromic shift of $\lambda_{\max}(x)$ (1.7-13f), whereas an electron withdrawing substituent produces a bathochromic shift (1.7-13d,e).

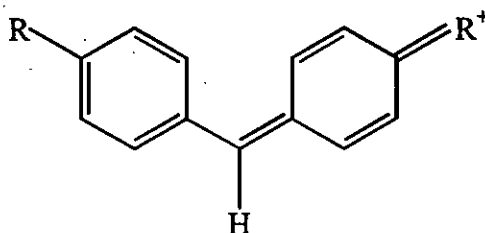
In order to understand better the influence of the terminal amino group on the chemistry of the DPM/TPM dye system, it is the intention of the present investigation to synthesise two series of dyes. The first series are symmetrical analogues of Michler's Hydrol Blue and the second series are unsymmetrical analogues of Malachite Green. The dye salts will be prepared from the dye bases. A discussion will be presented of the all preparative routes employed, their efficacy and the techniques for purification of the crude products.

The UV-Visible absorption spectrum of each dye will be recorded as will the ^1H and ^{13}C nmr spectra of both dye base and cation. A kinetic study of the rate of hydrolysis of the dye cations will also be conducted. Based upon the results of these measurements, a discussion will be presented in which the relative ability of each terminal amino group to conjugate with the chromophoric system will be appraised. The apparent donor ability will be justified in terms of steric and electronic factors by reference to previous, related work. From this discussion an understanding of the interaction between terminal amino groups and the DPM/TPM dye system will be derived.

2.

Results and Discussion

Prior to any discussion, a short note regarding the system of abbreviations adopted for the compounds studied in this investigation is given. This system was considered useful in defining the structure of the compound under discussion briefly but as clearly as possible. In this study, two series of compounds will be discussed in detail. The first series is based on the diphenylmethane dye Michler's Hydrol Blue (MHB) (2-1; R = NMe₂).



(2-1)

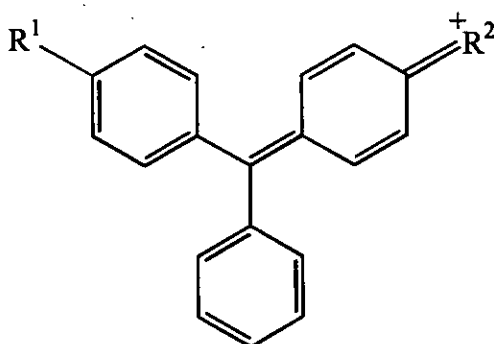
In this series of compounds, the terminal groups R will be selected from one of six amino groups: dimethylamino, diethylamino, pyrrolidino, piperidino, morpholino and *N*-methylpiperazino. Each amine function will be represented by an abbreviation and the suffix DPM will be used to denote a diphenylmethane type dye. The system of abbreviations used during this study is summarised in Table 2.1.

Table 2.1

Summary of abbreviations used for the Michler's Hydrol Blue analogues studied in this investigation

R	Abbreviation
Dimethylamino	MHB
Diethylamino	EtDPM
Pyrrolidino	PyDPM
Piperidino	PiDPM
Morpholino	MoDPM
<i>N</i> -Methylpiperazino	MPzDPM

The second series of compounds studied are analogues of the triphenylmethane dye Malachite Green (MG) (2-2; $R^1 = R^2 = NMe_2$). As with the analogues of MHB, modifications will involve only the amino groups R^1 and R^2 selected from the same list but with the addition of thiomorpholine. However, for the compounds studied in this series, R^1 and R^2 are always different. In total, 16 unsymmetrical MG derivatives have been studied.



(2-2)

The system of abbreviations used during this study are summarised in Table 2.2. As an example, the abbreviation MPz-Et refers to the dye 4'-diethylamino-4''-N-methylpiperazintriphenylmethane. The dye base from which the dye is generated is then abbreviated Mo-EtOH which, for example, represents 4'-diethylamino-4''-morpholinotriphenylmethanol.

Table 2.2
Summary of abbreviations used for the unsymmetrical Malachite Green
analogues studied in this investigation

R ¹	R ²	Abbreviation
NMe ₂	NEt ₂	Me-Et
Pyrrolidino	NEt ₂	Py-Et
Piperidino	NEt ₂	Pi-Et
Morpholino	NEt ₂	Mo-Et
NMe ₂	Pyrrolidino	Me-Py
Piperidino	Pyrrolidino	Pi-Py
Morpholino	Pyrrolidino	Mo-Py
NMe ₂	Piperidino	Me-Pi
Morpholino	Piperidino	Mo-Pi
NMe ₂	Morpholino	Me-Mo
<i>N</i> -Methylpiperazino	NEt ₂	MPz-Et
<i>N</i> -Methylpiperazino	NMe ₂	MPz-Me
<i>N</i> -Methylpiperazino	Pyrrolidino	MPz-Py
<i>N</i> -Methylpiperazino	Piperidino	MPz-Pi
<i>N</i> -Methylpiperazino	Morpholino	MPz-Mo
Thiomorpholino	NMe ₂	ThM-Me

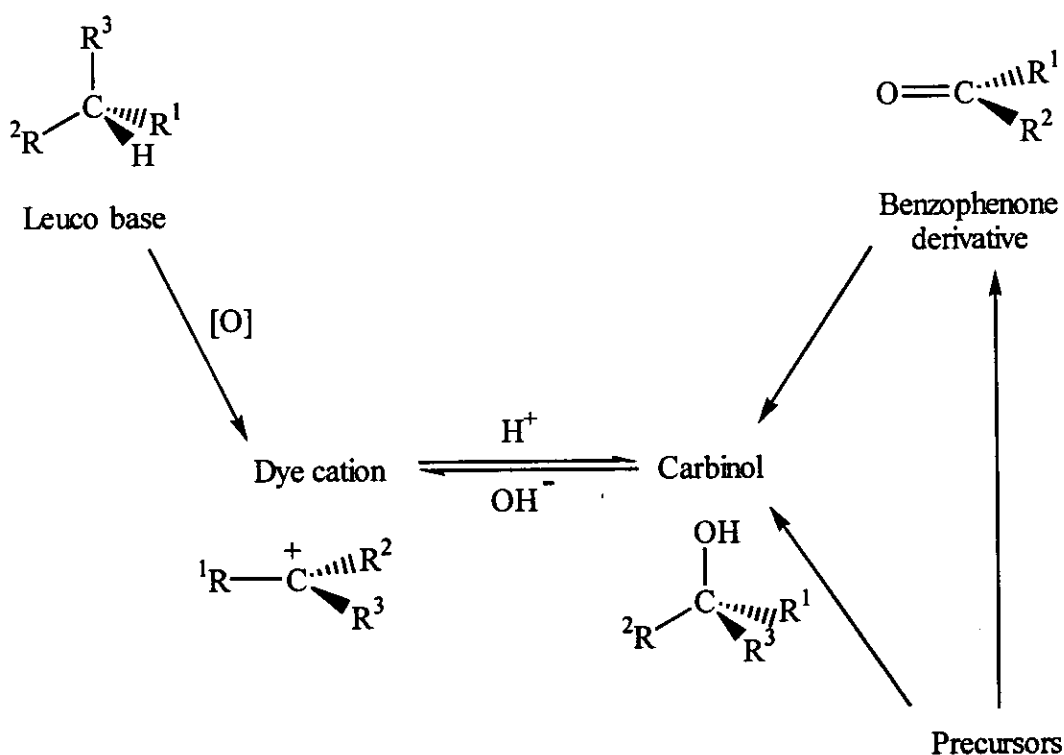
Except for thiomorpholine, for each of the amine functions substituted into the TPM system there are five examples with a different amino function in the x-axis of the molecule. Thus, there are five compounds containing morpholine with a different second amine function. There are, therefore, six series of compounds, one for each amine function, and five examples in each series with which to observe any effects. For the dimethylamino series there are six examples, the additional one having a thiomorpholino substituent.

2.1 Synthetic work

There have been several comprehensive reviews of the general preparative methods for TPM dyes (71MI1, 71MI2, 84RPCRT197). Within the scope of the present study it is not practical to discuss the preparative methods to the same depth as the reviews but an overview will be presented with a detailed discussion of pertinent methods. The relationship between a univalent, cationic TPM dye and its immediate precursors is shown in Figure 2A.

Figure 2A

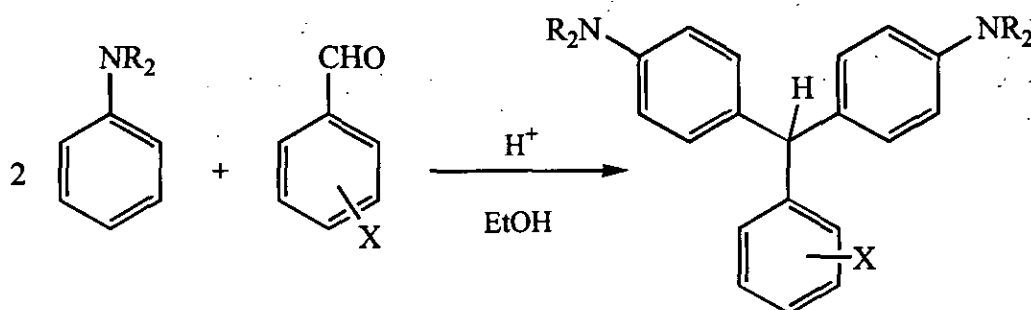
The relationship between a univalent cationic dye and its immediate precursors



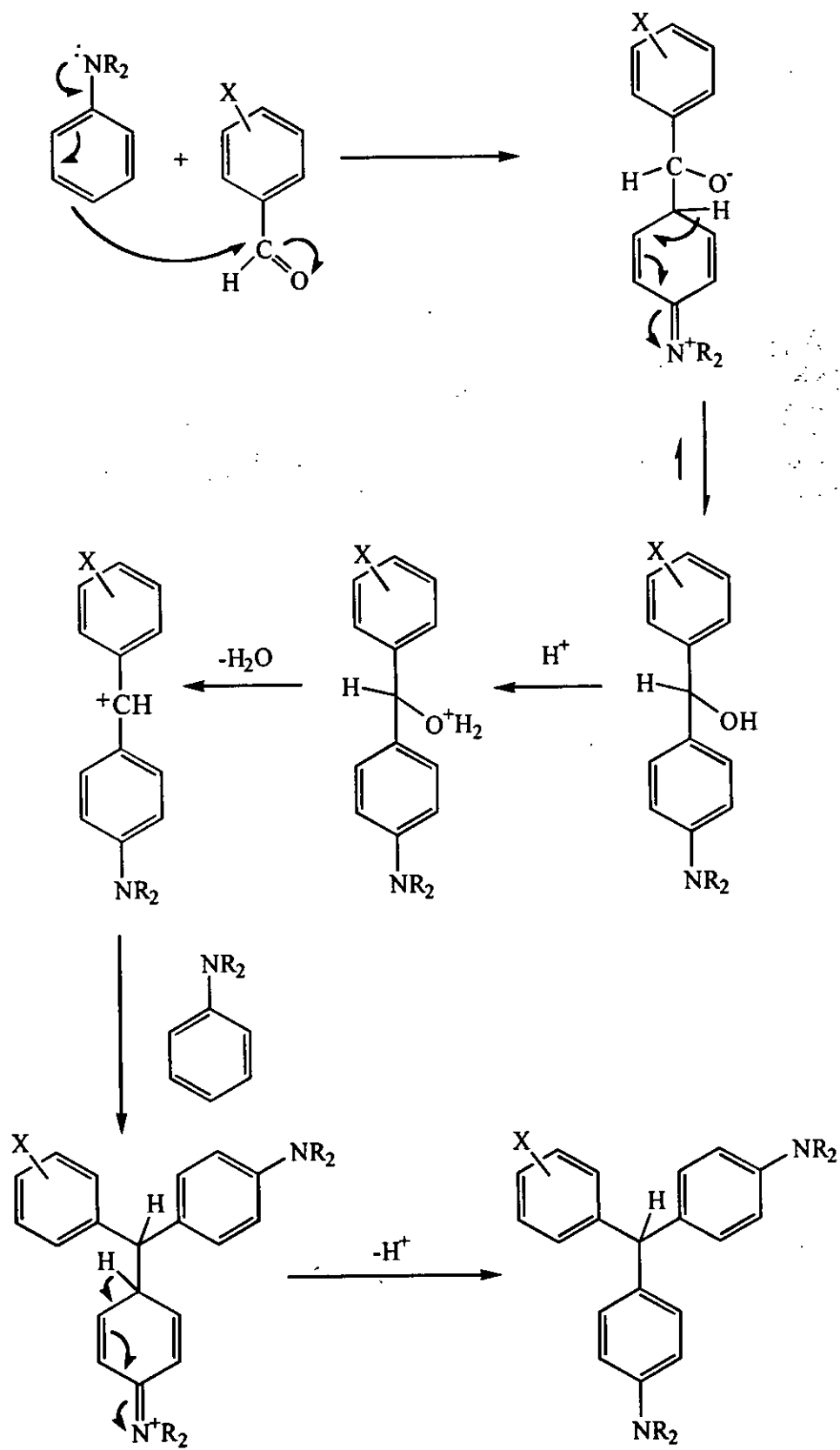
The formation of leuco bases, carbinols, benzophenones and their precursors will be discussed.

2.1.1 Preparation of Leuco Bases

There are two main routes for the preparation of a leuco base. The most widely used method involves the condensation of an excess of a tertiary amine with an aromatic aldehyde in the presence of an acid (61JCS1285). Ethanol is sometimes used to homogenise the mixture (49MI1).



The reaction mechanism is shown in Scheme 1.

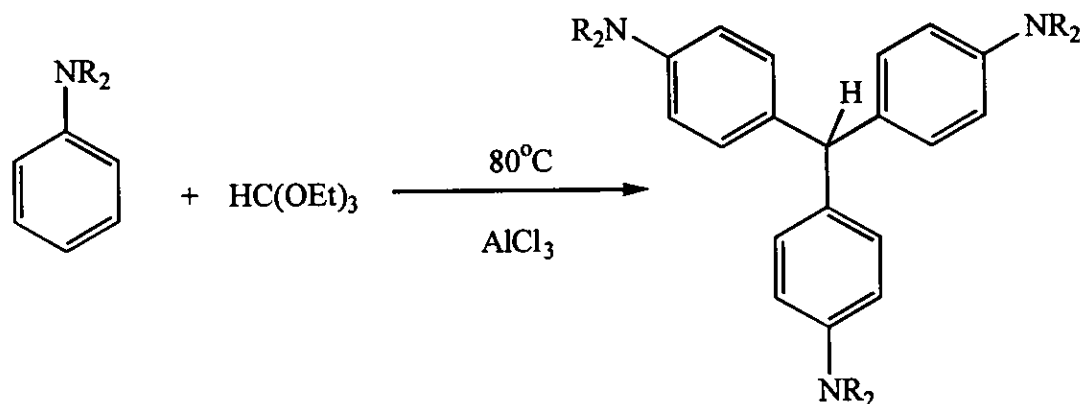


Scheme 1

Initially, a diarylmethanol intermediate is formed by the condensation of one mole of the arylamine with the aromatic aldehyde. Protonation and loss of water generates another cationic site allowing a second mole of the arylamine to react and produce the triarylmethane. The leuco base is then precipitated by neutralisation of the final reaction mixture with ethanolic ammonia. This acid-catalysed condensation of benzaldehydes and activated arenes has been used recently by Cano *et al.* for the ship-in-a-bottle synthesis of triarylmethyl cations during their work upon heterogeneous photosensitisers (96JA11006).

In a similar manner, three moles of an arylamine undergo an acid catalysed condensation with formaldehyde to generate a symmetrical leuco base (71MI1).

A further variant utilises the arylamine as both solvent and reagent in a Friedel-Crafts reaction catalysed by aluminium chloride, with triethyl orthoformate serving as the electrophilic species and the source of the central carbon atom.



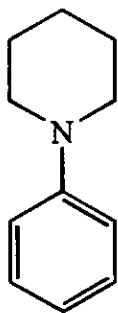
This route is particularly useful in the preparation of symmetrical leuco bases which are often difficult to make by other methods (31JCS118).

The leuco base requires oxidation in order to generate the dye cation and both lead dioxide and chloranil have been used for this purpose. The former leads to time consuming and difficult purification stages and so chloranil is preferable for small scale preparative work (62JA2349). Formation of the cation results from hydride ion transfer from the tertiary carbon atom of the leuco base. During this oxidative process, chloranil is reduced to the quinol.

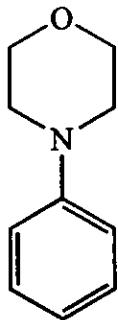
2.1.2 Preparation of intermediates and precursors

The unsymmetrical MG dye bases were prepared from a monosubstituted benzophenone by reaction with an aryllithium compound. The aryllithium compounds used in this study were prepared *in situ* by the addition of a substituted bromobenzene to an equimolar solution of *n*-BuLi in dry ether, cooled to -10°C . The mixture was then allowed to attain room temperature before being stirred for 30 minutes in order to generate the aryl-lithium species.

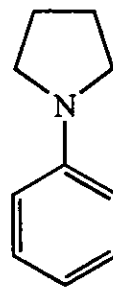
Piperidinobenzene (2.1-1), morpholinobenzene (2.1-2), 4-bromo-*N,N*-diethylaniline and 4-bromo-*N,N*-dimethylaniline were commercially available and were used as purchased from Aldrich Chemical Co., but pyrrolidinobenzene (2.1-3) had to be synthesised.



2.1-1

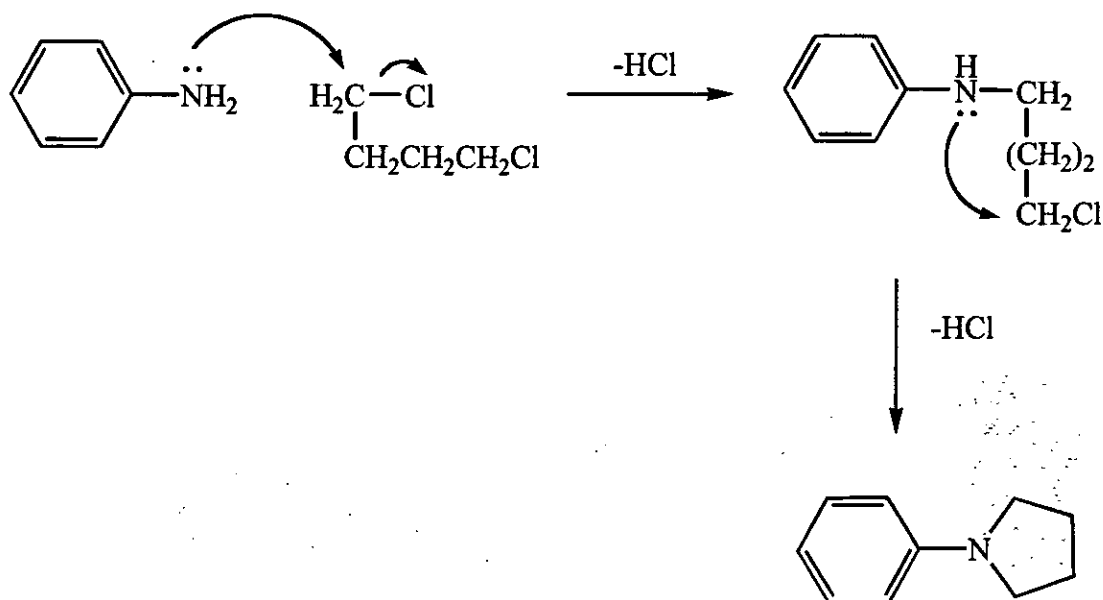


2.1-2

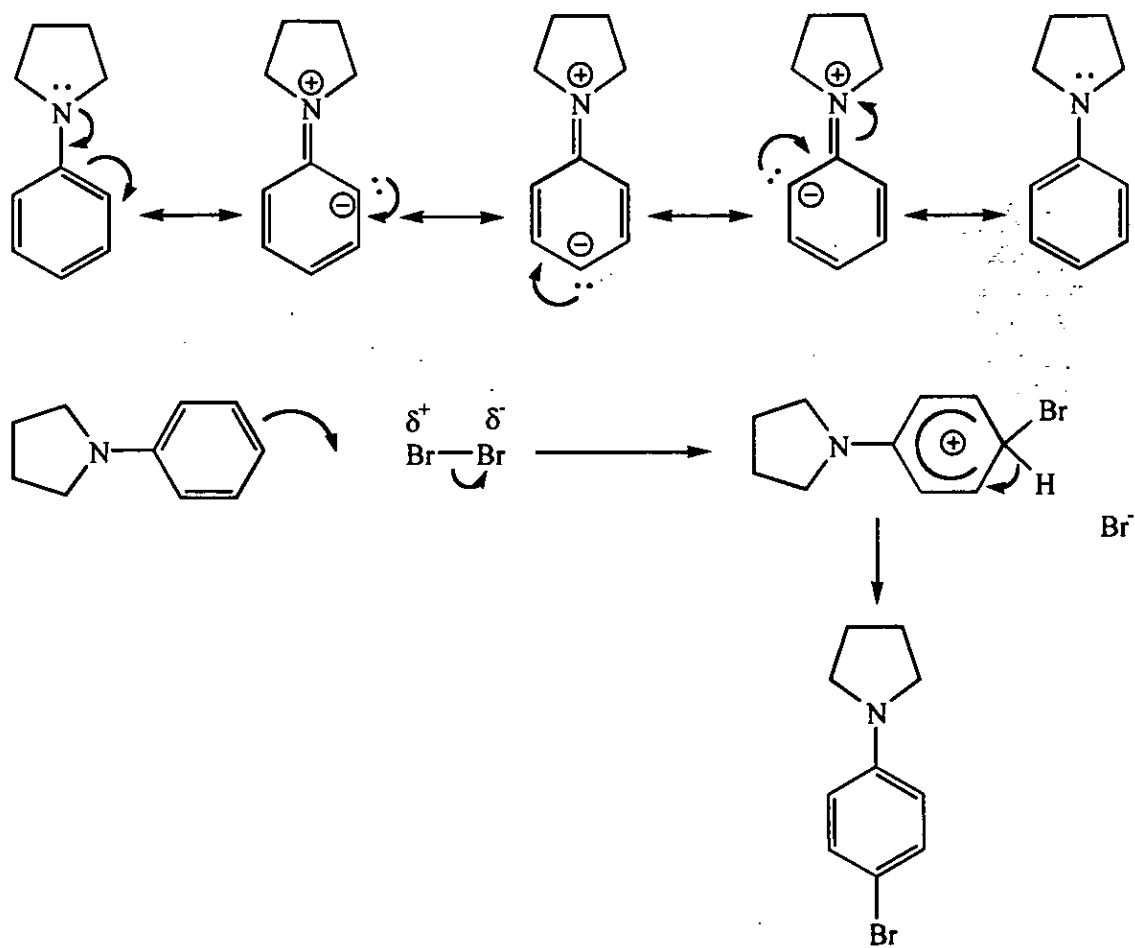


2.1-3

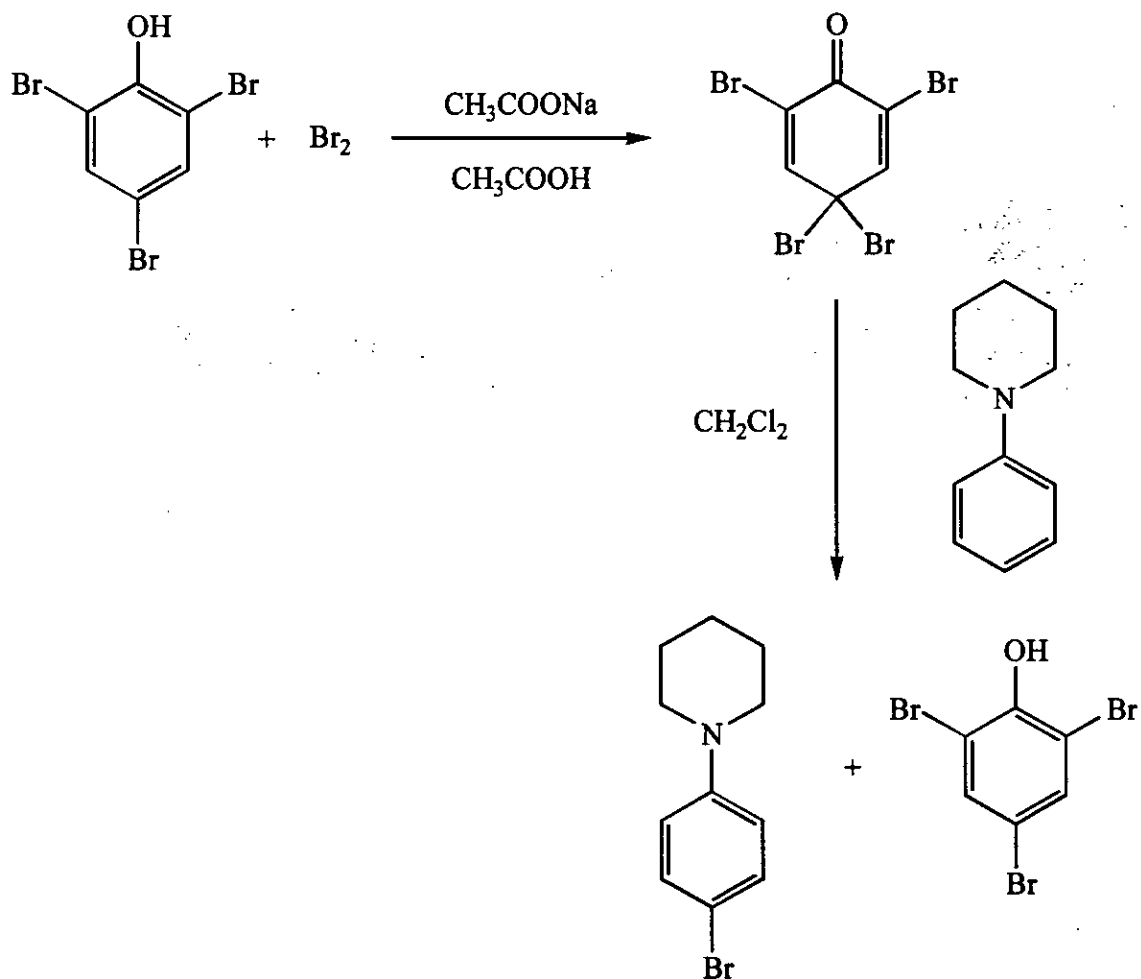
The nucleophilic attack of freshly distilled aniline on 1,4-dichlorobutane (30JA804) afforded pyrrolidinobenzene which was obtained as a pale yellow oil. Its purity and structure were supported by GC and mass spectroscopy which indicated an M^+ ion at 146 (m/z). A probable mechanism for the reaction is shown below.



Bromination of the aminobenzene compounds was conducted following one of two preparative routes. The first was by direct reaction with bromine and both 4-bromopyrrolidinobenzene and 4-bromomorpholinobenzene were prepared in this way. Although electrophilic aromatic bromination often requires assistance from a catalyst such as iron powder, arylamines are strongly activated towards electrophilic attack and the reaction is extremely facile. Thus, aniline itself readily yields 2,4,6-tribromoaniline, the amino function directing attack to the *ortho* and *para* positions as shown below. However, in the present work, good yields of the monobrominated amines were obtained. Presumably the bulky cycloalkylamino groups hinder attack at the *ortho* positions. Both 4-bromopyrrolidinobenzene and 4-bromomorpholinobenzene were characterised by their melting points and ^1H nmr spectra.



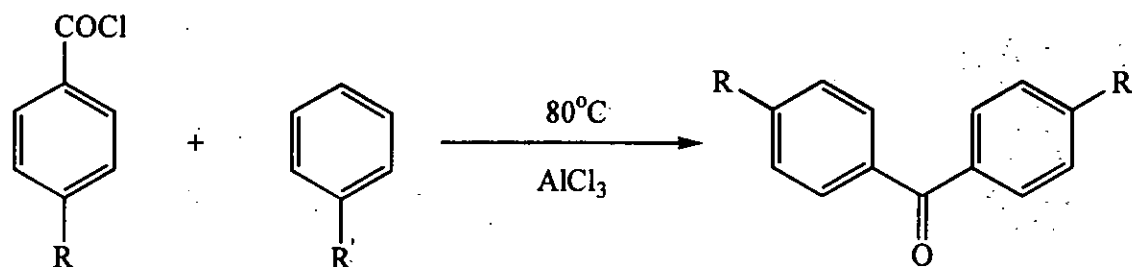
The second route employed for the bromination of certain aminobenzenes involved the use of 2,4,4,6-tetrabromocyclohexa-2,5-dien-1-one which is a brominating agent known for its efficiency at selectively brominating aromatic amines at the *para* position (71JCS3652). 4-Bromopiperidinobenzene was prepared in this manner as shown overleaf and was characterised by its melting point and its ^1H nmr spectrum.



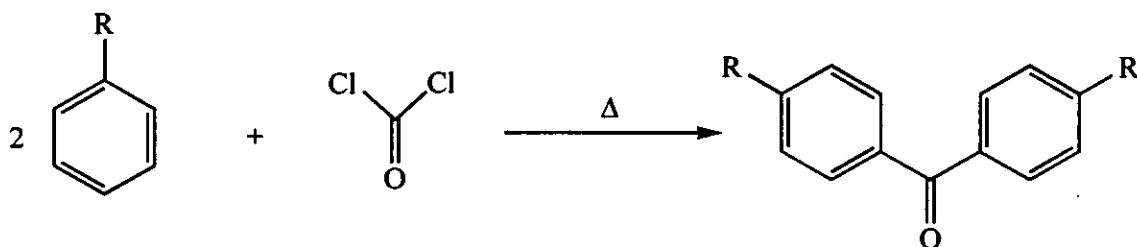
2,4,4,6-Tetrabromocyclohexa-2,5-dien-1-one was prepared by the bromination of 2,4,6-tribromophenol in the presence of sodium acetate trihydrate and glacial acetic acid following the method reported by Fox *et al.* (76OS20) and was prepared as required since it decomposes on storage.

2.1.3 Preparation of benzophenones

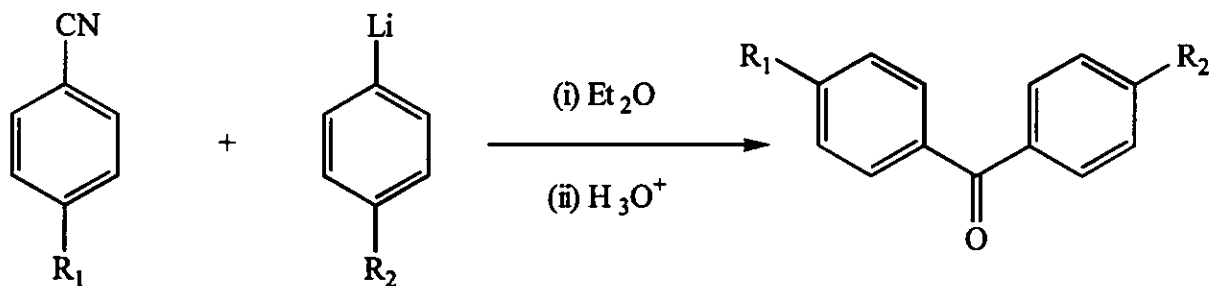
There are several routes available for the preparation of benzophenones. Friedel-Crafts electrophilic substitutions are commonly used to prepare both symmetrical and unsymmetrical ketones (77MI1).



A second method involves the condensation of two moles of an aromatic amine with either phosgene or formaldehyde. The extremely hazardous nature of phosgene results in other routes being preferred.



Organolithium compounds can also be used to prepare substituted benzophenones by reaction with benzonitriles (73JCS(P2)1792). The initial product of the reaction is a ketimine, which is subsequently hydrolysed in acid solution to generate the ketone.



However, the route used extensively in this study was the nucleophilic substitution of a 4-halo- or 4,4'-dihalo-benzophenone. This route was chosen because of its practical simplicity on a laboratory scale and the availability of the mono- and difluorobenzophenones. The analogous chlorobenzophenones are also available but are less reactive.

The symmetrically substituted benzophenones used in this study were prepared from 4,4'-difluorobenzophenone by refluxing in tetramethylenesulphone (sulfolane) with the appropriate amine. The experimental results are summarised in Table 2.3.

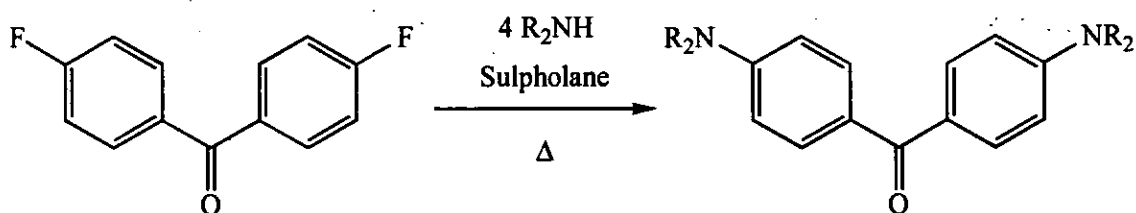


Table 2.3

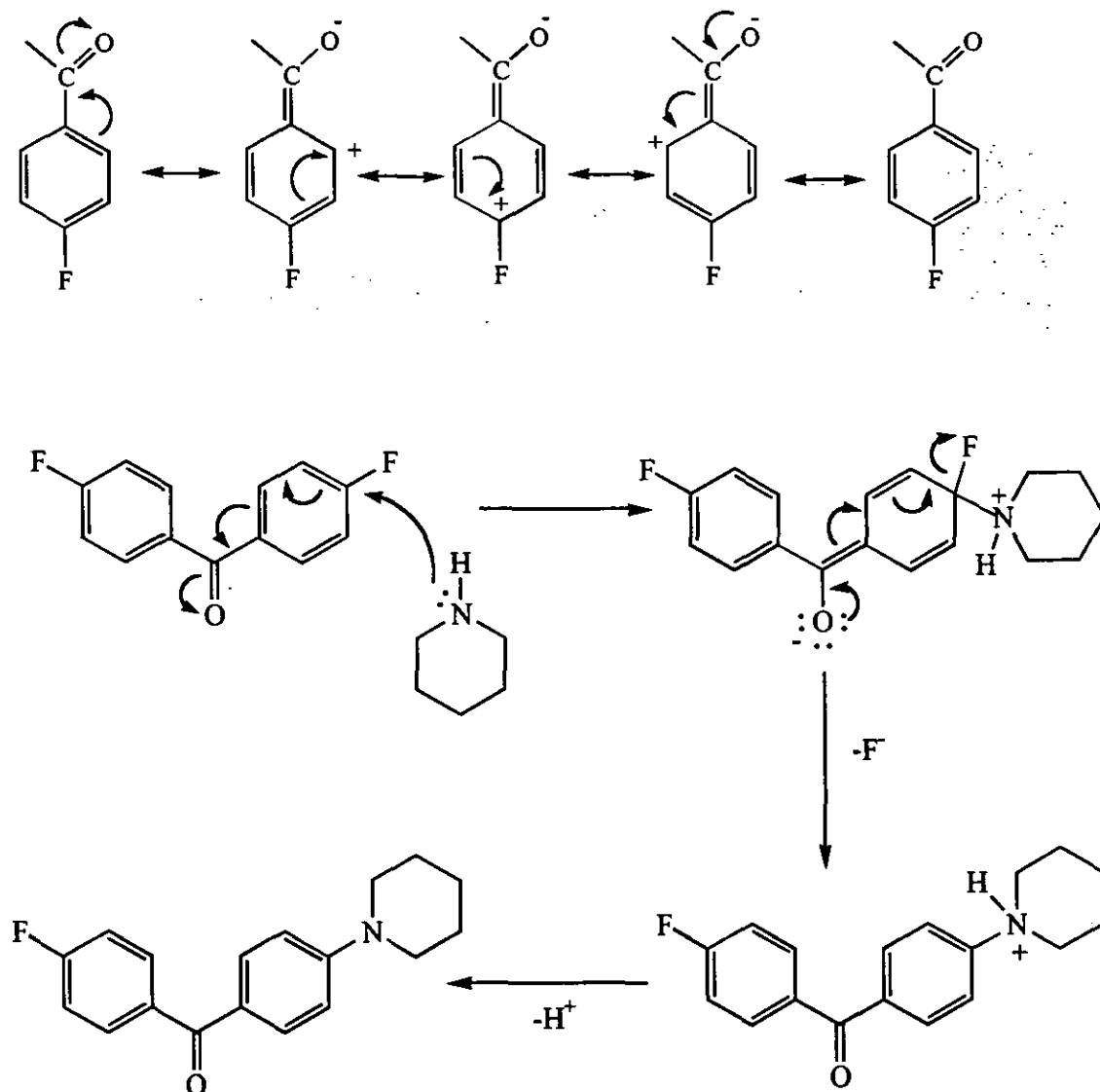
Preparative data for some 4,4'-diaminobenzophenones

Amine	Reaction time (hours)	Yield (%)
Piperidine	24	69
Morpholine	24	64
Pyrrolidine	24	58
<i>N</i> -Methylpiperazine	24	45

Commercially available 4,4'-dimethylaminobenzophenone was used as purchased from Aldrich Chemical Co., but 4,4'-diethylaminobenzophenone was quite crude and was purified prior to use by elution from alumina with dichloromethane.

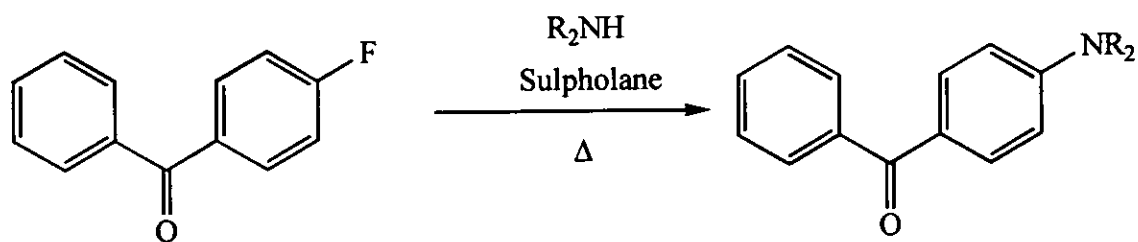
The preparation of the benzophenones was relatively straightforward. The high temperatures and long reaction times reflect the need for forcing conditions to accomplish replacement of both fluorine atoms. It might also be anticipated that for those amines that are liquids at room temperature, reacting the 4,4'-difluorobenzophenone directly with the liquid amine at or near its boiling point might reduce the reaction time, but this was not attempted. The electron withdrawing property

of the carbonyl group, illustrated by the following resonance structures, facilitates nucleophilic attack by the amine and the following reaction mechanism may be formulated using piperidine as the attacking amine.



Substitution then occurs at the second fluorophenyl group to produce the di-substituted amino compound. TLC of the final reaction mixture did not show the presence of any mono-substituted product which could arise through incomplete conversion.

The mono-substituted benzophenones used in this study were prepared by nucleophilic substitution of the 4-fluorobenzophenone:



The preparative data are shown in Table 2.4.

Table 2.4
Preparative data for some 4-aminobenzophenones

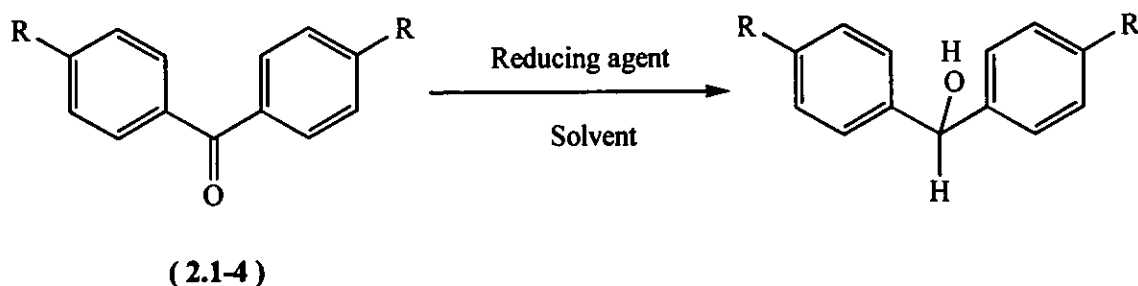
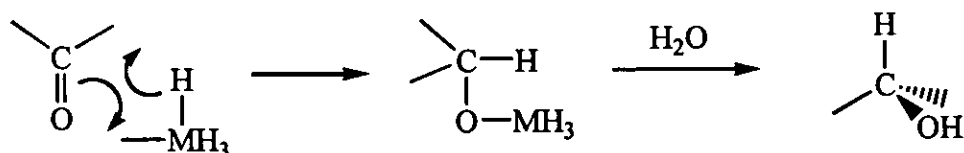
Amine	Reaction time (hours)	Yield %
Piperidine	5	70
Pyrrolidine	6	74
Morpholine	7	68
<i>N</i> -Methylpiperazine	24	50
Thiomorpholine	14	55

As expected, the reaction times required for mono-substitution were, for the most part, significantly shorter than those for the disubstituted product, but yields were comparable. 4-Dimethylaminobenzophenone was commercially available and was used as purchased from Aldrich Chemical Co.

2.1.4 Preparation of diarylcarbinols

There are variety of routes to diarylcarbinols and the choice of method normally depends on the availability of the precursors. Both symmetrical and unsymmetrical diarylcarbinols can be formed by reaction of an organolithium compound with a substituted benzaldehyde. Other routes to diarylcarbinols involve the oxidation of a diphenylmethane or the reduction of a benzophenone. The availability of substituted benzophenones results in their reduction being one of the most popular routes to benzhydrols and the diarylcarbinols used in this study were prepared by this method.

The most common reducing agents for the process are sodium borohydride (NaBH_4) and lithium aluminium hydride (LiAlH_4) (49JA122). Both function by facilitating a nucleophilic attack on the carbonyl carbon by a hydride ion in the form of the metal hydride (BH_4^- or AlH_4^-) as shown (77MI1). It has been shown that, in certain cases, the presence of the cation is essential for the reaction to occur. Effective removal of the Li^+ from LiAlH_4 by addition of a crown ether inhibits the reducing ability of the metal hydride (74T2317). From a practical viewpoint, NaBH_4 is easier to handle than LiAlH_4 .



The ease of reduction of the 4,4'-diaminobenzophenone was found to be dependent upon the nature of the amino-group. For example, Michler's ketone was reduced to the carbinol within a couple of hours using sodium borohydride in ethanol whereas for the diethylamino derivative substantially larger amounts of reducing agent were required, coupled with longer reaction times and the use of propan-2-ol as the solvent to achieve higher refluxing temperatures. For the pyrrolidino-, morpholino- and *N*-methylpiperazino-benzophenones, the effectiveness of NaBH₄ as the reducing agent proved to be less than satisfactory with low, unreliable yields, even with long reaction times and large amounts of reducing agent. In the case of 4,4'-dipiperidinobenzophenone, the yields were consistent but only moderate. As a result, the reducing agent sodium bis(2-methoxyethoxy)aluminium hydride (Red-al) was used in a modification of the published procedure (73JCE154) and produced quite satisfactory and consistent yields of the pyrrolidino, morpholino and *N*-methylpiperazino compounds. The reaction temperature for the reductions employing Red-al was maintained around 80°C since it has been reported that temperatures much greater than this may result in the reduction of the ketone to the substituted diphenylmethane (74CCCC842). The preparative data are shown in Table 2.5. The diarylcarbinols prepared during this study were purified by recrystallisation and were characterised by microanalysis and melting point data. 4,4'-Bis(dimethylamino)benzhydrol was characterised by its melting point alone since it is a well authenticated compound.

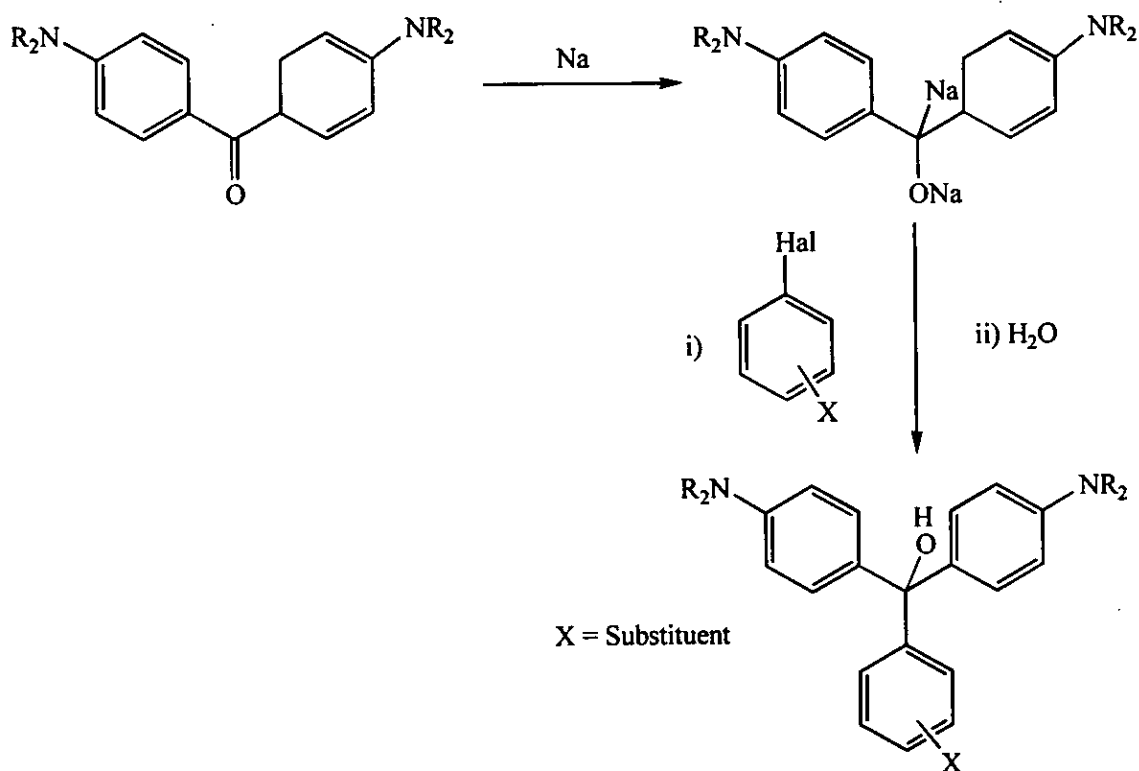
Table 2.5**Preparative data for the reduction of some 4,4'-diaminobenzophenones**

R in 2.1-4	Reagent	Solvent	Reaction time (hours)	Yield of hydrol %
NMe ₂	NaBH ₄	Ethanol	3	46
NEt ₂	NaBH ₄	Propan-2-ol	7 - 48	48 - 76
Pyrrolidino	NaBH ₄	Propan-2-ol	10 - 48	15 - 30
	Red-al	Toluene	2	73
Piperidino	NaBH ₄	Propan-2-ol	24 - 48	48 - 55
Morpholino	NaBH ₄	Propan-2-ol	24 - 48	15 - 20
	Red-al	Toluene	2	80
<i>N</i> -Methylpiperazino	NaBH ₄	Propan-2-ol	24 - 48	10 - 15
	Red-al	Toluene	2	57

The reactivity and selectivity of NaBH₄ may be increased by the formation of complexes such as sodium borohydride-palladium chloride (81BCJ1029), sulfurated borohydrides (68CJC2754, 70CJC2366, 72CJC526) and by adsorption of NaBH₄ on alumina. Preliminary investigations into the use of sulfurated borohydrides as a reducing agent for the substituted benzophenones used in this study suggested little or no improvement on the efficacy of sodium borohydride; however, a more involved investigation would be required to enable anything conclusive to be established.

2.1.5 Preparation of triarylcannabinols

There are several methods available for the preparation of triarylcannabinols. One of the earliest methods, reported by Rodd and Linch (27JCS2174), involved the reaction between a substituted diaryl ketone and an aryl aldehyde in the presence of metallic sodium. The reaction is shown in Scheme 3. However, this method produces relatively impure products and cannot be used in the presence of active hydrogen because of direct reaction with the sodium metal.



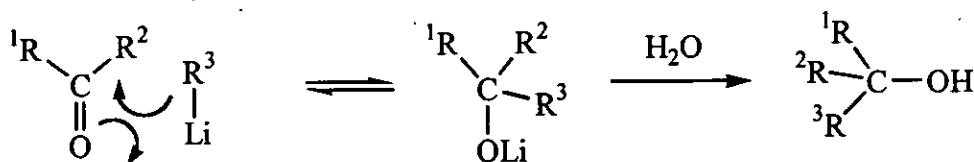
Scheme 3

In recent years, the use of organometallic compounds has become increasingly popular for the generation of di- and tri-arylcannabinols. Grignard reagents have a limited application unlike the more reactive organolithium compounds which form the basis of the principal synthetic route.

Organolithium compounds are extremely sensitive to air and moisture and must therefore be handled in anhydrous conditions under an inert atmosphere. As a result, the

organolithium compound is usually formed *in situ* before reaction with the electrophilic compound.

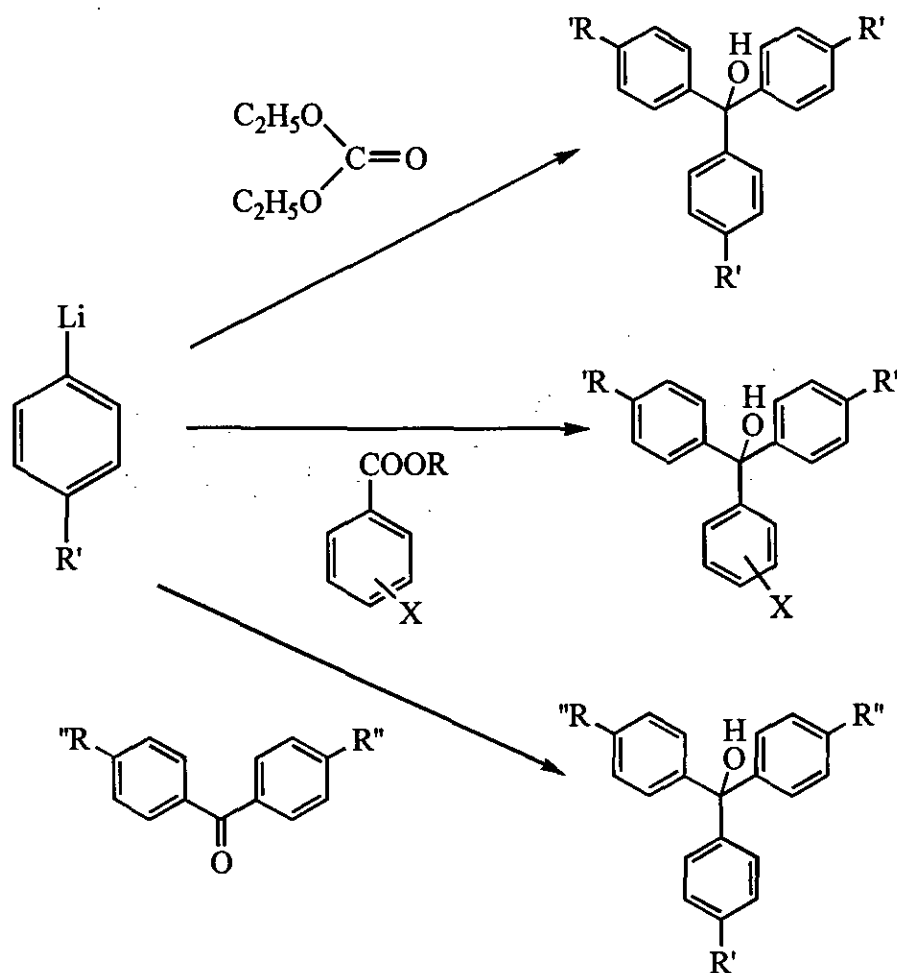
One method for the preparation of an organolithium compound is by the reaction of an aryl halide with freshly cut lithium metal in dry diethyl ether or tetrahydrofuran (THF) under nitrogen. More often, though, use is made of transmetalation with the source of lithium being *n*-butyllithium (*n*-BuLi). The mechanism for these types of reactions involves attack by the nucleophilic carbon of the organolithium compound at the electron deficient carbon of, say, a ketone as shown in Scheme 4.



Scheme 4

An equilibrium exists between the metallated and non-metallated aryl species. Sometimes only low yields of the products are obtained using this method because steric and/or electronic factors may result in the position of the equilibrium favouring the starting situation. To increase the reactivity of *n*-BuLi, a complex can be formed with tetramethylethylenediamine (TMEDA) (69CI620). The use of TMEDA produces reactive monomeric units of *n*-BuLi, whereas in ethereal solutions, the *n*-BuLi exists in bulkier, polymeric units (63JCS2058, 94T5861, 94T5903). Several studies have been conducted into the influence of solvent upon the degree of association of alkyllithium compounds and their consequent reactivity (63TFS2058, 70JA4664, 94T5861, 94T5903).

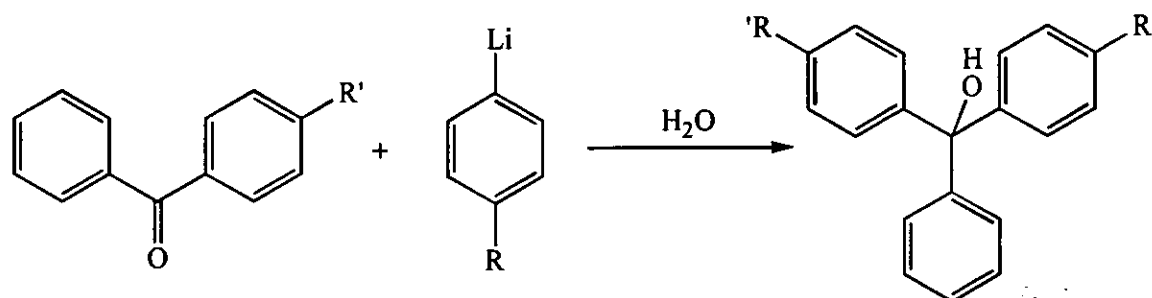
The electrophilic species which reacts with the organolithium compound can be chosen from an organic carbonate, an ester, ketone or aldehyde. Whilst the last substrate leads only to a diarylmethanol, the others lead to triarylmethanols in which the substituents can be identical or different depending on the substrate as illustrated in Scheme 5.



Scheme 5

These routes have been used previously to prepare symmetrical analogues of CV type dyes (81Th1), analogues of CV type dyes with mixed terminal groups (82Th1) and analogues of MG type dyes (82Th1).

For the unsymmetrical analogues of MG prepared in this study, a mono-substituted benzophenone was reacted with an appropriately substituted aryllithium compound, as shown where R^1 and R^2 are different and are selected from NMe_2 , NEt_2 , piperidino, pyrrolidino, morpholino, *N*-methylpiperazino and thiomorpholino.



Preparation of the organolithium compound was conducted in diethyl ether which had been cooled to $-10\text{ }^{\circ}\text{C}$ and was under an inert atmosphere of nitrogen. To this was added the *n*-butyl-lithium. After stirring for five minutes, TMEDA was added to the solution. This mixture was stirred for ten minutes, after which time a solution of the appropriate bromoamine in diethyl ether was added. This mixture was allowed to attain room temperature over a period of 15 minutes. A contact time of a further 30 minutes gave a solution of the aryl-lithium. It has been reported in the literature that for the bromine-lithium exchange of 4-bromo-*N,N*-dimethylamine with *n*-BuLi several side reactions may take place if the reaction is allowed to proceed for extended periods or at elevated temperatures (70JOC3756). However, the preparative method employed has been used extensively (81Th1, 82Th1, 86JSDC15, 89JCS(P2)1087) for similar systems without report of any such interferences. Indeed, no side reaction products were observed during the current preparative work.

The nature of the halogen in the halogen-metal exchange interconversion is limited almost entirely to the iodides and bromides. In general, chlorides and fluorides do not undergo metal-halogen exchange (51MI1, 74MI2). The bromides were chosen for this study for several reasons. Firstly their preparation is relatively straightforward and has been used successfully for similar studies (81Th1, 82Th1, 86JSDC15, 89JCS(P2)1087) and secondly, purification of the resulting product will be easier since the iodides, whilst undergoing metal-halogen interconversion at a greater rate and in higher yields, tend to also under coupling reactions more readily than the bromides (41JA545, 51MI1, 83Th2, 74MI2).

The 4-aminobenzophenone was then added to the aryllithium reagent thus formed and the reaction mixture stirred at room temperature for 2 - 3 hours. After the reaction was finished, the reaction mixture was worked up as detailed in the Experimental Section. In

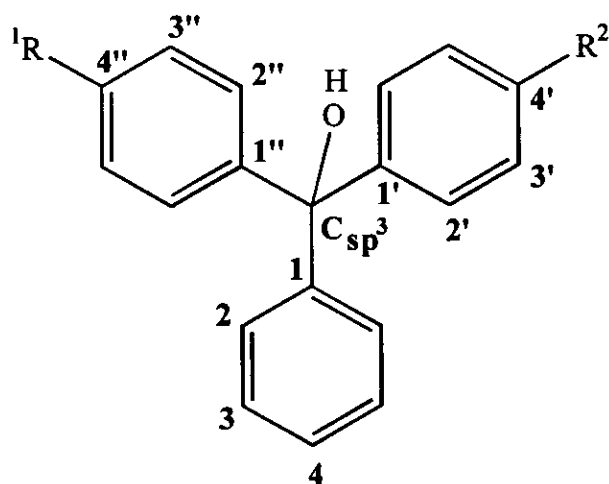
all cases, the crude product was obtained as an oil which failed to solidify without further treatment. The oils were encouraged to solidify by contacting them with a small volume of non-polar solvent to which had been added a drop of polar solvent. The flasks were then sealed and stored in the refrigerator for up to several weeks. For the dyes which solidified, several recrystallisations of the crude material were sufficient to purify these dyes. However, this method failed for seven out of the sixteen carbinols and flash column chromatography was necessary to purify these dyes. The early attempts at flash chromatography of the impure dyes were hampered by the carbinols forming brightly coloured cations and becoming irreversibly bound to the silica gel. This behaviour was prevented in one of two ways: either the silica gel was washed with triethylamine prior to elution of the dye or triethylamine was incorporated into the mobile phase of the column. For certain of the oils this treatment failed, Brockman I standard grade aluminium oxide (activated, neutral) was then used, since this has been found satisfactory for dye systems (69JCS(B)1068, 70JCS(B)979, 70JSDC200). However, the use of alumina as the stationary phase failed to give pure dyes in this study.

It has also been reported in the literature that the methyl ethers of TPM dyes are readily purified (69JSDC310, 77JSDC451). Preparation of the methyl ethers was attempted by the slow addition of a methanolic solution of the dye into methanol containing sodium methoxide, but only an impure green oil separated and therefore this technique was abandoned. Since previous workers have encountered problems with the purification of certain triphenylmethane dye bases, it was decided to suspend further work into the purification of the dye bases and attempt to generate the pure perchlorate salt by the methods illustrated in the Experimental Section.

The preparation of the unsymmetrical MG Me-Et has been reported previously using 4-diethylamino-4'-dimethylaminobenzophenone as the key intermediate. Several routes were investigated for the preparation of the dye but with mixed results. The Friedel-Crafts reaction between 4-dimethylaminobenzoyl chloride and *N,N*-diethylaniline and the reaction of 4-lithio-*N,N*-dimethylaniline with 4-diethylaminobenzonitrile both produced low yields of product as did the equivalent reaction with 4-lithio-*N,N*-diethylaniline (86JSDC15). The reaction between 4-diethylaminobenzoic acid and 4-dimethylaminophenyllithium produced a complex mixture of products. The route successfully employed was the interaction between 4-diethylaminophenyllithium and 4-dimethylaminobenzaldehyde to generate the unsymmetrically substituted

diphenylmethanol. Oxidation of this using chloranil produced the ketone and subsequent reaction with phenyllithium generated the TPM dye base. The routes investigated previously (86JSDC15) differ from the current method in that for this study a mono-substituted benzophenone was reacted with the appropriately substituted aryllithium compound. The present route produced satisfactory yields with simple reaction mixtures. None of the problems of low yields or complex reaction mixtures were encountered for the method currently used.

The carbinols prepared in this study were characterised by microanalysis and/or their ^1H and ^{13}C nmr spectra.



(2.1-5)

The ^{13}C chemical shifts for the analogues of 2.1-5 are shown overleaf in Tables 2.6 and 2.7.

Table 2.6
¹³C chemical shifts (ppm) for the carbinols (2.1-5)

Dye	R ¹	R ²	Csp ³	1''	2''	3''	4''	1'	2'	3'	4'	1	2	3	4
Me-Et	NEt ₂	NMe ₂	82.0	134.8	129.6	111.2	147.2	136.1	129.3	112.2	149.9	148.5	127.1	128.3	128.1
Py-Et	Pyr. ^a	NEt ₂	82.1	133.6	129.6	111.2	147.2	134.9	129.4	111.3	147.3	148.6	127.0	128.3	128.0
Pi-Et	NEt ₂	Pip. ^b	82.0	134.6	129.6	111.2	147.2	138.5	129.2	115.8	151.4	148.3	127.1	128.3	128.1
Mo-Et	NEt ₂	Mo. ^c	81.9 (81.2) ^f	134.4 (135.5) ^f	129.6 (129.6) ^f	111.2 (111.1) ^f	147.3 (147.0) ^f	139.5 (140.2) ^f	129.3 (129.3) ^f	115.1 (114.8) ^f	150.4 (150.6) ^f	148.2 (149.6) ^f	127.2 (126.8) ^f	128.6 (128.5) ^f	128.3 (127.8) ^f
Me-Py	Pyr. ^a	NMe ₂	82.1	133.3	129.5	111.3	147.3	135.9	129.4	112.2	149.9	148.2	127.5	128.3	128.1
Pi-Py	Pyr. ^a	Pip. ^b	87.1	135.2	130.9	111.0	147.0	130.5	130.1	115.6	151.0	146.6	126.6	128.4	128.0
Mo-Py	Pyr. ^a	Mo. ^c	82.0	134.6	129.4	111.2	147.4	139.6	129.3	115.1	150.4	148.2	127.2	128.3	128.1
Me-Pi	NMe ₂	Pip. ^b	82.0	135.9	129.3	112.1	149.9	138.4	129.2	115.8	151.4	148.2	127.2	128.3	128.1
Mo-Pi	Mo. ^c	Pip. ^b	81.9	138.0	129.1	115.1	151.4	139.2	129.3	115.8	150.4	147.9	127.3	128.2	128.1
Me-Mo	NMe ₂	Mo. ^c	81.9	135.7	129.3	112.1	150.0	139.4	129.3	115.1	150.4	148.1	127.3	128.3	128.2
MPz-Et	NEt ₂	MPz. ^d	81.9	134.5	129.6	111.2	147.2	139.1	129.3	115.4	150.4	148.3	127.1	128.3	128.1
MPz-Me	NMe ₂	MPz. ^d	81.9	135.8	129.3	112.1	150.0	139.0	129.3	115.4	150.4	148.2	127.2	128.3	128.1
MPz-Py	Pyr. ^a	MPz. ^d	82.0	134.7	129.5	111.2	147.3	139.2	129.3	115.4	150.4	148.3	127.1	128.3	128.1
MPz-Pi	MPz. ^d	Pip. ^b	81.9	138.1	129.2	115.4	151.4	138.8	129.3	115.8	150.5	148.0	127.3	128.3	128.2
MPz-Mo	Mo. ^c	MPz. ^d	81.9	139.5	129.3	115.1	150.5	139.1	129.2	115.4	150.4	147.9	127.4	128.2	128.2
ThM-Me	NMe ₂	ThM. ^e	81.9	135.7	129.3	112.2	150.0	139.2	129.4	116.5	150.4	148.1	127.3	128.3	128.2

a. Pyrrolidine
b. Piperidine

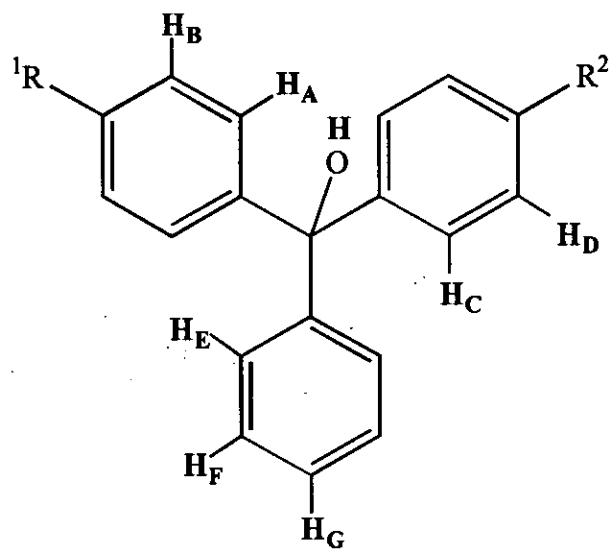
c. Morpholine
d. N-Methylpiperazine

e. Thiomorpholine
f. Spectrum run in acetone-d₆

Table 2.7
¹³C chemical shifts (ppm) for the carbinols (2.1-5)

Dye	R ¹	R ²	NMe ₂	NEt ₂		Pyrrolidine		Piperidine			Morpholine		N-Methylpiperazine			
			CH ₃	CH ₂	CH ₃	NCH ₂	CH ₂	NCH ₂	CH ₂	γ-CH ₂	NCH ₂	CH ₂ O	NCH ₂	CH ₂ N	NCH ₃	
Me-Et	NEt ₂	NMe ₂	41.1	44.7	13.1	-	-	-	-	-	-	-	-	-	-	-
Py-Et	Pyr. ^a	NEt ₂	-	44.8	13.1	48.1	26.0	-	-	-	-	-	-	-	-	-
Pi-Et	NEt ₂	Pip. ^b	-	44.7	13.1	-	-	50.9	26.3	24.8	-	-	-	-	-	-
Mo-Et	NEt ₂	Mo. ^c	-	44.7 (44.5) ^g	13.1 (12.7) ^g	-	-	-	-	-	49.6 (49.6) ^g	67.4 (67.1) ^g	-	-	-	-
Me-Py	Pyr. ^a	NMe ₂	41.1	-	-	48.1	26.0	-	-	-	-	-	-	-	-	-
Pi-Py	Pyr. ^a	Pip. ^b	-	-	-	48.0	26.0	50.8	26.4	24.8	-	-	-	-	-	-
Mo-Py	Pyr. ^a	Mo. ^c	-	-	-	48.0	26.0	-	-	-	49.6	67.4	-	-	-	-
Me-Pi	NMe ₂	Pip. ^b	41.0	-	-	-	-	50.8	26.3	24.8	-	-	-	-	-	-
Mo-Pi	Pip. ^b	Mo. ^c	-	-	-	-	-	50.7	26.3	24.7	49.5	67.3	-	-	-	-
Me-Mo	NMe ₂	Mo. ^c	41.0	-	-	-	-	-	-	-	49.6	67.4	-	-	-	-
MPz-Et	NEt ₂	MPz. ^d	-	44.7	13.1	-	-	-	-	-	-	-	55.6	49.3	46.7	-
MPz-Me	NMe ₂	MPz. ^d	41.0	-	-	-	-	-	-	-	-	-	55.6	49.2	46.7	-
MPz-Py	Pyr. ^a	MPz. ^d	-	-	-	48.0	26.0	-	-	-	-	-	55.6	49.3	46.6	-
MPz-Pi	Pip. ^b	MPz. ^d	-	-	-	-	-	50.7	26.3	24.7	-	-	55.6	49.2	46.6	-
MPz-Mo	Mo. ^c	MPz. ^d	-	-	-	-	-	-	-	-	49.5	67.4	55.6	49.2	46.6	-
ThM-Me	NMe ₂	ThM. ^e	41.0	-	-	-	-	-	-	-	52.4 ^f	27.2 ^f	-	-	-	-

a. Pyrrolidine b. Piperidine c. Morpholine d. N-Methylpiperazine e. Thiomorpholine f. For the thiomorpholine analogue g. Spectrum run in acetone-d₆



(2.1-6)

The ¹H chemical shifts for the analogues of 2.1-6 are shown overleaf in Tables 2.8 and 2.9.

Table 2.8
¹H chemical shifts (ppm) for the carbinols (2.1-6)

Dye	R ¹	R ²	OH	H _A	H _B	H _C	H _D	H _E , H _F , H _G
Me-Et	NEt ₂	NMe ₂	2.70	7.18	6.64	7.11	6.71	7.30 - 7.37
Py-Et	Pyr. ^a	NEt ₂	n.o. ^f	7.18	6.57	7.11	6.62	7.28 - 7.39
Pi-Et	NEt ₂	Pip. ^b	2.61	7.10	6.64	7.20	6.91	7.28 - 7.37
Mo-Et	NEt ₂	Mo. ^c	2.81 (n.o.) ^g	7.08 (7.20) ^g	6.63 (6.75) ^g	7.25 (7.33) ^g	6.88 (7.01) ^g	7.28 - 7.39 (7.38 - 7.53) ^g
Me-Py	Pyr. ^a	NMe ₂	3.14	7.09- 7.14	6.54	7.09- 7.14	6.77	7.21 - 7.39
Pi-Py	Pyr. ^a	Pip. ^b	3.10	7.54	6.54	7.21- 7.36	6.89	7.21 - 7.36
Mo-Py	Pyr. ^a	Mo. ^c	2.77	7.12	6.53	7.23	6.88	7.27 - 7.37
Me-Pi	NMe ₂	Pip. ^b	2.71	7.13- 7.18	6.69	7.13- 7.18	6.89	7.30 - 7.36
Mo-Pi	Pip. ^b	Mo. ^c	2.66	7.01	6.74- 6.79	7.05	6.74- 6.79	7.16 - 7.22
Me-Mo	NMe ₂	Mo. ^c	2.80	7.14	6.70	7.22	6.88	7.30 - 7.36
MPz-Et	NEt ₂	MPz. ^d	2.89	7.09	6.62	7.21	6.88	7.30 - 7.38
MPz-Me	NMe ₂	MPz. ^d	2.85	7.13	6.69	7.19	6.88	7.29 - 7.37
MPz-Py	Pyr. ^a	MPz. ^d	n.o. ^e	7.12	6.53	7.21	6.88	7.27 - 7.38
MPz-Pi	Pip. ^b	MPz. ^d	2.81	7.15	6.88	7.15	6.88	7.27 - 7.34
MPz-Mo	Mo. ^c	MPz. ^d	2.89	7.17	6.87	7.17	6.88	7.30 - 7.33
ThM-Me	NMe ₂	ThM. ^e	n.o. ^e	7.14	6.70	7.20	6.85	7.30 - 7.36

a. Pyrrolidine
b. Piperidine

c. Morpholine
d. *N*-Methylpiperazine

e. Thiomorpholine
f. Not observed

g. Spectrum run in acetone-d₆

Table 2.9
¹H chemical shifts (ppm) for the carbinols (2.1-6)

Dye	R ¹	R ²	NMe ₂	NEt ₂		Pyrrolidine		Piperidine			Morpholine		N-Methylpiperazine		
			NCH ₃	NCH ₂	CH ₃	NCH ₂	CH ₂	NCH ₂	CH ₂	γ-CH ₂	NCH ₂	CH ₂ O	NCH ₂	CH ₂ N	NCH ₃
Me-Et	NEt ₂	NMe ₂	2.99	3.38	1.20	-	-	-	-	-	-	-	-	-	-
Py-Et	Pyr. ^a	NEt ₂	-	3.39	1.19	3.32	2.03	-	-	-	-	-	-	-	-
Pi-Et	NEt ₂	Pip. ^b	-	3.39	1.21	-	-	3.21	1.75	1.64	-	-	-	-	-
Mo-Et	NEt ₂	Mo. ^c	-	3.38 (3.52) ^g	1.20 (1.28) ^g	-	-	-	-	-	3.19 (3.26) ^g	3.89 (3.91) ^g	-	-	-
Me-Py	Pyr. ^a	NMe ₂	3.00	-	-	3.34	2.08	-	-	-	-	-	-	-	-
Pi-Py	Pyr. ^a	Pip. ^b	-	-	-	3.33	2.03	3.19	1.74	1.61	-	-	-	-	-
Mo-Py	Pyr. ^a	Mo. ^c	-	-	-	3.32	2.03	-	-	-	3.19	3.89	-	-	-
Me-Pi	NMe ₂	Pip. ^b	2.98	-	-	-	-	3.19	1.73	1.65	-	-	-	-	-
Mo-Pi	Pip. ^b	Mo. ^c	-	-	-	-	-	3.07	1.63	1.49	3.07	3.77	-	-	-
Me-Mo	NMe ₂	Mo. ^c	2.99	-	-	-	-	-	-	-	3.19	3.89	-	-	-
MPz-Et	NEt ₂	MPz. ^d	-	3.39	1.19	-	-	-	-	-	-	-	3.22	2.60	2.38
MPz-Me	NMe ₂	MPz. ^d	2.98	-	-	-	-	-	-	-	-	-	3.24	2.60	2.38
MPz-Py	Pyr. ^a	MPz. ^d	-	-	-	3.32	2.03	-	-	-	-	-	3.24	2.60	2.38
MPz-Pi	Pip. ^b	MPz. ^d	-	-	-	-	-	3.17-3.26	1.71	1.62	-	-	3.17-3.26	2.60	2.38
MPz-Mo	Mo. ^c	MPz. ^d	-	-	-	-	-	-	-	-	3.17-3.26	3.89	3.17-3.26	2.60	2.38
ThM-Me	NMe ₂	ThM. ^e	2.98	-	-	-	-	-	-	-	3.58 ^f	2.77 ^f	-	-	-

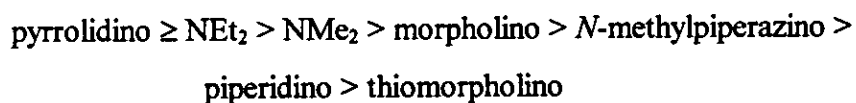
a. Pyrrolidine b. Piperidine c. Morpholine d. N-Methylpiperazine e. Thiomorpholine f. For the thiomorpholine analogue g. Spectrum run in acetone-d₆

The ^1H and ^{13}C nmr spectra for the carbinols were run in deuterated chloroform which had been stored over sodium hydroxide in order to prevent the formation of the cation during analysis. Tiny amounts of acidic substances in the chloroform have caused problems for previous workers (77JOC1657).

The ^1H and ^{13}C nmr spectra for the carbinols were interpreted using data obtained from the literature for similar systems (71T735, 80CJC339, 86TL5657, 90MRC1011, 95JA12889, 95JOC5016, 96MC895, 96MRC395).

It can be seen from the data presented in Tables 2.6 - 2.9 that certain trends can be established for the influence of the terminal amino group on the electronic density of the ring system. Similarly to the work by Nash (64JPC832), Eastes (71JOC3847) and Effenberger (78T2409), the donor strength of the terminal amino function can be correlated with the π -electron density of the phenyl ring as reflected by the chemical shifts. Conjugation with the phenyl ring results in an increase in electron density at the ring positions *ortho* and *para* to the carbon bearing the amino group, which results in shielding at these positions as reflected by the chemical shift data. In addition to the electronic considerations, steric inhibition of conjugation has been shown to have a marked effect on ring shieldings in the ^1H and ^{13}C nmr spectra of mono-substituted benzenes (61JCP731, 63CJC2339, 63JCP1415, 63JCP1432).

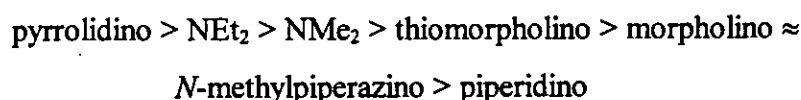
Considering the ^{13}C chemical shifts of the carbon atoms adjacent to the amine bearing carbon atom, the ability of the terminal amino group to conjugate with the phenyl ring is greatest with pyrrolidino and diethylamino and decreases in the order



This relative order is similar to the general order obtained from the visible absorption data for the dyes generated from these carbinols. Extending the alkyl chain by replacing a dimethylamino group with a diethylamino group increases the extent of electron donation. Also, when the diethylamino group is replaced by a pyrrolidino moiety, the increased electron donation is reflected in increased shielding at the carbon atoms adjacent to the amine bearing carbon atom. With the introduction of the 6-membered amino groups, steric interaction decreases the extent of electron donation into the system. It is interesting to note that the apparent electron donating ability for the six-

membered terminal amino groups as determined from their chemical shift data is the reverse of the Pauling electronegativity values for the heterocyclic γ -atom. This is in contrast to the order determined from the absorption spectra data for the dimethylamino-dye series and no explanation can be proffered for this. However, it must be remembered that a comparison is being made between a ground state property of the carbinols and an excited state property of the corresponding dyes and this may introduce discrepancies.

If the ^1H chemical shifts of the carbon atoms adjacent to the amine bearing carbon atom are considered, the ability of the terminal amino group to conjugate with the phenyl ring decreases in the order



This order is similar to that derived from the ^{13}C chemical shift data for the carbinols and a similar explanation can therefore be given for the general trend. The most significant difference between the two orders is the thiomorpholino group which now exhibits the greatest shielding of the six membered amine moieties. However, the ^{13}C chemical shift is considered to be more of a measure of the total electron density about a nucleus than the corresponding ^1H chemical shift which is more affected by magnetic anisotropy effects (72MI1). In addition, for the compounds studied in this investigation, a comparison of the variability of the ^1H and ^{13}C chemical shift values reveals that the ^1H chemical shift data display a greater variability than the corresponding ^{13}C chemical shift data. This may well be as a result of the susceptibility of the ^1H chemical shift data to magnetic anisotropic effects. The differences between respective ^1H chemical shifts for particular amino groups is small - in the range 0 - 0.35 ppm. As a consequence, it is more difficult to draw any firm conclusions regarding relative electron donating abilities from the ^1H chemical shift data. When it is also considered that only one example containing thiomorpholine has been studied, no definite conclusion regarding this seemingly anomalous behaviour can be confidently given.

The apparent order for pyrrolidino, diethylamino, dimethylamino and piperidino as derived in this work from the ^{13}C and ^1H chemical shifts is consistent with that derived by Nash (64JPC832) and Eastes (71JOC3847).

In their study, Effenberger *et al.* (78T2409) did not investigate the diethylamino group but did review the morpholino group. In their work on mono-, 1,3 bis- and 1,3,5-tris(dialkylamino)benzenes the relative order for piperidino and morpholino was the reverse of that found in this work. The present study and the earlier one by Effenberger *et al.* (78T2409) both used ^1H chemical shift data to relate the donor potential towards an uncharged π -system in the ground state and the discrepancy may lie in the different anisotropic effects present in each system (67JA2970).

Despite the minor variability of the ^1H chemical shifts, there are several points of note from the ^1H nmr. Firstly, the values for the H_A and H_C protons are reasonably constant and clearly distinct from the unsubstituted phenyl ring protons and secondly, the range for the unsubstituted phenyl ring protons (H_E , H_F and H_G) is fairly constant. In addition, the constancy for the ^1H chemical shifts for any given amine group is good which provides confidence in the ^1H chemical shift values used in this discussion.

One particular point worth a comment is for the carbinol Pi-Py. The ^{13}C chemical shift data show greater polarisation along certain bonds in this dye. This is not only apparent in the substituted phenyl rings but also in the unsubstituted phenyl ring suggesting an electronic distribution slightly different than the others. The positions closest to the central carbon atom display the greatest polarisation. Indeed, the central carbon atom in this dye ($\delta = 87.1$ ppm) is deshielded to a much greater extent than for all the other dyes. This effect does not appear to be due to inaccurate measurements since all the other positions display normal chemical shifts; to some extent, the effect is also observed in the ^1H nmr spectrum of Pi-Py. No apparent explanation for these observations can confidently be given but Pi-Py is different from the other dyes studied in that both terminal amino groups are relatively rigid ring systems and neither ring system contains a γ -heteroatom capable of inter-molecular bonding with the hydroxyl group of another molecule. The ^{13}C chemical shift for the central sp^3 hybridised carbon atom of triphenylmethanols is relatively invariant. A value of $\delta = 82$ ppm was reported by Tao and Maciel (95JA12889) for the unsubstituted triphenylmethanol, Arendano *et al.* (90MRC1011) obtained $\delta = 81.8$ ppm for MG dye base, Abarca *et al.* (86TL5657) reported $\delta = 77.2$ ppm again for unsubstituted triphenylmethanol and Robins *et al.* a value of $\delta = 79.9$ ppm in pararosanine carbinol base (80CJC339). When the variations in solvent and instrumentation is taken into account, these values are reasonably constant and the chemical shift values reported in this study are comparable to previous work.

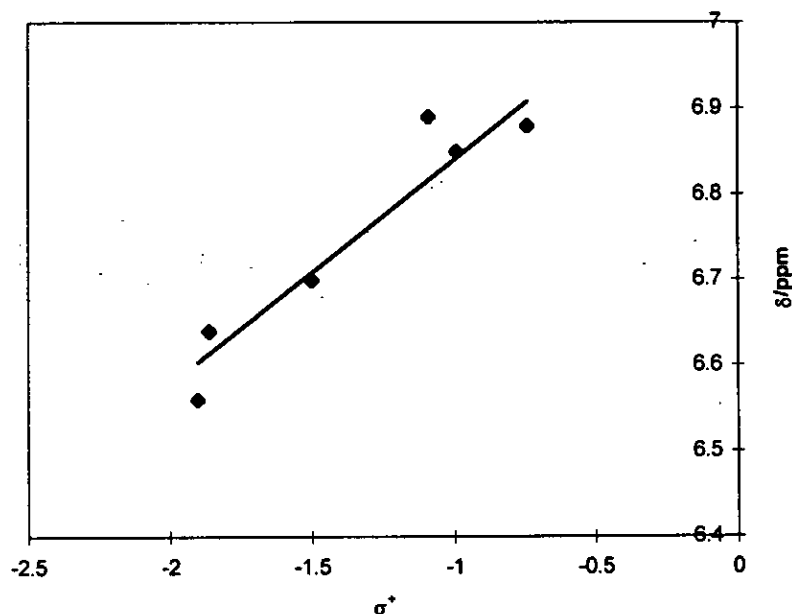
One point of note is the lack of variability in the ^{13}C chemical shifts of the central sp^3 hybridised carbon atom between triphenylmethanol and its terminally substituted analogues. This reflects the lack of electronic demand upon the terminal amino groups in the carbinol state.

The pattern of electronic distribution throughout the molecular framework of the carbinols reported herein is entirely consistent with that determined from previous work (71T735, 80CJC339, 86TL5657, 90MRC1011, 95JA12889, 95JOC5016, 96MC895, 96MRC395).

Many studies have been made with linear free energy relationships (LFER) applied to nmr chemical shift data, especially ^1H , ^{13}C and ^{19}F chemical shifts (71JCS(C)2847, 72MI1, 77JOC381, 78MI2, 79JOC1261, 81JOC2130). It was therefore considered worthwhile to investigate briefly any possible relationship for the systems studied in this work. Using the σ^+ substituent constants presented in Table 2.59 and in Table 2.72 for the thiomorpholine and N-methylpiperazine groups, a single substituent parameter Hammett line correlation was searched for between the σ^+ substituent constants and the ^1H and ^{13}C chemical shifts of the ring positions *ortho* to the amino group using a least squares computer program (HAM, Appendix A1). A less than satisfactory correlation ($r^2 < 0.9$) was observed between the σ^+ substituent constants and the ^{13}C chemical shifts. The plot for the ^1H regression is shown in Figure 2B.

Figure 2B

A plot of ^1H chemical shift for the proton adjacent to the amino-bearing carbon atom against σ^+ substituent constants



The regression equation obtained for the above plot was

$$\delta \text{ } ^1\text{H} = 0.26 \sigma^+ + 7.10 \quad 6.3$$
$$\pm 0.04 \quad \pm 0.04$$

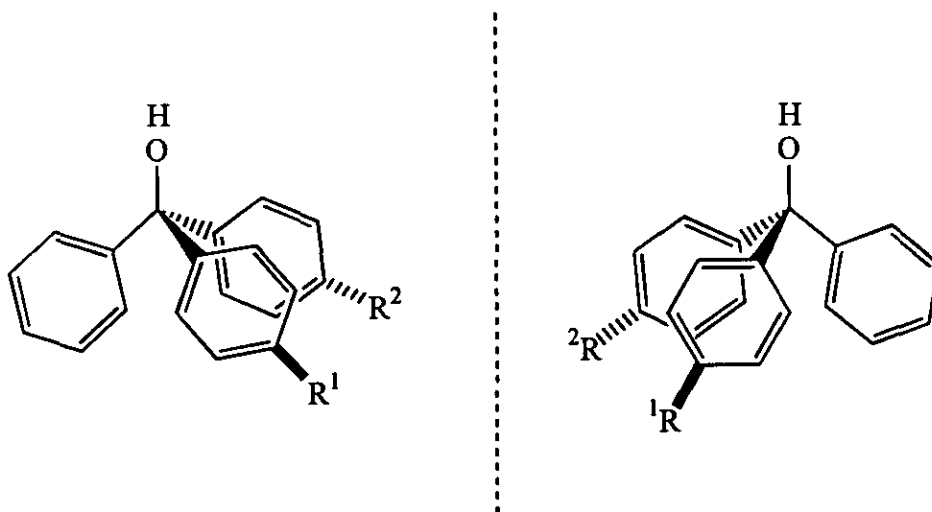
The correlation coefficient for the regression was 0.91 ($n = 7$) which reflects a fair correlation between the two parameters. The σ^+ substituent constants were used in preference to the σ substituent constants in order to reflect the greater resonance interaction between the terminal amino group and the reaction centre. From the regression above it would appear that, to at least a first approximation, a relationship exists between the chemical shift of the aromatic protons adjacent to the amino bearing carbon atom and the π -electron density within this class of compounds. However, during this treatment there has been a complete neglect of substituent anisotropy and whilst Zweig (63JA3940) has inferred no additional anisotropic effects in protons *ortho* to NMe_2 in substituted benzenes, it has been shown that for a more precise correlation these anisotropic effects should not be neglected (70JOC1555). Also, the σ^+ substituent

constants used in the correlation were obtained from kinetic and equilibrium data which relate the relative stabilities between precursors and transition states; these were then used in a correlation with spectroscopic measurements which directly measure the properties of the molecule itself (73JA7530). Hence, there is a fundamental difference in the two parameters employed for the regression, but despite this a satisfactory correlation was apparent.

As a *final* note, the unsymmetrical MGs prepared in this study have no plane of symmetry and can therefore exhibit stereoisomerism. This chirality is demonstrated in Figure 2C.

Figure 2C

Enantiomers for the unsymmetrical MGs



However, in view of their method of preparation the carbinols will be racemic mixtures and an investigation into any possible optical activity was not considered necessary. The stereoisomerism exhibited by the dye bases will be lost on protonation and formation of the dye cation.

2.1.6 Preparation of perchlorate salts

Several methods are detailed in the literature for the preparation and collection of the cationic salts of TPM and DPM dyes. Each method has in common the generation of the relatively unstable cation in sufficient quantities and in a medium in which it will combine with the desired anion before its destruction by some other reaction. The more unstable the cation, the greater the need to ensure the exclusion of any nucleophiles from the preparative medium.

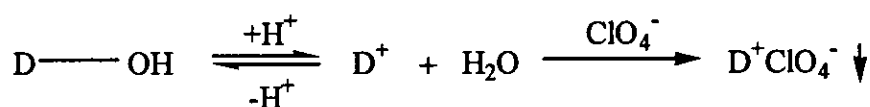
The method which has found widespread use in the field of TPM dye chemistry has been to generate the carbocation either from the leuco base by oxidation with chloranil (82JCS(P2)987) or by dissolving the dye base in glacial acetic acid (85JCS(P2)107, 86JSDC15) or ethanolic hydrogen chloride (74JCS(P2)59). Subsequent treatment with an aqueous solution of an alkali metal salt precipitates the dye salt. Perchlorate has been widely used as the anion, despite the fact that perchlorates are noted for their tendency to decompose explosively, but other counterions have been employed and commercial TPM dyes are available as the tetrafluoroborate, chloride and oxalate (57JCS674, 83JCSCC7, 88CS403, 91JCS(P2)1881). The salts can be purified by reprecipitation from acetone solution or by recrystallisation.

Alternative approaches to dye salt preparation include generation of the carbocation in a low boiling medium such as benzene by the controlled addition of the appropriate mineral acid. The salt is then recovered by evaporation or, depending upon solubilities, by allowing the mixture to stand (60JA1442, 81CL311, 88JCS(P2)3155).

For the preparation of the dye salts of the unsymmetrical MGs, a sample of the carbinol was dissolved in the minimum volume of glacial acetic acid and the solution was added to a saturated aqueous solution of sodium perchlorate. Purification of the resulting salt involved the dissolution of the crude material in dry acetone, filtration to remove any insoluble inorganic material and reprecipitation of the salt by addition of dry diethyl ether. If this failed to generate a pure salt, recrystallisation of the salt from a suitable solvent was undertaken. This method is basically that used by previous workers for similar dye systems (81Th1, 82Th1, 83Th1, 83Th2, 83Th3, 91Th1). This procedure also proved successful for the preparation of MHB perchlorate.

However, there were two groups of compounds for which this method did not prove satisfactory: (1) the other members of the DPM dyes and (2) the unsymmetrical MGs

which contained the *N*-methylpiperazine moiety. In the case of the DPM dyes, addition of the intensely coloured solution of the dye cation in glacial acetic acid to the aqueous sodium perchlorate solution resulted in decolourisation. The rate of decolourisation was sufficiently rapid to prevent the precipitation of any dye salt. It appears that the stability of the substituted diphenylmethyl cation is so low that the reaction of the cation with water is almost instantaneous, regenerating the dye base. The diphenylmethyl cation is much less efficiently stabilised than a triphenylmethyl cation, with delocalisation of the positive charge over two rings rather than three. Additionally, there is less congestion at the carbocation site in a DPM dye than in a TPM salt and hence nucleophilic attack by water is less hindered. Thus, the equilibrium between dye base and dye cation is more readily displaced toward the former. It is interesting to note therefore that, of the three DPM dyes which were collected as their perchlorate salt, only the MHB dye salt was obtained from the aqueous method. Both EtDPM and PyDPM had to be prepared using the non-aqueous method (see below) despite MHB displaying the largest rate constant for the reaction with hydroxide ion. This would suggest that the reaction with water is somehow kinetically unfavourable for MHB or some other factor is influencing the system.

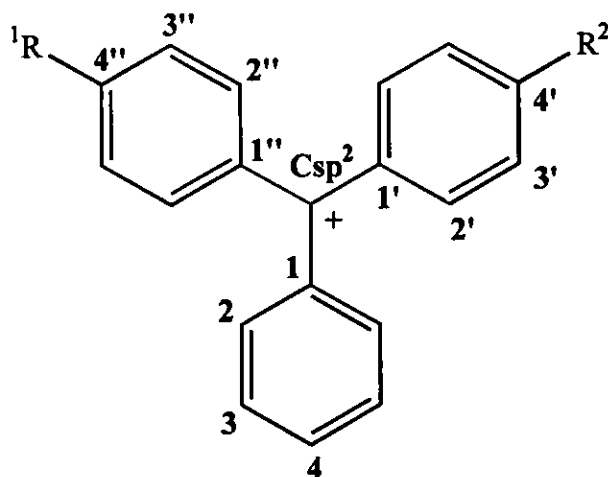


For the unsymmetrical MGs which contained the *N*-methylpiperazine moiety, addition of the dark blue solution of the dye cation in acetic acid to the aqueous sodium perchlorate solution generated a deep purple solution from which the dye salt could not be recovered. This behaviour was peculiar to dyes containing the *N*-methylpiperazine moiety.

For both the DPM dyes and the MGs containing the *N*-methylpiperazine moiety it was therefore decided to attempt the generation of the dye salt under non-aqueous conditions. In a modification of a procedure utilised previously (91JCS(P1)1881), the carbinol or hydrol was dissolved in the minimum volume of a mixture of methanol and dichloromethane (50/50 v/v) to which was added a molar equivalent of 60% HClO₄. The excess solvent was then removed by rotary evaporation but this failed to yield any salt, the salt seemingly decomposing before precipitation occurred. The route which proved

successful involved the dissolution of the hydrol in acetic anhydride and the addition to this mixture of a molar equivalent of 60% HClO₄, any water thus being removed by reaction with the acetic anhydride. The crude salt was then precipitated by adding a large excess of dry diethyl ether. Purification of the crude salt was by the reprecipitation procedure previously detailed since attempts to find a suitable recrystallisation medium proved unsuccessful. For MPzDPM, collection of the salt had to be carried out under anhydrous conditions. When the diethyl ether was being removed by suction it cooled to such an extent that water formed as ice crystals on the salt which was subsequently hydrolysed. It was therefore necessary to pass a stream of nitrogen over the filtration equipment. Once dried, the salt had to be stored in anhydrous condition and under nitrogen to prevent degradation.

The perchlorate salts prepared in this study were characterised by microanalysis and/or their ¹H and ¹³C nmr spectra. Some of the salts did not furnish satisfactory microanalysis, a feature noted in earlier work with related compounds (72JSDC25, 82Th1, 83Th2). Absorption of atmospheric moisture by the dye salts has also been a problem (64JA1860, 72JSDC25, 91JCS(P1)1881). However, the presence of moisture or organic impurities such as the unreacted parent dye base would result in elevated carbon, hydrogen and nitrogen microanalysis figures. Since this was not the case, the impurity was considered to be of an inorganic nature which should not interfere with the dye chemistry.



(2.1-7)

The ¹³C chemical shifts for the analogues of 2.1-7 are shown in Tables 2.10 and 2.11.

Table 2.10
¹³C chemical shifts (ppm) for the dye cations (2.1-7)

Dye	R ¹	R ²	Csp ²	1''	2''	3''	4''	1'	2'	3'	4'	1	2	3	4
Me-Et	NEt ₂	NMe ₂	177.3	127.5	141.0	114.2	156.2	127.6	140.3	114.4	157.5	141.7	133.4	129.2	135.0
Py-Et	Pyr. ^a	NEt ₂	177.0	126.3	140.4	114.1	155.2	127.7	140.4	115.2	155.5	141.3	133.4	129.2	134.9
Pi-Et	NEt ₂	Pip. ^b	176.2	128.4	141.3	114.5	156.2	128.7	140.3	114.9	156.3	141.5	133.4	129.2	134.9
Mo-Et	NEt ₂	Mo. ^c	177.3	128.1	140.6	114.3	156.8	128.5	140.2	115.2	157.1	142.3	133.6	129.2	135.1
Me-Py	Pyr. ^a	NMe ₂	178.0	128.1	141.5	114.8	156.0	128.5	141.1	116.1	158.0	142.1	134.1	129.9	135.7
Pi-Py	Pyr. ^a	Pip. ^b	177.8	129.2	141.4	114.8	155.3	127.9	140.3	115.4	156.3	141.4	133.4	131.7	134.9
Mo-Py	Pyr. ^a	Mo. ^c	177.2	128.4	140.4	114.3	156.0	128.5	140.3	116.3	156.6	142.1	133.5	129.2	135.0
Me-Pi	NMe ₂	Pip. ^b	176.5	128.4	141.0	114.4	156.7	128.7	140.3	115.0	157.7	141.5	133.4	129.2	135.0
Mo-Pi	Mo. ^c	Pip. ^b	176.5	128.4	140.2	114.4	156.8	128.6	140.5	115.6	156.8	142.3	133.6	129.2	135.0
Me-Mo	NMe ₂	Mo. ^c	177.6	128.1	140.8	114.4	156.9	128.5	140.2	115.2	158.5	141.9	133.6	129.2	135.1
MPz-Et	NEt ₂	MPz. ^d	177.4	128.7	140.1	115.0	155.2	128.9	139.6	116.2	158.1	143.2	133.7	129.7	135.1
MPz-Me	NMe ₂	MPz. ^d	177.7	128.5	140.1	115.0	155.4	128.6	139.8	116.3	159.5	142.7	133.8	129.3	135.2
MPz-Py	Pyr. ^a	MPz. ^d	177.0	128.9	140.2	115.0	155.0	129.1	139.3	117.2	156.9	142.8	133.6	129.8	135.0
MPz-Pi	MPz. ^d	Pip. ^b	176.3	128.4	139.3	115.0	158.2	128.9	140.1	116.5	155.1	143.2	133.7	129.3	135.0
MPz-Mo	Mo. ^c	MPz. ^d	178.5	129.5	140.4	115.1	155.9	129.3	140.1	116.0	158.5	143.0	134.1	129.6	135.4
ThM-Me	NMe ₂	ThM. ^e	177.4	128.0	140.2	114.9	156.0	128.1	141.1	115.1	158.4	141.8	133.7	129.2	135.1

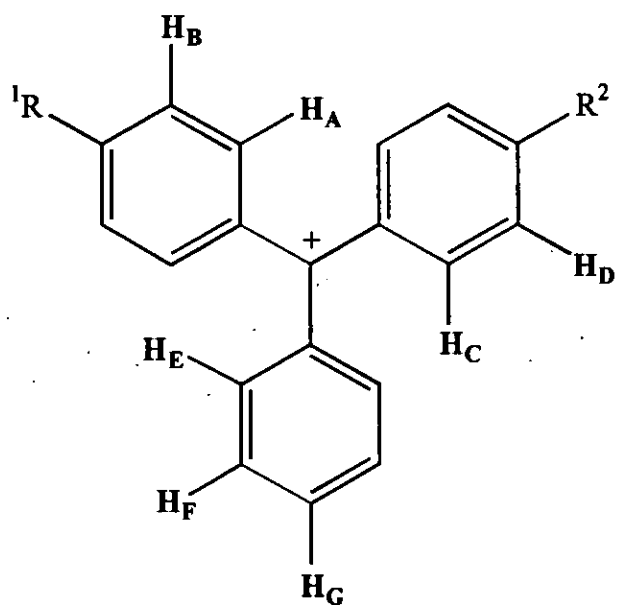
a. Pyrrolidine
b. Piperidine
c. Morpholine

d. *N*-Methylpiperazine
e. Thiomorpholine

Table 2.11
¹³C chemical shifts (ppm) for the dye cations (2.1-7)

Dye	R ¹	R ²	NMe ₂	NEt ₂		Pyrrolidine		Piperidine			Morpholine		N-Methylpiperazine		
			CH ₃	CH ₂	CH ₃	NCH ₂	CH ₂	NCH ₂	CH ₂	γ-CH ₂	NCH ₂	CH ₂ O	NCH ₂	CH ₂ N	NCH ₃
Me-Et	NEt ₂	NMe ₂	40.7	46.3	12.7	-	-	-	-	-	-	-	-	-	-
Py-Et	Pyr. ^a	NEt ₂	-	46.2	12.6	49.6	25.5	-	-	-	-	-	-	-	-
Pi-Et	NEt ₂	Pip. ^b	-	46.3	12.7	-	-	49.4	26.6	24.5	-	-	-	-	-
Mo-Et	NEt ₂	Mo. ^c	-	46.7	12.8	-	-	-	-	-	47.5	66.7	-	-	-
Me-Py	Pyr. ^a	NMe ₂	41.3	-	-	50.3	26.2	-	-	-	-	-	-	-	-
Pi-Py	Pyr. ^a	Pip. ^b	-	-	-	49.8	25.4	49.8	26.5	24.5	-	-	-	-	-
Mo-Py	Pyr. ^a	Mo. ^c	-	-	-	50.1	25.4	-	-	-	47.5	66.7	-	-	-
Me-Pi	NMe ₂	Pip. ^b	40.8	-	-	-	-	49.4	26.6	24.4	-	-	-	-	-
Mo-Pi	Pip. ^b	Mo. ^c	-	-	-	-	-	49.8	26.9	24.4	47.6	66.7	-	-	-
Me-Mo	NMe ₂	Mo. ^c	41.1	-	-	-	-	-	-	-	47.6	66.7	-	-	-
MPz-Et	NEt ₂	MPz. ^d	-	47.2	12.9	-	-	-	-	-	-	-	54.0	44.7	43.8
MPz-Me	NMe ₂	MPz. ^d	41.5	-	-	-	-	-	-	-	-	-	54.0	44.8	43.9
MPz-Py	Pyr. ^a	MPz. ^d	-	-	-	50.7	25.3	-	-	-	-	-	54.0	44.7	43.9
MPz-Pi	Pip. ^b	MPz. ^d	-	-	-	-	-	50.4	27.2	24.3	-	-	54.0	44.7	43.9
MPz-Mo	Mo. ^c	MPz. ^d	-	-	-	-	-	-	-	-	48.7	66.9	54.0	44.7	43.9
ThM-Me	NMe ₂	ThM. ^e	41.1	-	-	-	-	-	-	-	51.1 ^f	27.2 ^f	-	-	-

a. Pyrrolidine b. Piperidine c. Morpholine d. N-Methylpiperazine e. Thiomorpholine f. For the thiomorpholine analogue



(2.1-8)

The 1H chemical shifts for the analogues of 2.1-8 are shown in Tables 2.12 and 2.13.

Table 2.12
¹H chemical shifts (ppm) for the dye cations (2.1-8)

Dye	R ¹	R ²	H _A	H _B	H _C	H _D	H _E	H _F	H _G
Me-Et	NEt ₂	NMe ₂	7.56-7.64	7.27	7.56-7.64	7.29	7.80	7.56-7.64	7.94
Py-Et	Pyr. ^a	NEt ₂	7.57-7.65	7.16	7.57-7.65	7.31	7.81	7.57-7.65	7.93
Pi-Et	NEt ₂	Pip. ^b	7.57-7.65	7.33	7.57-7.65	7.46	7.81	7.57-7.65	7.93
Mo-Et	NEt ₂	Mo. ^c	7.58-7.71	7.39	7.58-7.71	7.43	7.83	7.58-7.71	7.95
Me-Py	Pyr. ^a	NMe ₂	7.56-7.64	7.17	7.56-7.64	7.27	7.80	7.56-7.64	7.92
Pi-Py	Pyr. ^a	Pip. ^b	7.56-7.66	7.19	7.56-7.66	7.49	7.80	7.56-7.66	7.94
Mo-Py	Pyr. ^a	Mo. ^c	7.55-7.70	7.24	7.55-7.70	7.42	7.81	7.55-7.70	7.93
Me-Pi	NMe ₂	Pip. ^b	7.50-7.64	7.30	7.50-7.64	7.49	7.80	7.50-7.64	7.93
Mo-Pi	Pip. ^b	Mo. ^c	7.57-7.70	7.43	7.57-7.70	7.53	7.81	7.57-7.70	7.95
Me-Mo	NMe ₂	Mo. ^c	7.56-7.65	7.36	7.56-7.65	7.43	7.81	7.56-7.65	7.92
MPz-Et	NEt ₂	MPz. ^d	7.46-7.61	7.19	7.46-7.61	7.31	7.89	7.46-7.61	7.94
MPz-Me	NMe ₂	MPz. ^d	7.41-7.60	7.18	7.41-7.60	7.30	7.79	7.41-7.60	7.94
MPz-Py	Pyr. ^a	MPz. ^d	7.38-7.58	7.20	7.38-7.58	7.31	7.79	7.38-7.58	7.93
MPz-Pi	Pip. ^b	MPz. ^d	7.46-7.61	7.46-7.61	7.46-7.61	7.46-7.61	7.80	7.46-7.61	7.92
MPz-Mo	Mo. ^c	MPz. ^d	7.51-7.75	7.51-7.75	7.51-7.75	7.51-7.75	7.82	7.51-7.75	7.97
ThM-Me	NMe ₂	ThM. ^e	7.54-7.66	7.33	7.54-7.66	7.43	7.80	7.54-7.66	7.94

a. Pyrrolidine
b. Piperidine

c. Morpholine
d. *N*-Methylpiperazine

e. Thiomorpholine

Table 2.13
¹H chemical shifts (ppm) for the dye cations (2.1-8)

Dye	R ¹	R ²	NMe ₂	NEt ₂		Pyrrolidine		Piperidine			Morpholine		N-Methylpiperazine			
			NCH ₃	NCH ₂	CH ₃	NCH ₂	CH ₂	NCH ₂	CH ₂	γ-CH ₂	NCH ₂	CH ₂ O	NCH ₂	CH ₂ N	NCH ₃	
Me-Et	NEt ₂	NMe ₂	3.55	3.94	1.50	-	-	-	-	-	-	-	-	-	-	-
Py-Et	Pyr. ^a	NEt ₂	-	3.90-3.99	1.49	3.90-3.99	2.33	-	-	-	-	-	-	-	-	-
Pi-Et	NEt ₂	Pip. ^b	-	3.94	1.50	-	-	4.02	1.96	1.96	-	-	-	-	-	-
Mo-Et	NEt ₂	Mo. ^c	-	3.94	1.52	-	-	-	-	-	4.00	4.00	-	-	-	-
Me-Py	Pyr. ^a	NMe ₂	3.55	-	-	3.91	2.34	-	-	-	-	-	-	-	-	-
Pi-Py	Pyr. ^a	Pip. ^b	-	-	-	3.93	2.34	4.02	1.97	1.97	-	-	-	-	-	-
Mo-Py	Pyr. ^a	Mo. ^c	-	-	-	3.91	2.35	-	-	-	4.00	4.00	-	-	-	-
Me-Pi	NMe ₂	Pip. ^b	3.58	-	-	-	-	4.05	1.97	1.97	-	-	-	-	-	-
Mo-Pi	Pip. ^b	Mo. ^c	-	-	-	-	-	4.12	1.99	1.99	4.00	3.92	-	-	-	-
Me-Mo	NMe ₂	Mo. ^c	3.63	-	-	-	-	-	-	-	4.01	3.93	-	-	-	-
MPz-Et	NEt ₂	MPz. ^d	-	4.09	1.55	-	-	-	-	-	-	-	4.29	3.92	3.40	-
MPz-Me	NMe ₂	MPz. ^d	3.72	-	-	-	-	-	-	-	-	-	4.30	3.90	3.40	-
MPz-Py	Pyr. ^a	MPz. ^d	-	-	-	3.87	2.36	-	-	-	-	-	4.08	3.78	3.51	-
MPz-Pi	Pip. ^b	MPz. ^d	-	-	-	-	-	3.92	2.01	2.01	-	-	4.20	3.92	3.40	-
MPz-Mo	Mo. ^c	MPz. ^d	-	-	-	-	-	-	-	-	4.04	3.92	4.17	4.04	3.41	-
ThM-Me	NMe ₂	ThM. ^e	3.61	-	-	-	-	-	-	-	4.32 ^f	2.98 ^f	-	-	-	-

a. Pyrrolidine b. Piperidine c. Morpholine d. N-Methylpiperazine e. Thiomorpholine f. For the thiomorpholine analogue

The ^1H and ^{13}C nmr spectra for the salts were measured in deuterated acetone. This solvent was used because the TPM salts were not sufficiently soluble in CDCl_3 to allow satisfactory nmr spectra to be achieved. The DPM salts were not sufficiently soluble in deuterated acetone to allow their nmr spectra to be analysed.

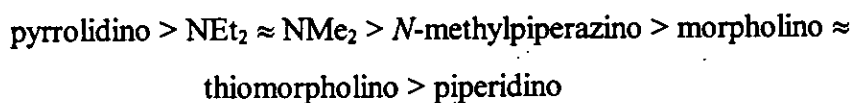
The ^1H and ^{13}C nmr spectra for the salts were interpreted with the help of data obtained from the literature for similar systems (71T735, 80CJC339, 86TL5657, 90MRC1011, 95JA12889, 95JOC5016, 96MC895, 96MRC395). In Table 2.12 the chemical shifts for the aromatic protons H_A and H_C are quoted as a range of values because the signals appeared as overlapping doublets which could not be resolved and ascribed to a particular group. This does imply a consistent electron density at these positions irrespective of the nature of the terminal amino group present.

From the ^{13}C chemical shift data reported in Table 2.10, the first point of interest is the extent of deshielding which has occurred at the central carbon atom upon formation of the carbocation. Values of δ in the range 176.2 - 178.5 ppm were obtained for the dye cations compared with 81.9 - 87.1 ppm for the carbinols. The magnitude of these shifts is consistent with previously reported values for similar dye systems (86TL5657, 90MRC1011, 95JA12889). Also, the ^{13}C nmr chemical shift for the central carbon atom in the dye cations is quite consistent irrespective of the nature of the terminal amino groups present. This reflects the extent to which the terminal amino groups are able to respond to the electronic demand of their environment and stabilise the dye system. The extent to which the paired amino groups stabilise the dye system by conjugation is more apparent when a comparison is made with the ^{13}C chemical shift for the central carbon atom of the trityl cation. Tao and Maciel report the $(\text{C}_6\text{H}_5)_3^{13}\text{C}^+$ peak at $\delta = 210$ ppm (95JA12889) and Abarca *et al.* at $\delta = 211.6$ ppm (86TL5657). These signals are shifted *ca.* 40 ppm further downfield in the absence of any terminal amino group.

For the dyes reported, very similar ^{13}C nmr chemical shifts are obtained for the ring carbon atoms adjacent to the amino-bearing carbons. As a result of this similarity, a definite relative electron donor ability cannot be determined from these chemical shifts. However, if the ^{13}C nmr chemical shifts for the non-aromatic carbon atoms adjacent to the conjugated terminal nitrogen atoms are considered, a pattern can be deduced. The dimethylamino, diethylamino and pyrrolidino all show a downfield shift whereas the piperidino, morpholino, *N*-methylpiperazino and thiomorpholino show an upfield shift.

This provides evidence for the former series displaying increased donation to compensate for the reduced electron donating ability of the latter series.

The ^1H nmr chemical shift data are greatly influenced by the presence of the single positive charge residing on the dye system. A comparison of the ^1H chemical shift data for the aromatic protons *ortho* to the terminal amino groups for the carbinol and the corresponding dye enable a relative donor ability to be determined:



This order is similar to that obtained from the ^{13}C chemical shift data for the non-aromatic carbon atoms adjacent to the conjugated terminal nitrogen atoms as mentioned previously in that pyrrolidino, diethylamino and dimethylamino display the greatest donor ability and the six-membered heterocycles perform less effectively. The relative order amongst the six-membered heterocycles is not the same and no explanation can be given for this. However, it must be remembered that a direct comparison between ^1H and ^{13}C chemical shift data will be difficult as a result of the greater susceptibility of the ^1H chemical shift data to magnetic anisotropic effects.

The phenyl protons of the unsubstituted aromatic ring display a significant downfield shift relative to the carbinol. The protons H_E and H_G are now *ortho* and *para* to a carbocation and are therefore deshielded due to the reduced electron density at these positions. The ^1H chemical shifts for the protons H_E and H_G are quite consistent and are the most downfield signals recorded in the ^1H nmr spectra of the dyes. This is to be expected since this phenyl ring is unsubstituted.

The protons of the non-aromatic carbon atoms adjacent to the conjugated terminal nitrogen atoms all show a downfield shift of 0.6 - 1.0 ppm compared to the carbinol which reflects the increased electron donation from the nitrogen atom into the dye system. However, no apparent donor order can be obtained for the amino groups from these signals.

Finally, it was considered worthwhile recording the ^1H and ^{13}C chemical shifts of one hydrol in deuterated acetone to determine whether the large shifts observed during the transition from hydrol to cation were as a consequence of the change of solvent in which the nmr spectra was recorded. In Tables 2.6 - 2.9, the ^1H and ^{13}C chemical shifts for

Mo-Et in acetone-d₆ are in parentheses. It can be seen that the shifts are virtually identical for those in CDCl₃ and hence the change of solvent has little effect upon the chemical shifts recorded.

2.2 Absorption spectra

In order to be consistent and to facilitate direct comparisons with the vast majority of previous work (81Th1, 82Th1, 83Th1), the absorption spectra of both the diphenylmethane and triphenylmethane carbinols were measured in 98% acetic acid with 2% water and at concentrations of 10^{-5} M. This solvent system has been established as a suitable medium for virtually complete ionisation of the hydrol to the univalent cation without the formation of the any other protonated species (63JCS2655). Complete ionisation in this medium has been predicted because of the constancy of ϵ_{\max} between MHB and its *ortho* bridged analogue (63JCS2655). For MHB, steric inhibition of conjugation as a result of interaction at the positions *ortho* to the central carbon atom can be reduced by increasing the phenyl-C-phenyl bond angle (59JCS3957). It is therefore accepted that the MHB system approaches planarity and exhibits maximum conjugation. This follows from the similarity in the absorption spectra of MHB and its *ortho* bridged analogue in which coplanarity is enforced upon the system (63JCS2655). In a more recent study, confirmation of the planarity of MHB was obtained from a photophysical study of its solutions in pure acetic acid or dichloromethane (92CP85). However, it has been observed that upon warming a solution of MHB in 98% acetic acid, the ϵ_{\max} value increases (71Th1) suggesting that even in this medium, the equilibrium between dye base and cation may not be completely shifted towards the cation and that the elevated temperatures shifts this equilibrium further towards the cation. However, it has been suggested that this increase in ϵ_{\max} upon warming may be due to the increased dissociation of aggregated dye molecules (82Th1, 84Th1).

Dye aggregation can also have a pronounced effect upon the solution absorption spectra of dyes (59JCS3957, 72JPC1772, 93CR381). As the dye concentration is increased, the α -band decreases in intensity and the β -band increases in intensity. The α and β bands are considered to be the two components of the main absorption band arising due to the presence of the two A and B rotational isomers of the dye (93CR381). The dye concentration used by previous workers (59JCS3957, 63JCS2655, 72JCS(P2)1792) and in this study was chosen to minimise dye aggregation.

The use of acetic acid also allows the rapid generation of more acidic solutions by the addition of more water which promotes the ionisation of the acetic acid. The

triphenylmethanols prepared in this investigation were studied at 100%, 98%, 50% and 10% acetic acid solutions with water. The perchlorate salts were measured in 98% acetic acid with water. The visible absorption spectra were measured immediately after preparation of the solutions and after a further one hour and 48 hours to ensure constant ϵ_{\max} values. The measurements were made using a Philips PU8740 UV/Vis scanning spectrophotometer. The instrument performance was checked prior to spectral data collection by measuring the absorption spectrum of a reference compound. The reference compound used was an analytically pure sample of the perchlorate salt of MHB which was kindly supplied by Dr.G.Hallas. The measured λ_{\max} value was 607.4 ± 0.2 nm compared with the published value of $\lambda_{\max} = 607.5$ nm. The precision of the instrument was ± 0.2 nm.

2.2.1 The absorption spectra of the dyes derived from diphenylcarbinols

The absorption spectral data of the diphenylmethane dyes are presented in Table 2.14. With the exception of the MPz-DPM analogue, these dyes have been reported previously (89JCS(P2)1087) but warrant a discussion in the context of this investigation.

Table 2.14

Absorption bands of some symmetrical MHB analogues in 98% acetic acid

Dye	λ_{\max}/nm	$10^{-4} \epsilon_{\max}/\text{dm}^3 \text{mol}^{-1} \text{cm}^{-1}$
MHB	607.4	14.7
EtDPM	613.0	17.6
PyDPM	613.2	15.5
PiDPM	619.1	0.21
MoDPM	612.8	3.3
MPzDPM	594.1	0.06

The first point to note is the similarity between the λ_{\max} values reported in Table 2.14 and the previously reported values (MHB: 607.5 nm; EtDPM: 613 nm; PyDPM: 613 nm;

PiDPM: 619 nm; MoDPM: 613 nm) (89JCS(P2)1087). This confirms the precision of the instrument used in this study and also the successful syntheses of the dye bases.

The terminal positions of MHB, CV and MG are starred or active sites. PMO theory (50JCS2329) predicts that any increase in the electron density at these positions will reduce the π^* energy level, thereby reducing the energy of the NBMO $\rightarrow \pi^*$ transition which will result in a bathochromic shift of λ_{\max} of the main absorption band. The magnitude of the shift in λ_{\max} will be related to the extent of electron donation by the terminal amino group. Therefore, studying the values in Table 2.14 will enable the electron donating nature of the substituents to be described. It is well known that increasing the length of the alkyl chain from dimethylamino to diethylamino increases the electron donating ability of the terminal group. This is reflected in the increased availability of the nitrogen lone pair of electrons to confer stability on the central carbon atom. Both λ_{\max} and ϵ_{\max} are increased.

The diethylamino and pyrrolidino groups have a similar electron donating ability as indicated by the λ_{\max} values for the respective derivatives, but the ϵ_{\max} value of the pyrrolidino derivative is lower than that of the diethylamino derivative. This has been ascribed to partial deconjugation of the 5-membered heterocyclic ring arising from a clash between the pyrrolidino α -methylene protons and the *ortho* protons of the phenyl ring (84JCS(P2)149, 89JCS(P2)1087).

When the terminal group is the 6-membered piperidine moiety, λ_{\max} is bathochromically shifted relative to the diethylamino and pyrrolidino derivatives indicating the greater inductive electron donating ability of the piperidino group. However, there is a dramatic reduction in ϵ_{\max} which has been attributed to the greater steric hindrance suffered by the 6-membered ring. Piperidine exists predominantly in the chair form (58JCS3002, 80MI1) and therefore the clash between its α -methylene protons and the *ortho* protons of the phenyl ring is quite significant, causing a greater degree of bond rotation than occurs for the near planar pyrrolidino group (74JCS(P2)1033, 78TS1, 85JA2305). This twisting results in a drastic reduction of the availability of the lone pair of electrons of the nitrogen for mesomeric interaction with the chromogen which is reflected in the lower ϵ_{\max} value.

With the introduction of morpholine as the terminal group, a reduced value of ϵ_{\max} is again observed and λ_{\max} is hypsochromically shifted relative to the piperidine derivative.

The presence of the oxygen with its inductive electron withdrawing effect results in an overall reduction in electron donation into the chromogen relative to the piperidine derivative. For the diarylmethyl cation (MPz-DPM), the introduction of *N*-methylpiperazino as the terminal group further destabilises the system so that in solution the equilibrium between dye base and univalent cation is displaced virtually entirely in favour of the former. Since PiDPM, MoDPM and MPzDPM are structurally similar, the decreased stability of MPzDPM relative to the PiDPM and MoDPM is presumably attributable to electronic factors. λ_{\max} for MPzDPM is hypsochromically shifted relative to MoDPM and PiDPM indicating a reduced electron density at the terminal nitrogen atom in line with PMO theory (50JCS2329). Electronically, MoDPM and MPzDPM appear similar in that both contain a heteroatom at the 4-position of the 6-membered ring. The greater electronegativity of an oxygen atom than a nitrogen atom would suggest a larger inductive electron withdrawing effect. However, the blue shift of λ_{\max} for MPzDPM relative to MoDPM indicates a lower electron density at the terminal nitrogen atom in MPzDPM. This seemingly anomalous behaviour may well be explained by the presence of the methyl group at the *N*-4 position in MPzDPM. The electron releasing nature of the methyl group will increase the electron density of the *N*-4 atom and it is likely that this position is preferentially protonated. Therefore the electron demand of the positively charged hetero-nitrogen atom will be greater than an oxygen atom and result in a reduced electron density at the terminal nitrogen position in MPzDPM. This would also explain the reluctance of MPzDPM to form the coloured species, as indicated by the low extinction coefficient, which would of necessity carry a double positive charge.

From the data given in Table 2.14, the apparent electron donating ability of the terminal amino groups in the diphenylmethane system is in the order:



If this order is compared to that obtained from the data in Table 2.15 for the corresponding MG analogues then a similar order is observed.

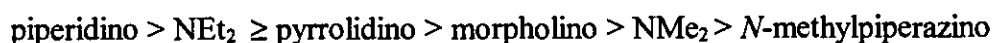
Table 2.15**Absorption spectra of some symmetrical MG analogues in 98% acetic acid**

Dye	x-band		y-band	
	λ_{\max}/nm	$10^{-4} \epsilon_{\max}/\text{dm}^3 \text{mol}^{-1} \text{cm}^{-1}$	λ_{\max}/nm	$10^{-4} \epsilon_{\max}/\text{dm}^3 \text{mol}^{-1} \text{cm}^{-1}$
Malachite Green ^a	621	10.4	427.5	2.0
Brilliant Green ^a	629.5	11.9	430	1.8
Morpholine Green ^a	623	9.0	433	1.9
Pyrrolidine Green ^a	629	11.1	426	1.7
Piperidine Green ^a	634	10.4	431	1.7
<i>N</i> -Methylpiperazine Green ^b	605.8	6.0	429.3	1.5

a. 82Th1

b. This study from a sample kindly supplied by Dr.A.M.Jones.

The apparent order of electron donating ability is:



It can be seen that there has been a reversal in the apparent electron donating ability between the diethylamino and pyrrolidino groups but the change is marginal. However, these two groups are known to be very similar in their ability to stabilise systems by electron donation (83Th1). These data also indicate that morpholino is a weaker electron donor than pyrrolidino and diethylamino, as expected. That the MHB and MG systems show a similar order is to be expected when one considers the structural similarity in the x-axis of the two series.

2.2.2 The absorption spectra of some unsymmetrical analogues of MG

Of the 16 unsymmetrical MGs prepared in this study, only Me-Et has been reported previously (86JSDC15). The spectral data are shown in Table 2.16.

Table 2.16

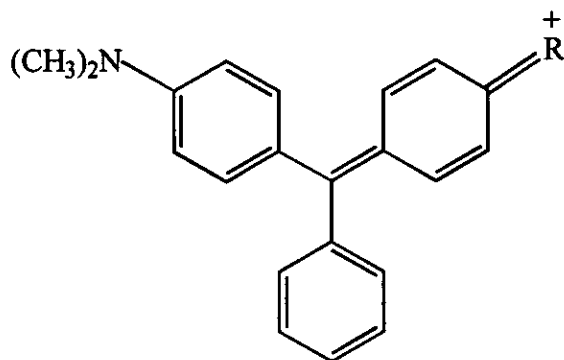
Absorption spectra of some unsymmetrical MGs in 98% acetic acid

Dye	x - band		y - band	
	λ_{\max}/nm	$10^{-4} \epsilon_{\max}/\text{dm}^3 \text{mol}^{-1} \text{cm}^{-1}$	λ_{\max}/nm	$10^{-4} \epsilon_{\max}/\text{dm}^3 \text{mol}^{-1} \text{cm}^{-1}$
Me-Et	624.6	10.0	427.5	1.8
Py-Et	628.3	5.2	429.2	1.1
Pi-Et	631.0	10.6	431.8	2.1
Mo-Et	622.5	9.3	429.1	2.2
Me-Py	624.6	2.4	430.1	0.6
Pi-Py	631.2	11.2	430.2	2.0
Mo-Py	623.4	8.8	428.3	1.9
Me-Pi	627.5	10.6	429.9	2.0
Mo-Pi	626.2	9.1	430.0	2.0
Me-Mo	621.1	9.6	428.9	2.2
MPz-Et	610.1	7.0	421.7	2.1
MPz-Me	608.3	7.4	423.1	2.2
MPz-Py	607.1	5.0	420.4	1.5
MPz-Pi	608.7	5.5	421.8	1.5
MPz-Mo	613.4	8.3	429.9	2.2
ThM-Me	624.8	9.4	433.0	1.8

In 98% acetic acid, all the absorption spectra of the dyes studied exhibited a shoulder on the high energy side of the main absorption band. The explanation for the presence of this shoulder has been the subject of much conjecture in the field of dye chemistry.

Lewis and Calvin (39CR273) predicted that two rotational isomers could exist, a propeller-like isomer and an isomer where one of the phenyl rings is rotated in the opposite direction to the other two. It was anticipated that the existence of these two rotamers would produce a splitting of the main band into two components - the α and β bands. However, subsequent studies by Barker (59JA3957), Korppi-Tomola (81CJC191, 84CPL373), Looney and Simpson (54JA6293) and Leuck *et al.* (92JA2342) suggest that only the propeller conformer exists for Crystal Violet in both solid and solution media. This has been further supported by a variety of other experimental techniques including Raman spectroscopy (79JRS305, 80JMS331), magnetic circular dichroism (76MP1001) and X-ray crystallography (65AC437) and the view is now (80JMS331, 89JCP279) that only one ground state conformer exists for CV with the phenyl rings rotated 32° to the central plane (65AC437). The relative intensities of the α and β bands have been shown to be affected by a variety of factors including dye concentration, solvent, pressure, temperature and the nature of the counterion (42JA1774, 65JCS(TFS)1800, 84JCP1024, 86JPC589). An excellent review of this aspect of TPM chemistry has been written by Duxbury (93CR381).

Once again, the extent of electron donation by the terminal amino groups into the triphenylmethane system can be estimated from the position and intensity of λ_{\max} . Previous studies into the extent of electron donation into an aromatic system by amines by studying nuclear magnetic resonance correlations (64JPC832, 71JOC3847, 78T2409), enamino structure relationships (67JA3289, 83JCS(P2)57) and electronic absorption spectra (62JA734, 84JCS(P2)149, 86JCS(P2)123, 89JCS(P2)1087) have revealed a complex relationship between chemical shift, extent of nitrogen hybridisation, steric environment and the base strength of the appropriate amine. Indeed, the situation is complicated even further by the differing nature of the amino substituents under investigation. Two essentially different substituent types are under investigation: these are the dialkylamino and nitrogen heterocyclic groups. If the unsymmetrical MGs containing the dimethylamino group (2.2-1) are considered, the influence of modifying the remaining terminal amino group upon the dye system can be determined.



(2.2-1)

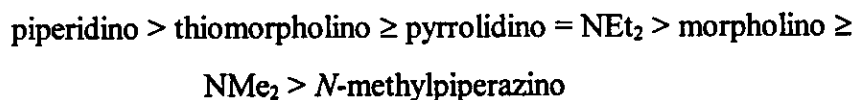
Table 2.17

Absorption spectra of some unsymmetrical MGs containing a dimethylamino group in 98% acetic acid

R in 2.2-1	x-band	
	λ_{\max}/nm	$\epsilon_{\max}/\text{dm}^3 \text{ mol}^{-1} \text{ cm}^{-1}$
NEt ₂	624.6	10.0
Pyrrolidino	624.6	2.4
Piperidino	627.5	10.6
<i>N</i> -Methylpiperazino	608.3	7.4
NMe ₂ ^a	621	10.4
Morpholino	621.1	9.6
Thiomorpholino	624.8	9.4

a 82Th1

For each of the compounds listed in Table 2.17 the only variant is the R group and hence it would seem reasonable to attribute any differences in their absorption spectrum to the changing nature of R. From the data in Table 2.17, the electron donating ability of the amino groups decreases in the order:



It is interesting to note the similarity in the order between these unsymmetrical MGs and the symmetrical parent Greens (Table 2.15). The position for the thiomorpholino group will be discussed later.

A similar order is found for all the other series of unsymmetrical dyes (Tables 2.18 - 2.20).

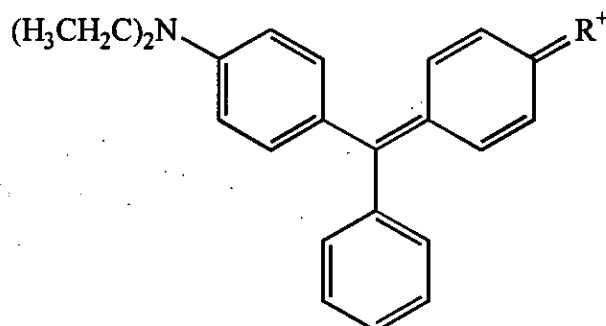


Table 2.18

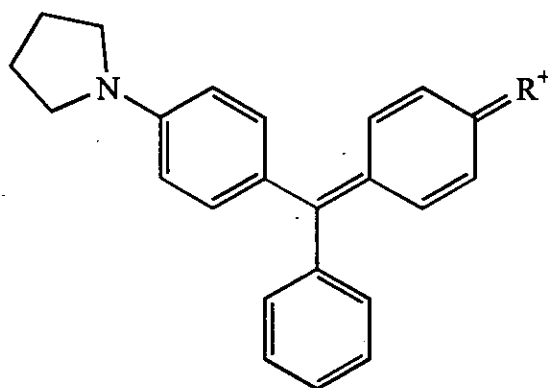
Absorption spectra of some unsymmetrical MGs containing a diethylamino group in 98% acetic acid

R in 2.2-2	x-band	
	λ_{\max}/nm	$\epsilon_{\max}/\text{dm}^3 \text{ mol}^{-1} \text{ cm}^{-1}$
NEt ₂ ^a	629.5	11.9
Pyrrolidino	628.3	5.2
Piperidino	631.0	10.6
N-Methylpiperazino	610.1	7.0
NMe ₂	624.6	10.0
Morpholino	622.5	9.3

a 82Th1

From the data in Table 2.18, the electron donating ability of the amino groups decreases in the order:

piperidino > NEt₂ > pyrrolidino > NMe₂ > morpholino > *N*-methylpiperazino



(2.2-3)

Table 2.19

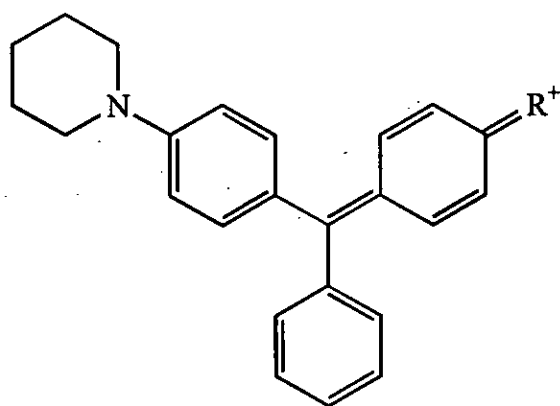
Absorption spectra of some unsymmetrical MGs containing a pyrrolidino group in 98% acetic acid

R in 2.2-3	x-band	
	λ_{\max}/nm	$\epsilon_{\max}/\text{dm}^3 \text{ mol}^{-1} \text{ cm}^{-1}$
NEt ₂	628.3	5.2
Pyrrolidino ^a	629	11.1
Piperidino	631.2	11.2
<i>N</i> -Methylpiperazino	607.1	5.0
NMe ₂	624.6	2.4
Morpholino	623.4	8.8

a 82Th1

From the data in Table 2.19, the electron donating ability of the amino groups decreases in the order:

piperidino > NEt₂ > pyrrolidino > NMe₂ > morpholino > N-methylpiperazino



(2.2-4)

Table 2.20

Absorption spectra of some unsymmetrical MGs containing a piperidino group in 98% acetic acid

R in 2.2-4	x-band	
	λ_{\max}/nm	$\epsilon_{\max}/\text{dm}^3 \text{ mol}^{-1} \text{ cm}^{-1}$
NEt ₂	631.0	10.6
Pyrrolidino	631.2	11.2
Piperidino ^a	634	10.4
N-Methylpiperazino	608.7	5.5
NMe ₂	627.5	10.6
Morpholino	626.2	9.1

a 82Th1

From the data in Table 2.20, the electron donating ability of the amino groups decreases in the order:



It can be seen from the relevant electron donating orders that a trend can be established. In each of the systems, dyes containing piperidine consistently exhibit the largest bathochromic shift. The position of pyrrolidine and diethylamine interchange readily indicating similar electron donating ability which is influenced by the structural environment. These are in turn bathochromically shifted relative to the morpholine and dimethylamino dyes. Finally, from the orders displayed, *N*-methylpiperazine has the weakest electron donating ability.

It is well established that an indication of the availability of a lone pair of electrons on a nitrogen can be obtained by studying the dissociation constants of nitrogen bearing compounds. Table 2.21 shows the values for some amino compounds.

Table 2.21
Dissociation constants for some amino compounds

R	4-NO ₂ C ₆ H ₄ R	4-COOHC ₆ H ₄ R	C ₆ H ₅ R		
	pK _a ^a	pK _a ^b	pK _a ^c	pK _a ^d	pK _a ^e
NMe ₂	0.65	1.40	4.22	5.07	4.39
NEt ₂	1.75	2.45	5.71	6.52	5.85
Pyrrolidino	-0.42	0.39	3.71	4.53	3.45
Piperidino	2.46	2.67	4.60	5.20	>5.2
Morpholino	-	-	-	3.20	-
Piperazino	-	-	-	9.02 ^f	-

a. 71JOC3847, H₂O, 20°C

b. 68RTC1372, 50% EtOH, 25°C

c. 56JCS451, 50% EtOH, 20°C

d. 82Th1, H₂O, 25°C

e. 64JPC832, 50% EtOH

f. 85JPP567, H₂O, 20°C

No literature value was available for the corresponding thiomorpholino and *N*-methylpiperazino compounds. However, it may be reasonably assumed as a result of the increased electron releasing ability of a methyl group that the pK_a of *N*-phenyl-*N*-methylpiperazine is greater or at least similar to *N*-phenylpiperazine and therefore the order of base strength for the *N*-phenyl derivatives and hence the ability of the heteroatom to protonate decreases in the order:



It is well known that mesomeric interaction of an amino function with an aromatic system reduces the basicity of the amine. Therefore, it is anticipated that the order of electron releasing ability into a conjugated system would be the reverse of the base strength order. However, this anticipated order bears little resemblance to the orders obtained from the spectral data for the dyes. It is therefore concluded that other factors such as steric interaction affect the overlap between the nitrogen lone pair and the conjugated system. Mesomeric interaction with the phenyl ring will increase the sp^2 character of the terminal nitrogen in order to facilitate the delocalisation of the nitrogen lone pair into the π -framework of the phenyl ring.

The increased inductive effect of an ethyl group relative to methyl results in the diethylamino derivatives consistently being more basic. This increased basicity is apparent in the unsymmetrical dyes presently studied by consideration of the data presented in Table 2.22. The unsymmetrical dyes containing diethylamino consistently display a bathochromic shift with respect to their corresponding dimethylamino bearing analogues.

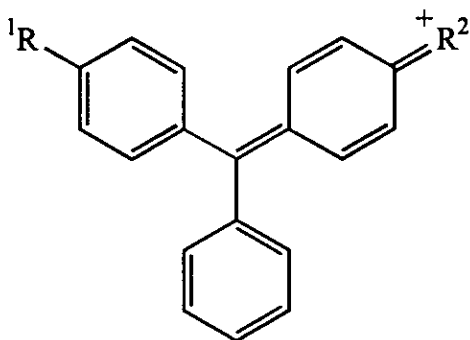


Table 2.22
Comparison of spectral shifts for some unsymmetrical MGs
bearing terminal dimethylamino and diethylamino groups
in 98% acetic acid

R ¹	R ² =NMe ₂	R ² =NEt ₂	Δ λ _{max} (x)/nm
NMe ₂	621 ^a	624.6	+3.6
NEt ₂	624.6	629.5 ^a	+4.9
Pyrrolidine	624.6	628.3	+3.7
Piperidine	627.5	631.0	+3.5
Morpholine	621.1	622.5	+1.4
<i>N</i> -Methylpiperazine	608.3	610.1	+1.8

a. 82Th1

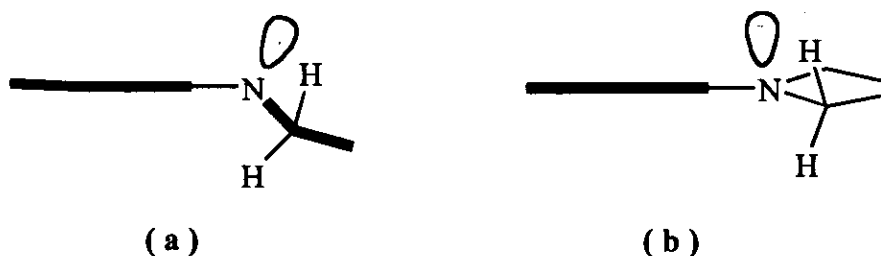
Steric considerations are thought to be at a minimum as a result of the non-rigid conformations for the dialkylamino moiety. In a study of the factors determining the structure of enamines of 2-substituted ketones, it was suggested that there is some degree of steric interaction between the methyl group of a diethylamino moiety with the 2- and 6- positions of a cyclohexene ring (67JA3289). However, for the planar ring system encountered here, if such interactions occur, it can be assumed that they have a negligible effect upon electron donation.

If a comparison is now made between the five and six membered terminal heterocyclic amino groups, in particular pyrrolidine and piperidine, steric considerations now become important. Studies into the structure of the pyrrolidine ring indicate that the system

exists as envelope or half-chair conformations (74JCS(P2)1033, 78TS1, 85JA2305). Thermodynamic studies (59JCP650, 59JCP655) of the conformational interconversion in the ring indicate little or no barrier to pseudorotation. This pseudorotation ensures that the system exists as a puckered five-membered ring and that internal bond angle strain will be averaged over all positions. Mesomeric interaction between the amine nitrogen and the phenyl ring will increase the sp^2 character of the nitrogen. This is illustrated in Figure 2D. This will result in the pyrrolidine ring adopting a more nearly planar conformation (Figure 2D(b)) which, in turn, will result in a decrease in the steric clash between the *ortho* protons of the phenyl ring and the α -methylene protons of the five-membered ring. Significant steric clash is experienced when the nitrogen has more sp^3 character (Figure 2D(a)). This more nearly planar conformation for the pyrrolidine ring will, however, cause the heterocyclic ring protons to be more eclipsed. As a consequence, a balance must be attained between these two opposing forces.

Figure 2D

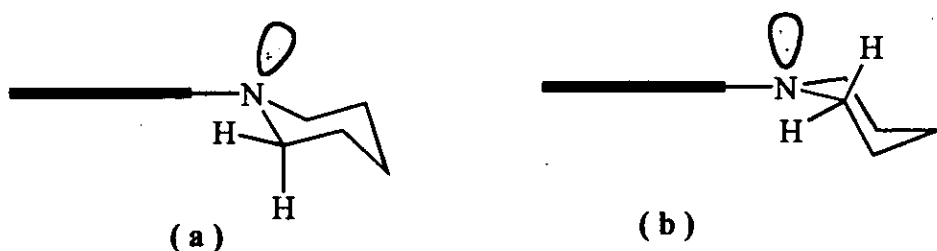
Nitrogen-phenyl ring resonance interaction for N-phenylpyrrolidine



The situation for piperidine is illustrated in Figure 2E.

Figure 2E

Nitrogen-phenyl ring resonance interaction for N-phenylpiperidine



Piperidine exists primarily in the rigid chair conformation (58JCS3002, 80MI2) and as a consequence there is significant steric clash between the α -methylene protons of the six-membered ring and the *ortho* protons of the phenyl ring (Figure 2E(a)). Mesomeric interaction (Figure 2E(b)) exacerbates this clash. Rotation of the piperidine moiety to obviate this conflict results in a reduction of the overlap between the nitrogen lone pair and the π -electron framework of the phenyl ring (84JCS(P2)149).

That the two amine moieties respond differently to crowding effects has been demonstrated to be consistent with steric and electronic considerations. Previously, the concept of I-strain has been proposed to explain the varying reactivities of cyclic five- and six-membered compounds (51JA212, 54JA467, 71JOC3847). I-strain is regarded as the change in internal strain which results from a change in co-ordination number of a ring position (51JA212). In five- and six-membered rings, this strain is primarily due to repulsions from unfavourable conformations (54JA467). A consequence of these interactions is that the formation of *exo*-double bonds is predicted to stabilise a five-membered ring but de-stabilise a six-membered ring (54JA467). In studies on some *N*-(4-nitrophenyl)polymethylenimines (71JOC3847, 71JOC3852), the basicities of the compounds studied were explained using Brown's generalisations regarding to I-strain (71JOC3847). The protonation reactions for aromatic amines involves a change in hybridisation of the nitrogen atom from sp^2 to sp^3 . The incursion of bond-opposition strain should result in this change of hybridisation being more difficult for five-membered ring compounds than six-membered rings. As a result, the piperidino compound is more easily protonated and displays a higher basic strength. The relative basic strengths of *N*-phenylpyrrolidine and *N*-phenylpiperidine have also been discussed by Klyne and de la Mare (58MI2) who attributed the lower basic strength of *N*-phenylpyrrolidine to steric promotion of mesomerism. In this concept, with a pyramidal configuration of the nitrogen, the nitrogen-phenyl carbon bond is in bond opposition with two of the pyrrolidine carbon-hydrogen bonds. If the nitrogen pyramid is flattened somewhat, there will be a two-fold effect: firstly, there will be a slight reduction in the steric strain and secondly, weak van der Waals attractive forces will stabilise the planar form with a subsequent increase in mesomeric interaction. With *N*-phenylpiperidine, the bond opposition which is set up opposes the mesomeric interaction. This evidence suggests that in aromatic amines, there is greater mesomeric interaction between the phenyl ring

and the nitrogen heterocycle in *N*-phenylpyrrolidine than for *N*-phenylpiperidine. However, when incorporated into TPM/DPM chromophores the relative electron donating ability of the two ring systems - as derived from the spectral data (82Th1, 89JCS(P2)1087) - suggest that piperidine has the greater electron donating ability. This was also observed during this study when unsymmetrical MGs containing piperidine consistently showed bathochromic shifts relative to the analogous pyrrolidine bearing dyes. This can be seen from the data in Table 2.23.

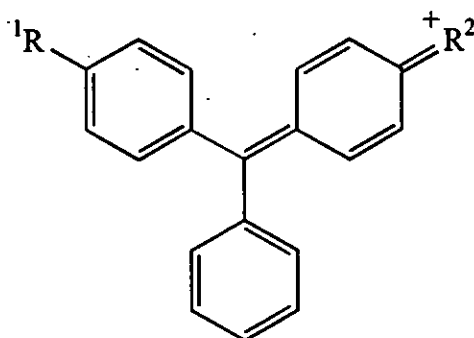


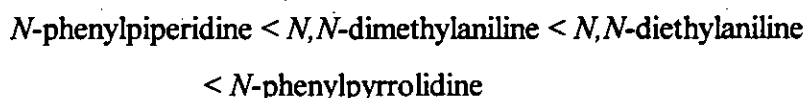
Table 2.23
Comparison of spectral shifts for some unsymmetrical MGs
bearing terminal pyrrolidino- and piperidino- groups
in 98% acetic acid

R ¹	R ² =Pyrrolidine	R ² =Piperidine	Δ λ _{max} (x)/nm
NMe ₂	624.6	627.5	+2.9
NEt ₂	628.3	631.0	+2.7
Pyrrolidino	629 ^a	631.2	+2.2
Piperidino	631.2	634 ^a	+2.8
Morpholino	623.4	626.2	+2.8
<i>N</i> -Methylpiperazino	607.1	608.7	+1.6

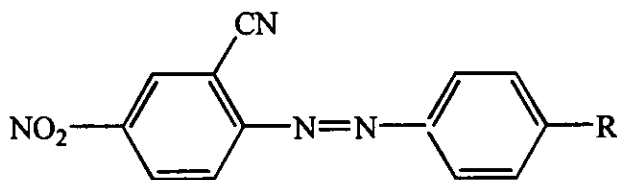
a. 82Th1

In a study of the effects of cyclic terminal groups in 4-aminoazobenzene and related azo dyes (84JCS(P2)149), Hallas *et al.* found that monoazo dyes which contain a terminal

piperidino group absorb hypsochromically compared to those in which the terminal group was pyrrolidine. In addition, in acid solution the pyrrolidino dyes protonated almost exclusively at the β -azo nitrogen whereas the piperidino analogues had a tendency to protonate at the terminal nitrogen. These observations were related to different conjugative abilities of the respective amino groups and are in agreement with previous findings. The molar refraction exaltation values - which are a measure of resonance interaction - for the corresponding anilines suggest increasing resonance interaction in the order (64JPC832):



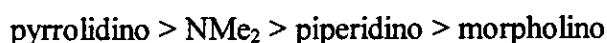
This order was not reflected in a study of the 4-aminoazobenzenes where 4-diethylaminoazobenzene has very similar λ_{max} values to 4-pyrrolidinoazobenzene in both polar and non-polar solvents. This was attributed to hybridisation differences in the ground state of the molecules. In the excited state, eclipsing of the pyrrolidino ring protons may offset any increased stabilisation arising from enhanced conjugation (84JCS(P2)149).



(2.2-5)

Also of interest from the study was the observation that the 2-cyano-4-nitro derivative of 4-pyrrolidinoazobenzene (2.2-5; R= pyrrolidino) shows additivity of substituent effects but that the analogous piperidino compound (2.2-5; R= piperidino) shows a reduced bathochromic shift of 17nm. The explanation of this was that the increased electron demand from the two electron withdrawing substituents was able to enforce improved conjugation of the piperidine nitrogen lone pair.

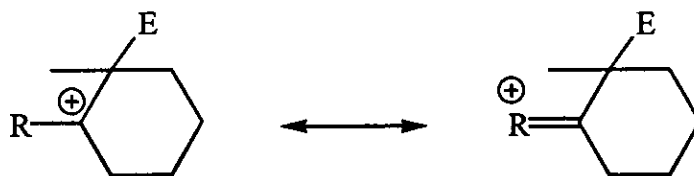
The contrasting ability of terminal amino substituents to donate electron density to π -systems has been studied by Effenberger (78T2409) using HMO π -electron density and ^1H nmr chemical shift correlations during an investigation of the effects of nitrogen substituents upon enamine reactivity. To a first approximation, it is well established that within a series of similar compounds the chemical shift of a specific proton is related to the π -charge density at the appropriate carbon (64JCP2796, 64JA4130). Hence, in the study into the resonance interaction between different amine groups and the aryl π -system of mono-, 1,3-bis-, and 1,3,5-tris-(dialkylamino)benzenes it was determined that the relative donor ability towards an uncharged π -system in the ground state decreases in the order:



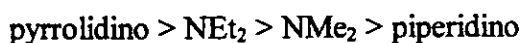
This order bears little resemblance to that derived from the absorption spectral data for the unsymmetrical MGs studied in this investigation. However, Effenberger (78T2409) concedes that whilst the order is derived using ^1H nmr chemical shift data - which is a ground state property - towards an uncharged π -system, no account is taken of the latent potential of each amino group to stabilise a partial or full positive charge such as that which is postulated to exist in the transition state formed during the reaction of enamines with electrophiles (Figure 2F; R= amino).

Figure 2F

Transition state formed during reaction of enamines with electrophile

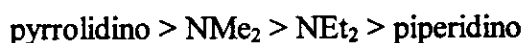


Similarly, a study by Nash and Maciel (64JPC832) into the ^{13}C nmr spectra of some aromatic amines and imines showed that the ^{13}C *para* chemical shifts correlate well with the predicted extent of nitrogen-phenyl ring resonance and that the order of donor ability was:



It was also reported that the ^{13}C *para* chemical shifts correlate well with the base strength of the compounds except for *N,N*-diethylaniline (64JPC832). This was attributed to a loss of solvation energy raising the free energy of the free base. This would have the effect of reducing the energy difference between the free base and its anilinium ion and hence increasing its base strength. From the chemical shifts, the pyrrolidino and diethylamino groups have very similar electron donating abilities. This is also demonstrated in the present work where the relative electron donating ability of the two amino groups as determined from spectral data may be interchanged.

Eastes *et al.* (71JOC3847) have used ultraviolet and nmr spectral data to determine the influence of the nitrogen hybridisation state on the relative basicities of a series of some *N*-(4-nitrophenyl)polymethylenimines. In their study, it was reasoned that deshielding of the *ortho* protons is consistent with reduced amine \leftrightarrow ring resonance interaction resulting from increased sp^3 character of the amine nitrogen. The apparent extent of resonance interaction decreased in the order:

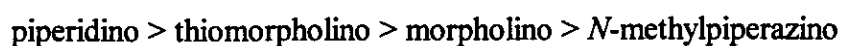


From the ultraviolet spectral data reported, which again was reasoned to relate to the hybridisation state of the nitrogen and hence the ability to interact with the aryl ring, the same approximate order is obtained but with the abilities of the dimethylamino and diethylamino analogues reversed. This may reflect some additional steric interaction for the diethylamino group. In their study on the structures of enamines of 2-substituted ketones (67JA3289), the diethylamino enamine of 2-methylcyclohexanone showed the largest vinyl chemical shift relative to its cyclohexanone analogue which was attributed to some degree of steric interaction with the methyl group of the diethylamino moiety.

From a study by Bottini and Nash (62JA734) of the ultraviolet spectra of *N*-phenyl substituted cyclic amines, the resonance energy due to phenyl ring \leftrightarrow nitrogen resonance interaction was greater for 1-phenylpyrrolidine than for 1-phenylpiperidine. When the spectra of these and related compounds were compared to *N,N*-dimethylaniline, it was concluded that the configuration about the ring nitrogen was more pyramidal than

trigonal suggesting greater sp^3 character than sp^2 . From this the authors concluded that $\pi-sp^3$ conjugation between an amine nitrogen and a phenyl ring was as effective as $\pi-\pi$ conjugation at lowering the energy of the system (62JA734). It may be concluded therefore that whilst the ability of piperidine to conjugate with a phenyl ring system in the ground state is lower than the corresponding pyrrolidine analogue, when increased electron demand is placed upon the system the piperidine responds to this enforced conjugation to a degree comparable if not greater than the five-membered ring. This enforced conjugation results in an increased steric interaction between the α -methylene ring protons and the *ortho* protons of the phenyl ring. An equilibrium is therefore reached whereby the increased rotation of the piperidine ring to alleviate the steric interaction is balanced by the electron demand of the system. This equilibrium manifests itself through a reduction in the extinction coefficient of the energy transition. It might be expected therefore that the more demand which was placed upon the heterocyclic ring system, the more this effect would be observed. This is indeed the case. Whereas the relative stabilities of the parent compounds decreases in the order CV > MG > MHB as indicated by the wider pH range over which the compounds are stable (pK_a, 9.36, 6.90 and 5.61 respectively) (49JCS1724) so the electronic demand increases. It follows therefore that, whilst MHB, EtDPM and PyDPM show increased ϵ_{\max} values for the main absorption band with respect to their MG analogues in accordance with the more planar configuration, the six membered analogues of MHB show a pronounced decrease in their ϵ_{\max} values when compared to their MG analogues.

With the introduction of a second hetero-atom at the 4-position of piperidine, additional electronic and steric interactions influence the ability of the terminal six-membered ring to conjugate with the phenyl ring. The effect which the second heteroatom has upon the heterocyclic ring will be both electronic arising from its electronegativity relative to nitrogen and steric through possible deformations of the ring. The greater the electronegativity of the second heteroatom relative to nitrogen, the larger will be the reduction in the availability of the nitrogen lone pair for conjugation. From their spectral data, the apparent electron donating ability of the six-membered terminal amino groups studied in this investigation decreases in the order:

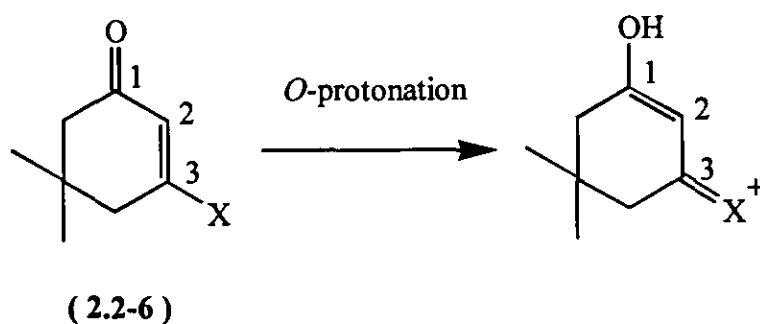


This order bears a similarity to the order for the Pauling electronegativity values of the second heteroatom (Table 2.24).

Table 2.24
Pauling electronegativity values

Element	C	N	O	S
Electronegativity value	2.55	3.04	3.44	2.58

The anomalously low ability of *N*-methylpiperazine to conjugate with the π -framework of the phenyl ring is believed to be related to the presence of the methyl group. The electron releasing ability of the methyl group will result in preferential protonation at the methyl-nitrogen atom thus enhancing its apparent electronegativity and therefore reducing still further the ability of the lone pair of electrons of the *N*-1 nitrogen to conjugate with the π -electron system of the phenyl ring. The effect of the second heteroatom to modify the availability of the nitrogen lone pair manifests itself in the relative basicities of *N*-phenylpiperidine and *N*-phenylmorpholine (Table 2.21). The unavailability of complete base strength data for the appropriate aromatic amines prevents a thorough discussion of this effect. However, a good comparison of the relative donor abilities of the terminal six-membered amino groups can be obtained from the work of Azzaro *et al.* into the basicities of enamino-ketones (83JCS(P2)57). In their study of a series of 3-aminocyclohex-2-enones (2.2-5) they demonstrated that the carbonyl oxygen is the basic site for protonation in aqueous or organic solvents and that the structural effects on the basicities can be linearly correlated using pK_{BH}^+ and the nitrogen substituent constants at the 3-position of the cyclohex-2-enone ring.



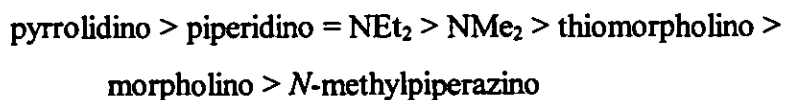
As the ability of the 3-amino substituent to stabilise the system increases so does the base strength of the 3-aminocyclohex-2-enone. The relative base strengths for the 3-aminocyclohex-2-enone compounds are shown in Table 2.25 (83JCS(P2)57).

Table 2.25

Base strengths for a series of some 3-aminocyclohex-2-enones

X in 2.2-6	pK_{BH^+}
NMe ₂	3.14
NEt ₂	3.28
Pyrrolidino	3.38
Piperidino	3.28
Morpholino	2.53
Thiomorpholino	2.57
N-Methylpiperazino	1.36

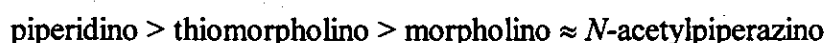
Hence it can be seen that the relative order of ability to stabilise the system decreases in the order:



Two points of note are that firstly, these data suggest that the piperidine group is as good as the diethylamino group at stabilising the system and that secondly, the relative

order for the six-membered ring substituents is the same as that derived from the spectral data collected during this investigation, with the *N*-methylpiperazine moiety having the lowest ability to stabilise a system by conjugation.

This order has also been reported in a study by Hallas *et al.* into the effects of cyclic terminal groups in 4-aminoazobenzenes (86JCS(P2)123). In the study, the absorption spectra of monoazo dyes bearing a terminal six-membered amino substituent were reported. The electron-donating power of the terminal substituent decreased in the order:



The effect upon λ_{max} of the amino groups was related to the relative inductive strength of the atom at the 4-position of the 6-membered ring. It would therefore appear as though monoazobenzene dyes respond in a similar manner to di- and tri-phenylmethane dyes to substitution at the *para* position.

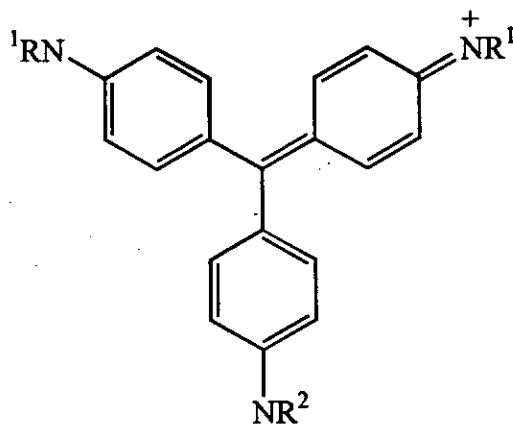
To conclude, the ability of the nitrogen atom of a terminal amino group to donate electron density to a π -system depends upon many factors: molecular conformation, the nature of the heterocycle in question, the intrinsic tendency of the pyramidal nitrogen to assume a planar conformation to maximise conjugation, the balance between steric and electronic effects and the ability of any substituent to enforce conjugation upon the amino moiety.

2.2.2.1 The effects of increased acidity

There have been several studies relating to the effects of increased acidity on the absorption spectra of TPM dyes and their derivatives (59JCS3957, 60JCS3790, 83JCS(P2)975, 89JCS(P2)1087). These studies have involved symmetrical or unsymmetrical Violets or symmetrical Greens. However, a study of the effect of increased acidity on the absorption spectra of unsymmetrical MGs has never been reported and because of the differing basicities of the terminal amino groups, these compounds may exhibit unusual spectral responses.

It has long been established that protonation of the dye base or colour salt can lead to the formation of several polyvalent cations. The preparation of the univalent cations of

the dye bases in 98% acetic acid facilitates the generation of a more acidic media simply by increasing the concentration of water. As the water content of the acetic acid medium is increased, further ionisation of the acetic acid occurs thereby increasing the acidity of the medium.



(2.2-7)

The spectral responses of both the symmetrical Violets (2.2-7; $R^2 = R^1$) and the unsymmetrical Violets (2.2-7; $R^2 \neq R^1$) to an increase in acidity are similar (82Th1, 89JCS(P2)1087). From the earlier discussion, for each of the Violet systems in 98% acetic acid the major band in the absorption spectrum corresponds to that for the univalent cation. As the acidity of the medium increases, protonation may occur at one of the terminal amino groups. This has the effect of generating a Malachite Green-like absorption spectrum with a shift in the main absorption band and the appearance of a low intensity band at shorter wavelength. The position, shape and intensity of the new bands are similar to the x- and y-bands of the Greens. The main absorption band of the original Violet is red shifted as a result of protonation. The spectral responses of the x- and y-bands of the protonated Violets relative to the analogous Greens are in accordance with theoretical predictions for electron-withdrawing groups in the phenyl ring of the parent Green (61JCS1285, 70JCS(B)530, 71JSDC187). An electron-withdrawing group in the phenyl ring of a Green will stabilise both the second highest filled and the lowest unfilled molecular orbitals but have no effect upon the NBMO (70JCS(B)530). Hence the main absorption band should show a red shift proportional to the stabilisation of the empty orbital. This has been utilised in a Hammett type correlation to determine substituent constants for the protonated amino group (82Th1, 83Th1). The response of the y-band

will depend upon the relative stabilisation of the orbitals, since both orbitals are now involved in the transition.

The ease of protonation of a terminal amino group will be dependent upon the basicity of that group. For the symmetrical Violets, protonation may occur at any of the identical terminal amino groups. The response of the symmetrical Violets to protonation may be used to relate the basic strength of the terminal amino groups. The spectral data for the symmetrical Violets are shown in Table 2.26 (82Th1).

Table 2.26
Absorption spectra of symmetrical Violet dyes in 98% and 10%
acetic acid

Dye	98% Acetic acid		10% Acetic acid			
			x-band		y-band	
	$\lambda_{\max} /$ nm	$10^4 \epsilon_{\max} /$ $\text{dm}^3 \text{mol}^{-1}$ cm^{-1}	$\lambda_{\max} /$ nm	$10^4 \epsilon_{\max} /$ $\text{dm}^3 \text{mol}^{-1}$ cm^{-1}	$\lambda_{\max} /$ nm	$10^4 \epsilon_{\max} /$ $\text{dm}^3 \text{mol}^{-1}$ cm^{-1}
Crystal Violet	589	11.6	592	9.2	425	0.3
Ethyl Violet	592.5	13.0	641	7.2	426	1.2
Pyrrolidine Violet	591	12.1	591	10.3	-	-
Piperidine Violet	602	11.5	643	5.1	426	1.6
Morpholine Violet	596	10.6	594	9.2	-	-

From the data in Table 2.26, it can be seen that a relationship exists between the basicity of the terminal amino group and the observed shift in $\lambda_{\max}(x)$ following an increase in the acidity of the solvent (82Th1). This relationship using the base strength values of the phenylamines (82Th1) is summarised in Table 2.27.

Table 2.27

Relationship between basicity of the terminal group and the observed shift in the main absorption band following an increase in the solvent acidity

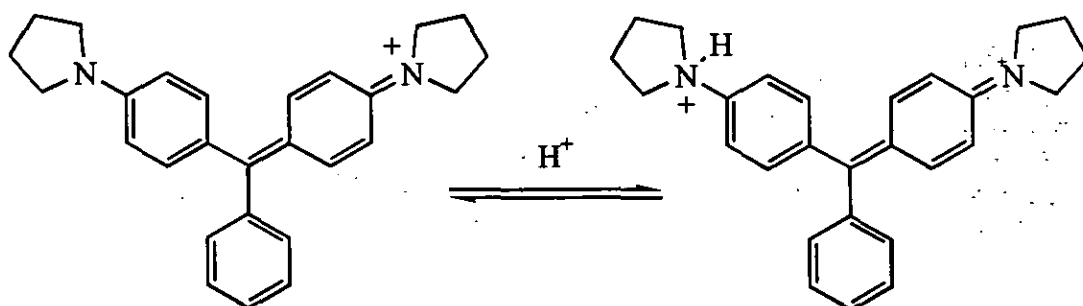
Dye	pK _a of phenylamine	Observed shift relative to parent Violet/nm
Ethyl Violet	6.52	+48.5
Piperidine Violet	5.20	+41
Crystal Violet	5.07	+3
Pyrrolidine Violet	4.53	0
Morpholine Violet	3.20	-2

In the unsymmetrical Violets, an increase in the acidity of the solvent produces a similar response as for the symmetrical Violets. This time, however, it is the most basic group which will be protonated first. A study of a whole series of unsymmetrical Violets bearing similar terminal amino groups as used in this study has shown that TPM dyes bearing the diethylamino or piperidino group readily undergo protonation whereas the ones bearing the dimethylamino, pyrrolidino and morpholino are not readily protonated (89JCS(P2)1087). This contrasting behaviour was explained in terms of the differences in electron density at the terminal heterocyclic nitrogen atoms. The reluctance of morpholine to undergo protonation was attributed to the greater inductive electron-withdrawing ability of the oxygen.

For the symmetrical Greens, protonation of one of the terminal amino groups will have a dramatic effect upon the absorption spectrum of the dye. Unlike the Violet system, where protonation of one of the terminal amino groups results in the generation of a MG type system containing a powerful electron-withdrawing group in one of the phenyl rings, protonation of one of the terminal amino moieties in a Green type dye will considerably destabilise the chromophoric system by destruction of one of the resonance systems. This can be illustrated by considering the example of Pyrrolidine Green

(83JCS(P2)975). Here, an increase in the acidity of the solvent containing the dye will generate the protonated Pyrrolidine Green as shown in Figure 2G.

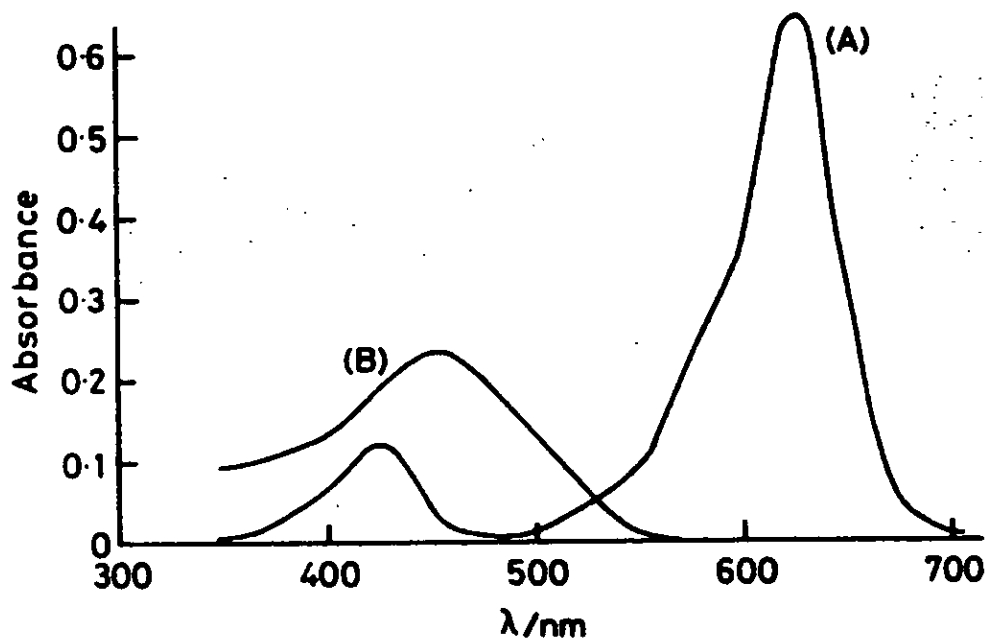
Figure 2G
The formation of protonated Pyrrolidine Green



It can be seen that upon protonation of one of the terminal pyrrolidino groups, the lone pair of electrons of the heterocyclic nitrogen will be utilised, thereby preventing the nitrogen lone pair from conjugating with the phenyl ring. The chromophoric system will be destabilised and the main absorption band will be significantly hypsochromically shifted. Indeed, the reported values for Pyrrolidine Green (PG^+) and its singly protonated form (PGH^{2+}) are 629 nm and 470 nm respectively. The absorption spectra of the two species are shown in Figure 2H.

Figure 2H

Visible absorption spectrum of Pyrrolidine Green, PG⁺, (A)
and protonated Pyrrolidine Green, PGH²⁺, (B)



The value for the main absorption band in PGH²⁺ is comparable to the value quoted for the singly substituted 4-dimethylaminotriphenylmethyl cation of 462 nm in acetic acid (63JGCU153). This would be expected when the similarity in electronic and structural properties of the two systems is considered.

The absorption spectral data for the dyes studied in this investigation were measured in 100%, 50% and 10% acetic acid with water and are presented in Tables 2.28, 2.29 and 2.30.

Table 2.28
Absorption spectra of some unsymmetrical MGs
in 100% acetic acid

Dye	x - band		y - band	
	λ_{\max}/nm	$10^4 \epsilon_{\max}/\text{dm}^3 \text{mol}^{-1} \text{cm}^{-1}$	λ_{\max}/nm	$10^4 \epsilon_{\max}/\text{dm}^3 \text{mol}^{-1} \text{cm}^{-1}$
Me-Et	623.7	10.1	428.7	1.9
Py-Et	626.9	5.3	427.7	1.2
Pi-Et	629.9	10.4	429.7	1.8
Mo-Et	623.0	8.9	428.4	1.8
Me-Py	625.3	2.2	426.2	0.5
Pi-Py	631.0	11.1	431.2	2.0
Mo-Py	623.4	9.0	427.0	2.2
Me-Pi	627.2	10.7	430.1	2.0
Mo-Pi	627.4	9.2	429.7	2.1
Me-Mo	621.4	9.5	430.3	2.3
MPz-Et	613.0	7.0	422.7	1.6
MPz-Me	611.0	7.6	425.3	2.0
MPz-Py	613.2	5.5	422.0	1.3
MPz-Pi	614.6	6.5	425.4	1.6
MPz-Mo	616.2	8.1	427.4	2.0
ThM-Me	625.1	9.5	433.7	1.9

Me: NMe₂; Et: NEt₂; Py: Pyrrolidine; Pi: Piperidine; Mo: Morpholine;
 ThM: Thiomorpholine; MPz: *N*-Methylpiperazine

Table 2.29
Absorption spectra of some unsymmetrical Malachite Greens
in 50% acetic acid

Dye	x - band		y - band	
	λ_{\max}/nm	$10^{-4} \epsilon_{\max}/\text{dm}^3 \text{mol}^{-1} \text{cm}^{-1}$	λ_{\max}/nm	$10^{-4} \epsilon_{\max}/\text{dm}^3 \text{mol}^{-1} \text{cm}^{-1}$
Me-Et	623.8	8.5	429.5	1.7
Py-Et	628.5	4.6	428.0	0.8
Pi-Et	629.9	1.3	431.6	0.3
Mo-Et	621.0	7.2	427.4	1.7
Me-Py	624.9	2.1	425.0	0.5
Pi-Py	630.4	8.1	431.1	2.1
Mo-Py	620.4	7.7	427.4	2.0
Me-Pi	627.0	4.7	432.1	1.2
Mo-Pi	623.7	4.4	428.3	1.2
Me-Mo	618.2	8.2	427.3	1.8
MPz-Et	598.9	4.7	419.6	1.5
MPz-Me	599.1	5.5	417.2	1.8
MPz-Py	598.1	4.3	418.4	1.6
MPz-Pi	600.7	2.8	417.8	1.0
MPz-Mo	607.0	6.8	427.0	1.9
ThM-Me	622.5	8.6	431.2	1.8

Me: NMe₂; Et: NEt₂; Py: Pyrrolidine; Pi: Piperidine; Mo: Morpholine;
ThM: Thiomorpholine; MPz: N-Methylpiperazine

Table 2.30
Absorption spectra of some unsymmetrical Malachite Greens
in 10% acetic acid

Dye	x - band		y - band	
	λ_{\max}/nm	$10^4 \epsilon_{\max}/\text{dm}^3 \text{mol}^{-1} \text{cm}^{-1}$	λ_{\max}/nm	$10^4 \epsilon_{\max}/\text{dm}^3 \text{mol}^{-1} \text{cm}^{-1}$
Me-Et	622.4	2.3	428.9	0.5
Py-Et	626.5	3.7	424.3	0.9
Pi-Et	-	-	-	-
Mo-Et	617.6	2.1	424.2	0.5
Me-Py	622.2	1.8	424.7	0.4
Pi-Py	631.1	3.2	435.1	2.0
Mo-Py	616.8	6.3	422.6	1.7
Me-Pi	627.0	0.4	428.0	0.2
Mo-Pi	621.3	0.7	-	^a
Me-Mo	614.9	6.1	424.1	1.6
MPz-Et	594.2	2.1	414.4	0.8
MPz-Me	592.2	4.2	416.3	1.5
MPz-Py	589.1	3.8	415.3	1.5
MPz-Pi	593.0	0.5	417.2	0.2
MPz-Mo	602.3	4.9	426.2	1.3
ThM-Me	620.2	5.9	428.8	1.4

a. ϵ value too small to be satisfactorily recorded.

Me: NMe₂; Et: NEt₂; Py: Pyrrolidine; Pi: Piperidine; Mo: Morpholine;
 ThM: Thiomorpholine; MPz: *N*-Methylpiperazine

It can be seen from Tables 2.28 - 2.30 that, for the majority of the dyes studied, as the water content of the solvent is increased there is a progressive but small blue shift of $\lambda_{\max}(x)$ and $\lambda_{\max}(y)$. It can be reasonably assumed that these changes are as a consequence of the change in polarity of the solvent. It has been established that, in

general, the main absorption band of TPM dyes is displaced to longer wavelengths in non-polar solvents (76MI1, 81CJC191). This is as a consequence of changing solute-solvent interactions. For symmetrically substituted TPMs such as CV, the resolution of the main absorption band into two separate bands is quite dramatic as the polarity of the solvent is changed. This has been attributed to splitting of the doubly degenerate HOMOs of CV by interaction with polar solvents or by counter-ion association in non-polar solvents (81CJC191, 92JA2342). For TPMs of the MG type which do not possess two degenerate states, the effect of solvent polarity will be much less dramatic (92JA2342). In general, as the water content of the acetic acid is increased there is a decrease in both $\epsilon_{\max}(x)$ and $\epsilon_{\max}(y)$. This can be attributed to the greater instability of the dye in the more acidic medium displacing the dye base \leftrightarrow dye cation equilibrium in favour of the former species. However, for particular dyes there are responses to the change in solvent nature which depart from the general trend. The most obvious case is that of Pi-Et which in 10% acetic acid is completely colourless. Pi-Et bears two of the most basic of the terminal amino groups studied and therefore it is likely that protonation of both of the terminal amino groups has occurred since there is no evidence of a significant absorption band at shorter wavelengths which would be predicted if only one of the terminal groups had been protonated. Indeed, it is noticeable that the dyes bearing the piperidino group (Mo-Pi, Me-Pi and MPz-Pi) display the most drastic reduction in ϵ_{\max} reflecting the increased tendency for piperidine to be protonated and hence destabilise the system. Following this line of reasoning, it might be expected that the dyes bearing *N*-methylpiperazino - predicted to be the most basic of the terminal amino groups used in this study - would display the greatest reduction in ϵ_{\max} . However, this is not the case since the series of dyes bearing *N*-methylpiperazine have amongst the largest ϵ_{\max} values (with the exception of MPz-Pi which unlike Pi-Et still displays a visible absorption spectrum in 10% acetic acid). This apparently anomalous behaviour can be attributed to the presence of the second nitrogen in the six-membered ring. It can be reasonably predicted that as the acidity of the solvent increases, protonation at the *N*-4 position occurs. This would create a strong electron-withdrawing centre which, by analogy with the oxygen in morpholine, would inductively draw electron density from the *N*-1 position and effectively prevent protonation from occurring at this position. This supposition is further supported by the magnitude of the shifts in λ_{\max} for this series

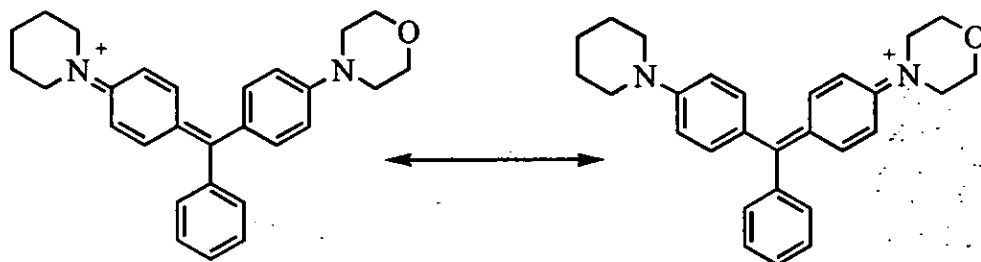
which are approximately two to three times larger than for comparable dyes which do not contain the *N*-methylpiperazino group.

It is also noticeable that the dyes Mo-Py, Me-Mo and ThM-Me which bear the least basic terminal groups display the largest $\epsilon_{\max}(x)$ values in 10% acetic acid, their reluctance to protonate providing greater stability in the increasingly acidic medium. For these dyes, the intensity of the second absorption band shows little or no decrease in 10% acetic acid suggesting a consistent electronic input from the unsubstituted phenyl ring into the chromophoric system. Of all the dyes studied, the responses of the γ -bands of Me-Et and Pi-Py require a comment. Here, rather than being hypsochromically shifted in 10% acetic acid relative to 98% acetic acid, their γ -bands show a bathochromic shift of 1.4 and 4.9 nm respectively which suggests an increase in the amount of electron donation from the phenyl ring into the system. For Pi-Py, this is further supported by the unchanged intensity of the γ -band in the two media. No apparent explanation can be given for this behaviour since neither dye possesses any obvious unique properties. To conclude, the responses of the dyes studied to an increasingly acidic medium are consistent with previously established patterns (82Th1, 83Th1, 89JCS(P2)1087), the exception being *N*-methylpiperazino dyes as discussed.

2.2.2.2 Electronic and structural symmetry

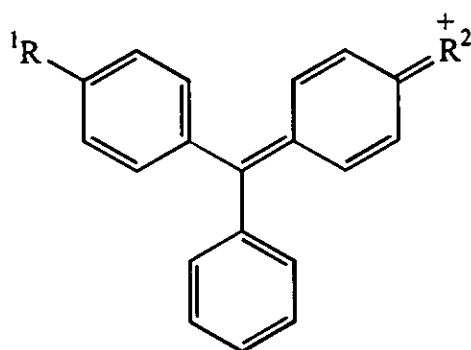
Earlier in this discussion (Section 2.2.2), it was stated that for each series of compounds listed in Table 2.17, the only variant is the nature of the R group and that it would seem reasonable to attribute any differences in their absorption spectra to the influence of changing the nature of R. Whilst this is indeed correct, consideration must be given to the nature of the common amino group and the similarity between the two terminal amino groups themselves. In valence bond terms, for the structurally unsymmetrical dyes studied in this investigation, two extreme resonance configurations can be predicted to exist as shown in Figure 2I using Mo-Pi as an example.

Figure 2I
Two extreme resonance configurations for the structurally
unsymmetrical dye Mo-Pi



In theory, the only difference between two resonance forms is the nature of the terminal amino group (41JA3214) and that, essentially, an unsymmetrical dye differs from a symmetrical dye only in the contributions of these two resonance forms to the resonance hybrid. It may also be inferred that the stability of the chromogen will be related to the ability of each terminal auxochrome to stabilise the positive charge residing upon it and as such, it would be expected that unsymmetrical dyes are less stable than symmetrical ones. Brooker *et al.* examined extensively the absorption spectra of unsymmetrical cyanines (41JA3214, 42JA199, 45JA1869, 45JA1875, 45JA1889). One of the interesting features of unsymmetrical cyanine dyes is that the polymethine chain is no longer uniform (58MI1) and substitution into the system will cause an uneven rotation about the chain; the consequence of this is that prediction of substitution effects is far more difficult. PPP calculations show that the loss of electronic symmetry destroys the relationship to the odd alternant hydrocarbons and perturbational theory can no longer be applied (81DP37). In a study of substitution into the phenyl ring of Me-Et (86JSDC15), Hallas found that the spectral shifts of the main absorption band brought about by substituents in the 3- and 4-positions were linearly related to the appropriate Hammett substituent constants. This is consistent with related symmetrical Green type systems (61JCS1285, 71JSDC187, 82JSDC10) and was explained in terms of transmission of the electronic effects to the central inactive carbon atom (81DP37). A value of $\lambda_{\max}(x) = 626 \text{ nm}$ was reported for the univalent cation of Me-Et (86JSDC15), which is very close to the one recorded for Me-Et during this investigation.

It is accepted that a structurally unsymmetrical cyanine dye having end-groups A and B is considered to be electronically symmetrical if $\lambda_{\max}AB$ is approximately equal to the arithmetic mean of $\lambda_{\max}AA$ and $\lambda_{\max}BB$ (37PRS138, 67JSDC368, 70JSDC237, 71JCS(B)1471). In such cases, the basicities of the end-groups are similar. An electronically unsymmetrical dye gives a value of $\lambda_{\max}AB$ which is less than the mean of $\lambda_{\max}AA$ and $\lambda_{\max}BB$ by an amount known as the deviation (71JCS(B)1471). The magnitude of the deviation will reflect the difference in basicity of the two end-groups. Table 2.31 reports the deviations for the dyes (2.2-8). The values used for the parent Greens were those reported by Sawyer (82Th1) except for *N*-methylpiperazine Green.



(2.2-8)

Table 2.31

Deviations in the electronic absorption spectra of some unsymmetrical MGs

R ¹ in 2.2-8	R ² in 2.2-8					
	NMe ₂	NEt ₂	Pyr. ^a	Pip. ^b	Mo. ^c	<i>N</i> -MPz. ^d
NMe ₂	-	-0.65	-0.4	0.0	-0.9	-5.1
NEt ₂	-0.65	-	-0.95	-0.75	-3.75	-7.55
Pyr. ^a	-0.4	-0.95	-	-0.3	-2.6	-10.3
Pip. ^b	0.0	-0.75	-0.3	-	-2.3	-11.2
Mo. ^c	-0.9	-3.75	-2.6	-2.3	-	-1.0
<i>N</i> -MPz. ^d	-5.1	-7.55	-10.3	-11.2	-1.0	-

a. Pyrrolidino; b. Piperidino; c. Morpholino; d. *N*-Methylpiperazino

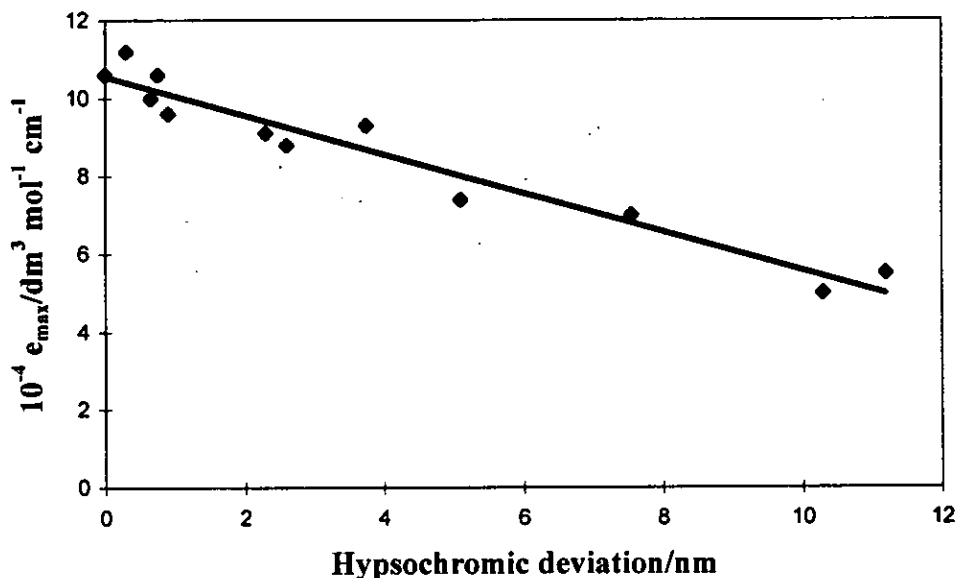
It is noticeable from the data in Table 2.31 that generally the unsymmetrical compounds containing piperidine tend to display the smallest deviations. This tendency is apparent when piperidine is paired with a dialkylamino or nitrogen heterocyclic amino group, but an exceptionally high deviation is shown when paired with *N*-methylpiperazine. Furthermore, there is no apparent deviation in Me-Pi suggesting that the piperidino and dimethylamino moieties have similar basicities and are able to stabilise the positive charge to a similar extent. This observation further supports the proposed tendency for the six-membered ring system to be protonated and hence for the nitrogen atom to adopt an sp^3 hybridised state. Similarly, deviations for the dimethylamino bearing compounds are also amongst the lowest - even for MPz-Me - which suggests the absence of any significant steric effect with the dimethylamino group. The deviations for the compounds bearing the diethylamino and pyrrolidino moieties are of a similar order as anticipated from their relative abilities to stabilise a positively charged system. The compounds bearing morpholino and *N*-methylpiperazino groups show the largest deviations reflecting their inability to stabilise a positive charge. In the case of morpholine, this can be attributed to the low basicity of the group but for *N*-methylpiperazine, whose basicity is predicted to be the greatest of all the amino groups employed in this investigation, this is apparently anomalous behaviour. However, if, as discussed previously, protonation occurs at the *N*-4 position this will create an electron-withdrawing region which will inductively draw electrons away from *N*-1 so reducing its ease of protonation. In this way, the *N*-methylpiperazino moiety will behave in a manner similar to that of morpholine. That protonation in *N*-methylpiperazino group occurs initially at the *N*-4 position is supported by the deviation for MPz-Mo which is only 1.0 nm. This value is significantly smaller than those for the other compounds bearing an *N*-methylpiperazino unit and indicates the greater electronic symmetry of the system arising from the presence of an electron-withdrawing atom at the *N*-4 position in each six-membered ring. This greater electronic symmetry in MPz-Mo may also explain the relative orders of electron releasing ability as derived from the absorption spectra for the *N*-methylpiperazino series. In this series, MPz-Mo displays the longest wavelength main absorption band suggesting the greatest electron releasing ability for the morpholino group relative to the other amino moieties when incorporated into the *N*-methylpiperazino series. This apparent enhanced electron releasing ability of the morpholino group is in contrast to the wealth of other data

collected (82Th1, 83Th1, 89JCS(P2)1087, 94Th1) and it is therefore concluded that the electronic symmetry of a TPM cation plays an important role in determining the position of the main absorption band. The near symmetrical electronic nature of MPz-Mo can be observed in the shape of its absorption spectrum. For the other members of the *N*-methylpiperazino series, broad absorption bands are observed, which results in a dull colour of the solutions. The broadening of the absorption spectra of this series of dyes is especially apparent with increasing acidity. The exception is MPz-Mo whose absorption spectrum is noticeably less broad than the other members of the series.

Various workers (82Th1, 83Th1, 94Th1) have attempted to relate the magnitude of the main absorption band in structurally symmetrical Violets and Greens to the relative ability of a terminal group to stabilise the system, though with variable success. The extinction coefficient of an absorption band can be taken as a measure of the probability of a specific transition occurring (94Th1). For simple Violets and Greens, it can therefore be used to assess the involvement of a terminal substituent in the delocalisation process. From an electronic consideration, it is accepted that the greater the degree of conjugation and hence stability of the system, the greater would be ϵ_{\max} . However, for the dyes studied in this investigation there appears to be no relationship between electron-donating ability as derived from $\lambda_{\max}(x)$ and the magnitude of $\epsilon_{\max}(x)$. This can be ascribed to the influence of other factors. As a consequence of the unsymmetrical nature of the dyes it was considered worthwhile to investigate the possibility of a relationship between $\epsilon_{\max}(x)$ and the deviation in $\lambda_{\max}(x)$. The plot is shown in Figure 2J.

Figure 2J

**A plot of $\epsilon_{\max}(x)$ against $\lambda_{\max}(x)$ deviation for twelve unsymmetrical
MG type dyes**



No deviation was calculable for ThM-Me. When fifteen of the dyes were considered there appeared to be no satisfactory correlation. However, Py-Et and Me-Py were not obtained in analytically pure condition and as such the accuracy of their recorded $\epsilon_{\max}(x)$ values is be open to question and MPz-Mo, as pointed out previously, is anomalous in its apparently symmetrical nature. Therefore, if these points are rejected, a correlation coefficient of $r^2 = 0.94$ is obtained which indicates a reasonable correlation. It can thus be concluded that for this series of dyes there is a relationship between the intensity of the main absorption band and the electronic symmetry of the dye. This can be explained by the differing electronic properties of the terminal groups. If two terminal amino groups have similar electron donating abilities the deviation of $\lambda_{\max}(x)$ will be small, each resonance form will make a similar contribution to the resonance hybrid which introduces a stabilising influence and the intensity of the transition will be greater. It would appear that the other contributing factors exert a negligible effect on the correlation.

If a comparison is made between $\epsilon_{\max}(x)$ for Morpholine Green ($90000 \text{ dm}^3 \text{ mol}^{-1} \text{ cm}^{-1}$) (82Th1), *N*-Methylpiperazine Green ($60000 \text{ dm}^3 \text{ mol}^{-1} \text{ cm}^{-1}$) (82Th1) and MPz-Mo

(83000 dm³ mol⁻¹ cm⁻¹), it can be seen that if the theoretical $\epsilon_{\max}(x)$ for MPz-Mo is a simple arithmetic average of the values for the respective parent Greens, the experimental value $\epsilon_{\max}(x)$ for MPz-Mo is exalted. This exaltation could be ascribed to the greater symmetry predicted for MPz-Mo as discussed previously. However, this is a very simple treatment and should be viewed with caution.

2.3 Kinetic investigations

2.3.1 General

Several experimental methods may be employed to conduct a kinetic study of TPM dyes but each has as its basis the tenet of monitoring the rate of change of concentration of the highly coloured dye with time. The experimental method outlined in the Experimental Section (3.2.4.a) has been used extensively by previous workers when studying relatively stable dyes (81Th1, 82Th1, 83Th1, 83Th2, 83Th3, 89Th1, 91Th1). Unsworth (91Th1) investigated three widely used methods and showed there was no variation between the results obtained from each method for Brilliant Green. Each of the three methods reported has an advantage over the others in the particular experimental circumstances in which it is most widely employed (91Th1).

During this work, preliminary investigations indicated that the DPM dyes and certain members of the unsymmetrical TPM dyes would require the stopped-flow method of study whilst the remainder could be adequately studied using the existing method for more stable dyes. In order to facilitate a direct comparison between this and previous work it was considered necessary to adopt a standard experimental method, namely the stopped-flow method, and determine whether there was any variation in the results obtained from this and other methods. The acetone concentration in each of the methods studied by Unsworth (91Th1) was 0.4% and this has been shown to have no significant effect upon the observed rate constant (80JCTB317). However, preliminary investigations also indicated that the stability of some of the dyes was so low that they decolourised in aqueous solution. It was therefore necessary to prepare them in a non-aqueous acetone medium. The acetone concentration in the reaction mixture for these reactions was 4.0% and it was considered necessary to investigate what possible effect this might have upon the observed rate constant. Therefore, Brilliant Green was studied using the two methods outlined in the Experimental Section and under increased acetone concentrations. A temperature of 298.2 K and an ionic strength of 0.01 mol dm^{-3} was used throughout. The observed rate constant data (k') are given in Table 2.32 and the rate constant values (k_2) in Table 2.33.

Table 2.32

The effect of hydroxide ion and acetone concentration on k' for Brilliant Green using different experimental techniques

Method 1		Method 2 ^a		Method 2 ^{a, b}	
$10^4[\text{OH}^-]/$ mol dm^{-3}	$10^4 k'/\text{s}^{-1}$	$10^3[\text{OH}^-]/$ mol dm^{-3}	$10^3 k'/\text{s}^{-1}$	$10^3[\text{OH}^-]/$ mol dm^{-3}	$10^3 k'/\text{s}^{-1}$
2.000	1.9203	1.923	1.1946	1.920	1.3747
4.000	3.3300	3.846	2.5858	3.848	2.7517
6.000	4.7650	5.769	3.9786	5.768	4.1279
8.000	6.1711	7.692	5.3715	7.688	5.5001
10.000	7.6121	9.615	6.7619	9.615	6.8812

- a. The ionic strength of the reaction solution in this method was $0.0096 \text{ mol dm}^{-3}$
 b. The acetone concentration of the reaction solution was 4.0%.

Table 2.33

Rate constant k_2 for the reaction between Brilliant Green and hydroxide ion using different experimental techniques

Method	$k_2/\text{dm}^3 \text{ mol}^{-1} \text{ s}^{-1}$	Reference
1 ^a	0.72 ± 0.01	80JCTB317
2 ^a	0.720 ± 0.002	91Th1
1 ^a	0.711 ± 0.002	This study
2 ^a	0.724 ± 0.001	This study
2 ^b	0.716 ± 0.001	This study

- a. Acetone concentration of reaction solution was 0.4%.
 b. Acetone concentration of reaction solution was 4.0%.

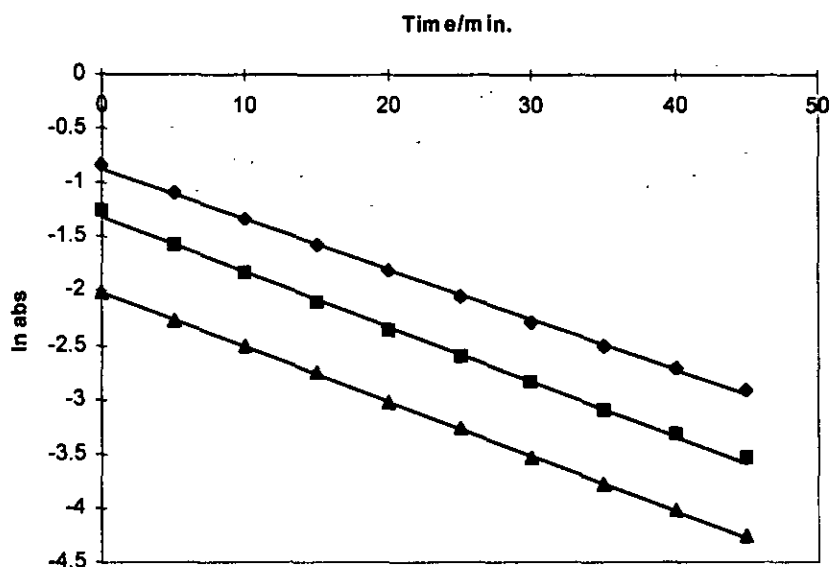
The values of k_2 were calculated using the least squares computer program (Appendix A1, PLOT). The k_2 values obtained are essentially constant, which indicates that the increased hydroxide ion and acetone concentration used do not cause any significant changes. It follows that the results obtained from the fast-kinetics method in which there was 4.0% acetone in the reaction solution can be directly compared with previous work. The effect of increased acetone concentration in the reaction solution of TPM dyes has been investigated previously (70JPC1382, 83Th1) and the findings from this investigation are in accordance with the previous, more extensive work. The stopped-flow technique is usually employed for dyes whose half-life times are less than 60 seconds but it has been established in this study that this technique is also suitable for more stable dyes.

For the reaction solutions, the plots of \ln absorbance against time were linear for at least 75% of the reaction. Unsworth (91Th1) encountered non-linearity after 60% of the reaction when employing the fast-kinetics technique. This was ascribed to excessive precipitation of the dye as a consequence of the increased dye concentration in the reaction solution. However, although this has been a problem for previous workers (52JA5988, 91Th1) it did not appear to be a problem during this study. Cigen *et al.* noted the problem of carbinol precipitation during their equilibrium and kinetic studies but found that the precipitation was sufficiently delayed in strongly alkaline solutions to allow reliable kinetic studies to be performed (64ACS157).

All the kinetic experiments were carried out in excess of hydroxide ion concentration which ensured pseudo first order reaction kinetics. Changes in the initial concentration of dye did not affect the observed rate constant k' for a particular hydroxide concentration and at a particular temperature thus confirming pseudo-first order kinetics. This is illustrated in Figure 2K using EtDPM as the example.

Figure 2K

Plot of \ln absorbance against time for varying initial concentrations of EtDPM at 293.8 K; (\blacklozenge) 4.67×10^{-4} , (\blacksquare) 2.52×10^{-4} and (\blacktriangle) $1.12 \times 10^{-4} \text{ mol dm}^{-3} \times 10^3$ $[\text{OH}^-] = 0.5 \text{ mol dm}^{-3}$, $I = 0.01 \text{ mol dm}^{-3}$



The observed rate constant for each reaction was computed using the Hewlett-Packard kinetics software. In order to minimise random experimental error, six values of k' were determined at each hydroxide concentration. The mean and standard error values for each set were calculated using a standard statistical treatment. Excellent results were obtained for the TPM dyes and the standard deviation on k' was less than 3% for all the experiments. For the DPM dyes, the standard deviation on k' was less than 10% for all experiments. The poorer precision for the DPM dyes is due to their increased reactivity - the drastically shorter reaction time reduced the amount of data collection available.

The graphical treatment of the data allowed suspect points to be repeated. The data suggest that a rate law of the following type can be predicted for both the DPM and TPM dyes studied in this investigation

$$\text{Rate} = -d[\text{Dye}^+]/dt = k_1[\text{Dye}^+][\text{H}_2\text{O}] + k_2[\text{Dye}^+][\text{OH}^-]$$

6.4

From the proposed equation, it can be seen that simultaneous reactions between dye cation and both water molecules and hydroxide ions occur. Since pseudo-first order kinetics are employed, the rate equation can be written as

$$\text{Rate} = k'[\text{Dye}^+] \quad 6.5$$

where

$$k' = k_1[\text{H}_2\text{O}] + k_2[\text{OH}^-] \quad 6.6$$

It can be seen that a plot of k' against hydroxide ion concentration will produce a straight line of slope equal to k_2 and with an intercept of $k_1[\text{H}_2\text{O}]$. Since water is a much weaker nucleophile than the hydroxide ion, the value of k_1 will be much smaller than k_2 . Previously, on similar studies of TPM dyes, k_2 has been obtained from the simple treatment of $k'/[\text{OH}^-]$ (61JIC861, 70BCJ601, 70TFS2305, 70JPC1382). However, k_1 is not insignificant, especially for the more reactive DPM dyes, and therefore it was standard to compute k_1 and k_2 from the plot of k' against hydroxide ion concentration using the weighted least squares computer program (Appendix A1, OHE). The correlation coefficients for all the plots of k' against hydroxide ion concentration were 0.995 or greater. Since k_1 is obtained from the intercept of the plot it is prone to very large errors and negative values may be derived. Therefore, the values of k_1 determined from the kinetic experiments will not be routinely reported. However, as an indication as to its magnitude, k_1 was typically of the order 10^{-5} to $10^{-7} \text{ dm}^3 \text{ mol}^{-1} \text{ s}^{-1}$.

The application of a weighted least squares computer program (Appendix A1, ACT) based on the equations of Margerison (69MI2) to the linear relationship between $\log k_2$ and $1/T$ generated a slope equal to $-E/2.303R$ and an intercept equal to $\log A$. From these Arrhenius plots, values for ΔH^\ddagger and ΔS^\ddagger were calculated together with their standard errors. Errors in ΔS^\ddagger can be relatively large as a consequence of the intercept being well removed from the experimental data. Previous workers (81Th1, 82Th1, 83Th1, 83Th2, 89Th1, 91Th1) have reported thermodynamic activation parameters for the reaction with water. However, due to nature of the data, these were only reported for completeness and only gave an indication as to their magnitude. For the present

investigation it was not considered necessary to report the thermodynamic activation parameters for the reaction with water.

Attempts to prepare pure samples of some of the dye salts proved unsuccessful. In view of the low carbon analysis figures for these dye salts and consistent with their method of preparation it was considered that the impurity was of an inorganic nature. Such inorganic impurities are not expected to interfere with the reaction in any way or behave catalytically towards the reaction. It was therefore considered acceptable to use these dyes for the kinetic investigation.

In addition, in view of the wealth of data covering the ionic nature of the reaction between dye cation and hydroxide ion (61JCS861, 70BCSJ601, 70TFS2305, 81Th1, 82JCS(P2)987, 82Th1, 85JCS(P2)107) it was viewed unnecessary to study ionic strength effects. It was considered reasonable to treat the reaction as occurring between two univalent but oppositely charged ions. Due to the nature of the fast-kinetics method in which two solutions are mixed at zero time, the ionic strength of the reaction solution was actually $0.009615 \text{ mol dm}^{-3}$ but this small difference in ionic strength did not have any significant effect upon the rate constants obtained.

As a final note, the computer programs presented in the Appendix have been used previously by employing a microcomputer but for this study the computer programs were translated into Microsoft Excel[®] spreadsheets. Numerous checks were conducted employing existing, independently obtained data to ensure correct translation.

2.3.2 Unsymmetrical MGs

The observed rate constant data for the sixteen unsymmetrical MG dyes studied during this investigation are shown in Tables 2.34 - 2.49. The kinetic plot for each dye is shown graphically in the Appendix (A2, Figures 1 – 16).

Table 2.34

The effect of temperature and hydroxide ion concentration on k' for 4'-dimethylamino-4''-diethylaminotriphenylmethyl perchlorate

$10^3 [\text{OH}^-]/\text{mol dm}^{-3}$	$10^2 k'/\text{s}^{-1}$	T/K
1.923	0.20 ± 0.01	298.2
3.846	0.42 ± 0.01	
5.769	0.65 ± 0.01	
7.692	0.86 ± 0.01	
3.846	0.60 ± 0.01	303.2
5.769	0.94 ± 0.03	
7.692	1.25 ± 0.04	
9.615	1.59 ± 0.02	
1.923	0.45 ± 0.01	309.2
3.846	0.90 ± 0.01	
7.692	1.98 ± 0.06	
9.615	2.50 ± 0.04	
1.923	0.67 ± 0.02	313.2
5.769	2.07 ± 0.04	
7.692	2.75 ± 0.07	
9.615	3.50 ± 0.11	

$I = 0.009615 \text{ mol dm}^{-3}$

95% confidence interval

Table 2.35

The effect of temperature and hydroxide ion concentration on k' for 4'-pyrrolidino-4''-diethylaminotriphenylmethyl perchlorate

$10^3[\text{OH}^-]/\text{mol dm}^{-3}$	$10^2 k'/\text{s}^{-1}$	T/K
1.923	0.12 ± 0.01	297.4
3.846	0.24 ± 0.01	
7.692	0.48 ± 0.01	
9.615	0.61 ± 0.01	
3.846	0.35 ± 0.01	302.4
5.769	0.55 ± 0.01	
7.692	0.74 ± 0.01	
9.615	0.92 ± 0.01	
1.923	0.28 ± 0.01	308.8
3.846	0.56 ± 0.01	
5.769	0.85 ± 0.02	
7.692	1.11 ± 0.03	
9.615	1.41 ± 0.02	
1.923	0.41 ± 0.01	313.2
3.846	0.85 ± 0.01	
5.769	1.29 ± 0.02	
7.692	1.69 ± 0.05	
9.615	2.12 ± 0.05	

$I = 0.009615 \text{ mol dm}^{-3}$

95% confidence interval

Table 2.36

The effect of temperature and hydroxide ion concentration on k'
for 4'-piperidino-4''-diethylaminotriphenylmethyl perchlorate

$10^3[\text{OH}^-]/\text{mol dm}^{-3}$	$10^2 k'/\text{s}^{-1}$	T/K
1.919	0.29 ± 0.01	297.2
5.765	0.862 ± 0.01	
7.692	1.17 ± 0.04	
9.612	1.48 ± 0.04	
1.919	0.65 ± 0.01	307.4
3.846	1.19 ± 0.02	
7.692	2.53 ± 0.03	
9.612	3.18 ± 0.04	
1.919	0.94 ± 0.02	308.8
3.846	1.78 ± 0.04	
5.765	2.71 ± 0.08	
9.612	4.61 ± 0.15	

$I = 0.009615 \text{ mol dm}^{-3}$

95% confidence interval

Table 2.37

**The effect of temperature and hydroxide ion concentration on k'
for 4'-morpholino-4''-diethylaminotriphenylmethyl perchlorate**

$10^3[\text{OH}^-]/\text{mol dm}^{-3}$	$10^2 k'/\text{s}^{-1}$	T/K
1.925	0.66 ± 0.02	297.2
3.850	1.42 ± 0.03	
5.775	2.31 ± 0.03	
7.692	3.01 ± 0.04	
9.617	3.87 ± 0.05	
1.925	0.96 ± 0.02	301.4
3.850	1.94 ± 0.06	
5.775	3.06 ± 0.04	
9.617	5.05 ± 0.06	
1.925	1.49 ± 0.02	306.6
5.775	4.39 ± 0.12	
7.692	5.96 ± 0.08	
9.617	7.28 ± 0.10	
1.925	2.13 ± 0.05	311.4
3.850	4.26 ± 0.05	
5.775	6.39 ± 0.06	
7.692	8.50 ± 0.19	

$I = 0.009615 \text{ mol dm}^{-3}$

95% confidence interval

Table 2.38

The effect of temperature and hydroxide ion concentration on k'
for 4'-dimethylamino-4''-pyrrolidinotriphenylmethyl perchlorate

$10^3[\text{OH}^-]/\text{mol dm}^{-3}$	$10^2 k'/\text{s}^{-1}$	T/K
1.925	0.11 ± 0.01	292.4
3.842	0.20 ± 0.01	
5.767	0.28 ± 0.01	
9.617	0.50 ± 0.01	
3.842	0.31 ± 0.01	297.4
5.767	0.45 ± 0.01	
7.692	0.62 ± 0.02	
9.617	0.79 ± 0.02	
1.925	0.25 ± 0.01	302.8
3.842	0.47 ± 0.01	
5.767	0.71 ± 0.02	
7.692	0.96 ± 0.02	
3.842	0.73 ± 0.02	308.4
5.767	1.08 ± 0.01	
7.692	1.47 ± 0.03	
9.617	1.87 ± 0.03	

$I = 0.009615 \text{ mol dm}^{-3}$

95% confidence interval

Table 2.39

The effect of temperature and hydroxide ion concentration on k'
for 4'-piperidino-4''-pyrrolidinotriphenylmethyl perchlorate

$10^3[\text{OH}^-]/\text{mol dm}^{-3}$	$10^2 k'/\text{s}^{-1}$	T/K
1.921	0.16 ± 0.01	292.4
3.842	0.33 ± 0.01	
7.692	0.67 ± 0.02	
9.613	0.87 ± 0.01	
3.842	0.51 ± 0.01	297.4
5.771	0.77 ± 0.01	
7.692	1.05 ± 0.02	
9.613	1.33 ± 0.03	
1.921	0.39 ± 0.01	302.6
3.842	0.77 ± 0.02	
5.771	1.18 ± 0.03	
7.692	1.57 ± 0.03	
3.842	1.18 ± 0.03	308.4
5.771	1.78 ± 0.02	
7.692	2.38 ± 0.02	
9.613	2.99 ± 0.03	

I = 0.009615 mol dm⁻³

95% confidence interval

Table 2.40

The effect of temperature and hydroxide ion concentration on k'
for 4'-morpholino-4''-pyrrolidinotriphenylmethyl perchlorate

$10^3[\text{OH}^-]/\text{mol dm}^{-3}$	$10^2k'/\text{s}^{-1}$	T/K
1.922	0.44 ± 0.01	292.8
3.844	0.89 ± 0.02	
5.766	1.38 ± 0.04	
7.688	1.83 ± 0.05	
3.844	1.31 ± 0.03	297.8
5.766	2.00 ± 0.02	
7.688	2.68 ± 0.02	
9.611	3.38 ± 0.02	
1.922	1.02 ± 0.02	303.0
3.844	2.08 ± 0.02	
7.688	4.36 ± 0.03	
9.611	4.99 ± 0.16	
1.922	1.45 ± 0.02	308.6
3.844	2.87 ± 0.06	
5.766	4.37 ± 0.06	
9.611	7.32 ± 0.06	

I = 0.009615 mol dm⁻³

95% confidence interval

Table 2.41

The effect of temperature and hydroxide ion concentration on k'
for 4'-dimethylamino-4''-piperidinotriphenylmethyl perchlorate

$10^3[\text{OH}^-]/\text{mol dm}^{-3}$	$10^2k'/\text{s}^{-1}$	T/K
1.923	0.28 ± 0.01	292.6
3.846	0.54 ± 0.01	
5.769	0.81 ± 0.02	
7.692	1.09 ± 0.02	
1.923	0.39 ± 0.01	297.4
3.846	0.77 ± 0.02	
5.769	1.17 ± 0.02	
7.692	1.57 ± 0.03	
1.923	0.61 ± 0.01	303.4
3.846	1.19 ± 0.02	
5.769	1.84 ± 0.01	
9.615	3.11 ± 0.01	
1.923	0.91 ± 0.02	309.0
3.846	1.83 ± 0.02	
7.692	3.70 ± 0.03	
9.615	4.72 ± 0.03	

$I = 0.009615 \text{ mol dm}^{-3}$

95% confidence interval

Table 2.42

The effect of temperature and hydroxide ion concentration on k'
for 4'-morpholino-4''-piperidinotriphenylmethyl perchlorate

$10^3[\text{OH}^-]/\text{mol dm}^{-3}$	$10^2k'/\text{s}^{-1}$	T/K
1.923	0.52 ± 0.01	292.4
3.845	1.04 ± 0.03	
5.768	1.60 ± 0.03	
7.691	2.31 ± 0.04	
1.923	0.85 ± 0.02	297.4
3.845	1.68 ± 0.04	
7.691	3.54 ± 0.03	
9.613	4.47 ± 0.02	
1.923	1.43 ± 0.02	302.4
5.768	3.93 ± 0.12	
7.691	5.23 ± 0.18	
9.613	6.66 ± 0.16	
3.845	3.99 ± 0.06	308.6
5.768	5.78 ± 0.14	
7.691	8.38 ± 0.12	
9.613	9.51 ± 0.05	

$I = 0.009615 \text{ mol dm}^{-3}$

95% confidence interval

Table 2.43

The effect of temperature and hydroxide ion concentration on k'
for 4'-dimethylamino-4''-morpholinotriphenylmethyl perchlorate

$10^3[\text{OH}^-]/\text{mol dm}^{-3}$	$10^2k'/\text{s}^{-1}$	T/K
1.921	0.80 ± 0.02	292.2
3.842	1.59 ± 0.05	
5.771	2.40 ± 0.02	
7.692	2.97 ± 0.05	
9.612	3.90 ± 0.02	
1.921	1.17 ± 0.02	297.2
3.842	2.18 ± 0.05	
5.771	3.49 ± 0.02	
7.692	4.64 ± 0.01	
3.842	3.31 ± 0.01	302.2
5.771	5.04 ± 0.01	
7.692	6.53 ± 0.12	
9.612	8.36 ± 0.04	
1.921	2.58 ± 0.03	308.4
3.842	5.08 ± 0.03	
5.771	8.36 ± 0.09	
9.612	14.5 ± 0.1	

$I = 0.009615 \text{ mol dm}^{-3}$

95% confidence interval

Table 2.44

The effect of temperature and hydroxide ion concentration on k'
for 4'-N-methylpiperazino-4''-diethylaminotriphenylmethyl perchlorate

$10^3[\text{OH}^-]/\text{mol dm}^{-3}$	$10^2k'/\text{s}^{-1}$	T/K
0.481	0.17 ± 0.01	294.4
0.963	0.31 ± 0.01	
1.925	0.60 ± 0.01	
3.850	1.16 ± 0.03	
0.963	0.40 ± 0.01	297.6
1.444	0.56 ± 0.01	
1.925	0.76 ± 0.01	
3.850	1.43 ± 0.03	
0.481	0.31 ± 0.01	302.8
0.963	0.59 ± 0.02	
1.444	0.86 ± 0.01	
1.925	1.12 ± 0.02	
0.481	0.48 ± 0.02	308.8
0.963	0.88 ± 0.02	
1.444	1.31 ± 0.03	
1.925	1.69 ± 0.04	

$I = 0.009615 \text{ mol dm}^{-3}$

95% confidence interval

Table 2.45

The effect of temperature and hydroxide ion concentration on k'
for 4'-N-methylpiperazino-4''-dimethylaminotriphenylmethyl perchlorate

$10^3[\text{OH}^-]/\text{mol dm}^{-3}$	$10^2k'/\text{s}^{-1}$	T/K
1.924	0.74 ± 0.01	293.0
3.848	1.46 ± 0.04	
5.772	2.18 ± 0.03	
9.619	3.64 ± 0.05	
1.924	1.09 ± 0.03	297.4
3.848	2.14 ± 0.05	
7.695	4.12 ± 0.15	
9.619	5.16 ± 0.19	
1.924	1.60 ± 0.02	303.0
3.848	3.02 ± 0.16	
7.695	6.11 ± 0.07	
9.619	7.64 ± 0.10	
1.924	2.45 ± 0.05	309.0
3.848	4.83 ± 0.12	
5.772	7.04 ± 0.25	
7.695	8.87 ± 0.38	

$I = 0.009615 \text{ mol dm}^{-3}$

95% confidence interval

Table 2.46

The effect of temperature and hydroxide ion concentration on k'
for 4'-N-methylpiperazino-4''-pyrrolidinotriphenylmethyl perchlorate

$10^3[\text{OH}^-]/\text{mol dm}^{-3}$	$10^2k'/\text{s}^{-1}$	T/K
1.922	0.39 ± 0.01	292.6
3.844	0.80 ± 0.01	
5.766	1.21 ± 0.03	
7.688	1.62 ± 0.03	
1.922	0.58 ± 0.01	297.4
3.844	1.16 ± 0.04	
5.766	1.75 ± 0.05	
9.610	2.90 ± 0.02	
1.922	0.87 ± 0.02	303.0
3.844	1.75 ± 0.03	
7.688	3.51 ± 0.02	
9.610	4.26 ± 0.14	
1.922	1.36 ± 0.02	309.0
3.844	2.68 ± 0.06	
5.766	4.08 ± 0.06	
7.688	5.47 ± 0.10	

$I = 0.009615 \text{ mol dm}^{-3}$

95% confidence interval

Table 2.47

The effect of temperature and hydroxide ion concentration on k'
for 4'-N-methylpiperazino-4''-piperidinotriphenylmethyl perchlorate

$10^3[\text{OH}^-]/\text{mol dm}^{-3}$	$10^2k'/\text{s}^{-1}$	T/K
1.923	0.73 ± 0.02	293.6
3.846	1.63 ± 0.02	
5.769	2.45 ± 0.04	
9.615	3.90 ± 0.17	
1.923	1.06 ± 0.03	297.4
3.846	2.00 ± 0.02	
5.769	3.14 ± 0.06	
7.692	4.12 ± 0.15	
1.923	1.67 ± 0.04	303.6
3.846	3.16 ± 0.13	
5.769	4.80 ± 0.39	
7.692	6.59 ± 0.12	
1.923	2.41 ± 0.09	309.6
3.846	4.68 ± 0.34	
5.769	7.27 ± 0.18	
7.692	9.70 ± 0.27	

I = 0.009615 mol dm⁻³

95% confidence interval

Table 2.48

The effect of temperature and hydroxide ion concentration on k'
for 4'-N-methylpiperazino-4''-morpholinotriphenylmethyl perchlorate

$10^3[\text{OH}^-]/\text{mol dm}^{-3}$	$10^2k'/\text{s}^{-1}$	T/K
1.923	2.65 ± 0.04	292.4
3.846	5.55 ± 0.06	
5.769	8.69 ± 0.36	
9.615	14.6 ± 0.6	
1.923	3.66 ± 0.09	297.4
3.846	7.30 ± 0.39	
5.769	12.0 ± 0.4	
7.692	15.1 ± 0.5	
1.923	6.55 ± 0.24	303.2
3.846	12.5 ± 0.5	
5.769	19.3 ± 0.4	
7.692	25.5 ± 1.3	
1.923	9.63 ± 0.30	308.8
3.846	18.8 ± 0.7	
5.769	28.2 ± 0.5	
7.692	37.5 ± 0.5	

$I = 0.009615 \text{ mol dm}^{-3}$

95% confidence interval

Table 2.49

The effect of temperature and hydroxide ion concentration on k' for 4'-thiomorpholino -4''-dimethylaminotriphenylmethyl perchlorate

$10^3[\text{OH}^-]/\text{mol dm}^{-3}$	$10^2k'/\text{s}^{-1}$	T/K
1.922	0.49 ± 0.01	292.8
3.844	0.98 ± 0.02	
5.766	1.54 ± 0.02	
7.688	2.02 ± 0.02	
1.922	0.76 ± 0.02	297.8
3.844	1.49 ± 0.02	
7.688	3.01 ± 0.04	
9.611	3.83 ± 0.04	
3.844	2.17 ± 0.04	303.0
5.766	3.37 ± 0.04	
7.688	4.51 ± 0.05	
9.611	5.68 ± 0.08	
1.922	1.66 ± 0.04	308.8
5.766	5.13 ± 0.05	
7.688	6.81 ± 0.11	
9.611	8.72 ± 0.10	

$I = 0.009615 \text{ mol dm}^{-3}$

95% confidence interval

The values for the rate constant, k_2 together with its standard error are reported in Tables 2.50 - 2.65. It must be stated at this point that throughout the discussion, the terms k_1 , ΔH_1^\ddagger , and ΔS_1^\ddagger refer to the reaction between dye cation and water and the terms k_2 , ΔH_2^\ddagger , and ΔS_2^\ddagger refer to the reaction between dye cation and hydroxide ion.

Table 2.50

The effect of temperature on the rate constant k_2 for the hydrolysis of the 4'-dimethylamino-4''-diethylaminotriphenylmethyl cation

Temperature/K	$k_2/ \text{dm}^3 \text{mol}^{-1} \text{s}^{-1}$
298.2	1.15 ± 0.01
303.2	1.71 ± 0.01
309.2	2.72 ± 0.06
313.2	3.65 ± 0.04

Table 2.51

The effect of temperature on the rate constant k_2 for the hydrolysis of the 4'-pyrrolidino-4''-diethylaminotriphenylmethyl cation

Temperature/K	$k_2/ \text{dm}^3 \text{mol}^{-1} \text{s}^{-1}$
297.4	0.64 ± 0.01
302.4	0.98 ± 0.01
307.8	1.47 ± 0.01
313.2	2.22 ± 0.02

Table 2.52

The effect of temperature on the rate constant k_2 for the hydrolysis of the 4'-piperidino-4''-diethylaminotriphenylmethyl cation

Temperature/K	$k_2/ \text{dm}^3 \text{mol}^{-1} \text{s}^{-1}$
297.2	1.54 ± 0.03
307.4	3.33 ± 0.07
312.4	4.79 ± 0.10

Table 2.53

The effect of temperature on the rate constant k_2 for the hydrolysis of the 4'-morpholino-4''-diethylaminotriphenylmethyl cation

Temperature/K	$k_2/ \text{dm}^3 \text{mol}^{-1} \text{s}^{-1}$
297.2	4.19 ± 0.08
301.4	5.30 ± 0.08
306.6	7.58 ± 0.12
311.4	11.0 ± 0.1

Table 2.54

The effect of temperature on the rate constant k_2 for the hydrolysis of the 4'-dimethylamino-4''-pyrrolidinotriphenylmethyl cation

Temperature/K	$k_2/ \text{dm}^3 \text{mol}^{-1} \text{s}^{-1}$
292.4	0.52 ± 0.03
297.4	0.81 ± 0.04
302.8	1.24 ± 0.03
308.4	2.01 ± 0.05

Table 2.55

The effect of temperature on the rate constant k_2 for the hydrolysis of the 4'-piperidino-4''-pyrrolidinotriphenylmethyl cation

Temperature/K	$k_2/ \text{dm}^3 \text{mol}^{-1} \text{s}^{-1}$
292.4	0.92 ± 0.01
297.4	1.43 ± 0.02
302.6	2.05 ± 0.01
308.4	3.16 ± 0.01

Table 2.56

The effect of temperature on the rate constant k_2 for the hydrolysis of the 4'-morpholino-4''-pyrrolidinotriphenylmethyl cation

Temperature/K	$k_2/ \text{dm}^3 \text{mol}^{-1} \text{s}^{-1}$
292.8	2.41 ± 0.03
297.8	3.60 ± 0.03
303.0	5.77 ± 0.24
308.6	7.66 ± 0.03

Table 2.57

The effect of temperature on the rate constant k_2 for the hydrolysis of the 4'-dimethylamino-4''-piperidinotriphenylmethyl cation

Temperature/K	$k_2/ \text{dm}^3 \text{mol}^{-1} \text{s}^{-1}$
292.6	1.41 ± 0.02
297.4	2.04 ± 0.01
303.4	3.30 ± 0.03
309.0	4.98 ± 0.08

Table 2.58

The effect of temperature on the rate constant k_2 for the hydrolysis of the 4'-morpholino-4''-piperidinotriphenylmethyl cation

Temperature/K	$k_2/ \text{dm}^3 \text{mol}^{-1} \text{s}^{-1}$
292.4	3.14 ± 0.17
297.4	4.78 ± 0.05
302.4	6.74 ± 0.10
308.6	9.58 ± 0.04

Table 2.59

The effect of temperature on the rate constant k_2 for the hydrolysis of the 4'-dimethylamino-4''-morpholinotriphenylmethyl cation

Temperature/K	$k_2/ \text{dm}^3 \text{mol}^{-1} \text{s}^{-1}$
292.2	3.82 ± 0.18
297.2	6.06 ± 0.10
302.2	8.77 ± 0.10
308.4	16.0 ± 0.4

Table 2.60

The effect of temperature on the rate constant k_2 for the hydrolysis of the 4'-N-methylpiperazino-4''-diethylaminotriphenylmethyl cation

Temperature/K	$k_2/ \text{dm}^3 \text{mol}^{-1} \text{s}^{-1}$
294.4	2.94 ± 0.01
297.6	3.57 ± 0.07
302.8	5.62 ± 0.07
308.8	8.41 ± 0.16

Table 2.61

The effect of temperature on the rate constant k_2 for the hydrolysis of the 4'-N-methylpiperazino-4''-dimethylaminotriphenylmethyl cation

Temperature/K	$k_2/ \text{dm}^3 \text{mol}^{-1} \text{s}^{-1}$
293.0	3.77 ± 0.01
297.4	5.26 ± 0.05
303.0	7.84 ± 0.03
309.0	11.4 ± 0.4

Table 2.62

The effect of temperature on the rate constant k_2 for the hydrolysis of the 4'-N-methylpiperazino-4''-pyrrolidinotriphenylmethyl cation

Temperature/K	$k_2/ \text{dm}^3 \text{mol}^{-1} \text{s}^{-1}$
292.6	2.12 ± 0.01
297.4	3.01 ± 0.01
303.0	4.54 ± 0.08
309.0	7.13 ± 0.06

Table 2.63

The effect of temperature on the rate constant k_2 for the hydrolysis of the 4'-N-methylpiperazino-4''-piperidinotriphenylmethyl cation

Temperature/K	$k_2/ \text{dm}^3 \text{mol}^{-1} \text{s}^{-1}$
293.6	4.16 ± 0.18
297.4	5.47 ± 0.24
303.6	8.57 ± 0.13
309.6	12.7 ± 0.1

Table 2.64

The effect of temperature on the rate constant k_2 for the hydrolysis of the 4'-N-methylpiperazino-4''-morpholinotriphenylmethyl cation

Temperature/K	$k_2/ \text{dm}^3 \text{mol}^{-1} \text{s}^{-1}$
292.4	15.5 ± 0.2
297.4	20.2 ± 0.9
303.2	33.2 ± 0.6
308.8	48.3 ± 0.1

Table 2.65

The effect of temperature on the rate constant k_2 for the hydrolysis of the 4'-thiomorpholino -4''-dimethylaminotriphenylmethyl cation

Temperature/K	$k_2/ \text{dm}^3 \text{mol}^{-1} \text{s}^{-1}$
292.8	2.67 ± 0.05
297.8	4.03 ± 0.05
303.0	6.07 ± 0.05
308.8	9.21 ± 0.15

The Arrhenius plots for each dye are shown graphically in the Appendix (A3, Figures 1 – 16). From the data in Tables 2.50 - 2.65, thermodynamic activation parameters were calculated for each of the dyes by the weighted least squares method as described earlier (Section 2.3.1). The results together with their standard error are shown in Table 2.66.

Table 2.66

Thermodynamic activation parameters for the reaction between some unsymmetrical MG type dyes and hydroxide ion (298.2K)

Dye	$\Delta H^\ddagger / \text{kJ mol}^{-1}$	$\Delta S^\ddagger / \text{J K}^{-1} \text{mol}^{-1}$
Me-Et	62.4 ± 0.3	-51.1 ± 0.8
Py-Et	57.6 ± 1.2	-55.0 ± 3.9
Pi-Et	55.0 ± 0.2	-56.2 ± 0.5
Mo-Et	52.6 ± 2.2	-56.4 ± 7.2
Me-Py	61.1 ± 1.4	-41.3 ± 4.6
Pi-Py	55.0 ± 0.8	-57.3 ± 2.7
Mo-Py	51.6 ± 1.0	-60.9 ± 3.4
Me-Pi	56.0 ± 0.8	-50.7 ± 2.7
Mo-Pi	44.9 ± 1.3	-81.0 ± 4.1
Me-Mo	62.1 ± 4.8	-21.3 ± 16.0
MPz-Et	53.4 ± 1.6	-54.4 ± 5.4
MPz-Me	51.5 ± 0.3	-57.9 ± 1.1
MPz-Py	52.4 ± 1.3	-59.4 ± 4.5
MPz-Pi	49.6 ± 0.7	-64.0 ± 2.2
MPz-Mo	49.8 ± 0.8	-51.7 ± 2.7
ThM-Me	55.8 ± 0.8	-45.8 ± 2.7

The thermodynamic activation parameters reported in Table 2.66 are similar in magnitude to those reported previously for structurally similar dyes (82Th1). The most stable dye was Py-Et ($k_2 = 0.64 \text{ dm}^3 \text{ mol}^{-1} \text{ s}^{-1}$ at 297.4 K). This result was consistent with the predicted reactivity when the nature of the terminal amino groups is considered. The k_2 value obtained for Py-Et was intermediate between those of Pyrrolidine Green ($k_2 = 0.57 \text{ dm}^3 \text{ mol}^{-1} \text{ s}^{-1}$) (82Th1) and Brilliant Green ($k_2 = 0.72 \text{ dm}^3 \text{ mol}^{-1} \text{ s}^{-1}$) (82JCS(P2)987). The least stable dye studied was MPz-Mo ($k_2 = 20.2 \text{ dm}^3 \text{ mol}^{-1} \text{ s}^{-1}$ at 297.4 K). This result is in agreement with predictions in view of the basicities of the terminal amino groups and the findings from the previous absorption spectra investigation.

As stated previously, the influence upon cation stability of modifying one of the terminal amino groups within a series can be assessed by consideration of the rate constant for the reaction between the cation and hydroxide ion. If the interpolated rate data at 298.2 K for the unsymmetrical MGs studied in this investigation and the data for the parent dyes are considered together a general order can be determined for the relative ability of each amine group to stabilise the cation. The values of k_2 for the parent dyes are given in Table 2.68. The correlation coefficients for the Arrhenius plots of all the unsymmetrical dyes studied were 0.99 or greater and therefore it was considered reasonable, where necessary, to use interpolated values of k_2 to facilitate complete data manipulation. The regression equation which described the Arrhenius plot of each unsymmetrical dye was used to calculate the interpolated k_2 values at several fixed temperatures. The interpolated k_2 values for the unsymmetrical MGs are given in Table 2.67.

Table 2.67**Interpolated kinetic data for the unsymmetrical MGs**

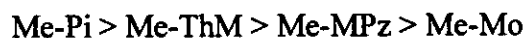
Dye	Interpolated log k_2 values at quoted temperature				
	288.2 K	293.2 K	298.2 K	303.2 K	308.2 K
Me-Et	-0.304	-0.119	0.060	0.233	0.400
Py-Et	-0.534	-0.346	-0.164	0.012	0.182
Pi-Et	-0.128	0.050	0.222	0.388	0.549
Mo-Et	0.320	0.483	0.640	0.792	0.939
Me-Py	-0.449	-0.254	-0.066	0.116	0.292
Pi-Py	-0.179	-0.002	0.169	0.335	0.495
Mo-Py	0.232	0.405	0.573	0.735	0.892
Me-Pi	-0.011	0.168	0.342	0.509	0.672
Mo-Pi	0.376	0.536	0.690	0.839	0.983
Me-Mo	0.416	0.618	0.814	1.002	1.185
MPz-Et	0.245	0.420	0.589	0.752	0.909
MPz-Me	0.426	0.587	0.743	0.894	1.040
MPz-Py	0.171	0.343	0.509	0.669	0.824
MPz-Pi	0.444	0.607	0.765	0.917	1.064
MPz-Mo	1.034	1.200	1.359	1.513	1.663
ThM-Me	0.264	0.444	0.618	0.786	0.948

Table 2.68**Kinetic data for the parent dyes at 298.2K and ionic strength 0.01 mol dm⁻³**

Dye	$k_2 / \text{dm}^3 \text{mol}^{-1} \text{s}^{-1}$	Reference
Pyrrolidine Green	0.565 ± 0.035	82Th1
Brilliant Green	0.72 ± 0.01	80JCTB317
Malachite Green	1.45 ± 0.01	82Th1
Piperidine Green	2.08 ± 0.05	82Th1
Morpholine Green	23.54 ± 1.79	82Th1

No kinetic study has been reported for *N*-Methylpiperazine Green. In much the same way as the $\lambda_{\max}(x)$ values for the dyes were used to establish an order of electron releasing ability for the terminal amino groups, the values of k_2 for each dye can be used to deduce a relative order. The general trend observed is that pyrrolidine consistently has the greatest stabilising effect upon the system followed closely by diethylamine. Both dimethylamine and piperidine stabilise the system to a lesser extent and their ability relative to each other varies. The least stabilising groups are the morpholine and the *N*-methylpiperazine whose ability relative to each other also varies. This ability of the terminal amino groups to stabilise the system by electron donation is reflected to a large extent by their substituent constants (72MI1, 78MI2) and their electron donating potentials as derived by Effenberger (78T2409) where such values have been reported. No values for the substituent constants of *N*-methylpiperazine or thiomorpholine have been reported in the literature.

The relative ability of the six-membered rings to stabilise the system reflects the relative electronegativity of the γ -atom as can be seen from the dimethylamino series of dyes whose relative stability decreases in the order:



As we cross the series, the electronegativity of the γ -atom of the heterocyclic moiety increases. This will have the effect of reducing the electron donation by the terminal heterocyclic nitrogen into the chromophoric system and thereby the cation will be destabilised. However, the relative order of morpholine and *N*-methylpiperazine varies in other dye series and so the behaviour is not simply a consequence of the electronegativity of the γ -atom and may also be system dependent. In each series of dyes, the morpholino and *N*-methylpiperazino derivatives are the most unstable and it would seem reasonable to attribute this increased instability to the nature of the γ -atom of the heterocyclic moiety. The incorporation of both of these amino groups into one dye (MPz-Mo) results in a drastically destabilised dye cation with a hydroxide reaction rate constant comparable to Morpholine Green. When Sawyer first studied Morpholine Green, its decreased stability measured by its extremely fast reaction with hydroxide ion was noted and several explanations were considered (82Th1). In light of the present work, it would

seem appropriate to discuss the possible explanations for the relative order of stability of the unsymmetrical MG dyes bearing six-membered heterocyclic functions.

Studies into the conformational equilibrium of a series of piperidine and piperazine derivatives have indicated that the energetic preferences of methyl and hydrogen groups are for the equatorial positions in the gas phase and non-polar solvents (64TL3345, 65JA1232, 75ACR300). It was suggested that in polar solvents this may not always be the case (75ACR300). It has been reported that polar solvents such as methanol may affect the equilibrium by decreasing the energy barrier to ring inversion (94JMS137). In a review of the literature relating to this area, Blackburne and Katritzky (75ACS300) have noted that the piperidine equilibrium is relatively unaffected by the presence of a second heteroatom at the 4-position of the ring and this conclusion coupled with the dynamic nature of the ring-chair equilibrium and the relatively low energy barriers to the inversion mean that it may be reasonably assumed that in the solvent system employed during the present kinetic investigation the conformational considerations for all the six-membered rings will be similar. A direct comparison between morpholine and *N*-methylpiperazine would be problematic as a consequence of the presence of the additional methyl group in the latter compound. However, if a comparison is drawn between analogous morpholino- and thiomorpholino-bearing dyes – Me-ThM and Me-Mo respectively - it is noted that k_2 for Me-Mo is more than 50% larger than for the analogous reaction with Me-ThM. If it is assumed that the conformational considerations for each six-membered ring are similar then this difference must be attributed to the very nature of the γ -atom. In his work, Sawyer suggests that the γ -oxygen atoms of Morpholine Green may utilise their lone pairs of electrons to form bonds with the solvent molecules (82Th1). This would generate a relatively rigid structure which would have fewer degrees of freedom and could explain the positive ΔS_2^\ddagger value ($51 \pm 47 \text{ J K}^{-1} \text{ mol}^{-1}$) obtained for Morpholine Green for the reaction with hydroxide ion. A value for ΔS_2^\ddagger of $-21 \pm 16.0 \text{ J K}^{-1} \text{ mol}^{-1}$ was obtained for Me-Mo which was the least negative value for the dimethylamino dye series under discussion. However, this distinction for the morpholino analogue is not reflected in the other dye series and even for the dimethylamino dye series both entropy and enthalpy values fluctuate. Sulphur also being a Group VI element has two lone pairs of electrons with which to form bonds with solvent molecules and so it might also be reasonably expected to display a more positive ΔS_2^\ddagger . The ΔS_2^\ddagger value obtained for Me-ThM of $-45.8 \pm 2.7 \text{ J}$

$\text{K}^{-1} \text{mol}^{-1}$ is low but not especially so. Sulphur is known to exhibit weak hydrogen bonds in certain circumstances but both oxygen and nitrogen have a far greater tendency to form such bonds (77MI1). It is therefore to be expected that the compounds containing morpholine and *N*-methylpiperazine would display less negative ΔS_2^\ddagger values, especially in the case of MPz-Mo. However, there are variations in both the entropy and enthalpy values for each dye series for the reaction between dye cation and hydroxide ion. Therefore, in order to gain a better understanding of the reaction mechanism it was considered worthwhile to determine the isokinetic relationship for the reaction. Previous workers have already attempted to establish an isokinetic relationship for related TPM dyes and to obtain a value for β , the isokinetic temperature.

There are several algebraic expressions for the testing of an isokinetic relationship and for the determination of β for a reaction series (73PPOC411). A plot of ΔH^\ddagger versus ΔS^\ddagger may produce a linear relationship, from the slope of which β may be derived. It was employing this technique that Fox *et al.* (82JCS(P2)987) deduced an isokinetic relationship and obtained a value of β of $130 \pm 32 \text{ K}$ for a series of Brilliant Green derivatives. When Beach (85JCS(P2)107) used the same method on a series of 3-substituted Pyrrolidine Greens, a value of $370 \pm 70 \text{ K}$ was obtained. This result is very similar to the value of 330 K obtained by Idlis and Ginsburg for some substituted Malachite Greens (65RSOS46). However, it was acknowledged by these workers that the linearity observed for their data may simply arise from experimental error alone (64CCC1094, 73PPOC411, 76JPC2335). That this is the case is a consequence of the method by which ΔH^\ddagger and ΔS^\ddagger are calculated. In the first instance both ΔH^\ddagger and ΔS^\ddagger are computed from the same equation and in the second a relationship between the two parameters is searched for. It has been shown that such a linear relationship can be observed from random errors in the determination of rate constants (61JA3819, 64JOC3133). It has thus been accepted that a linear ΔH^\ddagger versus ΔS^\ddagger plot by itself cannot be taken to show the existence of an isokinetic relationship. The plot of ΔH^\ddagger versus ΔS^\ddagger for the dyes studied in this investigation showed no correlation and therefore a value of β could not be calculated using this technique.

Another expression which may be used for the determination of the isokinetic relationship involves the measurement of the rate of reaction at two temperatures T_1 and T_2 . The linear relationship predicted is

$$\log k_{2T_1} = a + b \log k_{2T_2} \quad 6.7$$

The isokinetic temperature can then be calculated by the equation

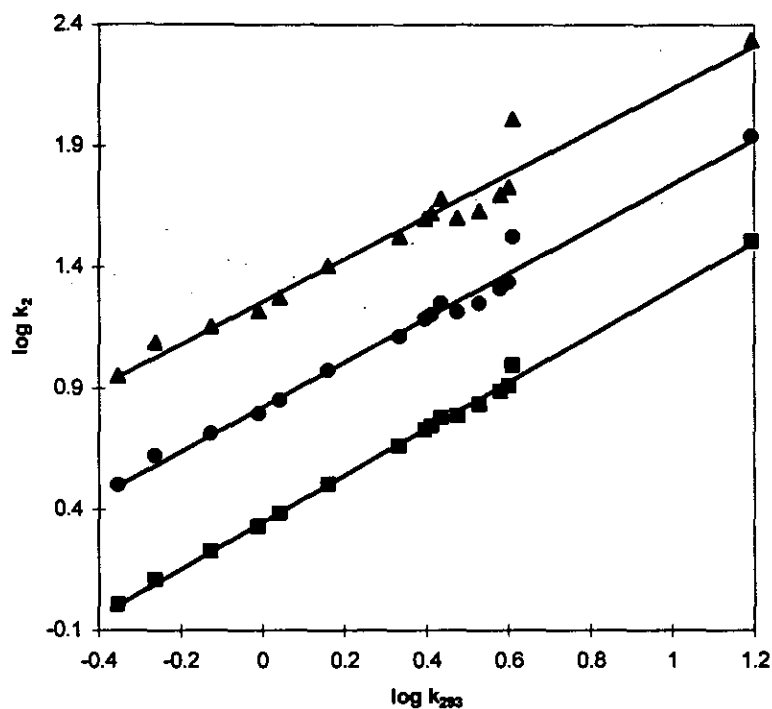
$$\beta = T_1 T_2 (1 - b/T_1 - b/T_2) \quad 6.8$$

This method was also used by Beach for the 3-substituted Pyrrolidine Greens (85JCS(P2)107). Using a $\log k_2 (293.2)$ versus $\log k_2 (313.2)$ plot, Beach obtained a value for β of 460 ± 200 K by application of a least squares computer program. Similarly but using a $\log k_2 (293.2)$ versus $\log k_2 (308.2)$ plot, Unsworth determined β to be 490 K for a series of 3- and 4-substituted Brilliant Greens (91Th1). This method is more statistically correct than the ΔH^\ddagger versus ΔS^\ddagger plot since the values of $\log k_2$ are determined by independent experiments. In addition, the computation of β is simpler and can be carried out to a greater degree of accuracy (73PPOC411). However, this method does have its limitations in the choice of the temperature interval examined. If the interval is too small, the error in β will be large. Also, if the temperature interval is too small, the existence of an exact isokinetic temperature can be erroneously detected since when $T_1 \cong T_2$, equation 6.8 holds exactly. If the temperature interval is too large, extrapolated values must replace actual ones (73PPOC411).

When a plot of $\log k_2 (T_1)$ versus $\log k_2 (T_2)$ for various temperature intervals is made for the dyes studied in this investigation the results are as shown in Figure 2L.

Figure 2L

Isokinetic relationship in the co-ordinates $\log k_2$ versus $\log k_{293}$ with k_2 at 303 K (■), 318 K (●) and 333 K (▲)



From the plots in Figure 2L, it can be seen that with only a 10 K difference between T_1 and T_2 a very good correlation is obtained ($r^2 = 0.997$, $n = 16$) but no real proof of the existence of an isokinetic relationship can be deduced. As the temperature difference is increased to 40 K, it becomes apparent that some of the data points are deviating from the general regression. The point which deviates the greatest is for Me-Mo and therefore this point was omitted for the calculation of β from the data for 333 K and 318 K. Hence, from the plot of $\log k_2$ (₂₉₃) versus $\log k_2$ (₃₃₃) a situation is reached where a real but limited isokinetic relationship can be proposed ($r^2 = 0.985$, $n = 15$). Calculation of β for each of the plots produces the values reported in Table 2.69.

Table 2.69

Isokinetic temperature determined from log k_2 versus log k_{293} with k_2 at 333 K, 318 K and 303 K

Temperature of k_2 / K	Isokinetic temperature, β / K	Characterisation
303	∞	Isoentropic
318	1457	Isoenthalpic
333	1459	Isoenthalpic

The characterisation of each set of data shown in Table 2.69 is derived from the classification as outlined by Blackadder and Hinshelwood (58JCS2720, 58JCS2728). In it, reaction series are characterised into three types:

- 1) Series with constant entropy. The value of b from the slope in equation 6.7 is equivalent to T_1/T_2 and no value for the isokinetic temperature can be determined ($\beta = \infty$)
- 2) Series with constant enthalpy. The value of b from the slope in equation 6.7 is either 1 or between 0 and T_1/T_2 with isokinetic temperatures of 0 or $>T_{exp}$ respectively
- 3) Series where changes in ΔH^\ddagger are paralleled by changes in ΔS^\ddagger in such a direction that the resulting reactivity is less than it would be if it were controlled by either ΔH^\ddagger or ΔS^\ddagger alone. This is also known as the compensation effect. The value of b from the slope in equation 6.7 is either >1 or <0 with isokinetic temperatures of $0 < \beta < T_{exp}$ or in the experimental interval respectively

It can be seen that for the dyes studied in this investigation, the choice of the temperature interval employed may produce drastically different isokinetic temperatures and the reaction series can be incorrectly described. It would seem reasonable to reject the conclusions from the log k_2 (293) versus log k_2 (303) plot on the grounds of the narrow temperature interval employed and therefore predict that an isokinetic relationship exists and that the hydrolysis of the dyes is under enthalpy control in the region investigated.

However, it would appear that there are certain exceptions to this conclusion, the most obvious being Me-Mo. An explanation for these exceptions can be ventured when an attempt is made to establish an isokinetic relationship using the temperature dependence of the reaction constant.

In this approach, the relationship between $\log k$ and some parameter is used to indirectly determine β . The most common form of this treatment is using the Hammett equation where a relationship between $\log k$ and the substituent constant, σ , is used to determine the temperature dependence of the reaction constant, ρ , and therefore β . This is an example of using an empirically determined constant to generate a LFER. The relationship is

$$\rho = \text{constant} (1 - \beta/T) \quad 6.9$$

Beach (85JCS(P2)107) has reported a value for β of 580 ± 70 K when applying this method to a series of 3-substituted Pyrrolidine Greens which was consistent with the values of β obtained when using other methods for the same series of dyes (85JCS(P2)107). In this exercise, each series of dyes is investigated separately producing six treatments in which a common amino substituent is studied whilst changing the nature of the remaining amino substituent. Large numbers of substituent constants are compiled in the literature (72MI1, 75MI1, 78MI2, 81PPOC119) but little is reported for amino substituents except for the dimethylamino and diethylamino moieties. One exception to this is the σ_R° parameter (68JA1757) which was formulated by Brownlee *et al.* from the integrated intensities for the ν_{16} mode of some mono-substituted benzenes. However, as a consequence of their origin, their suitability for use in this study is questionable and therefore it was decided to use the values derived by Beach (83Th1) from a single substituent parameter correlation of the rate of hydrolysis for a series of 4-substituted Pyrrolidine Greens. The σ^+ value obtained for the diethylamino substituent from this work (83Th1) was in close agreement with that obtained in a separate study by Antonova *et al.* (75ZOK1970). However, no value was derived for the dimethylamino substituent and it was therefore decided to employ a value obtained from the literature in order to have a sufficient number of data points. The σ^+ constant used for NMe₂ was -1.50 reported by Clementi and Linda which was evaluated

by the Extended Selectivity Treatment (73JCS(P2)1887). The σ^+ values used in this study are shown in Table 2.70. σ_p^+ substituent constants were used to express the enhanced interaction since the reaction centre is directly conjugated with the substituent constant (78MI2).

Table 2.70
The σ^+ values used for the determination of the temperature
dependence of the reaction constant, ρ

Substituent	σ^+	Reference
NMe ₂	-1.5	73JCS(P2)1887
NEt ₂	-1.86	83Th1
Pyrrolidine	-1.90	83Th1
Piperidine	-1.09	83Th1
Morpholine	-0.74	83Th1

It can be seen from the values for the σ^+ parameter that the substituents are electron releasing in nature.

In addition, to ensure a complete set of data points, values of $\log k_2$ were calculated for the symmetrical parent Greens at the temperatures to be used in the investigation: 288.2, 293.2, 298.2, 303.2 and 308.2 K. These values of $\log k_2$ were interpolated from the data for the rate of hydrolysis for each dye from the work of Fox (Brilliant Green) (81Th1) and Sawyer (Malachite Green, Pyrrolidine Green, Piperidine Green and Morpholine Green) (82Th1). An error limit of $\pm 3\%$ was applied to the interpolated $\log k_2$ values in line with the rate constants calculated from this study. No study has been reported for *N*-Methylpiperazine Green which therefore could not be included in this treatment.

During the graphical examination of the relationship between $\log k_2$ and σ^+ it became apparent that satisfactory correlation could only be achieved if the value for the piperidine substituent was omitted; in every case the piperidine σ^+ value employed was too low. It was therefore decided to omit this value from the correlation. This can be justified when one considers the system under investigation and the nature of the

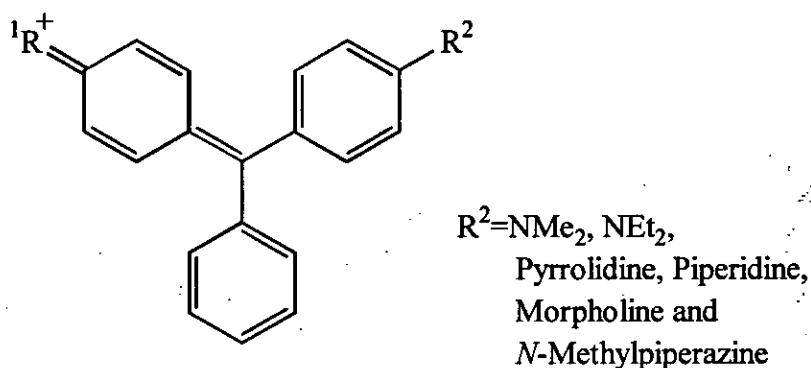
piperidine moiety. It has been established that the range of values of σ_p^+ constants for NR_2 groups in the literature suggest that other factors characteristic of the reaction may influence the magnitude of the substituent constant (84JCS(P2)771). Azzaro, Gal and Garibaldi have concluded from their studies (84JCS(P2)771) that σ_p^+ constants for NR_2 groups depend upon the reaction centre strength which is related to reaction constant, solvent properties such as acidity, basicity and polarity and steric factors which may influence the extent of through conjugation. Oparin *et al.* have substantiated this by a qualitative study of the acid-base equilibrium constants of a series of arylcarbinol bases (81OR308). In addition, it has already been established from the absorption spectra study of this investigation that piperidine has the ability to enhance its electron donation when required. The value of σ^+ for piperidine was derived by Beach from a series of 4-substituted Pyrrolidine Greens which could therefore be better described as a series of unsymmetrical Crystal Violet type molecules. As such, there would be less demand upon the piperidine ring to supply electron donation than would be expected when employed in the dyes studied in this investigation. It would therefore seem reasonable to predict a greater σ^+ constant for piperidine than that derived by Beach when it is substituted into an unsymmetrical MG type system. This is further supported by the work of Azzaro *et al.* (84JCS(P2)771) from pK_{R^+} data who report that σ_p^+ (NMe_2) is -2.00 when it is employed in a series of symmetrically substituted diarylcarbinols but only -1.55 in the case of symmetrically trisubstituted triarylcarbinols. This discrepancy is attributed to the greater delocalisation of the charge in the triarylcarbinols and to the increased steric crowding. It would therefore appear from the correlation coefficients obtained that the σ_p^+ constants utilised for the remaining terminal amino groups were a fair representation of their relative electron donating ability.

Correlation analysis was carried out for each series of unsymmetrical dyes using a weighted least squares computer program by plotting interpolated $\log k_2$ values against the σ^+ constants (Table 2.70) at five temperatures. The results are shown graphically in the Appendix (A6, Figures 1 – 5) and correlation coefficients were generally better than 0.93 except for the pyrrolidino series which produced a correlation coefficient of only 0.87. The reaction constant and its error at each temperature was calculated from the slope of the plots using the regression

$$\log k_2 = \rho \sigma^+ + \log k_0$$

6.10

Figure 2.3-1 shows the unsymmetrical dyes employed in this study. R^1 is as specified in the Tables 2.71 – 2.76.



(2.3-1)

The results for the regression equations for the dyes shown in 2.3-1 are reported in Tables 2.71 - 2.76.

Table 2.71
Reaction constants determined from $\log k_2$ versus σ^+ for some
unsymmetrical MGs (2.3-1; $R^1 = \text{NMe}_2$)

Temperature/ K	Calculated ρ	Calculated $\log k_0$
288.2	0.70 ± 0.06	0.931 ± 0.101
293.2	0.71 ± 0.06	1.134 ± 0.100
298.2	0.72 ± 0.07	1.331 ± 0.106
303.2	0.73 ± 0.07	1.521 ± 0.117
308.2	0.74 ± 0.08	1.705 ± 0.131

Table 2.72

Reaction constants determined from log k_2 versus σ^+ for some unsymmetrical MGs (2.3-1; $R^1 = \text{NEt}_2$)

Temperature/ K	Calculated ρ	Calculated log k_0
288.2	0.72 ± 0.06	0.832 ± 0.091
293.2	0.70 ± 0.05	0.985 ± 0.076
298.2	0.69 ± 0.04	1.133 ± 0.062
303.2	0.67 ± 0.03	1.276 ± 0.051
308.2	0.58 ± 0.11	1.342 ± 0.176

Table 2.73

Reaction constants determined from log k_2 versus σ^+ for some unsymmetrical MGs (2.3-1; $R^1 = \text{Pyrrolidine}$)

Temperature/ K	Calculated ρ	Calculated log k_0
288.2	0.71 ± 0.10	0.726 ± 0.154
293.2	0.70 ± 0.09	0.893 ± 0.143
298.2	0.69 ± 0.08	1.054 ± 0.132
303.2	0.68 ± 0.08	1.210 ± 0.123
308.2	0.60 ± 0.16	1.300 ± 0.250

Table 2.74

Reaction constants determined from log k_2 versus σ^+ for some unsymmetrical MGs (2.3-1; R¹ = Piperidine)

Temperature/ K	Calculated ρ	Calculated log k_0
288.2	0.47 ± 0.03	0.713 ± 0.045
293.2	0.45 ± 0.03	0.863 ± 0.040
298.2	0.43 ± 0.02	1.007 ± 0.035
303.2	0.42 ± 0.02	1.147 ± 0.033
308.2	0.41 ± 0.02	1.282 ± 0.033

Table 2.75

Reaction constants determined from log k_2 versus σ^+ for some unsymmetrical MGs (2.3-1; R¹ = Morpholine)

Temperature/ K	Calculated ρ	Calculated log k_0
288.2	0.54 ± 0.06	1.277 ± 0.087
293.2	0.60 ± 0.05	1.565 ± 0.072
298.2	0.66 ± 0.04	1.843 ± 0.057
303.2	0.72 ± 0.03	2.112 ± 0.043
308.2	0.78 ± 0.02	2.372 ± 0.030

Table 2.76

Reaction constants determined from log k_2 versus σ^+ for some unsymmetrical MGs (2.3-1; $R^1 = N$ -Methylpiperazine)

Temperature/ K	Calculated ρ	Calculated log k_0
288.2	0.73 ± 0.05	1.558 ± 0.071
293.2	0.72 ± 0.05	1.716 ± 0.081
298.2	0.71 ± 0.06	1.868 ± 0.090
303.2	0.71 ± 0.06	2.016 ± 0.098
308.2	0.70 ± 0.07	2.158 ± 0.107

The temperature dependence of the reaction constants shown in Tables 2.71 - 2.76 used in equation 6.10, enabled values for β to be derived for each of the dye series studied. The correlation analysis was carried out using a weighted least squares computer program by plotting the reaction constant versus the reciprocal of the temperature. The results are shown in Table 2.77.

Table 2.77

Values of β determined from the temperature dependence of the reaction constant for a series of unsymmetrical MGs

R^1 in 2.3-1	β/ T
NMe ₂	-177 ± 2
NEt ₂	334 ± 106
Pyrrolidino	276 ± 122
Piperidino	260 ± 27
Morpholino	-1083 ± 12
<i>N</i> -Methylpiperazino	126 ± 17

Since the data for each dye series (with the exception of the *N*-methylpiperazino series) contains the parent Green it is worthwhile to quote the reaction constants as for the parent Greens. The observed ρ values at 293.2 K are given in Table 2.78 together with data from other work.

Table 2.78
Reaction constant values for parent Green dyes

Dye	Reaction constant	Reference
Malachite Green	0.50 ± 0.02	65RSOS46
	0.63 ± 0.04	83Th2
	0.57	66ACS444
	0.71 ± 0.06	This study
Brilliant Green	0.60 ± 0.07	82JCS(P2)987
	0.60 ± 0.02	81Th1
	0.70 ± 0.05	This study
Pyrrolidine Green	0.64 ± 0.04	85JCS(P2)107
	0.70 ± 0.09	This study
Piperidine Green	0.45 ± 0.03	This study
Morpholine Green	0.60 ± 0.05	This study
<i>N</i> -Methylpiperazine Green	0.72 ± 0.05	This study

It can be seen from the calculated values for ρ from this study that the cations are stabilised by electron donation and destabilised by electron withdrawing groups in the terminal positions. The magnitude of ρ indicates that the reaction centre is relatively insensitive to substituent effects and that there is a relatively small change in charge density at the central carbon atom.

The isokinetic temperatures calculated for each reaction series (Table 2.77) show considerable variation. From the values calculated, the diethylamino series of dyes appear to be under enthalpy control but the large variation of β prevents a definite

conclusion being drawn. The piperidino and pyrrolidino series of dyes appear to be indeterminable. However, it appears that the dimethylamino, morpholino and *N*-methylpiperazino series are under entropy control with the gradient of the reaction constant temperature dependence plot for the dimethylamino and morpholino series being negative. This may then be an explanation as to why the data point for Me-Mo - the dye which contains both groups predicted to be under entropy control- in the plot of $\log k_{2(293)}$ versus $\log k_{2(333)}$ was seen to deviate from the relationship. This suggests that the mechanism of reaction for this dye may be different from that for the others. However, it must be borne in mind that the results obtained from this treatment have been based upon establishing a reliable Hammett relationship with which to generate a LFER. Topsom (76PPOC1) has listed the criteria for the application of experimental data for a specific form of the Hammett equation but these criteria still apply to the more general form such as that employed in this study. The basic requirements for any set of experimental data are:

- 1) The data generally should be on an energy dependent scale such as $\log k/k_0$
- 2) Unless careful standardisation is carried out the data should be obtained from one source for each series
- 3) The spread of energy values should be considerable compared to the relative accuracy and reproducibility of the measurements
- 4) Where protic or polar solvents are involved, data for the substituents, such as hydroxyl and amino, that can interact specifically should be disregarded in overall correlations
- 5) Where possible, concentration studies should be undertaken to check for solute-solute interactions
- 6) A sufficient range of substituent behaviour

The above list indicates the limited application afforded to the data in this study. For the most part the data is from one source but the dimethylamino- σ^+ constant was taken from another source and no standardisation was possible between the two sets of data. The spread of the values was by their nature not very wide which suggests that precision errors may become significant. In addition, the entire set of data was made up of amino-groups which it was suggested should be avoided since specific interactions may occur. Finally, concentration studies were not conducted to eliminate solute-solute interactions and therefore it may be possible that these have occurred. Where possible adherence to

Topsom's (76PPOC1) criteria was maintained but certain limitations prevented full compliance. However, despite these deficiencies, satisfactory correlations were achieved for the majority of the regressions which enabled comparable reaction constants to be calculated and isokinetic temperatures to be evaluated. The values of β thus derived should be viewed with caution and merely indicate a general trend for a particular reaction series.

Of the methods reviewed by Exner for the determination of an isokinetic relationship (73PPOC411), the most general representation is the plot of $\log k$ against the reciprocal of temperature (73PPOC411, 79CJC3041). If the Arrhenius relationship holds then each reaction of the series is given as a straight line. Additionally, if the isokinetic relationship holds then all of the lines should intersect at one point equal to the isokinetic temperature. Since $\log k$ and temperature are independent such plots are statistically sound. However, the estimation of β from a graphical representation can be problematic if all the lines do not appear to cross at one point or if the point of intersection is well removed from the region of experimental data. It was by using this visual inspection of the Arrhenius plot that Unsworth determined the isokinetic temperature of a series of 3- and 4-substituted Brilliant Greens to be $\cong 480$ K for which the $\log k_{(293.2)}$ versus $\log k_{(308.2)}$ technique produced a value of 490 K (91Th1). Beach used the $\log k_{(293.2)}$ versus $\log k_{(313.2)}$ plot to obtain a value for β of 460 ± 200 K which was substantiated by visible and statistical interpretation of the Arrhenius plots for a series of 3-substituted Pyrrolidine Greens (85JCS(P2)107). The equations proposed by Exner (73PPOC411) for the determination of β and a test of its statistical validity were applied to the current data for each unsymmetrical MG type dye series. These equations (Appendix A1, EXN) have been used previously by employing a microcomputer (83Th1) but for this study the equations were translated into a Microsoft Excel[®] spreadsheet. The equations were checked rigorously with existing, independently derived data to confirm their accuracy. The values for β with its error or confidence interval for each of the dye series are given in Table 2.79.

Table 2.79

**Values of β determined from Arrhenius plots for some unsymmetrical
MG type dye series**

Dye series	β / K	Confidence interval/ K
NMe ₂	701	600 → 910
NEt ₂	878	730 → 1180
Pyrrolidino	865	710 → 1250
Piperidino	677	600 → 810
Morpholino	-39	-200 → 40
<i>N</i> -Methylpiperazino	-240	-630 → -80

From the results given in Table 2.79 it can be seen that values for the isokinetic temperature, β , can be obtained for each dye series.

For the determination of β for the dimethylamino and morpholino series the data for Me-Mo was not included. Following on from previous arguments, the determination of an isokinetic relationship for these two dye series with the data for Me-Mo included proved problematic and hence the effect of the inclusion of this data was investigated. With the inclusion of the Me-Mo data, the value of β for the dimethylamino and morpholino series was -286 K and -17 K respectively. This shows a dramatic reversal for the dimethylamino series. Using the spreadsheet, values for the standard deviation for the data assuming a common point of intersection (s_u) were obtained as a function of reciprocal temperature. Comparison of these values with the standard deviation for the data assuming an isokinetic relationship exists (s_o) (73PPOC411) determined the confidence interval for β . However, with the inclusion of the Me-Mo data in both dye series it was not possible to quote confidence intervals for β and it was therefore decided to omit this data from each series. In addition, a value for s_{∞} - the standard deviation for the data with no constraint of a common point of intersection - was calculated for each series. This parameter may be taken as an estimate of the experimental error (73CCCC781). Comparison of this parameter with s_o and the actual experimental error,

if known, can provide statistical proof for several conclusions. However, for the interpolated data employed in this study a true value for s_{∞} could not be calculated. Interpolated data were used in this study to facilitate the simpler mathematical treatment proposed by Exner (73PPOC411). Exner and Beranek have reported a more involved treatment (73CCCC781) but the application of this method was beyond the scope of this study. It was felt by the author that the use of interpolated data would not detract from the establishment of an isokinetic relationship. As a consequence, whilst from a visual inspection of the $\log k$ against $1/T$ plots the Arrhenius law can be accepted, it cannot be statistically proven. In addition, the existence of an isokinetic relationship cannot be statistically, unconditionally accepted. However, for this to be the case $s_{\infty} \leq s_0$; this can occur in the unrealistic case when all the constrained regression lines intersect in one point or for only two sets of data (73PPOC411, 73CCCC781). Therefore it would seem reasonable to accept the isokinetic relationships as derived.

The values obtained for the pyrrolidino and the diethylamino series are slightly higher than the values obtained previously by Beach (470 K with a confidence interval 430 to 610 K) (85JCS(P2)107) using the same mathematical treatment and Unsworth (480 K) (91Th1) for the parent Green dyes. However, the difference is not significant when one considers the confidence intervals for β and that Unsworth's determination was based upon visual inspection alone. The data reported by Fox (82JCS(P2)987) for a series of 3- and 4-substituted Brilliant Greens were re-examined by Beach (83Th1) using the mathematical procedures presented by Exner (73PPOC411) but the results did not provide a better estimation of β . Values of β have not been reported previously for the piperidino, morpholino and *N*-methylpiperazino dyes. The values reported in Table 2.79 show two distinct trends: for the morpholino and *N*-methylpiperazino series the values for β are negative and for the remaining dye series β is large and positive. This would suggest that for the morpholino and *N*-methylpiperazino series the reaction is under entropy control whilst for the dimethylamino, diethylamino, pyrrolidino and piperidino series the reaction is under enthalpy control. However, since each dye series is composed of members of other dye systems it would only be correct to ascribe a general trend for β . Indeed too much emphasis can be attributed to β when the only unambiguous statements are the confidence interval and the corresponding standard deviation (73CCCC781); it is more correct to determine whether an isokinetic relationship holds. The very idea of an isokinetic temperature at which all members of a

reaction series react at the same rate and beyond which their reactivity is reversed is open to question. Examples do exist for which this reversal has been recorded (55AC75) particularly in heterogeneous catalysis. For solution kinetics, the narrow temperature range in which the reaction can be studied tends to prevent a thorough investigation although examples are known, one of which is for the hydrolysis of a series of some substituted Malachite Greens (66RSOS162). The results reported in Table 2.79 clearly confirm that an isokinetic relationship exists for all the dye systems and that a common reaction mechanism can be predicted. It would be reasonable to conclude that whilst the differing values for β suggest either enthalpy or entropy control the situation is not straightforward since each dye series is composed of members of other dye series. As such, no one thermodynamic activation parameter can be considered more influential than the other and the rate of the reaction is determined by both entropy and enthalpy considerations to varying degrees. This is further supported by the variations in both ΔH_2^* and ΔS_2^* displayed by the dyes in each dye series.

The various algebraic and graphical representations of the isokinetic relationship allow the possibility of investigating each case from different sides (89MI1). A particular representation may prove useful for a particular case and no one can be considered to be erroneous in itself (73PPOC411).

When a comparison is made between the results from the $\log k$ against $1/T$ and the temperature dependence of ρ methods there is, in general, good agreement. The exception being for the dimethylamino series where seemingly conflicting results are obtained. However, each method has at its core a series of assumptions and models and it must be concluded that for the dimethylamino series either one of the models is not a true reflection of the kinetics studied or that each model reflects a specific but opposing aspect of the reaction. That this is the case is supported by the results for the plot of $\log k_2$ (293) versus $\log k_2$ (333). This type of plot provides the best way to observe any deviations from a common mechanism (73PPOC411). The members of the dimethylamino series of dyes are well correlated by the overall regression. A number of dyes - Mo-Et, Mo-Pi, MPz-Me and MPz-Pi - are seen to deviate slightly from the linear relationship. These dyes contain the morpholino and *N*-methylpiperazino moieties which have been shown to be predominantly under entropy control. However, these dyes are well represented during the other mathematical treatments and therefore no firm conclusions as to the nature of the deviation can be drawn. This is not the case for Me-

Mo which, as well as displaying a noticeable deviation from the linear regression in the plot of $\log k_2$ (293) versus $\log k_2$ (333) (Figure 2L), has consistently shown anomalous behaviour during the other mathematical treatments. It must therefore be concluded that there is a high probability that the reaction mechanism for Me-Mo is different from that proposed for the other dyes. The magnitude of k_2 for Me-Mo is also larger than that predicted purely upon the relative electron donating abilities of the two terminal amino groups. Interestingly though, from the work conducted, ThM-Me is predicted to react by the common mechanism and does not display any anomalous behaviour. It is the presence of the oxygen atom that promotes this behaviour albeit in conjunction with the dimethylamino group. It is likely that the lone pair of electrons of the oxygen play an important role in this mechanism which from the work conducted has a similar order and molecularity as in the mechanism for the other dyes. It is interesting to postulate upon the possible nature of this difference. From the study on Morpholine Green, Sawyer (82Th1) proposed intermolecular bonding between the morpholino oxygen of one molecule with the central carbon atom of another molecule to explain the positive ΔS^\ddagger_2 obtained for the reaction. In a similar manner, it would not be too difficult to envisage a situation where intermolecular attraction could occur between the lone pair of electrons of a morpholino oxygen atom and a neighbouring positively charged dimethylamino nitrogen atom. The lower steric considerations predicted for a dimethylamino group would certainly facilitate this interaction. This intermolecular bonding would create a sterically more rigid structure which could explain the less negative ΔS^\ddagger_2 value obtained for the Me-Mo dye. This mechanism has not, however, been tested.

Hammett relationships of the form shown in equation 6.11 have already been established for the dye series during this investigation.

$$\log k_2 = \rho \sigma_p^+ + \log k_0 \quad 6.11$$

It would therefore seem appropriate to calculate σ_p^+ substituent constants using these regressions for the substituents for which no previous substituent constants have been reported. Interpolated values of σ_p^+ substituent constants for the thiomorpholino and *N*-methylpiperazino groups were calculated from the relevant regression equations. In addition, a revised value for the piperidino group was also calculated. The error quoted for $\log k_2$ was $\pm 3\%$. The values of σ_p^+ calculated are given in Tables 2.80 - 2.82.

Table 2.80 **σ_p^+ Substituent constants calculated for *N*-methylpiperazine**

Dye series	σ_p^+ constants at quoted temperatures					
	288.2	293.2	298.2	303.2	308.2	Average
NMe ₂	-0.72 ± 0.16	-0.77 ± 0.16	-0.82 ± 0.17	-0.86 ± 0.19	-0.90 ± 0.21	-0.81
NEt ₂	-0.81 ± 0.14	-0.81 ± 0.13	-0.79 ± 0.11	-0.78 ± 0.10	-0.75 ± 0.34	-0.79
Pyrrolidine	-0.78 ± 0.24	-0.79 ± 0.23	-0.79 ± 0.21	-0.80 ± 0.21	-0.79 ± 0.47	-0.79
Piperidine	-0.57 ± 0.11	-0.57 ± 0.11	-0.56 ± 0.11	-0.55 ± 0.12	-0.53 ± 0.13	-0.56

Table 2.81 **σ_p^+ Substituent constants calculated for piperidine**

Dye series	σ_p^+ constants at quoted temperatures					
	288.2	293.2	298.2	303.2	308.2	Average
NMe ₂	-1.34 ± 0.18	-1.36 ± 0.18	-1.37 ± 0.20	-1.39 ± 0.21	-1.40 ± 0.24	-1.37
NEt ₂	-1.33 ± 0.17	-1.34 ± 0.14	-1.32 ± 0.12	-1.33 ± 0.10	-1.37 ± 0.40	-1.34
Pyrrolidine	-1.28 ± 0.28	-1.28 ± 0.26	-1.28 ± 0.24	-1.29 ± 0.24	-1.34 ± 0.55	-1.29
<i>N</i> -Methyl- -piperazine	-1.53 ± 0.14	-1.54 ± 0.16	-1.55 ± 0.19	-1.55 ± 0.20	-1.56 ± 0.23	-1.55

Table 2.82 **σ_p^+ Substituent constants calculated for thiomorpholine**

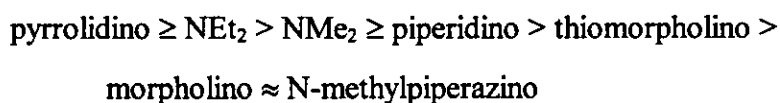
Dye series	σ_p^+ constants at quoted temperatures					
	288.2	293.2	298.2	303.2	308.2	Average
NMe ₂	-0.95 ± 0.22	-0.97 ± 0.16	-0.99 ± 0.18	-1.01 ± 0.19	-1.02 ± 0.21	-0.99

The σ_p^+ substituent constants obtained from the regression equations for several dye series show good consistency between series. Over this temperature range, the average σ_p^+ value for *N*-methylpiperazine from the collected dye series was -0.74 and for piperidine was -1.39. The same arguments proposed earlier in this discussion as to the validity of a Hammett plot when used to determine an isokinetic relationship still apply in this case. The consistency of σ_p^+ constants obtained between different dye series indicates the method has merit and that a Hammett relationship can be applied but only to a certain degree. A complete set of σ_p^+ substituent constants for the terminal amino groups used in this study can now be reported (Table 2.83).

Table 2.83**Summary of σ_p^+ substituent constants for the terminal amino groups used in the present investigation**

Substituent	σ_p^+	Source
NMe ₂	-1.5	73JCS(P2)1887
NEt ₂	-1.86	83Th1
Pyrrolidine	-1.90	83Th1
Piperidine	-1.39	This study
Morpholine	-0.74	83Th1
Thiomorpholine	-0.99	This study
<i>N</i> -Methylpiperazine	-0.74	This study

From the values reported in Table 2.83 a relative order of electron donating ability can be determined. The order of decreasing ability to donate electron density to the chromophoric system is



This order bears some similarity to that obtained during the present study from the absorption spectra data except the electron donating potential of the piperidine group is realised more fully in the spectral work. The new σ_p^+ constant evaluated for piperidine is significantly greater than that obtained by Beach (83Th1) and reflects the greater electron demand placed upon the amino group in the unsymmetrical MGs presently studied. Table 2.84 shows some of the σ_p^+ constants obtained by previous workers using a range of techniques and serves to illustrate the variability of these constants even when similar techniques are employed.

Table 2.84
Comparison of σ_p^+ constants

Substituent	σ_p^+	Method	Reference
NMe ₂	-1.70	Solvolysis of t-Cumyl Chlorides	58JA4979
	-1.67	Protonolysis of Arylsilanes	57JA804
	-1.50	Extended Selectivity Treatment	73JCS(P2)1887
	-1.67	Thermodynamic pKa	73JA5357
	-1.95	¹³ C nmr DMSO of β -Nitrostyrenes	76AJC2607
	-1.86	¹³ C nmr CDCl ₃ of β -Nitrostyrenes	
	-1.98 to	Thermodynamic measurements of	84JCS(P2)771
	-2.32	carbonyl compounds	
-1.82	Rate of Hydrolysis of Brilliant Greens	91Th1	
NEt ₂	-2.07	Apparent pKa values	75ZOK1991
	-1.86	Rate of Hydrolysis of Pyrrolidine Greens	83Th1
	-2.10	Rate of Hydrolysis of Brilliant Greens	91Th1
Pyrrolidine	-1.8	Rate of Hydrolysis of Pyrrolidine Greens	83Th1
	-2.14	Rate of Hydrolysis of Brilliant Greens	91Th1
Piperidine	-1.09	Rate of Hydrolysis of Pyrrolidine Greens	83Th1
	-1.39	Rate of Hydrolysis of Unsymmetrical Malachite Greens	This study

From this discussion it can be concluded that the unsymmetrical MG dyes studied react following the mechanism indicated earlier (Section 1.3) and which has been proposed from previous studies for TPM dyes in general. In view of the range of ΔH_2^\ddagger and ΔS_2^\ddagger values determined for the series of dyes studied it can be concluded that whilst both entropy and enthalpy considerations can be shown to be important for virtually all the dyes, the seemingly anomalous behaviour of Me-Mo can be attributed to a greater predominance of entropy control.

2.3.3 Analogues of Michler's Hydrol Blue

The observed rate constant data for the diphenylmethane dyes studied during this investigation are shown in Tables 2.85 - 2.87. The kinetic plot for each dye is shown graphically in the Appendix (A4, Figures 1 – 3).

Table 2.85

The effect of temperature and hydroxide ion concentration on k'
for 4,4'-bis(dimethylamino)diphenylmethyl perchlorate

$10^3 [\text{OH}^-]/\text{mol dm}^{-3}$	$10^1 k'/\text{s}^{-1}$	T/K
0.481	0.96 ± 0.02	293.6
0.962	1.9 ± 0.1	
1.923	3.8 ± 0.1	
5.769	11.4 ± 0.7	
0.481	1.6 ± 0.1	297.8
0.962	2.9 ± 0.1	
1.923	5.6 ± 0.3	
3.846	10.7 ± 1.4	
0.481	2.1 ± 0.3	303.2
0.962	3.8 ± 1.1	
1.923	7.8 ± 1.5	
5.769	25.8 ± 6.3	
0.481	2.5 ± 0.4	308.2
0.962	4.9 ± 0.2	
1.923	10.3 ± 1.2	
3.846	26.6 ± 4.9	

$I = 0.009615 \text{ mol dm}^{-3}$

95% confidence interval

Table 2.86

The effect of temperature and hydroxide ion concentration on k'
for 4,4'-bis(diethylamino)diphenylmethyl perchlorate

$10^3 [\text{OH}^-]/\text{mol dm}^{-3}$	$10^1 k'/\text{s}^{-1}$	T/K
0.481	0.51 ± 0.02	296.0
0.962	1.1 ± 0.1	
1.923	2.3 ± 0.1	
3.846	4.4 ± 0.2	
0.481	0.67 ± 0.04	298.0
0.962	1.3 ± 0.1	
1.923	2.5 ± 0.1	
3.846	4.9 ± 0.3	
0.481	1.1 ± 0.2	303.2
0.962	2.1 ± 0.2	
1.923	4.0 ± 0.1	
3.846	7.8 ± 0.4	
0.481	1.2 ± 0.2	308.6
0.962	2.5 ± 0.3	
1.442	4.3 ± 0.2	
3.846	12.1 ± 0.5	

$I = 0.009615 \text{ mol dm}^{-3}$

95% confidence interval

Table 2.87

The effect of temperature and hydroxide ion concentration on k'
for 4,4'-dipyrrolidinodiphenylmethyl perchlorate

$10^3 [\text{OH}^-]/\text{mol dm}^{-3}$	$10^1 k'/\text{s}^{-1}$	T/K
0.385	0.38 ± 0.03	293.8
0.962	0.86 ± 0.05	
1.442	1.4 ± 0.1	
1.923	1.8 ± 0.1	
0.385	0.54 ± 0.02	297.6
0.962	1.2 ± 0.1	
1.442	1.9 ± 0.1	
1.923	2.4 ± 0.2	
0.385	0.69 ± 0.03	302.8
0.577	1.1 ± 0.1	
0.962	1.8 ± 0.2	
1.442	2.7 ± 0.3	
0.385	1.1 ± 0.1	308.8
0.577	1.7 ± 0.1	
0.769	2.3 ± 0.1	
0.962	2.8 ± 0.2	

$$I = 0.009615 \text{ mol dm}^{-3}$$

95% confidence interval

The values for the rate constant, k_2 , together with its standard error are reported in Tables 2.88 - 2.90.

Table 2.88

The effect of temperature on the rate constant k_2 for the hydrolysis of the 4,4'-bis(dimethylamino)diphenylmethyl cation

Temperature/K	$k_2/ \text{dm}^3 \text{mol}^{-1} \text{s}^{-1}$
293.6	197 ± 1
297.8	273 ± 4
303.2	446 ± 14
308.2	703 ± 65

Table 2.89

The effect of temperature on the rate constant k_2 for the hydrolysis of the 4,4'-bis(diethylamino)diphenylmethyl cation

Temperature/K	$k_2/ \text{dm}^3 \text{mol}^{-1} \text{s}^{-1}$
296.0	116 ± 4
298.0	126 ± 1
303.2	199 ± 1
308.6	327 ± 2

Table 2.90

The effect of temperature on the rate constant k_2 for the hydrolysis of the 4,4'-dipyrrolidinodiphenylmethyl cation

Temperature/K	$k_2/ \text{dm}^3 \text{mol}^{-1} \text{s}^{-1}$
293.8	97 ± 3
297.6	124 ± 5
302.8	187 ± 3
308.8	287 ± 1

The Arrhenius plots for each dye are shown graphically in the Appendix (A5, Figures 1 – 3). From the data in Tables 2.88 - 2.90, thermodynamic activation parameters were calculated for each of the dyes by the weighted least squares method as described earlier (Section 2.3.1). The results together with their standard error are shown in Table 2.91.

Table 2.91
Thermodynamic activation parameters for the reaction between
some MHB analogues and hydroxide ion (298.2K)

Dye	$\Delta H^\ddagger_2 / \text{kJ mol}^{-1}$	$\Delta S^\ddagger_2 / \text{J K}^{-1} \text{mol}^{-1}$
MHB	58.2 ± 2.5	-2.6 ± 8.6
EtDPM	65.4 ± 2.0	14.6 ± 6.8
PyDPM	52.9 ± 0.6	-26.7 ± 2.1

Six diphenylcarbinols were prepared from which it was intended to generate the carbocation and study its reaction with hydroxide ion. However, the very low extinction coefficient for PiDPM prevented the preparation of a satisfactory carbocation salt and therefore no study was conducted upon this salt. Investigation into the rate of reaction of the MoDPM and MPzDPM cations was complicated by their very much increased reactivity. The HP89531A kinetics software employed to analyse the kinetic data has a minimum cycle and integration time of 0.1s but the minimum time over which reaction data can be collected is 1s. It was observed that for both MoDPM and MPzDPM the reaction was over in less than 1s even at low temperatures (ca. 20°C). Therefore, it was not possible to measure the rate of reaction for these two dyes. In an attempt to bring the reaction into a range manageable for the instrument, the reaction was investigated briefly in pure water and employing a buffer solution (pH 4, potassium hydrogen phthalate). Under both conditions the reaction was still complete in less than 1s. It was then considered as to whether the use of an oscilloscope with a faster operating speed would solve the problem. However, the slowest operation in the kinetic experiment was the manual depression of the plunger on the stopped-flow apparatus which, even at its

maximum rate was still very significant in comparison to the anticipated rate of reaction. It was decided to abandon any further attempt to measure the rate of reaction for these two dyes. From the kinetic data collected for the remaining three dyes their reactivity towards hydroxide ion can be deduced from the large k_2 values obtained. In each case their rate of reaction towards hydroxide ion is approximately 200 times greater than for the corresponding Green type system (Table 2.92).

Table 2.92
Comparison of k_2 values for related dye systems

Dye	$k_2/ \text{dm}^3 \text{mol}^{-1} \text{s}^{-1}$	Ratio DPM/TPM
Malachite Green	1.45 ^a	188
MHB	273.3	
Brilliant Green	0.72 ^b	174
EtDPM	125.6	
Pyrrolidine Green	0.57 ^a	217
PyDPM	123.9	

a. 82Th1

b. 81Th1

This increased reactivity can be attributed to the absence of the third phenyl ring. In the TPM systems there is some degree of steric restriction to the approach of the hydroxide ion to the central carbon atom. However, in the DPM systems there is a much reduced restriction and hence the greater reactivity. Conjugation between the terminal amino groups and the phenyl rings would be expected to be at a maximum due to the increased coplanarity in the DPM system (59JCS3957, 63JCS2655). The DPM dyes studied are greatly stabilised by this conjugation. For the diarylmethyl cation, laser flash photolysis techniques have to be employed in order to study the rate of reaction (89JA3966, 92JA1816) which rapidly approaches the diffusion limit for solution based reactions. Ritchie (86CJC2239) has reported a value of $\log k_{\text{OH}}$ for the trityl cation of 6.72. However, the presence of a terminal substituent that conjugates with the phenyl ring system greatly increases the stability of the system. It is not possible to ascribe the

greater reactivity of the MoDPM and MPzDPM cations to either reduced conjugation or entropy effects.

The ΔS_2^* values obtained for the DPM dyes studied are less negative than for the unsymmetrical MGs studied and this reflects the reduced steric inhibition to reaction with hydroxide ion. It can be visualised that for the diarylmethyl cation a closely held solvation sphere of solvent molecules might exist. This sphere will have a high degree of order and therefore upon reaction with hydroxide ion this order is reduced considerably. The disruption of this shell will increase the number of degrees of freedom for the molecule which results in the more positive ΔS_2^* parameter.

From the k_2 values obtained for the dyes a relative order of electron donating ability can once again be established. The order shown below displays the anticipated ability for the terminal amino groups studied



A discussion into the applicability of several methods for the determination of a possible isokinetic relationship for a series of compounds has already been given and therefore it was decided to only employ the statistical treatment of Exner (73PPOC411) for the DPM dyes studied. The Arrhenius plots for the dyes are shown in the Appendix (A5, Figures 1 – 3). The interpolated values of $\log k_2$ used in the computation of β are shown in Table 2.93.

Table 2.93
Interpolated values of $\log k_2$ used for the computation of the isokinetic relationship

Dye	Interpolated $\log k_2$ values at quoted temperature			
	293.2 K	298.2 K	303.2 K	308.2 K
MHB	5.222	5.675	6.113	6.537
EtDPM	4.454	4.895	5.321	5.734
PyDPM	4.508	4.889	5.257	5.614

From the data given in Table 2.93, a value for β of 229 K was obtained with a confidence interval between 200 and 240 K. Once again, too much emphasis should not be placed on the value of β but rather that an isokinetic relationship has been established and the confidence interval set for β . Considering this, it can be stated that the three diarylmethyl dyes studied all react by a common mechanism and that the reaction is under entropy control. This conclusion appears sound in view of the qualitative discussion presented earlier. This mechanism is the same as that proposed for the TPM dyes and is shown in Section 1.3.

^1H and ^{13}C nmr spectra were recorded on a Brüker Avance DPX250MHz multinuclear nuclear magnetic resonance spectrometer at 250 MHz. The solvent peak was used as reference for CDCl_3 and acetone- d_6 solutions. The ^1H and ^{13}C nmr spectra of the dye perchlorates were recorded in acetone- d_6 (99.9 atom % D) used as purchased from Aldrich Chemical Co. The ^1H and ^{13}C nmr spectra of all other compounds were run in Euriso-top CDCl_3 ($\text{H}_2\text{O} < 0.01\%$) used as purchased. The electronic absorption spectra were recorded using a Philips PU8740 UV/Vis scanning spectrophotometer using a 10mm silica cell. The spectra were determined in AnalaR[®] grade acetic acid. Melting points were determined using a Gallenkamp melting point apparatus and are uncorrected. Gas chromatography-mass spectrometry was obtained using a Perkin Elmer 8500 gas chromatograph employing a Perkin Elmer ITD ion trap detector. The distillation apparatus used in this study was a bulb-to-bulb Kugelrohr (Büchi GKR-50 Glass Tube Oven). The boiling points quoted are the oven temperatures at which distillation began. Microanalyses were carried out at the University of Leeds. Flash column chromatography was performed following the published procedure (78JOC2923) using a Rhône-Poulenc C60 40/60 H, activated silica gel.

3.1 Organic synthesis

3.1.1 Preparation of disubstituted benzophenones

a) 4,4'-Bis(diethylamino)benzophenone

Commercial grade 4,4'-bis(diethylamino)benzophenone was eluted from alumina with dichloromethane. Evaporation of the dichloromethane and recrystallisation of the residue from hexane gave the ketone, m.p. 97.5 - 98.0 °C as pale yellow crystals [(53MI1) gives m.p. 95.0 - 96.0 °C].

b) 4,4'-Dipiperidinobenzophenone

A solution of 4,4'-difluorobenzophenone (20.0 g; 0.10 mol) and piperidine (31.0 cm³; 0.32 mol) in sulfolane (100 cm³) was refluxed for 24 hours. The reaction mixture was then poured into ice-water (2000 cm³), with stirring, whereupon a precipitate was formed. The solid was collected, washed with water, ethanol and finally diethyl ether and then crystallised from aqueous acetone to give 4,4'-dipiperidinobenzophenone (24.0 g; 69 %), m.p. 142.0 - 143.0 °C as pale brown crystals [(89JCS(P2)1087) gives m.p. 140 - 142 °C].

The following compounds were prepared in a similar manner.

c) 4,4'-Dimorpholinobenzophenone

4,4'-Dimorpholinobenzophenone was prepared from 4,4'-difluorobenzophenone (20.0g; 0.10 mol) and morpholine (30.0 cm³; 0.34 mol). Recrystallisation from ethanol gave 4,4'-dimorpholinobenzophenone (22.5 g; 64 %), m.p. 167.5 - 168.0 °C as off-white flakes [(89JCS(P2)1087) gives m.p. 162 - 164 °C].

d) 4,4'-Di-*N*-methylpiperazinobenzophenone

4,4'-Di-*N*-methylpiperazinobenzophenone was prepared from 4,4'-difluorobenzophenone (5.0 g; 0.03 mol) and *N*-methylpiperazine (10.2 cm³; 0.09 mol). The crude product was dissolved in chloroform (50 cm³) and the solution was washed three times with water (25 cm³) before being dried (Na₂SO₄). Removal of the solvent and recrystallisation of the crude solid from aqueous ethanol gave 4,4'-di-*N*-methylpiperazinobenzophenone (5.1 g; 45 %), m.p. 194.0 - 195.0 °C as brown crystals [(83Th3) gives m.p. 194 °C].

e) 4,4'-Dipyrrolidinobenzophenone

4,4'-Dipyrrolidinobenzophenone was prepared from 4,4'-difluorobenzophenone (20.0 g; 0.10 mol) and pyrrolidine (22.0 cm³; 0.26 mol). The crude product was triturated with hot diethyl ether before crystallisation from toluene to give 4,4'-dipyrrolidinobenzophenone (18.6 g; 58 %), m.p. 264.5 - 265.0 °C as orange-brown crystals [(85JCS(P2)107) gives m.p. 262 - 264 °C].

3.1.2 Preparation of monosubstituted benzophenones

a) 4-Piperidinobenzophenone

4-Fluorobenzophenone (20.0 g; 0.1 mol) and piperidine (9.9 cm³; 0.1 mol) were refluxed together in sulfolane (100 cm³) for five hours. The reaction mixture was then poured into ice-water (2000 cm³), with stirring, whereupon a precipitate was formed. The crude solid was collected, washed with water, ethanol and finally diethyl ether and then crystallised from aqueous acetone to give 4-piperidinobenzophenone (18.6 g; 70 %), m.p. 92.0 - 93.0 °C as yellow flakes [(87JOC1710) gives m.p. 85 -87 °C].

The following compounds were prepared in a similar manner.

b) 4-Pyrrolidinobenzophenone

4-Pyrrolidinobenzophenone was prepared from 4-fluorobenzophenone (20.0 g; 0.1 mol) and pyrrolidine (8.3 cm³; 0.1 mol) after refluxing for six hours. Recrystallisation from aqueous acetone gave 4-pyrrolidinobenzophenone (18.6 g; 74 %), m.p. 149.0 - 149.5 °C as pale yellow crystals [(97JOC1264) gives m.p. 138 °C]. (Found: C, 81.2; H, 6.9; N, 5.3. C₁₇H₁₇NO requires C, 81.3; H, 6.8; N, 5.6 %). ¹H nmr δ 2.06 (4H, m, (CH₂)₂), 3.04 (4H, m, N(CH₂)₂), 6.58 (2H, d, 8.7 Hz, 3-H, 5-H), 7.45 - 7.59 (3H, m, Ar'), 7.74 (2H, d, 2'-H, 6'-H), 7.84 (2H, d, 8.7 Hz, 2-H, 6-H). ¹³C nmr δ 25.9, 48.0, 111.1, 124.6, 128.5, 129.9, 131.4, 133.4, 139.9, 151.3, 195.6.

c) 4-Morpholinobenzophenone

4-Morpholinobenzophenone was prepared from 4-fluorobenzophenone (40.0 g; 0.2 mol) and morpholine (17.4 cm³; 0.2 mol) after refluxing for seven hours. Recrystallisation from light petroleum (b.p. 60 - 80 °C) gave 4-morpholinobenzophenone (36.4 g; 68 %), m.p. 145.0 - 146.0 °C as yellow needles [(90S1145) gives m.p. 140 - 142 °C].

d) 4-N-Methylpiperazinobenzophenone

4-N-Methylpiperazinobenzophenone was prepared from 4-fluorobenzophenone (15.0 g; 0.075 mol) and N-methylpiperazine (11.1 cm³; 0.1 mol) after refluxing for 24 hours. Basification of the ice-water mixture using sodium hydroxide solution (2M) resulted in precipitation of the crude product. Crystallisation from light petroleum (b.p. 60 - 80 °C) gave 4-N-methylpiperazinobenzophenone (10.5 g; 50 %) as bright yellow flakes. ¹H nmr δ 2.40 (3H, s, N(CH₃)), 2.60 (4H, t, 5.0 Hz, N-4(CH₂)₂), 3.43 (4H, t, 5.0 Hz, N-1(CH₂)₂), 6.93 (2H, d, 8.9 Hz, 3-H, 5-H), 7.47 - 7.59 (3H, m, Ar'), 7.77 (2H, d, 2'-H, 6'-H), 7.83 (2H, d, 8.9 Hz, 2-H, 6-H). ¹³C nmr δ 46.6, 47.8, 55.2, 113.8, 127.6, 128.5, 130.0, 131.9, 133.0, 139.3, 154.4, 195.7.

e) 4-Thiomorpholinobenzophenone

4-Thiomorpholinobenzophenone was prepared from 4-fluorobenzophenone (15.0 g; 0.075 mol) and thiomorpholine (10.0 cm³; 0.075 mol) after refluxing for 14 hours. The crude solid was triturated with hot light petroleum (b.p. 60 - 80 °C), filtered and crystallised from aqueous acetone to give 4-thiomorpholinobenzophenone (11.7 g; 55 %), m.p. 144.0 - 144.5 °C as brown crystals. ¹H nmr δ 2.75 (4H, t, 5.0 Hz, S(CH₂)₂), 3.84 (4H, t, 5.0 Hz, N(CH₂)₂), 6.88 (2H, d, 8.9 Hz, 3-H, 5-H), 7.47 - 7.62 (3H, m, Ar'), 7.77 (2H, d, 2'-H, 6'-H), 7.83 (2H, d, 8.9 Hz, 2-H, 6-H). ¹³C nmr δ 26.3, 50.8, 114.0, 127.3, 128.6, 130.0, 131.9, 133.3, 139.2, 153.2, 195.6.

3.1.3 Preparation of diarylhydrols

a) 4,4'-Bis(dimethylamino)benzhydrol

A solution of 4,4'-bis(dimethylamino)benzophenone (1.0 g; 5.0 mmol) and sodium borohydride (0.3 g; 7.9 mmol) in ethanol (100 cm³) was refluxed for three hours. The reaction mixture was then poured into water (1200 cm³), made slightly alkaline by the addition of 2M NaOH (20 cm³), whereupon a bright yellow precipitate formed. This solid was collected, dried and recrystallised from light petroleum (b.p. 60 - 80 °C) to give 4,4'-bis(dimethylamino)benzhydrol (0.82 g; 46 %), m.p. 100 - 102 °C as pale green crystals [(89Th1) gives m.p. 100 - 101 °C].

The following compounds were prepared in a similar manner.

b) 4,4'-Bis(diethylamino)benzhydrol

4,4'-Bis(diethylamino)benzhydrol was prepared from 4,4'-bis-(diethylamino)-benzophenone (2.0 g; 6.2 mmol) and sodium borohydride (5.0 g; 0.13 mol) after refluxing in propan-2-ol (150 cm³) for 48 hours. Recrystallisation from light petroleum (b.p. 60 - 80 °C) gave 4,4'-bis(diethylamino)benzhydrol (1.54 g; 76 %), m.p. 77.5 -

78.5 °C as a pale yellow green solid [(89JCS(P2)1087) gives m.p. 72 - 74 °C] (Found: C, 77.3; H, 9.5; N, 8.5. C₂₁H₃₀N₂O requires C, 77.3; H, 9.3; N, 8.6 %).

c) 4,4'-Dipiperidinobenzhydrol

4,4'-Dipiperidinobenzhydrol was prepared from 4,4'-dipiperidinobenzophenone (2.0 g; 5.7 mmol) and sodium borohydride (3.0 g; 0.078 mol) after refluxing in propan-2-ol (150 cm³) for 48 hours. Recrystallisation from light petroleum (b.p. 60 - 80 °C) gave 4,4'-dipiperidinobenzhydrol (1.12 g; 55 %), m.p. 119.0 - 119.5 °C as a white powder [(89JCS(P2)1087) gives m.p. 117 - 118 °C] (Found: C, 78.9; H, 8.6; N, 7.8 C₂₃H₃₀N₂O requires C, 78.9; H, 8.6; N, 8.0 %).

d) 4,4'-Dipyrrolidinobenzhydrol

A solution of commercially available sodium bis(2-methoxyethoxy)aluminium hydride (12 cm³; 0.04 mol) in sodium-dried toluene (50 cm³) was placed in a 2-necked round bottomed flask (250 cm³) equipped with a Claisen adapter to which was fitted a water-cooled condenser and a stoppered dropping funnel. A calcium chloride drying tube was fitted to the condenser. The solution was heated to ca. 80 °C whereupon the apparatus was removed from the heat and a slurry of 4,4'-dipyrrolidinobenzophenone (1.0g; 3.1 mmol) in sodium dried toluene (20 cm³) was slowly added over a 10 minute period. After the addition was complete, the mixture was heated at 80 °C for two hours. After cooling to 0 °C, a 20% aqueous solution of sodium hydroxide (20 cm³) was cautiously added *via* the dropping funnel whilst swirling the flask, followed by water (20 cm³). The aqueous layer was then removed. The organic layer was washed with water (2 x 25 cm³), saturated sodium chloride solution (30 cm³) and then dried (Na₂SO₄). Removal of the solvent and recrystallisation of the crude solid from light petroleum (b.p. 80 - 100 °C) gave 4,4'-dipyrrolidinobenzhydrol (0.73 g; 73 %), m.p. 135.5 - 136.0 °C as a pale yellow green powder [(89JCS(P2)1087) gives m.p. 138 °C] (Found: C, 78.1; H, 7.9; N, 8.5 C₂₁H₂₆N₂O requires C, 78.3; H, 8.1; N, 8.7 %).

The following compounds were prepared in the same way.

e) 4,4'-Dimorpholinobenzhydrol

4,4'-Dimorpholinobenzhydrol was prepared from 4,4'-dimorpholinobenzophenone (1.2 g; 3.4 mmol) as described in 3.1.3.d. Recrystallisation of the crude solid from light petroleum (b.p. 100 - 120 °C) gave 4,4'-dimorpholinobenzhydrol (0.88 g; 80 %), m.p. 168.0 - 168.5 °C as cream crystals [(89JCS(P2)1087) gives m.p. 152 - 154 °C] (Found: C, 71.4; H, 7.6; N, 8.0 C₂₁H₂₆N₂O₃ requires C, 71.2; H, 7.3; N, 7.9 %).

f) 4,4'-Di-*N*-methylpiperazinobenzhydrol

4,4'-Di-*N*-methylpiperazinobenzhydrol was prepared from 4,4'-di-*N*-methylpiperazinobenzophenone (1.06 g; 2.8 mmol). Recrystallisation of the crude solid from light petroleum (b.p. 100 - 120 °C) gave 4,4'-di-*N*-methylpiperazinobenzhydrol (0.61 g; 57 %), m.p. 175.0 - 175.5 °C as pale yellow crystals [(83Th3) gives m.p. 167 - 169 °C] (Found: C, 72.4; H, 8.5; N, 14.5 C₂₃H₃₂N₄O requires C, 72.7; H, 8.4; N, 14.7 %).

3.1.4 Preparation of intermediates

a) 2,4,4,6-Tetrabromo-2,5-cyclohexadien-1-one

a) A solution of 2,4,6-tribromophenol (66.0 g; 0.2 mol) and sodium acetate trihydrate (27.0 g; 0.34 mol) in glacial acetic acid (400 cm³) was gently heated. Once all the solids were dissolved, the solution was cooled to room temperature at which time a solution of bromine (32.0 g; 0.2 mol) in glacial acetic acid (200 cm³) was added slowly, maintaining the temperature below 25 °C. The resulting mixture was stirred at room temperature for 30 minutes and then poured onto crushed ice (2000 g). Recrystallisation of the damp solid from chloroform gave 2,4,4,6-tetrabromo-2,5-cyclohexadien-1-one (49.2 g; 60 %), m.p. 122.0 - 122.5 °C as a yellow solid [(76OS20) gives m.p. 125 - 130 °C].

b) Purification of aniline

Commercially available aniline (100 g) was boiled under reflux with acetic anhydride (75 g) for three hours. After removal of the acetic anhydride, distillation under reduced pressure afforded pure aniline (75 g), b.p. 120 °C at 10 mmHg.

c) Pyrrolidinobenzene

A mixture of 1,4-dichlorobutane (58.0 g; 0.46 mol) and freshly distilled aniline (77.0 g; 0.83 mol) was boiled under reflux for 30 minutes. The reaction mixture was quenched with water. Extraction with ether and removal of the dried (Na_2SO_4) solvent yielded an oil which, after boiling with acetic anhydride (100 cm³) for one hour, was distilled under reduced pressure to give pyrrolidinobenzene as a pale yellow oil (53.7 g; 80 %), b.p. 160 °C at 10 mmHg [(83JCS(P2)975) gives b.p. 110 °C at 0.7 mmHg]. m/z 146 (M^+).

d) 4-Bromomorpholinobenzene

To a solution of commercially available *N*-phenylmorpholine (38.8 g; 0.24 mol) in glacial acetic acid (100 cm³), cooled to below 15 °C, was added a solution of bromine (37.7 g; 0.24 mol) in glacial acetic acid (70 cm³), whilst maintaining the temperature below 15 °C. The resulting mixture was poured into water (700 cm³) and neutralised with sodium hydroxide (10 M). Extraction with ether and removal of the dried (Na_2SO_4) solvent yielded a crude solid which was recrystallised from light petroleum (b.p. 60 - 80 °C) to give 4-bromomorpholinobenzene (31.9 g; 54.2 %), m.p. 114.0 - 114.5 °C as colourless needles [(43JA479) gives m.p. 114.5 - 115.5 °C].

e) 4-Bromopyrrolidinobenzene

4-Bromopyrrolidinobenzene was prepared from pyrrolidinobenzene (35.0 g; 0.24 mol) and bromine (37.3 g; 0.24 mol) as described in 3.1.4.d. Recrystallisation from ethanol gave 4-bromopyrrolidinobenzene (46.1 g; 83.3 %), m.p. 105.0 - 105.5 °C as a pale yellow powder [(51OKN166) gives 103 °C].

f) 4-Bromopiperidinobenzene

A solution of commercially available *N*-phenylpiperidine (10.0 g; 0.05 mol) in dichloromethane (100 cm³) was cooled to -10 °C, whereupon a suspension of 2,4,4,6-tetrabromo-2,5-cyclohexadien-1-one (20.0 g; 0.05 mol) in dichloromethane (200 cm³) was added slowly. The temperature of the reaction mixture was maintained around 0 °C. After an additional 30 minutes, the reaction mixture was shaken with an aqueous sodium hydroxide solution (2 x 50 cm³, 2 M). The organic layer was separated, dried (Na₂SO₄) and removed to yield a crude solid which was recrystallised from ethanol to give 4-bromopiperidinobenzene (7.2 g; 60 %), m.p. 74.5 - 75.0 °C as off-white flakes [(68RTC1372) gives 74 - 76 °C].

3.1.5 Preparation of aryllithium compounds

The general method of preparation of the aryllithium compounds was as follows.

To diethyl ether (50 cm³), cooled to -10 °C and under an atmosphere of nitrogen, was added a solution of *n*-butyllithium in hexane (4.5 cm³; 0.011 mol). After stirring for five minutes, *N,N,N',N'*-tetramethylethylenediamine (TMEDA) (1.7 cm³; 0.011 mol) was added to the solution. This mixture was stirred for ten minutes, after which time a solution of the appropriate bromo-compound (0.011 mol) in diethyl ether (50 cm³) was added. This mixture was allowed to attain room temperature over a period of 15 minutes. A contact time of a further 30 minutes gave a solution of the aryllithium.

3.1.6 Preparation of the unsymmetrical derivatives of Malachite Green

a) 4'-Dimethylamino-4''-diethylaminotriphenylmethanol

To a solution of 4-diethylaminophenyllithium was added a solution of commercially available 4-dimethylaminobenzophenone (2.5 g; 0.011 mol) in dry diethyl ether (50 cm³) under nitrogen. The reaction mixture was allowed to stir at room temperature for 2-3 hours, whereupon the reactants were poured into water (500 cm³). The organic layer was then washed with water and the ether layer collected. Evaporation of the dried (Na₂SO₄) extracts yielded an oil. Flash chromatography of the crude oil on silica which had been basified using triethylamine and employing a mobile phase of hexane, ethyl acetate and triethylamine (2:2:1) produced 4'-dimethylamino-4''-diethylaminotriphenylmethanol (2.47 g; 60.0 %) as a pale brown oil which would not solidify (Found: C, 79.6; H, 8.6; N, 7.7 C₂₅H₃₀N₂O requires C, 80.2; H, 8.0; N, 7.5 %). ¹H nmr δ 1.20 (6H, t, 6.8 Hz, N(CH₂CH₃)₂), 2.70 (1H, s, OH), 2.99 (6H, s, N(CH₃)₂), 3.38 (4H, q, 6.8 Hz, N(CH₂CH₃)₂), 6.64 (2H, d, 8.9 Hz, 3''-H, 5''-H), 6.71 (2H, d, 8.9 Hz, 3'-H, 5'-H), 7.11 (2H, d, 8.9 Hz, 2'-H, 6'-H), 7.18 (2H, d, 8.9 Hz, 2''-H, 6''-H), 7.30 - 7.37 (5H, m, Ar). ¹³C nmr δ 13.1, 41.1, 44.7, 82.0, 111.2, 112.2, 127.1, 128.1, 128.3, 129.3, 129.6, 134.8, 136.1, 147.2, 148.5, 149.9.

The following compounds were prepared in a similar manner.

b) 4'-Pyrrolidino-4''-diethylaminotriphenylmethanol

From 4-diethylaminophenyllithium and 4-pyrrolidinobenzophenone (2.75 g; 0.011 mol). Evaporation of the organic layer yielded 4'-pyrrolidino-4''-diethylaminotriphenylmethanol (2.85 g; 64.8 %) as a green oil which would not solidify and could not be purified. ¹H nmr δ 1.19 (6H, t, 6.8 Hz, N(CH₂CH₃)₂), 2.03 (4H, m, (CH₂)₂), 3.32 (4H, m, N(CH₂)₂), 3.39 (4H, q, 6.8 Hz, N(CH₂CH₃)₂), 6.57 (2H, d, 8.9 Hz, 3'-H, 5'-H), 6.62 (2H, d, 8.9 Hz, 3''-H, 5''-H), 7.11 (2H, d, 8.9 Hz, 2'-H, 6'-H), 7.18 (2H, d, 8.9 Hz, 2''-H, 6''-H), 7.28 - 7.39 (5H, m, Ar), no hydroxyl proton signal

could be detected. ^{13}C nmr δ 13.1, 26.0, 44.8, 48.1, 82.1, 111.2, 111.3, 127.0, 128.0, 128.3, 129.4, 129.6, 133.6, 134.9, 147.2, 147.3, 148.6.

c) 4'-Piperidino-4''-diethylaminotriphenylmethanol

From 4-diethylaminophenyllithium and 4-piperidinobenzophenone (2.92 g; 0.011 mol). Evaporation of the organic layer yielded a green oil. Flash chromatography of the crude oil on silica which had been basified using triethylamine and employing a mobile phase of hexane produced 4'-piperidino-4''-diethylaminotriphenylmethanol (2.98 g; 65.5 %) as a pale brown oil which would not solidify (Found: C, 81.0; H, 8.2; N, 6.6 $\text{C}_{28}\text{H}_{34}\text{N}_2\text{O}$ requires C, 81.2; H, 8.2; N, 6.6 %). ^1H nmr δ 1.21 (6H, t, 7.2 Hz, $\text{N}(\text{CH}_2\text{CH}_3)_2$), 1.64 (2H, m, CH_2), 1.75 (4H, m, $(\text{CH}_2)_2$), 2.61 (1H, s, OH), 3.21 (4H, t, $\text{N}(\text{CH}_2)_2$), 3.39 (4H, q, 7.2 Hz, $\text{N}(\text{CH}_2\text{CH}_3)_2$), 6.64 (2H, d, 8.9 Hz, 3''-H, 5''-H), 6.91 (2H, d, 8.9 Hz, 3'-H, 5'-H), 7.10 (2H, d, 8.9 Hz, 2''-H, 6''-H), 7.20 (2H, d, 8.9 Hz, 2'-H, 6'-H), 7.28 - 7.37 (5H, m, Ar). ^{13}C nmr δ 13.1, 24.8, 26.3, 44.7, 50.9, 82.0, 111.2, 115.8, 127.1, 128.1, 128.3, 129.2, 129.6, 134.6, 138.5, 147.2, 148.3, 151.4.

d) 4'-Morpholino-4''-diethylaminotriphenylmethanol

From 4-diethylaminophenyllithium and 4-morpholinobenzophenone (2.94 g; 0.011 mol). Evaporation of the organic layer yielded a pale yellow oil, which solidified after several weeks. Recrystallisation of the crude solid from light petroleum (b.p. 60 - 80 $^\circ\text{C}$) yielded 4'-morpholino-4''-diethylaminotriphenylmethanol (3.4 g; 74.5 %), m.p. 131.5 - 132.0 $^\circ\text{C}$ as a yellow powder (Found: C, 78.0; H, 7.9; N, 6.6 $\text{C}_{27}\text{H}_{32}\text{N}_2\text{O}_2$ requires C, 77.9; H, 7.7; N, 6.7 %). ^1H nmr δ 1.20 (6H, t, 7.0 Hz, $\text{N}(\text{CH}_2\text{CH}_3)_2$), 2.81 (1H, s, OH), 3.19 (4H, t, 5.0 Hz, $\text{N}(\text{CH}_2)_2$), 3.38 (4H, q, 7.0 Hz, $\text{N}(\text{CH}_2\text{CH}_3)_2$), 3.89 (4H, t, 5.0 Hz, $\text{O}(\text{CH}_2)_2$), 6.63 (2H, d, 8.7 Hz, 3''-H, 5''-H), 6.88 (2H, d, 8.7 Hz, 3'-H, 5'-H), 7.08 (2H, d, 8.7 Hz, 2''-H, 6''-H), 7.25 (2H, d, 8.7 Hz, 2'-H, 6'-H), 7.28 - 7.39 (5H, m, Ar). ^{13}C nmr δ 13.1, 44.7, 49.6, 67.4, 81.9, 111.2, 115.1, 127.2, 128.3, 128.6, 129.3, 129.6, 134.3, 139.5, 147.3, 148.2, 150.4.

e) 4'-Dimethylamino-4"-pyrrolidinotriphenylmethanol

From 4-pyrrolidinophenyllithium and 4-dimethylaminobenzophenone (2.5 g; 0.011 mol). Evaporation of the organic layer yielded 4'-dimethylamino-4"-pyrrolidinotriphenylmethanol (3.15 g; 77.3 %) as a green oil which would not solidify and could not be purified. ^1H nmr δ 2.08 (4H, m, $(\text{CH}_2)_2$), 3.00 (6H, s, $\text{N}(\text{CH}_3)_2$), 3.14 (1H, s, OH), 3.34 (4H, m, $\text{N}(\text{CH}_2)_2$), 6.54 (2H, d, 8.7 Hz, 3"-H, 5"-H), 6.77 (2H, d, 8.7 Hz, 3'-H, 5'-H), 7.09 - 7.14 (4H, 2d, 8.7 Hz, 2'-H, 6'-H, 2"-H, 6"-H), 7.21 - 7.39 (5H, m, Ar). ^{13}C nmr δ 26.0, 41.1, 48.1, 82.1, 111.3, 112.2, 127.5, 128.1, 128.3, 129.4, 129.5, 133.3, 135.9, 147.3, 148.2, 149.9.

f) 4'-Piperidino-4"-pyrrolidinotriphenylmethanol

From 4-pyrrolidinophenyllithium and 4-piperidinobenzophenone (2.92 g; 0.011 mol). Evaporation of the organic layer yielded a pale yellow oil, which solidified after several weeks. Recrystallisation of the crude solid from methanol which had been made slightly alkaline by the addition of a trace of 2M sodium hydroxide solution yielded 4'-piperidino-4"-pyrrolidinotriphenylmethanol (2.86 g; 62.7 %), m.p. 144.5 - 145.0 °C as greenish brown flakes (Found: C, 81.4; H, 8.1; N, 6.5 $\text{C}_{28}\text{H}_{32}\text{N}_2\text{O}$ requires C, 81.6; H, 7.8; N, 6.8 %). ^1H nmr δ 1.61 (2H, m, CH_2), 1.74 (4H, m, $(\text{CH}_2)_2$), 2.03 (4H, m, $(\text{CH}_2)_2$), 3.10 (1H, s, OH), 3.19 (4H, m, $\text{N}(\text{CH}_2)_2$), 3.33 (4H, m, $\text{N}(\text{CH}_2)_2$), 6.54 (2H, d, 8.7 Hz, 3"-H, 5"-H), 6.89 (2H, d, 8.7 Hz, 3'-H, 5'-H), 7.21 - 7.36 (7H, m, 2'-H, 6'-H, Ar), 7.54 (2H, d, 8.7 Hz, 2"-H, 6"-H). ^{13}C nmr δ 24.8, 26.0, 26.4, 48.0, 50.8, 87.1, 111.0, 115.6, 126.6, 128.0, 128.4, 130.1, 130.5, 130.9, 135.2, 146.6, 147.0, 151.0.

g) 4'-Morpholino-4"-pyrrolidinotriphenylmethanol

From 4-pyrrolidinophenyllithium and 4-morpholinobenzophenone (2.94 g; 0.011 mol). Evaporation of the organic layer yielded a pale yellow oil, which solidified after several weeks. Recrystallisation of the crude solid from hexane yielded 4'-morpholino-4"-pyrrolidinotriphenylmethanol (3.04 g; 66.4 %), m.p. 143.0 - 143.5 °C as pale greenish

yellow crystals (Found: C, 78.1; H, 7.3; N, 6.7 $C_{27}H_{30}N_2O_2$ requires C, 78.3; H, 7.2; N, 6.8 %). 1H nmr δ 2.03 (4H, m, $(CH_2)_2$), 2.77 (1H, s, OH), 3.19 (4H, t, 4.7 Hz, $N(CH_2)_2$), 3.32 (4H, m, $N(CH_2)_2$), 3.89 (4H, t, 4.7 Hz, $O(CH_2)_2$), 6.53 (2H, d, 8.7 Hz, 3''-H, 5''-H), 6.88 (2H, d, 8.7 Hz, 3'-H, 5'-H), 7.12 (2H, d, 8.7 Hz, 2''-H, 6''-H), 7.23 (2H, d, 8.7 Hz, 2'-H, 6'-H), 7.27 - 7.37 (5H, m, Ar). ^{13}C nmr δ 26.0, 48.0, 49.6, 67.4, 82.0, 111.2, 115.1, 127.2, 128.2, 128.3, 129.3, 129.4, 134.6, 139.6, 147.4, 148.2, 150.4.

h) 4'-Dimethylamino-4''-piperidinotriphenylmethanol

From 4-piperidinophenyllithium and 4-dimethylaminobenzophenone (2.48 g; 0.011 mol). Evaporation of the organic layer yielded a pale yellow oil, which solidified after several weeks. Recrystallisation of the crude solid from light petroleum (b.p. 60 - 80 °C) yielded 4'-dimethylamino-4''-piperidinotriphenylmethanol (2.69 g; 63.6 %), m.p. 124.0 - 124.5 °C as pale yellowish green needles (Found: C, 81.0; H, 7.8; N, 7.1 $C_{26}H_{30}N_2O$ requires C, 80.8; H, 7.7; N, 7.3 %). 1H nmr δ 1.65 (2H, m, CH_2), 1.73 (4H, m, $(CH_2)_2$), 2.71 (1H, s, OH), 2.98 (6H, s, $N(CH_3)_2$), 3.19 (4H, t, $N(CH_2)_2$), 6.69 (2H, d, 8.9 Hz, 3'-H, 5'-H), 6.89 (2H, d, 8.9 Hz, 3''-H, 5''-H), 7.13 - 7.18 (4H, 2d, 2'-H, 6'-H, 2''-H, 6''-H), 7.30 - 7.36 (5H, m, Ar). ^{13}C nmr δ 24.8, 26.3, 41.0, 50.8, 82.0, 112.1, 115.8, 127.2, 128.1, 128.3, 129.2, 129.3, 135.9, 138.4, 148.2, 149.9, 151.4.

i) 4'-Morpholino-4''-piperidinotriphenylmethanol

From 4-piperidinophenyllithium and 4-morpholinobenzophenone (2.94 g; 0.011 mol). Evaporation of the organic layer yielded 4'-morpholino-4''-piperidinotriphenylmethanol (2.17 g; 48.2 %) as a green oil which would not solidify and could not be purified. 1H nmr δ 1.49 (2H, m, CH_2), 1.63 (4H, m, $(CH_2)_2$), 2.66 (1H, s, OH), 3.07 (8H, m, $N(CH_2)_2$, $N(CH_2)_2$), 3.77 (4H, t, $O(CH_2)_2$), 6.74 - 6.79 (4H, 2d, 3'-H, 5'-H, 3''-H, 5''-H), 7.01 (2H, d, 8.7 Hz, 2''-H, 6''-H), 7.05 (2H, d, 8.7 Hz, 2'-H, 6'-H), 7.16 - 7.22 (5H, m, Ar). ^{13}C nmr δ 24.7, 26.3, 49.5, 50.7, 67.3, 81.9, 115.1, 115.8, 127.3, 128.1, 128.2, 129.1, 129.3, 138.0, 139.2, 147.9, 150.4, 151.4.

j) 4'-Morpholino-4''-dimethylaminotriphenylmethanol

From 4-dimethylaminophenyllithium and 4-morpholinobenzophenone (2.94 g; 0.011 mol). Evaporation of the organic layer yielded a pale yellow oil, which solidified after several weeks. Recrystallisation of the crude solid from light petroleum (b.p. 100 - 120 °C) yielded 4'-morpholino-4''-dimethylaminotriphenylmethanol (3.25 g; 76.4 %), m.p. 163.5 - 164.0 °C as a pale green powder (Found: C, 77.3; H, 7.5; N, 7.1 C₂₅H₂₈N₂O₂ requires C, 77.3; H, 7.2; N, 7.2 %). ¹H nmr δ 2.80 (1H, s, OH), 2.99 (6H, s, N(CH₃)₂), 3.19 (4H, t, 4.7 Hz, N(CH₂)₂), 3.89 (4H, t, 4.7 Hz, O(CH₂)₂), 6.70 (2H, d, 8.9 Hz, 3''-H, 5''-H), 6.88 (2H, d, 8.9 Hz, 3'-H, 5'-H), 7.14 (2H, d, 8.9 Hz, 2''-H, 6''-H), 7.22 (2H, d, 8.9 Hz, 2'-H, 6'-H), 7.30 - 7.36 (5H, m, Ar). ¹³C nmr δ 41.0, 49.6, 67.4, 81.9, 112.1, 115.1, 127.3, 128.2, 128.3, 129.3, 129.4, 135.7, 139.4, 148.1, 150.0, 150.4.

k) 4'-N-Methylpiperazino-4''-diethylaminotriphenylmethanol

From 4-diethylaminophenyllithium and 4-N-methylpiperazinobenzophenone (3.08 g; 0.011 mol). Evaporation of the organic layer yielded a pale yellow oil, which solidified after several weeks. Recrystallisation of the crude solid from ethyl acetate yielded 4'-N-methylpiperazino-4''-diethylaminotriphenylmethanol (2.47 g; 52.7 %), m.p. 144.2 - 144.7 °C as pale brown flakes (Found: C, 78.3; H, 8.4; N, 9.8 C₂₈H₃₅N₃O requires C, 78.3; H, 8.2; N, 9.8 %). ¹H nmr δ 1.19 (6H, t, 6.9 Hz, N(CH₂CH₃)₂), 2.38 (3H, s, NCH₃), 2.60 (4H, t, N-4(CH₂)₂), 2.89 (1H, s, OH), 3.22 (4H, t, N-1(CH₂)₂), 3.39 (4H, q, 6.9 Hz, N(CH₂CH₃)₂), 6.62 (2H, d, 8.7 Hz, 3''-H, 5''-H), 6.88 (2H, d, 8.7 Hz, 3'-H, 5'-H), 7.09 (2H, d, 8.7 Hz, 2''-H, 6''-H), 7.21 (2H, d, 8.7 Hz, 2'-H, 6'-H), 7.30 - 7.38 (5H, m, Ar). ¹³C nmr δ 13.1, 44.7, 46.7, 49.3, 55.6, 81.9, 111.2, 115.4, 127.1, 128.1, 128.3, 129.3, 129.6, 134.5, 139.1, 147.2, 148.3, 150.4.

l) 4'-N-Methylpiperazino-4''-dimethylaminotriphenylmethanol

From 4-dimethylaminophenyllithium and 4-*N*-methylpiperazinobenzophenone (3.08 g; 0.011 mol). Evaporation of the organic layer yielded a pale yellow oil, which solidified after several weeks. Recrystallisation of the crude solid from light petroleum (b.p. 100 - 120 °C) yielded 4'-*N*-methylpiperazino-4''-dimethylaminotriphenylmethanol (3.22 g; 72.7 %), m.p. 157.1 - 157.7 °C as an off-white powder (Found: C, 77.7; H, 7.9; N, 10.3 C₂₆H₃₁N₃O requires C, 77.8; H, 7.7; N, 10.5 %). ¹H nmr δ 2.38 (3H, s, NCH₃), 2.60 (4H, t, 4.7 Hz, N-4(CH₂)₂), 2.85 (1H, s, OH), 2.98 (6H, s, N(CH₃)₂), 3.24 (4H, t, 4.7 Hz, N-1(CH₂)₂), 6.69 (2H, d, 8.7 Hz, 3''-H, 5''-H), 6.88 (2H, d, 8.7 Hz, 3'-H, 5'-H), 7.13 (2H, d, 8.7 Hz, 2''-H, 6''-H), 7.19 (2H, d, 8.7 Hz, 2'-H, 6'-H), 7.29 - 7.34 (5H m, Ar). ¹³C nmr δ 41.0, 46.7, 49.2, 55.6, 81.9, 112.1, 115.4, 127.2, 128.1, 128.3, 129.3, 129.3, 135.8, 139.0, 148.2, 150.0, 150.4.

m) 4'-N-Methylpiperazino-4''-pyrrolidinotriphenylmethanol

From 4-pyrrolidinophenyllithium and 4-*N*-methylpiperazinobenzophenone (3.08 g; 0.011 mol). Evaporation of the organic layer yielded a pale brown oil which would not solidify. Flash chromatography of the crude oil on silica which had been basified using triethylamine and employing a mobile phase of toluene, ethyl acetate and triethylamine (2:2:1) produced 4'-*N*-methylpiperazino-4''-pyrrolidinotriphenylmethanol (2.62 g; 55.5 %) as a pale brown oil which would not solidify (Found: C, 77.4; H, 7.9; N, 9.3 C₂₈H₃₃N₃O requires C, 78.7; H, 7.7; N, 9.8 %). ¹H nmr δ 2.03 (4H, t, 6.5 Hz, (CH₂)₂), 2.38 (3H, s, NCH₃), 2.60 (4H, t, 5.0 Hz, N-4(CH₂)₂), 3.24 (4H, t, 5.0 Hz, N-1(CH₂)₂), 3.32 (4H, t, 6.5 Hz, N(CH₂)₂), 6.53 (2H, d, 8.7 Hz, 3''-H, 5''-H), 6.88 (2H, d, 8.7 Hz, 3'-H, 5'-H), 7.12 (2H, d, 8.7 Hz, 2''-H, 6''-H), 7.21 (2H, d, 8.7 Hz, 2'-H, 6'-H), 7.27 - 7.38 (5H, m, Ar). ¹³C nmr δ 26.0, 46.6, 48.0, 49.3, 55.6, 82.0, 111.2, 115.4, 127.1, 128.1, 128.3, 129.3, 129.5, 134.7, 139.2, 147.3, 148.3, 150.4.

n) 4'-N-Methylpiperazino-4''-piperidinotriphenylmethanol

From 4-piperidinophenyllithium and 4-*N*-methylpiperazinobenzophenone (3.08 g; 0.011 mol). Evaporation of the organic layer yielded a pale yellow oil, which solidified after several weeks. Repeated recrystallisation of the crude solid from light petroleum (b.p. 60 - 80 °C) yielded 4'-*N*-methylpiperazino-4''-piperidinotriphenylmethanol (3.32 g; 68.2 %), m.p. 146.0 - 146.6 °C as pale yellow crystals (Found: C, 78.7; H, 7.9; N, 9.3 C₂₉H₃₅N₃O requires C, 78.9; H, 7.9; N, 9.5 %). ¹H nmr δ 1.62 (2H, m, CH₂), 1.71 (4H, m, (CH₂)₂), 2.38 (3H, s, NCH₃), 2.60 (4H, t, 4.7 Hz, N-4(CH₂)₂), 2.81 (1H, s, OH), 3.17 - 3.26 (8H, m, N(CH₂)₂, N-1(CH₂)₂), 6.88 (4H, 2d, 8.7 Hz, 3''-H, 5''-H, 3'-H, 5'-H), 7.15 (4H, 2d, 8.7 Hz, 2''-H, 6''-H, 2'-H, 6'-H), 7.27 - 7.34 (5H, m, Ar). ¹³C nmr δ 24.7, 26.3, 46.6, 49.2, 50.7, 55.6, 81.9, 115.4, 115.8, 127.3, 128.2, 128.3, 129.2, 129.3, 138.1, 138.8, 148.0, 150.5, 151.4.

o) 4'-N-Methylpiperazino-4''-morpholinotriphenylmethanol

From 4-morpholinophenyllithium and 4-*N*-methylpiperazinobenzophenone (3.08 g; 0.011 mol). Evaporation of the organic layer yielded a pale yellow oil, which solidified after several weeks. Repeated recrystallisation of the crude solid from light petroleum (b.p. 60 - 80 °C) yielded 4'-*N*-methylpiperazino-4''-morpholinotriphenylmethanol (2.52 g; 51.8 %), m.p. 76.0 - 76.6 °C as a white powder (Found: C, 75.4; H, 7.6; N, 8.8 C₂₈H₃₃N₃O₂ requires C, 75.8; H, 7.4; N, 9.5 %). ¹H nmr δ 2.38 (3H, s, NCH₃), 2.60 (4H, t, 4.7 Hz, N-4(CH₂)₂), 2.89 (1H, s, OH), 3.17 - 3.26 (8H, m, N(CH₂)₂, N-1(CH₂)₂), 3.89 (4H, t, 4.7 Hz, O(CH₂)₂), 6.87 (2H, d, 8.7 Hz, 3''-H, 5''-H), 6.88 (2H, d, 8.7 Hz, 3'-H, 5'-H), 7.17 (4H, 2d, 2'-H, 6'-H, 2''-H, 6''-H), 7.30 - 7.33 (5H, m, Ar). ¹³C nmr δ 46.6, 49.2, 49.5, 55.6, 67.4, 81.9, 115.1, 115.4, 127.4, 128.2, 128.2, 129.2, 129.3, 139.1, 139.5, 147.9, 150.4, 150.5.

p) 4'-Thiomorpholino-4"-dimethylaminotriphenylmethanol

From 4-dimethylaminophenyllithium and 4-thiomorpholinobenzophenone (3.11 g; 0.011 mol). Evaporation of the organic layer yielded a pale yellow oil, which solidified after several weeks. Flash chromatography of the crude solid on silica which had been basified using triethylamine and employing a mobile phase of benzene followed by ethyl acetate produced 4'-thiomorpholino-4"-dimethylaminotriphenylmethanol (2.01 g; 45.5 %) as a pale green powder (Found: C, 73.4; H, 7.2; N, 7.0 C₂₅H₂₈N₂OS requires C, 74.3; H, 6.9; N, 6.9 %). ¹H nmr δ 2.77 (4H, m, S(CH₂)₂), 2.98 (6H, s, N(CH₃)₂), 3.58 (4H, m, N(CH₂)₂), 6.70 (2H, d, 8.7 Hz, 3"-H, 5"-H), 6.85 (2H, d, 8.7 Hz, 3'-H, 5'-H), 7.14 (2H, d, 8.7 Hz, 2"-H, 6"-H), 7.20 (2H, d, 8.7 Hz, 2'-H, 6'-H), 7.30 - 7.36 (5H, m, Ar). ¹³C nmr δ 27.2, 41.0, 52.4, 81.9, 112.2, 116.5, 127.3, 128.2, 128.3, 129.3, 129.4, 135.7, 139.2, 148.1, 150.0, 150.4.

3.1.7 Preparation of the perchlorate salts

Two methods were used to generate the perchlorate salts of the dye bases studied in this project.

Method 1

A solution of the dye base dissolved in the minimum volume of glacial acetic acid was added dropwise to a saturated aqueous solution of sodium perchlorate (50 cm³). The solid which formed was collected, washed thoroughly with water, ethanol and then with diethyl ether. Purification of the crude salt was a two step process. The first step involved dissolution of the salt in acetone (previously dried over 4A molecular sieve) and filtering the solution into a clean, dry conical flask. Addition of a large excess of diethyl ether (Na-dried) brought about the reprecipitation of the salt. The salt was then collected, washed with diethyl ether (Na-dried) and collected. If the salt was still impure, the second stage of purification involved recrystallisation of the salt from a suitable organic solvent such as ethyl acetate. The salt was then collected, washed and dried.

Method 2

The dye base (0.2 g) was dissolved in a solution of acetic anhydride (30 cm³) containing glacial acetic acid (5 cm³). The solution was then gently warmed. To the warmed solution was added an equimolar amount of 60% perchloric acid. The solution was then gently warmed for a further 20 minutes after which time it was filtered into a clean, dry conical flask. Addition of a large excess of diethyl ether (Na-dried) brought about the precipitation of the salt. The salt was washed a further three times with diethyl ether (Na-dried). The diethyl ether was then removed under vacuum. The crude salt was collected and dissolved in acetone (dried over 4A molecular sieve). This solution was then filtered into a clean, dry conical flask. Addition of a large excess of diethyl ether (Na-dried) brought about the reprecipitation of the salt. The salt was washed a further three times with diethyl ether (Na-dried). The diethyl ether was then removed under vacuum.

The following perchlorate salts were prepared using Method 1:

a) 4,4'-Bis(dimethylamino)diphenylmethyl perchlorate

4,4'-Bis(dimethylamino)diphenylmethyl perchlorate (0.26 g; 33 %) as lustrous purple metallic crystals (Found: C, 57.8; H, 5.9; N, 7.9 C₁₇H₂₁O₄N₂Cl requires C, 57.9; H, 6.0; N, 7.9 %).

b) 4'-Dimethylamino-4"-diethylaminotriphenylmethyl perchlorate

4'-Dimethylamino-4"-diethylaminotriphenylmethyl perchlorate (0.21 g; 58 %) as lustrous green metallic crystals, after recrystallisation from ethyl acetate (Found: C, 65.4; H, 6.4; N, 6.0 C₂₅H₂₉O₄N₂Cl requires C, 65.7; H, 6.4; N, 6.1 %). ¹H nmr δ 1.50 (6H, t, 7.2 Hz, N(CH₂CH₃)₂), 3.55 (6H, s, N(CH₃)₂), 3.94 (4H, q, 7.2 Hz, N(CH₂CH₃)₂), 7.27 (2H, d, 9.4 Hz, 3"-H, 5"-H), 7.29 (2H, d, 9.4 Hz, 3'-H, 5'-H), 7.56 - 7.64 (6H, m, 2'-H, 6'-H, 2"-H, 6"-H, 3-H, 5-H), 7.80 (2H, t, 9.2 Hz, 2-H, 6-H), 7.94 (1H, t, 9.2 Hz, 4-H).

^{13}C nmr δ 12.7, 40.7, 46.3, 114.2, 114.4, 127.5, 127.6, 129.2, 133.4, 135.0, 140.3, 141.0, 141.7, 156.2, 157.5, 177.3.

c) 4'-Pyrrolidino-4''-diethylaminotriphenylmethyl perchlorate

4'-Pyrrolidino-4''-diethylaminotriphenylmethyl perchlorate (0.17 g; 47 %) as lustrous purple crystals for which a satisfactory analysis could not be obtained. ^1H nmr δ 1.49 (6H, t, 7.0 Hz, $\text{N}(\text{CH}_2\text{CH}_3)_2$), 2.33 (4H, t, 6.7 Hz, $(\text{CH}_2)_2$), 3.90 - 3.99 (8H, m, $\text{N}(\text{CH}_2)_2$, $\text{N}(\text{CH}_2\text{CH}_3)_2$), 7.16 (2H, d, 8.9 Hz, 3'-H, 5'-H), 7.31 (2H, d, 8.9 Hz, 3''-H, 5''-H), 7.57 - 7.65 (6H, m, 2'-H, 6'-H, 2''-H, 6''-H, 3-H, 5-H), 7.81 (2H, t, 7.5 Hz, 2-H, 6-H), 7.93 (1H, t, 7.5 Hz, 4-H). ^{13}C nmr δ 12.6, 25.5, 46.2, 49.6, 114.1, 115.2, 126.3, 127.7, 129.2, 133.4, 134.9, 140.4, 140.4, 141.3, 155.2, 155.5, 177.0.

d) 4'-Piperidino-4''-diethylaminotriphenylmethyl perchlorate

4'-Piperidino-4''-diethylaminotriphenylmethyl perchlorate (0.12 g; 33 %) as lustrous purple crystals for which a satisfactory analysis could not be obtained. ^1H nmr δ 1.50 (6H, t, 7.0 Hz, $\text{N}(\text{CH}_2\text{CH}_3)_2$), 1.96 (6H, m, CH_2 , $(\text{CH}_2)_2$), 3.94 (4H, q, 7.0 Hz, $\text{N}(\text{CH}_2\text{CH}_3)_2$), 4.02 (4H, m, $\text{N}(\text{CH}_2)_2$), 7.33 (2H, d, 9.2 Hz, 3''-H, 5''-H), 7.46 (2H, d, 9.2 Hz, 3'-H, 5'-H), 7.57 - 7.65 (6H, m, 2'-H, 6'-H, 2''-H, 6''-H, 3-H, 5-H), 7.81 (2H, t, 7.5 Hz, 2-H, 6-H), 7.93 (1H, t, 7.5 Hz, 4-H). ^{13}C nmr δ 12.7, 24.5, 26.6, 46.3, 49.4, 114.5, 114.9, 128.4, 128.7, 129.2, 133.4, 134.9, 140.3, 141.3, 141.5, 156.2, 156.3, 176.2.

e) 4'-Morpholino-4''-diethylaminotriphenylmethyl perchlorate

4'-Morpholino-4''-diethylaminotriphenylmethyl perchlorate (0.26 g; 72 %) as lustrous metallic green crystals (Found: C, 64.8; H, 6.4; N, 5.6 $\text{C}_{27}\text{H}_{31}\text{O}_5\text{N}_2\text{Cl}$ requires C, 65.0; H, 6.2; N, 5.6 %). ^1H nmr δ 1.52 (6H, t, 7.0 Hz, $\text{N}(\text{CH}_2\text{CH}_3)_2$), 3.94 (4H, q, 7.0 Hz, $\text{N}(\text{CH}_2\text{CH}_3)_2$), 4.00 (8H, m, $\text{N}(\text{CH}_2)_2$, $\text{O}(\text{CH}_2)_2$), 7.39 (2H, d, 9.0 Hz, 3''-H, 5''-H), 7.43 (2H, d, 9.0 Hz, 3'-H, 5'-H), 7.58 - 7.71 (6H, m, 2'-H, 6'-H, 2''-H, 6''-H, 3-H, 5-H), 7.83 (2H, t, 7.5 Hz, 2-H, 6-H), 7.95 (1H, t, 7.5 Hz, 4-H). ^{13}C nmr δ 12.8, 46.7, 47.5, 66.7,

114.3, 115.2, 128.1, 128.5, 129.2, 133.6, 135.1, 140.2, 140.6, 142.3, 156.8, 157.1, 177.3.

f) 4'-Dimethylamino-4"-pyrrolidinotriphenylmethyl perchlorate

4'-Dimethylamino-4"-pyrrolidinotriphenylmethyl perchlorate (0.26 g; 70 %) after recrystallisation from ethyl acetate as lustrous green metallic crystals (Found: C, 65.7; H, 6.1; N, 6.0 $C_{25}H_{27}O_4N_2Cl$ requires C, 66.0; H, 5.9; N, 6.2 %). 1H nmr δ 2.34 (4H, m, $(CH_2)_2$), 3.55 (6H, s, $N(CH_3)_2$), 3.91 (4H, m, $N(CH_2)_2$), 7.17 (2H, d, 8.7 Hz, 3"-H, 5"-H), 7.27 (2H, d, 8.7 Hz, 3'-H, 5'-H), 7.56 - 7.64 (6H, m, 2'-H, 6'-H, 2"-H, 6"-H, 3-H, 5-H), 7.80 (2H, t, 7.5 Hz, 2-H, 6-H), 7.92 (1H, t, 7.5 Hz, 4-H). ^{13}C nmr δ 26.2, 41.3, 50.3, 114.8, 116.1, 128.1, 128.5, 129.9, 134.1, 135.7, 141.1, 141.5, 142.1, 156.0, 158.0, 178.0.

g) 4'-Piperidino-4"-pyrrolidinotriphenylmethyl perchlorate

4'-Piperidino-4"-pyrrolidinotriphenylmethyl perchlorate (0.19 g; 52 %) after recrystallisation from ethyl acetate as lustrous green metallic crystals (Found: C, 67.6; H, 6.4; N, 5.5. $C_{28}H_{31}O_4N_2Cl$ requires C, 67.9; H, 6.3; N, 5.7 %). 1H nmr δ 1.97 (6H, m, CH_2 , $(CH_2)_2$), 2.34 (4H, m, $(CH_2)_2$), 3.93 (4H, m, $N(CH_2)_2$), 4.02 (4H, m, $N(CH_2)_2$), 7.19 (2H, d, 8.4 Hz, 3"-H, 5"-H), 7.49 (2H, d, 8.4 Hz, 3'-H, 5'-H), 7.56 - 7.66 (6H, m, 2'-H, 6'-H, 2"-H, 6"-H, 3-H, 5-H), 7.80 (2H, t, 7.5 Hz, 2-H, 6-H), 7.94 (1H, t, 7.5 Hz, 4-H). ^{13}C nmr δ 24.5, 25.4, 26.5, 49.8, 49.8, 114.8, 115.4, 127.9, 129.2, 131.7, 133.4, 134.9, 140.3, 141.4, 141.4, 155.3, 156.3, 177.8.

h) 4'-Morpholino-4"-pyrrolidinotriphenylmethyl perchlorate

4'-Morpholino-4"-pyrrolidinotriphenylmethyl perchlorate (0.15 g; 42 %) after recrystallisation from ethyl acetate as lustrous purple crystals for which a satisfactory analysis could not be obtained. 1H nmr δ 2.35 (4H, m, $(CH_2)_2$), 3.91 (4H, m, $N(CH_2)_2$), 4.00 (8H, m, $N(CH_2)_2$, $O(CH_2)_2$), 7.24 (2H, d, 8.9 Hz, 3"-H, 5"-H), 7.42 (2H, d, 8.9 Hz,

3'-H, 5'-H), 7.55 - 7.70 (6H, m, 2'-H, 6'-H, 2''-H, 6''-H, 3-H, 5-H), 7.81 (2H, t, 7.4 Hz, 2-H, 6-H), 7.93 (1H, t, 7.4 Hz, 4-H). ^{13}C nmr δ 25.4, 47.5, 50.1, 66.7, 114.3, 116.3, 128.4, 128.5, 129.2, 133.5, 135.0, 140.3, 140.4, 142.1, 156.0, 156.6, 177.2.

i) 4'-Dimethylamino-4''-piperidinotriphenylmethyl perchlorate

4'-Dimethylamino-4''-piperidinotriphenylmethyl perchlorate (0.13 g; 36 %) after recrystallisation from ethyl acetate as lustrous green metallic crystals (Found: C, 64.1; H, 6.4; N, 5.6. $\text{C}_{26}\text{H}_{29}\text{O}_4\text{N}_2\text{Cl}$ requires C, 66.6; H, 6.2; N, 6.0 %). ^1H nmr δ 1.97 (6H, m, CH_2 , $(\text{CH}_2)_2$), 3.58 (6H, s, $\text{N}(\text{CH}_3)_2$), 4.05 (4H, m, $\text{N}(\text{CH}_2)_2$), 7.30 (2H, d, 9.2 Hz, 3'-H, 5'-H), 7.49 (2H, d, 9.2 Hz, 3''-H, 5''-H), 7.50 - 7.64 (6H, m, 2'-H, 6'-H, 2''-H, 6''-H, 3-H, 5-H), 7.80 (2H, t, 7.2 Hz, 2-H, 6-H), 7.93 (1H, t, 7.2 Hz, 4-H). ^{13}C nmr δ 24.4, 26.6, 40.8, 49.4, 114.4, 115.0, 128.4, 128.7, 129.2, 133.4, 135.0, 140.3, 141.0, 141.5, 156.7, 157.7, 176.5.

j) 4'-Morpholino-4''-piperidinotriphenylmethyl perchlorate

4'-Morpholino-4''-piperidinotriphenylmethyl perchlorate (0.10 g; 28 %) after recrystallisation from ethyl acetate as lustrous purple metallic crystals for which a satisfactory analysis could not be obtained. ^1H nmr δ 1.99 (6H, m, CH_2 , $(\text{CH}_2)_2$), 3.92 (4H, t, 5.2 Hz, $\text{O}(\text{CH}_2)_2$), 4.00 (4H, t, 5.2 Hz, $\text{N}(\text{CH}_2)_2$), 4.12 (4H, m, $\text{N}(\text{CH}_2)_2$), 7.43 (2H, d, 9.2 Hz, 3''-H, 5''-H), 7.53 (2H, d, 9.2 Hz, 3'-H, 5'-H), 7.57 - 7.70 (6H, m, 2'-H, 6'-H, 2''-H, 6''-H, 3-H, 5-H), 7.81 (2H, t, 7.2 Hz, 2-H, 6-H), 7.95 (1H, t, 7.2 Hz, 4-H). ^{13}C nmr δ 24.4, 26.9, 47.6, 49.8, 66.7, 114.4, 115.6, 128.4, 128.6, 129.2, 133.6, 135.0, 140.2, 140.5, 142.3, 156.8, 156.8, 176.5.

k) 4'-Morpholino-4''-dimethylaminotriphenylmethyl perchlorate

4'-Morpholino-4''-dimethylaminotriphenylmethyl perchlorate (0.21 g; 58 %) after recrystallisation from ethyl acetate as lustrous green metallic crystals (Found: C, 63.2; H, 6.2; N, 5.4. $C_{25}H_{27}O_5N_2Cl$ requires C, 63.8; H, 5.7; N, 6.0 %). 1H nmr δ 3.63 (6H, s, $N(CH_3)_2$), 3.93 (4H, m, $O(CH_2)_2$), 4.01 (4H, m, $N(CH_2)_2$), 7.36 (2H, d, 9.2 Hz, 3''-H, 5''-H), 7.43 (2H, d, 9.2 Hz, 3'-H, 5'-H), 7.56 - 7.65 (6H, m, 2'-H, 6'-H, 2''-H, 6''-H, 3-H, 5-H), 7.81 (2H, t, 7.2 Hz, 2-H, 6-H), 7.92 (1H, t, 7.2 Hz, 4-H). ^{13}C nmr δ 41.1, 47.6, 66.7, 114.4, 115.2, 128.1, 128.5, 129.2, 133.6, 135.1, 140.2, 140.8, 141.9, 156.9, 158.5, 177.6.

The following perchlorate salts were prepared using Method 2:

l) 4,4'-Bis(diethylamino)diphenylmethyl perchlorate

4,4'-Bis(diethylamino)diphenylmethyl perchlorate (0.13 g; 45 %) as lustrous blue crystals (Found: C, 57.9; H, 6.9; N, 6.4. $C_{21}H_{29}O_4N_2Cl$ requires C, 61.7; H, 7.1; N, 6.9 %).

m) 4,4'-Dimorpholinodiphenylmethyl perchlorate

4,4'-Dimorpholinodiphenylmethyl perchlorate (0.07 g; 26 %) replacing glacial acetic acid with formic acid as lustrous green crystals for which a satisfactory analysis could not be obtained.

n) 4,4'-Dipyrrolidinodiphenylmethyl perchlorate

4,4'-Dipyrrolidinodiphenylmethyl perchlorate (0.09 g; 36 %) as lustrous grey crystals (Found: C, 61.4; H, 6.4; N, 6.3. $C_{21}H_{25}O_4N_2Cl$ requires C, 62.3; H, 6.2; N, 6.9 %).

o) 4,4'-Di-*N*-methylpiperazinodiphenylmethyl perchlorate

4,4'-Di-*N*-methylpiperazinodiphenylmethyl perchlorate (0.07 g; 30 %) as a purple powder for which a satisfactory analysis could not be obtained.

p) 4'-*N*-Methylpiperazino-4''-diethylaminotriphenylmethyl perchlorate

4'-*N*-Methylpiperazino-4''-diethylaminotriphenylmethyl perchlorate (0.15 g; 62 %) as lustrous purple crystals for which a satisfactory analysis could not be obtained. ^1H nmr δ 1.55 (6H, t, 6.7 Hz, $\text{N}(\text{CH}_2\text{CH}_3)_2$), 3.40 (3H, s, NCH_3), 3.92 (4H, m, $\text{N-4}(\text{CH}_2)_2$), 4.09 (4H, q, 6.7 Hz, $\text{N}(\text{CH}_2\text{CH}_3)_2$), 4.29 (4H, m, $\text{N-1}(\text{CH}_2)_2$), 7.19 (2H, d, 9.4 Hz, 3''-H, 5''-H), 7.31 (2H, d, 9.4 Hz, 3'-H, 5'-H), 7.46 - 7.61 (6H, m, 2'-H, 6'-H, 2''-H, 6''-H, 3-H, 5-H), 7.89 (2H, t, 7.2 Hz, 2-H, 6-H), 7.94 (1H, t, 7.2 Hz, 4-H). ^{13}C nmr δ 12.9, 43.8, 44.7, 47.2, 54.0, 115.0, 116.2, 128.7, 128.9, 129.7, 133.7, 135.1, 139.6, 140.1, 143.2, 155.2, 158.1, 177.4.

q) 4'-*N*-Methylpiperazino-4''-dimethylaminotriphenylmethyl perchlorate

4'-*N*-Methylpiperazino-4''-dimethylaminotriphenylmethyl perchlorate (0.11 g; 46 %) as lustrous purple crystals for which a satisfactory analysis could not be obtained. ^1H nmr δ 3.40 (3H, s, NCH_3), 3.72 (6H, s, $\text{N}(\text{CH}_3)_2$), 3.90 (4H, m, $\text{N-4}(\text{CH}_2)_2$), 4.30 (4H, m, $\text{N-1}(\text{CH}_2)_2$), 7.18 (2H, d, 9.4 Hz, 3''-H, 5''-H), 7.30 (2H, d, 9.4 Hz, 3'-H, 5'-H), 7.41 - 7.60 (6H, m, 2'-H, 6'-H, 2''-H, 6''-H, 3-H, 5-H), 7.79 (2H, t, 7.2 Hz, 2-H, 6-H), 7.94 (1H, t, 7.2 Hz, 4-H). ^{13}C nmr δ 41.5, 43.9, 44.8, 54.0, 115.0, 116.3, 128.5, 128.6, 129.3, 133.8, 135.2, 139.8, 140.1, 142.7, 155.4, 159.5, 177.7.

r) 4'-*N*-Methylpiperazino-4''-pyrrolidinotriphenylmethyl perchlorate

4'-*N*-Methylpiperazino-4''-pyrrolidinotriphenylmethyl perchlorate (0.12g; 51%) as lustrous purple crystals for which a satisfactory analysis could not be obtained. ^1H nmr δ 2.36 (4H, m, $(\text{CH}_2)_2$), 3.51 (3H, s, NCH_3), 3.78 (4H, m, $\text{N-4}(\text{CH}_2)_2$), 3.87 (4H, m,

$N(CH_2)_2$), 4.08 (4H, m, $N-1(CH_2)_2$), 7.20 (2H, d, 9.0 Hz, 3''-H, 5''-H), 7.31 (2H, d, 9.0 Hz, 3'-H, 5'-H), 7.38 - 7.58 (6H, m, 2'-H, 6'-H, 2''-H, 6''-H, 3-H, 5-H), 7.79 (2H, t, 7.2 Hz, 2-H, 6-H), 7.93 (1H, t, 7.2 Hz, 4-H). ^{13}C nmr δ 25.3, 43.9, 44.7, 50.7, 54.0, 115.0, 117.5, 128.9, 129.1, 129.8, 133.6, 135.0, 139.3, 140.2, 142.8, 155.0, 156.9, 177.0.

s) 4'-N-Methylpiperazino-4''-piperidinotriphenylmethyl perchlorate

4'-N-Methylpiperazino-4''-piperidinotriphenylmethyl perchlorate (0.12 g; 51 %) as lustrous purple crystals for which a satisfactory analysis could not be obtained. 1H nmr δ 2.01 (6H, m, CH_2 , $(CH_2)_2$), 3.40 (3H, s, NCH_3), 3.92 (6H, m, $N(CH_2)_2$, $N-4(CH_2)_2$), 4.20 (4H, m, $N-1(CH_2)_2$), 7.46 - 7.61 (10H, m, 2'-H, 3'-H, 5'-H, 6'-H, 2''-H, 3''-H, 5''-H, 6''-H, 3-H, 5-H), 7.80 (2H, t, 7.7 Hz, 2-H, 6-H), 7.92 (1H, t, 7.7 Hz, 4-H). ^{13}C nmr δ 24.3, 27.2, 43.9, 44.7, 50.4, 54.0, 115.0, 116.5, 128.4, 128.9, 129.3, 133.7, 135.0, 139.3, 140.1, 143.2, 155.1, 158.2, 176.3.

t) 4'-N-Methylpiperazino-4''-morpholinotriphenylmethyl perchlorate

4'-N-Methylpiperazino-4''-morpholinotriphenylmethyl perchlorate (0.11 g; 47 %) as lustrous purple crystals for which a satisfactory analysis could not be obtained. 1H nmr δ 3.41 (3H, s, NCH_3), 3.92 (4H, m, $O(CH_2)_2$), 4.04 (8H, m, $N(CH_2)_2$, $N-4(CH_2)_2$), 4.17 (4H, m, $N-1(CH_2)_2$), 7.51 - 7.75 (10H, m, 2'-H, 3'-H, 5'-H, 6'-H, 2''-H, 3''-H, 5''-H, 6''-H, 3-H, 5-H), 7.82 (2H, t, 7.7 Hz, 2-H, 6-H), 7.97 (1H, t, 7.7 Hz, 4-H). ^{13}C nmr δ 43.9, 44.7, 48.7, 54.0, 66.9, 115.1, 116.0, 129.3, 129.5, 129.6, 134.1, 135.4, 140.1, 140.4, 143.0, 155.9, 158.5, 178.5.

u) 4'-Thiomorpholino-4''-dimethylaminotriphenylmethyl perchlorate

4'-Thiomorpholino-4''-dimethylaminotriphenylmethyl perchlorate (0.15 g; 62 %) as lustrous purple crystals (Found: C,60.3; H,5.9 $C_{25}H_{27}O_4N_2S$ Cl requires C, 61.7; H, 5.5; N, 5.8 %). 1H nmr δ 2.98 (4H, m, $S(CH_2)_2$), 3.61 (6H, s, $N(CH_3)_2$), 4.32 (4H, m, $N(CH_2)_2$), 7.33 (2H, d, 9.4 Hz, 3''-H, 5''-H), 7.43 (2H, d, 9.4 Hz, 3'-H, 5'-H), 7.54 - 7.66 (6H, m, 2'-H, 6'-H, 2''-H, 6''-H, 3-H, 5-H), 7.80 (2H, t, 8.0 Hz, 2-H, 6-H), 7.94 (1H, t,

8.0 Hz, 4-H). ^{13}C nmr δ 27.2, 41.1, 51.1, 114.9, 115.1, 128.0, 128.1, 129.2, 133.7, 135.1, 140.2, 141.1, 141.8, 156.0, 158.4, 177.4.

3.2 Kinetic Studies

3.2.1 Chemicals

All the chemicals employed for the kinetic studies were obtained from commercial sources as AnalaR grades or equivalent. The 0.1M sodium hydroxide used was purchased from Fisher Chemicals as Soltrate grade carbonate free volumetric solution. Potassium nitrate (B.D.H. AnalaR grade) was used as purchased. Potassium hydrogen phthalate (B.D.H. AnalaR grade) was dried overnight at 105 - 110 °C and cooled in a vacuum dessicator prior to use. Acetone (B.D.H. AnalaR grade) was dried over 3Å molecular sieve. Nitric acid (B.D.H. AnalaR grade) was diluted as required. Decon 90[®] was used as the cleaning solution and was diluted as required. Pure water (\cong 18 M Ω) was obtained from a Barnstead E-pure deioniser unit fitted with a filter to remove organic impurities.

The sodium hydroxide solutions used throughout this study were freshly prepared and were standardised against potassium hydrogen phthalate which had been dissolved in freshly boiled and cooled deionised water as described in the literature (89MI2).

All materials and volumetric solutions were carbonate free and were stored under a nitrogen atmosphere.

3.2.2 Apparatus

Previous studies involving triphenylmethane dyes have been troubled with dye adsorption upon glassware and plastic components (70JPC1382, 70JCS(B)205, 80JCTB317) and great care has been exercised to prevent dye adsorption. Meticulous care was taken to ensure all apparatus was free from adsorbed dye before any investigation began. All glassware and plastic tubing that were in contact with dye solution were thoroughly cleaned after each kinetic study. The cleaning procedure involved soaking in 2M nitric acid for 12 hours, a thorough rinse with pure water, a further soak in a 5% Decon 90[®] solution for 48 hours before a final thorough rinse with pure water followed by acetone and finally pure water again. The stopped-flow kinetics apparatus was similarly treated.

Volumetric flasks, pipettes and burettes were of grade A quality.

3.2.3 Instrumentation

Hewlett-Packard HP8452A Diode-array UV/Visible spectrophotometer.

Hewlett-Packard Chemstation with HP89531A kinetic software.

Hewlett-Packard HP89090A Peltier Cell Temperature Control Accessory.

Hi-Tech Scientific SFA-11 Rapid Kinetics Accessory.

Pye-Unicam SP6-350 visible spectrophotometer with thermostatted cell block.

Techne[®] Tempette TE-8A thermostatted water bath.

Townson and Mercer Series III thermostatted water bath.

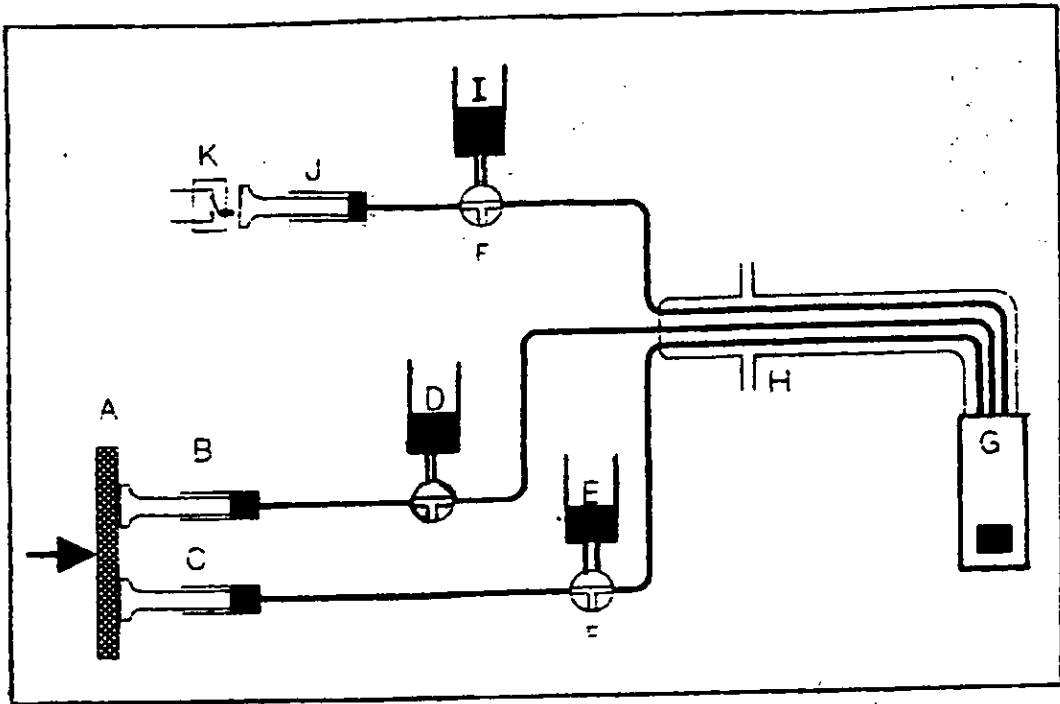
Barnstead E pure deioniser unit.

A schematic diagram of the Hi-Tech Scientific SFA-11 Rapid Kinetics Accessory is given in Figure 3A.

Figure 3A

Schematic diagram of the Hi-Tech Scientific SFA-11 Rapid Kinetics

Accessory



- A Drive bar
- B Reagent 1 syringe
- C Reagent 2 syringe
- D Reagent 1 reservoir
- E Reagent 2 reservoir
- F 3-way port valve
- G Flow cell
- H Jacketed umbilical
- I Waste reservoir
- J Waste syringe
- K Microswitch

3.2.4 Experimental Methods

Prior to each kinetic study, the applicability of the Beer-Lambert Law to the dye under investigation was established. The procedure used takes into account any reaction between cationic dye and water molecules. A dye solution of known concentration was prepared by dissolution of the salt in acetone and quantitative dilution with pure water up to the required volume. The absorbance (A) of this solution was then monitored with time. Extrapolation of the plot of \ln absorbance against time produced a value for the absorbance at zero time (A_0). This procedure was then repeated for several initial concentrations of dye cation. A plot of A_0 against initial concentration produced a linear relationship indicating the applicability of the Beer-Lambert Law at dye concentrations of $5.0 \mu\text{mol dm}^{-3}$ or less. This was in agreement with the findings of other workers (70BCJ601, 70JPC1382, 73JA2293, 80JCTB317, 82JCS(P2)987, 85JCS(P2)107). All the dyes studied in this investigation were found to obey the Beer-Lambert Law at the concentrations used in the kinetic experiments.

For this study, two methods were used in the kinetic investigation of the dyes. The first method has been widely used by other workers in related investigations (81Th1, 82Th1, 83Th1, 83Th2, 89Th1, 91Th1). The second method has had only a limited use by previous workers (91Th1).

(a) Method 1

In this method, a dye stock solution ($2.5 \times 10^{-5} \text{ mol dm}^{-3}$) was prepared by dissolution of a known mass of dye salt in acetone (20 cm^3) and quantitative dilution to 1000 cm^3 with pure water. Also prepared were stock solutions of potassium nitrate (0.1 mol dm^{-3} , added to maintain ionic strength of reaction mixture) and sodium hydroxide ($0.025 \text{ mol dm}^{-3}$). Reaction solutions were then prepared by mixing dye stock solution, potassium nitrate solution and pure water in clean, dry stoppered conical flasks such that on addition of the sodium hydroxide solution a reaction solution of constant ionic strength (0.01 mol dm^{-3}) was produced. The conical flasks were then filled with nitrogen, stoppered and temperature equilibrated for thirty minutes in a water bath. After factorisation against potassium hydrogen phthalate using the standard method (89MI2),

the sodium hydroxide solution was similarly temperature equilibrated. After temperature equilibration, at zero time, the required aliquot of sodium hydroxide was added to the dye reaction solution. The solution was quickly but thoroughly mixed and a 4 cm³ cuvette filled with the solution and placed in the SP6-350 spectrophotometer. The cell holder of the spectrophotometer was temperature controlled using the Townson and Mercer Series III thermostatted water bath. The absorbance of the solution was then measured against time at the wavelength of maximum absorbance for each dye studied. In the reaction solution, the initial dye concentration was *ca.* 5 μmol dm⁻³ and the initial sodium hydroxide concentration ranged from 0.2 - 1.0 mmol dm⁻³. The acetone concentration in the reaction solution was 0.4%. This was shown to have a negligible effect upon the rates of hydrolysis which is in agreement with the findings of other workers (80JCTB317, 83Th1).

The dependence of rate of reaction on hydroxide ion concentration was then studied over several temperatures.

(b) Method 2

In this method, a dye stock solution (*ca.* 0.3 mmol dm⁻³) was prepared by dissolution of a known mass of dye salt in acetone (5 cm³) and quantitative dilution to 50 cm³ with pure water or acetone. The reservoir syringe connected to the 100 μL drive syringe was filled with this solution. Also prepared were stock solutions of potassium nitrate (0.1 mol dm⁻³) and sodium hydroxide (0.1 mol dm⁻³). The sodium hydroxide solution was factorised against potassium hydrogen phthalate using the standard method (89MI2). All stock solutions were stored under nitrogen. From these stock solutions, reaction solutions containing varying concentrations of sodium hydroxide and potassium nitrate were then prepared such that the ionic strength of the reaction mixture was 0.01 mol dm⁻³. The reservoir syringe connected to the 2.5 cm³ drive syringe was filled with this solution. Both drive syringes were then filled; care being taken to ensure no air bubbles were trapped. The solutions were then temperature equilibrated by circulating thermostatted water from a Techne[®] Tempette TE-8A thermostatted water bath through the insulated umbilical of the SFA-11 rapid kinetics apparatus. A port on the SFA-11 kit allowed the temperature of the water to be recorded. The reaction cell attached to the end of the umbilical was seated in the Hewlett-Packard HP89090A Peltier Cell

Temperature Control Accessory. After temperature equilibration, the drive bar was manually depressed which presented fresh reactants into the thermostatted cell. The cell was filled until the stopping syringe made contact with the microswitch fitted to the SFA-11 apparatus. This action automatically triggered the data acquisition using the HP Chemstation of the HP8452A spectrophotometer. The mixing ratio of the two reactants was 1:25, dye solution: aqueous solution. The sodium hydroxide concentration in the reaction solution for the kinetic work involving the unsymmetrical MGs was 2 - 10 mmol dm⁻³ and for the kinetic work involving the diphenylmethane dyes 0.2 - 1.0 mmol dm⁻³. For some of the very unstable dyes, preparation of the dye stock solution in only acetone resulted in an acetone concentration in the reaction solutions of 4%, which was again shown to have no significant effect upon the rate of reaction.

The rate of reaction was followed by measuring the absorbance of the reaction solution at the wavelength of maximum absorbance for each particular dye studied. The data was collected using an integration time of 0.1s and a cycle time of 0.1s. The rate constant for each reaction was calculated using the HP89512A kinetics software using data collected over 75% of the reaction. The kinetic data for each reaction were saved.

For each sodium hydroxide concentration studied, several test runs were conducted in order to optimise the data collection and to condition the system. Once conditioned, six analyses were then carried out from which the average rate constant and error were determined using a standard statistical treatment.

4.

CONCLUSIONS

4.1 Fifteen previously unknown unsymmetrical Malachite Green type dye bases have been prepared. The method of synthesis was reaction of the mono-substituted benzophenone with the appropriately substituted aryllithium compound. The dye cation of each carbinol was generated and collected as the perchlorate salt.

4.2 Six symmetrical analogues of Michler's Hydrol Blue dye base have been prepared. The method of preparation was reduction of the appropriate di-substituted benzophenone. The dye cation of some of the hydrols was generated and collected as the perchlorate salt.

4.3 The rate equation

$$\text{Rate} = -d[\text{Dye}^+]/dt = k_1[\text{Dye}^+][\text{H}_2\text{O}] + k_2[\text{Dye}^+][\text{OH}^-]$$

is proposed for the hydrolysis of all the symmetrical MHB analogues and unsymmetrical MG type dyes studied kinetically in this work.

4.4 Isokinetic relationships have been established for the unsymmetrical MG type dyes by investigating i) the rate of reaction at two temperatures, ii) the temperature dependence of the reaction constant and iii) a statistical treatment of the Arrhenius relationship. The results indicate that the hydrolysis of the dyes containing dimethylamino, diethylamino, pyrrolidino and piperidino is under enthalpy control and the hydrolysis of the dyes containing morpholino and *N*-methylpiperazino is under entropy control. The establishment of isokinetic relationships provides evidence for the constancy of reaction mechanism throughout each reaction series.

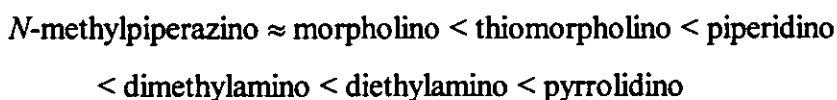
4.5 From the isokinetic relationship studies it was concluded that the 4'-dimethylamino-4"-morpholinotriphenylmethyl cation may react by a different mechanism from other members of the dye series. An alternative mechanism has been discussed but not proven.

4.6 An isokinetic relationship has been established for the hydrolysis reaction of the symmetrical MHB analogues. The hydrolysis for this series has been shown to be under entropy control.

4.7 Of the various methods used to determine β which have been investigated, no single one can be concluded to be the definitive method. Rather it is more accurate to determine whether a relationship exists and the confidence intervals.

4.8 The rates of hydrolysis of some unsymmetrical MG type dyes are linearly related to the σ_p^+ constants. The magnitude of the reaction constant, ρ , for the dye series indicates that the reaction is relatively insensitive to substituent effects. The positive nature of the reaction constant indicates that the reaction rate is increased by electron withdrawing substituents and decreased by electron donating substituents.

4.9 The kinetic investigation has enabled interpolated values of σ_p^+ for the dialkylamino and heterocyclic amines studied in this work to be determined. The electron donor ability of the substituents increases in the order



4.10 The enhanced reactivity of the Michler's Hydrol Blue analogues compared to the equivalent parent Green dyes is attributed to the absence of the third phenyl ring which effectively removes any steric hindrance to the approach of a nucleophile. In addition, there is less resonance stabilisation of the positive charge.

4.11 The stopped flow method developed in this study can be used to accurately determine rate constants for hydrolysis reactions with half-life times ranging from 1s to greater than 60s. The increased acetone concentration of 4.0% in the reaction mixture does not interfere with the hydrolysis reaction studied.

4.12 The instability of the *N*-methylpiperazino and morpholino analogues of Michler's Hydrol Blue was so great that their rate of hydrolysis could not be recorded using the stopped-flow equipment available.

4.13 λ_{\max} for the *N*-methylpiperazino derivative of Michler's Hydrol Blue displays a hypsochromic shift relative to the other members of the series. There is also a drastic reduction in ϵ_{\max} . Both of these observations can be attributed to the reduced ability of the *N*-methylpiperazino group to stabilise the dye by electron donation.

4.14 The relative influence of the six-membered heterocycles on $\lambda_{\max}(x)$ of the unsymmetrical Malachite Green type dyes is affected by the electronegativity of the γ -atom.

4.15 Hypsochromic shifts and reduced intensity of the $\lambda_{\max}(x)$ absorption bands were generally observed for the unsymmetrical Malachite Green type dyes containing the *N*-methylpiperazino group when compared to other related dyes. This is consistent with the *N*-methylpiperazino moiety displaying a marked inability to stabilise the system by conjugation.

4.16 In a solvent of increasing acidity, the unsymmetrical Malachite Green type dyes containing *N*-methylpiperazino display enhanced deviation from electronic/structural symmetry. This behaviour is consistent with the *N*-methylpiperazino moiety being more susceptible to protonation at the methyl-nitrogen atom of the six-membered heterocycle.

4.17 A linear relationship exists between $\epsilon_{\max}(x)$ and the deviation of $\lambda_{\max}AB$ from the arithmetic mean of $\lambda_{\max}AA$ and $\lambda_{\max}BB$ for the unsymmetrical Malachite Green type dyes studied. This is consistent with similarities in the terminal amino groups enabling effective conjugation throughout the dye.

4.18 The ^{13}C and 1H nmr spectra of the carbinols have been measured. The ^{13}C and 1H chemical shifts of the ring position adjacent to the carbon atom bearing the amino group have been used to deduce a relative order of electron donating ability amongst the amino moieties. The order determined from the nmr investigation has similarities to the

orders derived from both the UV-visible absorption and the kinetic investigations but discrepancies also exist. Each method is sound in principle but as a consequence of the assumptions made in each method and their inherent nature it is not possible to draw a definitive conclusion as to the absolute electron donor ability of each amino moiety studied.

4.19 The ^{13}C and ^1H nmr spectra of the dye cations have also been obtained. From the ^{13}C chemical shift of the central sp^2 hybridised carbon atom, the extent of electron shielding at this position is relatively insensitive to the nature of the terminal amino group present.

4.20 The ^1H chemical shifts of the ring positions *ortho* to the amino group in the dye cations are linearly related to the σ_p^+ constants. This is consistent with, to at least a first approximation, a relationship between the chemical shift of the *ortho* aromatic protons and their π -electron density within this class of compounds.

REFERENCES

- 1868BER106 C.Graebe and C.Liebermann, Chem.Ber., 1868, 1, 106.
- 1876BER522 O.N.Witt, Chem.Ber., 1876, 9, 522.
- 1888PCS27 H.E.Armstrong, Proc.Chem.Soc., 1888, 27.
- 27JCS2174 E.H.Rodd and F.W.Linch, J.Chem.Soc., 1927, 2174.
- 30JA804 L.C.Craig and R.M.Hixon, J.Amer.Chem.Soc., 1930, 52, 804.
- 31JCS118 B.Gokhle and F.A.Mason, J.Chem.Soc., 1931, 118.
- 32CR229 G.Scratchard, Chem.Rev., 1932, 10, 229.
- 37PRS138 B.Beilenson, N.I.Fisher and F.M.Hamer, Proc.Roy.Soc., 1937, A163, 138.
- 39CR273 G.N.Lewis and M.Calvin, Chem.Rev., 1939, 25, 273.
- 41JA545 W.Langham, R.Q.Brewster and H.Gilman, J.Amer.Chem.Soc., 1941, 63, 545.
- 41JA3214 L.G.S.Brooker and R.H.Sprague, J.Amer.Chem.Soc., 1941, 63, 3214.
- 42JA199 L.G.S.Brooker, G.H.Keyes and W.W.Williams, J.Amer.Chem.Soc., 1942, 64, 199.
- 42JA1774 G.N.Lewis, T.T.Magel and D.Lipkin, J.Amer.Chem.Soc., 1942, 64, 1774.
- 43JA479 R.A.Henry and W.M.Dehn, J.Amer.Chem.Soc., 1943, 65, 479.
- 45JA1869 L.G.S.Brooker and R.H.Sprague, J.Amer.Chem.Soc., 1945, 67, 1869.
- 45JA1875 L.G.S.Brooker, A.L.Sklar, H.W.J.Cressman, G.H.Keyes, L.A.Smith, R.H.Sprague, E.Van Lare, G.Van Zandt, F.L.White and W.W.Williams, J.Amer.Chem.Soc., 1945, 67, 1875.
- 45JA1889 L.G.S.Brooker, R.H.Sprague and H.W.J.Cressman, J.Amer.Chem.Soc., 1945, 67, 1889.
- 49JA122 S.W.Chaikin and W.G.Brown, J.Amer.Chem.Soc., 1949, 71, 122.
- 49JCS1724 R.J.Goldacre and J.N.Philips, J.Chem.Soc., 1949, 1724.
- 49MI1 H.E.Fiertz-David and L.Bangley, 'Fundamental Processes of Dye Chemistry', Wiley-Interscience, 1949.
- 50JCP265 H.C.Longuet-Higgins, J.Chem.Phys., 1950, 18, 265.
- 50JCP275 H.C.Longuet-Higgins, J.Chem.Phys., 1950, 18, 275.

- 50JCP283 H.C.Longuet-Higgins, J.Chem.Phys., 1950, **18**, 283.
- 50JCS2329 M.J.S.Dewar, J.Chem.Soc., 1950, 2329.
- 50MI1 K.J.Laidler, 'Chemical Kinetics', McGraw-Hill, 1950.
- 51CR1043 C.Dufraisse, J.Lefranc and P.Barbieri, Compt.Rend., 1951, **232**, 1043.
- 51CR1977 C.Dufraisse, J.Lefranc and P.Barbieri, Compt.Rend., 1951, **232**, 1977.
- 51JA212 H.C.Brown, R.S.Fletcher and R.B.Johannesen, J.Am.Chem.Soc., 1951, **73**, 212.
- 51MI1 R.G.Jones and H.Gilman, 'Organic Reactions', Vol. VI, R.Adams Ed., J.Wiley & Sons, 1951.
- 51OKN166 Yu.K.Yur'ev, I.S.Korsakova and A.V.Arbatskii, Izv.Akad.Nauk.SSSR, Otd.Khim.Nauk., 1951, 166.
- 52JA3341 M.J.S.Dewar, J.Am.Chem.Soc., 1952, **74**, 3341.
- 52JA3345 M.J.S.Dewar, J.Am.Chem.Soc., 1952, **74**, 3345.
- 52JA3350 M.J.S.Dewar, J.Am.Chem.Soc., 1952, **74**, 3350.
- 52JA3353 M.J.S.Dewar, J.Am.Chem.Soc., 1952, **74**, 3353.
- 52JA3357 M.J.S.Dewar, J.Am.Chem.Soc., 1952, **74**, 3357.
- 52JA5988 J.C.Turgeon and V.K. la Mer, J.Am.Chem.Soc., 1952, **74**, 5988.
- 53JPC466 R.Pariser and R.G.Parr, J.Phys.Chem., 1953, **21**, 466.
- 53MI1 I.Heilbron and H.M.Bunbury, 'Dictionary of Organic Compounds', Eyre and Spottiswoode, 1953, **4**, p.430.
- 53JCS(TFS)1375 J.A.Pople, J.Chem.Soc., Trans.Far. Soc., 1953, **49**, 1375.
- 54JA467 H.C.Brown, J.H.Brewster and H.Shechter, J.Am.Chem.Soc., 1954, **76**, 467.
- 54JA6293 C.W.Looney and W.T.Simpson, J.Am.Chem.Soc., 1954, **76**, 6293.
- 54JOC155 N.C.Deno, J.Jaruzeski and A.Schrieschein, J.Org.Chem., 1954, **19**, 155.
- 55AC75 E.Cremer, Adv.Catalysis, 1955, **7**, 75.
- 56JCS451 G.Baddeley, J.Chadwick and H.T.Taylor, J.Chem.Soc., 1956, 451.
- 56MI1 R.W.Taft, 'Steric Effects in Organic Chemistry', Wiley, 1956.
- 57JCS674 D.W.A.Sharp and Sheppard, J.Chem.Soc., 1957, 674.
- 58JA2436 R.W.Taft and I.C.Lewis, J.Am.Chem.Soc., 1958, **80**, 2436.

- 58JA4979 H.C.Brown and Y.Okamoto, J.Am.Chem.Soc., 1958, **80**, 4979.
- 58JCS2720 D.A.Blackadder and C.Hinshelwood, J.Chem.Soc., 1958, 2720.
- 58JCS2728 D.A.Blackadder and C.Hinshelwood, J.Chem.Soc., 1958, 2728.
- 58JCS3002 M.Aroney and R.J.W. le Fèvre, J.Chem.Soc., 1958, 3002.
- 58MI1 G.W.Gray, 'Steric Effects in Conjugated Systems', Butterworths Scientific Publ., 1958.
- 58MI2 W.Klyne and P.B.D. de la Mare, Prog. in Stereochem., 1958, **2**, 129.
- 59JA5343 R.W.Taft and I.C.Lewis, J.Am.Chem.Soc., 1959, **81**, 5343.
- 59JCP650 D.L.Hildenbrand, G.C.Sinke, R.A.McDonald, W.R.Kramer and D.R.Stull, J.Chem.Phys., 1959, **31**, 650.
- 59JCP655 J.C.Evans and J.C.Wahr, J.Chem.Phys., 1959, **31**, 655.
- 59JCS3957 C.C.Barker, M.H.Bride and A.Stamp, J.Chem.Soc., 1959, 3957.
- 59RTC815 H.van Bekkum, P.E.Verkaide and B.M.Wepster, Rec.Trav.Chim., 1959, **78**, 815.
- 60JA1442 H.J.Dauben, L.R.Honnen and K.M.Harmon, J.Am.Chem.Soc., 1960, **82**, 1442.
- 60JCS3790 C.C.Barker, G.Hallas and A.Stamp, J.Chem.Soc., 1960, 3790.
- 60JCS3812 S.S.Malhatra and M.C.Whiting, J.Chem.Soc., 1960, 3812.
- 61JA3819 R.C.Petersen, J.H.Markgraf and S.D.Ross, J.Am.Chem.Soc., 1961, **83**, 3819.
- 61JCP731 H.Spiesecke and W.G.Schneider, J.Chem.Phys., 1961, **35**, 731.
- 61JCS1285 C.C.Barker, M.H.Bride, G.Hallas and A.Stamp, J.Chem.Soc., 1961, 1285.
- 61JCS1529 C.C.Barker and G.Hallas, J.Chem.Soc., 1961, 1529.
- 61JCS861 N.A.Ramaiah and S.S.Katiyar, J.Ind.Chem.Soc., 1961, **38**, 861.
- 61PRFR14 A.H.Gomes de Mesquita, Pet.Res.Fund.Rep., 1961, **6**, 14.
- 62ACS2251 R.Cigén and G.Bengtsson, Acta.Chem.Scand., 1962, **16**, 2251.
- 62JA734 A.T.Bottini and C.P.Nash, J.Am.Chem.Soc., 1962, **84**, 734.
- 62JA2349 C.D.Ritchie, W.F.Sager and E.S.Lewis, J.Am.Chem.Soc., 1962, **84**, 2349.
- 62JPC2179 R.Hoffman and W.N.Lipscomb, J.Phys.Chem., 1962, **36**, 2179.
- 62JPC2872 R.Hoffman and W.N.Lipscomb, J.Phys.Chem., 1962, **36**, 2872.

- 62JPC3489 R.Hoffman and W.N.Lipscomb, J.Phys.Chem., 1962, **36**, 3489.
- 63ACS2083 R.Cigén and C.G.Ekström, Acta.Chem.Scand., 1963, **17**, 2083.
- 63CJC2339 W.F.Reynolds and T.Schaefer, Can.J.Chem., 1963, **41**, 2339.
- 63JA3940 A.Zweig, J.E.Lehnsen, J.E.Lancaster and M.T.Neglia,
J.Am.Chem.Soc., 1963, **85**, 3940.
- 63JCP1415 P.C.Lauterbur, J.Chem.Phys., 1963, **38**, 1415.
- 63JCP1432 P.C.Lauterbur, J.Chem.Phys., 1963, **38**, 1432.
- 63JCS2655 C.Aaron and C.C.Barker, J.Chem.Soc., 1963, 2655.
- 63JCS(TFS)2058 D.Margerison and J.P.Newport, J.Chem.Soc., Trans.Far.Soc., 1963,
59, 2058.
- 63JGCU153 N.G.Belotserkovskaya and O.F.Ginzburg, J.Gen.Chem.USSR,
1963, **33**, 153.
- 63JPC1397 R.Hoffman, J.Phys.Chem., 1963, **39**, 1939.
- 64ACS157 R.Cigén and C.G.Ekström, Acta.Chem.Scand., 1964, **18**, 157.
- 64ACS447 G.Bengtsson, Acta.Chem.Scand., 1964, **18**, 447.
- 64CCCC1094 O.Exner, Coll.Czech.Chem.Comm., 1964, **29**, 1094.
- 64JA4130 A.Zweig, J.E.Lancaster, M.T.Neglia and W.H.Jura,
J.Am.Chem.Soc., 1964, **86**, 4130.
- 64JCP2796 T.K.Wu and B.P.Dailey, J.Chem.Phys., 1964, **41**, 2796.
- 64JOC3133 R.C.Petersen, J.Org.Chem., 1964, **29**, 3133.
- 64JPC832 C.P.Nash and G.E.Maciel, J.Phys.Chem., 1964, **68**, 832.
- 64TL3345 N.L.Allinger, J.G.D.Carpenter and F.M.Karkowski, Tetrahedron
Lett., 1964, **45**, 3345.
- 65AC437 A.H.Gomes de Mesquita, C.H.MacGilliarvy and K.Eriks, Acta
Crystallogr., 1965, **18**, 437.
- 65JA1232 N.L.Allinger, J.G.D.Carpenter and F.M.Karkowski, J.Amer. Chem.
Soc., 1965, **87**, 1232.
- 65JCS(TFS)1800 R.B.McKay and P.J.Hillson, J.Chem.Soc., Trans. Faraday Soc.,
1965, **61**, 1800.
- 65RSOS46 G.S.Idlis and O.F.Ginsburg, Reakts.Sposobnost.Org.Soedin., 1965,
2,46.
- 66ACS444 C.G.Ekström, Acta.Chem.Scand., 1966, **20**, 444.

- 66BCJ2274 Y.Yukawa, Y.Tsuno and M.Sawada, Bull.Chem.Soc.Japan, 1966, 39, 2274.
- 66JCP3289 J.A.Pople and G.A.Segal, J.Chem.Phys., 1966, 44, 3289.
- 66MI1 A.G.Sykes, 'Kinetics of Inorganic Reactions', Pergamon Press Ltd., 1966.
- 66RSOS162 G.S.Idlis and O.F.Ginsburg, Reakts.Sposobnost.Org.Soedin., 1966, 3, 162.
- 67JA2970 D.G.Farnum, J.Amer.Chem.Soc., 1967, 89, 2970.
- 67JA3089 M.J.S.Dewar and G.Klopman, J.Amer.Chem.Soc., 1967, 89, 3089.
- 67JSDC368. G.Hallas, J.Soc.Dyers and Colourists, 1967, 83, 368.
- 67MP83 R.N.Dixon, Mol.Phys., 1967, 12, 83.
- 68CJC2754 J.M.Lalancette, A.Frêche and R.Montoux, Can.J.Chem., 1968, 46, 2754.
- 68JA1757 R.T.C.Brownlee, R.E.J.Hutchinson, A.R.Katritzky, T.T.Tidwell and R.D.Topsom, J.Amer.Chem.Soc., 1968, 90, 1757.
- 68RTC1372 W.D.Weringa and M.J.Janssen, Rec.Trav.Chim.Pays-Bas., 1968, 87, 1372.
- 69CI620 G.Hallas and D.R.Waring, Chem. and Industry, 1969, 620.
- 69JCS(B)1068 C.C.Barker and G.Hallas, J.Chem.Soc.(B), 1969, 1068.
- 69JCS(B)1138 A.A.Humffray and J.J.Ryan, J.Chem.Soc.(B), 1969, 1138.
- 69JCP1262 N.C.Baird and M.J.S.Dewar, J.Chem.Phys., 1969, 50, 1262.
- 69MI1 M.J.S.Dewar, 'The Molecular Orbital Theory of Organic Chemistry', McGraw-Hill, 1969.
- 69MI2 D.Margerison, 'The Practice of Kinetics', Chpt.5, Eds. C.H.Bamford and C.F.H.Tipper, Elsevier, 1969.
- 70BCJ601 S.S.Katiyar, Bull.Chem.Soc.Japan, 1970, 43, 601.
- 70CJC2366 J.M.Lalancette and A.Frêche, Can.J.Chem., 1970, 48, 2366.
- 70JA590 M.J.S.Dewar and E.Haselbach, J.Amer.Chem.Soc., 1970, 92, 590.
- 70JA4664 H.L.Lewis and T.L.Brown, J.Amer.Chem.Soc., 1970, 92, 4664.
- 70JCS(B)205 P.Bruck, A.Ledwith and A.C.White, J.Chem.Soc.(B), 1970, 205.
- 70JCS(B)530 A.C.Hopkinson and P.A.H.Wyatt, J.Chem.Soc.(B), 1970, 530.
- 70JCS(B)975 G.Hallas, J.D.Hepworth and D.R.Waring, J.Chem.Soc.(B), 1970, 975.

- 70JCS(B)979 G.Hallas and D.R.Waring, J.Chem.Soc.(B), 1970, 979.
- 70JCS(TFS)2305 S.S.Katiyar, J.Chem.Soc., Trans.Far.Soc., 1970, 66, 2305.
- 70JOC1555 M.E.Kuehne and T.Garbacik, J.Org.Chem., 1970, 35, 1555.
- 70JOC3756 A.G.Giumanini and G.Lercker, J.Org.Chem., 1970, 35, 3756.
- 70JPC1382 S.K.Sinka and S.S.Katiyar, J.Phys.Chem., 1970, 74, 1382.
- 70JSDC200 D.E.Grocock, G.Hallas and J.D.Hepworth, J.Soc.Dyers and Colourists, 1970, 86, 200.
- 70JSDC237 G.Hallas, J.Soc.Dyers and Colourists, 1970, 86, 237.
- 71JCS(B)319 C.Aaron and C.C.Barker, J.Chem.Soc.(B), 1971, 319.
- 71JCS(B)1471 R.W.Castelino and G.Hallas, J.Chem.Soc.(B), 1971, 1471.
- 71JCS(C)2847 G.Hallas, J.Chem.Soc.(C), 1971, 2847.
- 71JOC3847 J.W.Eastes, M.H.Aldridge, R.R.Minesinger and M.J.Kamlet, J.Org.Chem., 1971, 36, 3847.
- 71JOC3852 M.J.Kamlet, R.R.Minesinger, E.G.Kayser, M.H.Aldridge and J.W.Eastes, J.Org.Chem., 1971, 36, 3852.
- 71JSDC187 A.S.Ferguson and G.Hallas, J.Soc.Dyers and Colourists, 1971, 87, 187.
- 71MI1 R.L.M.Allen, 'Colour Chemistry', Nelson, 1971.
- 71MI2 K.Venkateraman, 'The Chemistry of Synthetic Dyes and Pigments', Vol(IV), Chpt.3, Academic Press, 1971.
- 71T735 G.J.Ray, R.J.Kurland and A.K.colter, Tetrahedron, 1971, 27, 735.
- 71Th1 D.R.Waring, PhD., C.N.A.A., Univ. of Leeds, 1971.
- 72CJC526 J.M.Lalancette, A.Freche, J.R.Brindle and M.Laliberte, Can.J.Chem., 1972, 50, 526.
- 72JCS(P2)1792 D.E.Grocock, G.Hallas and J.D.Hepworth, J.Chem.Soc., Perkin Trans 2, 1972, 1792.
- 72JCS(P2)2281 G.Hallas, K.N.Paskins and D.R.Waring, J.Chem.Soc., Perkin Trans 2, 1972, 2281.
- 72JPC1772 W.H.J.Stork, G.J.M.Lippits and M.Mandel, J.Phys.Chem., 1972, 76, 1772.
- 72JSDC25 R.W.Castelino, G.Hallas and D.C.Taylor, J.Soc.Dyers and Colourists, 1972, 88, 25.

- 72MI1 J.Shorter, 'Advances in Linear Free Energy Relationships', Plenum, 1972.
- 73JA2293 T.Okubo and N.Ise, J.Amer.Chem.Soc., 1973, **95**, 2293.
- 73JA5357 A.Hoefnagel and B.M.Wepster, J.Amer.Chem.Soc., 1973, **95**, 5357.
- 73JA7530 G.Olah and P.W.Westerman, J.Amer.Chem.Soc., 1973, **95**, 7530.
- 73CCCC781 O.Exner and V.Beránek, Coll.Czech.Chem.Comm., 1973, **38**, 781.
- 73JCS(P2)1792 D.E.Grocock, G.Hallas and J.D.Hepworth, J.Chem.Soc., Perkin Trans 2, 1973, 1792.
- 73JCS(P2)1887 S.Clementi and P.Linda, J.Chem.Soc., Perkin Trans 2, 1973, 1887.
- 73JCE154 A.S.Kushner and T.Vaccariello, J.Chem.Ed., 1973, **50**, 154.
- 73PPOC411 O.Exner, Prog.Phys.Org.Chem., 1973, **10**, 411.
- 74CCCC842 M.Cerný and J.Málek, Coll.Czech.Chem.Comm., 1974, **39**, 842.
- 74JCS(P2)59 G.Hallas and R.M.Potts, J.Chem.Soc., Perkin Trans 2, 1974, 59.
- 74JCS(P2)1033 B.C.Gilbert, R.O.C.Norman and M.Trenwith, J.Chem.Soc., Perkin Trans 2, 1974, 1033.
- 74MI1 H.E.Avery, 'Basic Reaction Kinetics and Mechanisms', MacMillan, 1974.
- 74MI2 B.J.Wakefield, 'The Chemistry of Organolithium Compounds', Pergamon, 1974.
- 74T2317 T.Pierre and R.Handel, Tetrahedron, 1974, 2317.
- 75ACR300 I.D.Blackburne, A.R.Katritzky and Y.Takeuchi, Acc.Chem.Res., 1975, **8**, 300.
- 75JA1285 R.C.Bingham, M.J.S.Dewar and D.H.Lo, J.Amer.Chem.Soc., 1975, **97**, 1285.
- 75MI1 M.J.Pilling, 'Reaction Kinetics', Clarendon Press, 1975.
- 75ZOK197 G.S.Antonova, S.M.Ramsh and A.I.Ginak, Zh.Org.Khim., 1975, **11**, 1970.
- 75ZOK1991 C.Hansch, Zh.Org.Khim., 1975, **11**, 1991.
- 76AJC2607 D.A.R.Happer, Aust.J.Chem., 1976, **29**, 2607.
- 76JPC2335 R.R.Krug, W.G.Hunter and R.A.Grieger, J.Phys.Chem., 1976, **8**, 2335.

- 76MI1 J.Griffiths, 'Colour and Constitution of Organic Molecules', Academic Press, 1976.
- 76MP1001 H.P.J.M.Dekkers and E.C.Kielman van Luyt, Mol.Phys., 1976, 31, 1001.
- 76OS20 G.J.Fox, G.Hallas, J.D.Hepworth and K.N.Paskins, Org.Synth., 1976, 55, 20.
- 76PPOC1 R.D.Topsom, Prog.Phys.Org.Chem., 1976, 12, 1.
- 77JOC381 A.Cornélis, S.Lambert and P.Laszlo, J.Org.Chem., 1977, 42, 381.
- 77JOC1657 J.A.Turner and W.Herz, J.Org.Chem., 1977, 42, 1657.
- 77JSDC451 S.S.Gandhi, G.Hallas and J.Thomasson, J.Soc.Dyers and Colourists, 1977, 93, 451.
- 77MI1 J.March, 'Advanced Organic Chemistry: Reactions, Mechanisms and Structure', 2nd Ed., McGraw-Hill, 1977.
- 78JOC2923 W.C.Still, M.Khan and A.Mitra, J.Org.Chem., 1978, 43, 2923.
- 78MI1 P.W.Atkins, 'Physical Chemistry', Oxford University Press, 1978.
- 78MI2 O.Exner, 'Correlation Analysis in Organic Chemistry: Recent Advances', Plenum, 1978.
- 78T2409 F.Effenberger, P.Fischer, W.W.Schoeller and W.D.Stohrer, Tetrahedron, 1978, 34, 2409.
- 78TS1 B.Fuchs, Top.Stereochem., 1978, 10, 1.
- 79BCJ2244 Y.Matsuoka and K.Yamaoka, Bull.Chem.Soc.Japan, 1979, 52, 2244.
- 79CJC3041 R.J.Taillefer, S.E.Thomas, Y.Nadeau and H.Beierbeck, Can.J.Chem., 1979, 57, 3041.
- 79JOC1261 J.Bromilow and R.T.C.Brownlee, J.Org.Chem., 1979, 44, 1261.
- 79ML111 Microbios.Lett., 1979, 11, 111.
- 79JRS305 L.Angeloni, G.Smulevich and M.P.Marzocchi, J.Raman Spectroc., 1979, 8, 305.
- 80CJC339 J.H.Robins, G.D.Abrams and J.A.Pincock, Can.J.Chem., 1980, 58, 339.
- 80JCTB317 B.M.Fox, G.Hallas, J.D.Hepworth and D.Mason, J.Chem.Tech.Biotechnol., 1980, 30, 317.

- 80JMS331 L. Angeloni, G. Smulevich and M.P. Marzocchi, J.Mol.Struct., 1980, 61, 331.
- 80JPC1361 Y. Matsuoka, J.Phys.Chem., 1980, 84, 1361.
- 80MI1 H.C. Brown, D.P. Kelly and M. Periasamy, Proc.Natl.Acad.Sci.USA, 1980, 77, 6956.
- 80MI2 F.G. Riddell, 'The Conformational Analysis of Heterocyclic Compounds', Academic Press, 1980.
- 81BCJ1029 T. Satoh, N. Matsuo, M. Nishiki, K. Nanba and S. Suzuki, Bull.Chem.Soc.Japan, 1981, 54, 1029.
- 81CJC191 J. Korppi-Tömmola and R. Yip, Can.J.Chem., 1981, 59, 191.
- 81CL311 S. Akiyama and M. Iyoda, Chem.Lett., 1981, 311.
- 81DP37 J. Griffiths and K.J. Pender, Dyes and Pigments, 1981, 59, 37.
- 81JOC2130 A. Cornélis, S. Lambert, P. Laszlo and P. Schaus, J.Org.Chem., 1981, 46, 2130.
- 81OR308 D.A. Oparin, T. Melentyeva and L.A. Pavlova, Org. React., 1981, 18, 308.
- 81PPOC119 M. Charton, Prog.Phys.Org.Chem., 1981, 13, 119.
- 81Th1 B.M. Fox, PhD., C.N.A.A., Preston Polytechnic, 1981.
- 82JCS(P2)987 B.M. Fox, J.D. Hepworth, D. Mason and G. Hallas, J.Chem.Soc., Perkin Trans 2, 1982, 987.
- 82JCS(P2)991 B.M. Fox, J.D. Hepworth, D. Mason and G. Hallas, J.Chem.Soc., Perkin Trans 2, 1982, 991.
- 82JCS(P2)1037 A.T. Brown and G. Hallas, J.Chem.Soc., Perkin Trans 2, 1982, 1037.
- 82JSDC10 B.M. Fox, J.D. Hepworth, D. Mason, J. Sawyer and G. Hallas, J.Soc.Dyers and Colourists, 1982, 98, 10.
- 82Th1 J. Sawyer, PhD., C.N.A.A., Preston Polytechnic, 1982.
- 83JA6782 Y. Taniguchi and A. Iguchi, J.Amer.Chem.Soc., 1983, 105, 6782.
- 83JCSCC7 K. Takeuchi, T. Kitagawa and K. Okamoto, J.Chem.Soc., Chem.Comm., 1983, 7.
- 83JCS(P2)57 M. Azzaro, J.F. Gal, S. Geribaldi and B. Videau, J.Chem.Soc., Perkin Trans 2, 1983, 57.
- 83JCS(P2)975 S.F. Beach, J.D. Hepworth, D. Mason and G. Hallas, J.Chem.Soc., Perkin Trans 2, 1983, 975.

- 83Th1 S.F.Beach, PhD., C.N.A.A., Preston Polytechnic, 1983.
- 83Th2 D.E.Giles, PhD., C.N.A.A., Preston Polytechnic, 1983.
- 83Th3 P.J.Haslam, PhD., C.N.A.A., Preston Polytechnic, 1983.
- 84CPL373 J.Korppi-Tommola, E.Kolehmainen, E.Salo and R.Yip, Chem.Phys.Lett., 1984, **104**, 373.
- 84JCP1024 F.T.Clark and H.G.Drickamer, J.Chem.Phys., 1984, **81**, 1024.
- 84JCS(P2)149 G.Hallas, R.Marsden, J.D.Hepworth and D.Mason, J.Chem.Soc., Perkin Trans 2, 1984, 149.
- 84JCS(P2)771 M.Azzaro, J.F.Gal and S.Geribaldi, J.Chem.Soc., Perkin Trans 2, 1984, 771.
- 84RPCRT197 R.Raue, Rev.Prog.Col.Relat.Top., 1984, **14**, 197.
- 84Th1 D.J.Lythgoe, PhD., C.N.A.A., Preston Polytechnic, 1984.
- 85JA2305 G.Pfafferott, H.Oberhammer, J.E.Boggs and W.Caminati, J.Amer.Chem.Soc., 1985, **107**, 2305.
- 85JCS(P2)107 S.F.Beach, J.D.Hepworth, D.Mason, G.Halas and B.May, J.Chem.Soc., Perkin Trans 2, 1985, 107.
- 85JPP567 S.Caccia, M.H.Fong, J.Pharm.Pharmacol., 1985, **37**, 567.
- 85PP78 S.Mitra, Polym.Prep., 1985, **26**, 78.
- 86AB242 R.Kraupse and A.Scheer, Anal.Biochem., 1986, **153**, 242.
- 86CIB997 J.Griffiths, Chem. In Brit., 1986, **22**, 997.
- 86CJC2239 C.D.Ritchie, Can.J.Chem., 1986, **64**, 2239.
- 86CL329 S.Nakatsuji and S.Akiyama, Chem.Lett., 1986, 329.
- 86JCS(P2)123 G.Hallas, R.Marsden, J.D.Hepworth and D.Mason, J.Chem.Soc., Perkin Trans 2, 1986, 123.
- 86JIS9 N.Ohta, J.Imaging Sci., 1986, **30**, 9.
- 86JPC589 F.T.Clark and H.G.Drickamer, J.Phys.Chem., 1986, **90**, 589.
- 86JSDC15 G.Hallas and M.Mitchell, J.Soc.Dyers and Colourists, 1986, **102**, 15.
- 86TL5657 B.Abarca, G.Asensio, R.Ballesteros and C.Luna, Tetrahedron Lett., 1986, **27**, 5657.
- 87JCSCC710 S.Akiyama, S.Nakatsuji, K.Nakashima and M.Watanabe, J.Chem.Soc., Chem.Commun., 1987, 710.

- 87JOC1710 A-H.Khuthier, K.Y.Al-Mallah, S.Y.Hanna and N-A.I.Abdulla, J.Org.Chem., 1987, **52**, 1710.
- 87P24756 S.Koike and K.Iwata, Chem.Abs., 1987, **107**, P24756.
- 88CS403 C. de Diego, C.Avendaño and J.Elguero, Chemica.Scripta., 1988, **28**, 403.
- 88JCS(P1)3155 S.Akiyama, S.Nakatsuji, K.Nakashima, M.Watanabe and H.Nakazumi, J.Chem.Soc., Perkin Trans 1, 1988, 3155.
- 89JA3966 R.A.McClelland, V.M.Kanagasabapathy, N.S.Banait and S.Steenken, J.Amer.Chem.Soc., 1989, **111**, 3966.
- 89JCP279 M.M.Martin, E.Breheret, F.Nesa and Y.H.meyer, J.Phys.Chem., 1989, **130**, 279.
- 89JCS(P2)1087 S.F.Beach, J.D.Hepworth, P.Jones, D.Mason, J.Sawyer, G.Hallas and M.Mitchell, J.Chem.Soc., Perkin Trans 2, 1989, 1087.
- 89MI1 O.Exner, 'Correlation Analysis of Chemical Data', Plenum, 1989.
- 89MI2 A.Vogel, 'Vogel's Textbook of Quantitative Chemical Analysis', 5th Ed., Longman Scientific and Technical, 1989.
- 89Th1 E.A.Swarbrick, PhD., C.N.A.A., Preston Polytechnic, 1987.
- 90MI1 D.R.Waring and G.Hallas, 'The Chemistry and Application of Dyes', Plenum, 1990.
- 90MRC1011 C.Avendaño, C. de Diego and J.Elguero, Magn.Reson.Chem., 1990, **28**, 1011.
- 90S1145 H.Kotsuki, S.Kobayashi, H.Suenaga and H.Nishizawa, Synth., 1990, 1145.
- 91JCS(P1)1881 S.Nakatsuji, H.Nakazumi, H.Fukuma, T.Yahiro, K.Nakashima, M.Iyoda and S.Akiyama, J.Chem.Soc., Perkin Trans 1, 1991, 1881.
- 91MI1 H.Zollinger, 'Colour Chemistry', VCH, 1991.
- 91Th1 C.Unsworth, PhD., C.N.A.A., Preston Polytechnic, 1991.
- 92CP85 I.Baraldi, A.Carnevali, F.Momicchioli and G.Ponterini, Chem.Phys., 1992, **160**, 85.
- 92JA1816 R.A.McClelland, V.M.Kanagasabapathy, N.S.Banait and S.Steenken, J.Amer.Chem.Soc., 1992, **114**, 1816.
- 92JA2342 H.B.Leuck, J.L.McHale and W.D.Edwards, J.Amer.Chem.Soc., 1992, **114**, 2342.

- 93CR381 D.F.Duxbury, Chem.Rev., 1993, **93**, 381.
- 93MI1 J.P.J.Pinel, 'Biopsychology', Allen and Bacon, 1993.
- 94CM412 E.Kelderman, W.A.J.Starmans, J.P.M. van Duynhoven, W.Verboom, J.F.J.Engbersen and D.N.Reinhoudt, Chem.Mater., 1994, **6**, 412.
- 94JMS137 T.Mohsen, C.Suarez, N.S.True, C.B.LeMaster and C.L.LeMaster, J.Mol.Struct., 1994, **317**, 137.
- 94T5861 K.Bergander, R.He, N.Chandrakumar, O.Eppers and H.Günther, Tetrahedron, 1994, **50**, 5861.
- 94T5903 N.J.R.van Eikema Hommes and P.von Rague Schleyer, Tetrahedron, 1994, **50**, 5903.
- 94Th1 S.G.R.Guinot, PhD., C.N.A.A., University of Central Lancashire, 1994.
- 95CIB547 O.Meth-Cohn and A.S.Travis, Chem. in Brit., 1995, **31**, 547.
- 95CM945 K.Kimura, M.Kaneshige and M.Yokoyama, Chem.Mater., 1995, **7**, 945.
- 95JA12889 T.Tao and G.E.Maciell, J.Amer.Chem.Soc., 1995, **117**, 12889.
- 95JOC5016 M.P.Sibi, M.Marvin and R.Sharma, J.Org.Chem., 1995, **60**, 5016.
- 96JA11006 M.L.Cano, A.Corma, V.Fornés, H.Garcia, M.A.Miranda, C.Baerlocher and C.Lengauer, J.Amer.Chem.Soc., 1996, **118**, 11006.
- 96MC895 W.Franek, Monatsh.Chem., 1996, **127**, 895.
- 96MRC395 H.Hönig, Magn.Reson.Chem., 1996, **34**, 395. 6
- 97JA2062 K.Kimura, R.Mizutani, M.Yokoyama, R.Arakawa, G.Matsubayashi, M.Okamoto and H.Doe, J.Amer.Chem.Soc., 1997, **119**, 2062.
- 97JOC1264 J.P.Wolfe and S.L.Buchwald, J.Org.Chem., 1997, **62**, 1264.

APPENDICES

Appendix A1

ACT

```
10 S1=0
20 S2=0
30 S3=0
40 S4=0
50 S5=0
60 S6=0
70 PRINT " INPUT NO. OF POINTS "
80 INPUT N
90 FOR I= 1.TO N
100 PRINT " INPUT TEMP., K, ERROR "
110 INPUT T(I), K(I), S(I)
120 X(I) = 1/T(I)
130 Y(I) = LOG(K(I))
140 W(I) = K(I)*K(I)/(S(I)*S(I))
150 S1 = S1+W(I)
160 S2 = S2+W(I)*X(I)
170 S3 = S3+W(I)*X(I)*X(I)
180 S4 = S4+W(I)*Y(I)
190 S5 = S5+W(I)*X(I)*Y(I)
200 NEXT I
210 D = S1*S3-S2*S2
220 G = (S1*S5-S2*S4)/D
230 A = (S4*S3-S2*S5)/D
240 FOR I = 1 TO N
250 Y = G*X(I)+A
260 Y = Y(I)-Y
270 S6 = S6+W(I)*Y*Y
280 NEXT I
290 E1 = 8.314001E-03*SQR(S6*S1/(D*(N-2)))
300 E2 = 8.314*SQR(S6*S3/(D*(N-2)))
310 A1 = -8.314001E-03*G
320 H = A1-2.48
330 A2 = (A-30.458)*8.314
340 PRINT " ACT ENERGY = ",A1" AND ERROR = ",E1
350 PRINT "ACT ENTHALPY = ",H
360 PRINT "ACT ENTROPY = ",A2" AND ERROR = ",E2
370 END
```

OHE

```
10 S1=0
20 S2=0
30 S3=0
40 S4=0
50 S5=0
60 S6=0
70 PRINT " INPUT NO. OF POINTS "
80 INPUT N
90 PRINT " INPUT OH CONC., K, ERROR "
100 FOR I = 1 TO N
110 INPUT T(I), K(I), S(I)
120 X(I) = T(I)
130 Y(I) = K(I)
140 W(I) = K(I)*K(I)/(S(I)*S(I))
150 S1 = S1+W(I)
160 S2 = S2+W(I)*X(I)
170 S3 = S3+W(I)*X(I)*X(I)
180 S4 = S4+W(I)*Y(I)
190 S5 = S5+W(I)*X(I)*Y(I)
200 NEXT I
210 D = S1*S3-S2*S2
220 G = (S1*S5-S2*S4)/D
230 A = (S4*S3-S2*S5)/D
240 FOR I = 1 TO N
250 Y = G*X(I)+A
260 Y = Y(I)-Y
270 S6 = S6+W(I)*Y*Y
280 NEXT I
290 E1 = SQR(S6*S1/(D*(N-2)))
300 E2 = SQR(S6*S3/(D*(N-2)))
310 A = A*0.018
320 E1 = E1*0.018
330 PRINT " SLOPE = ",G"AND ERROR = ",E1
340 PRINT "INTERCEPT = ",A" AND ERROR = ",E2
350 END
```

HAM

```
10 S1=0
20 S2=0
30 S3=0
40 S4=0
50 S5=0
60 S6=0
70 PRINT " INPUT NO. OF POINTS "
80 INPUT N
90 PRINT " INPUT SIGMA VALUE, K, ERROR "
100 FOR I = 1 TO N
110 INPUT T(I), K(I), S(I)
120 X(I) = T(I)
130 Y(I) = LOG (K(I))/2.303
140 W(I) = K(I)*K(I)/(S(I)*S(I))
150 S1 = S1+W(I)
160 S2 = S2+W(I)*X(I)
170 S3 = S3+W(I)*X(I)*X(I)
180 S4 = S4+W(I)*Y(I)
190 S5 = S5+W(I)*X(I)*Y(I)
200 NEXT I
210 D = S1*S3-S2*S2
220 G = (S1*S5-S2*S4)/D
230 A = (S4*S3-S2*S5)/D
240 FOR I = 1 TO N
250 Y = G*X(I)+A
260 Y = Y(I)-Y
270 S6 = S6+W(I)*Y*Y
280 NEXT I
290 E1 = SQR(S6*S1/(D*(N-2)))
300 E2 = SQR(S6*S3/(D*(N-2)))
310 PRINT " SLOPE = ",G"AND ERROR = ",E1
320 PRINT "INTERCEPT = ",A" AND ERROR = ",E2
330 END
```

PLOT

```
10 S1=0
20 S2=0
30 S3=0
40 S4=0
50 S5=0
60 PRINT " NOW INPUT NO. OF POINTS, TEMP "
70 INPUT N,T
80 PRINT " NOW INPUT OH CONC, KOBS IN PAIRS "
90 FOR I = 1 TO N
100 INPUT X(I), Y(I)
110 S1 = S1+X(I)
120 S2 = S2+Y(I)
130 S3 = S3+X(I)*Y(I)
140 S4 = S4+X(I)*X(I)
150 NEXT I
160 G = (N*S3-S1*S2)/(N*S4-S1*S1)
170 A = (S2-G*S1)/N
180 FOR I = 1 TO N
190 S6 = Y(I)-(G*X(I)+A)
200 S5 = S5+S6*S6
210 NEXT I
220 S7 = SQR(S5/(N-1))
230 S8 = (S5/((N-2)*(S4-S1*S1/N)))
240 S8 = SQR(S8)
250 LET A = A* 0.018
260 LET S7 = S7*0.018
272 PRINT "TEMP =",T
280 PRINT " K2 = ",G"AND ERROR IN K2 IS =",S8
290 PRINT " K1 =",A" AND ERROR IN K1 IS =",S7
300 END
```

EXN

$$u = T^{-1} - \frac{1}{m} \sum_j T_j^{-1}$$

$$p_i = \frac{1}{m} \sum_j u_j \log k_{ij}$$

$$X = \frac{1}{m} \sum_j (x_j - \bar{x})^2 = \frac{1}{m} \sum_j u_j^2$$

$$Y = \frac{1}{m} \sum_i \left(\sum_j \log k_{ij} \right)^2 - \frac{1}{ml} \left(\sum_{ij} \log k_{ij} \right)^2$$

$$Z = \sum_{ij} (\log k_{ij})^2 - \frac{1}{ml} \left(\sum_{ij} \log k_{ij} \right)^2$$

$$P = \sum_{ij} u_j \log k_{ij}$$

$$Q = \frac{1}{m} \sum_i \left(\sum_j u_j \log k_{ij} \right)^2$$

$$U = \frac{2}{m} \sum_i \left(\sum_j u_j \log k_{ij} \sum_l \log k_{il} \right) - \frac{2}{ml} \left(\sum_{ij} u_j \log k_{ij} \right) \left(\sum_{ij} \log k_{ij} \right)$$

$$u_o = \beta^{-1} - \sum_j \frac{T_j^{-1}}{m} = \left[Q - P^2 / ml - XY - \sqrt{(Q - P^2 / ml - XY)^2 + XU^2} \right] / U$$

$$y_o = \frac{1}{ml} \left(\sum_{ij} \log k_{ij} + u_o P / X \right)$$

$$b_i = \frac{p_i + u_o \left(y_o - \frac{1}{m} \sum_j \log k_{ij} \right)}{X + u_o^2}$$

$$S_o = Z - \left[Q + P^2 / ml + XY + \sqrt{(Q - P^2 / ml - XY)^2 + XU^2} \right] / 2X$$

Where the number of degrees of freedom, $f = (m-1)! - 2$

$$S_{oo} = Z - Y - Q/X$$

Where the number of degrees of freedom, $f = (m-2)!$

$$S_u = Z - \frac{Q - uU + u^2(Y + P^2 / mlX)}{X + u^2}$$

Where the number of degrees of freedom, $f = (m-1)! - 1$

Appendix A2

Figure 1: Kinetic plots for 4'-dimethylamino-4''-diethylaminotriphenylmethyl perchlorate

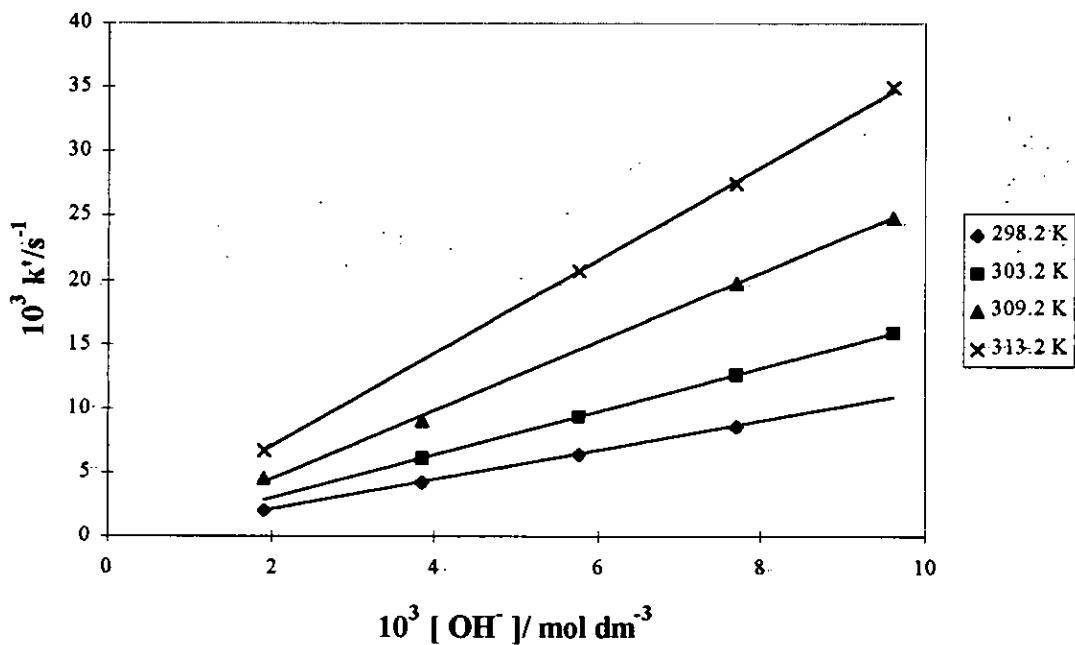


Figure 2: Kinetic plots for 4'-pyrrolidino-4''-diethylaminotriphenylmethyl perchlorate

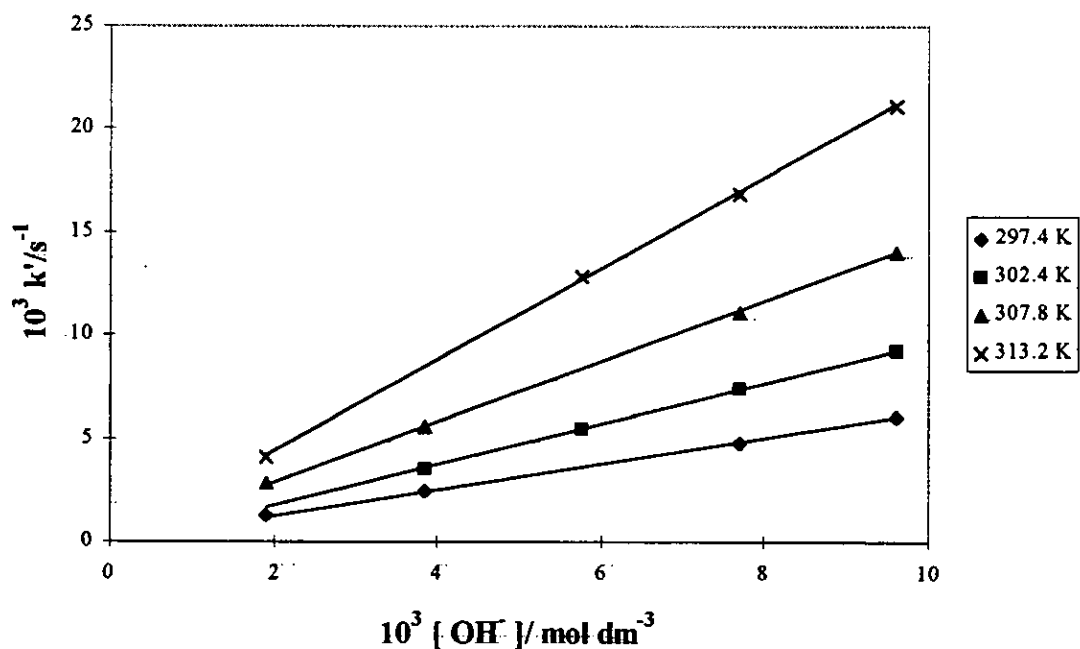


Figure 3: Kinetic plots for 4'-piperidino-4''-diethylaminotriphenylmethyl perchlorate

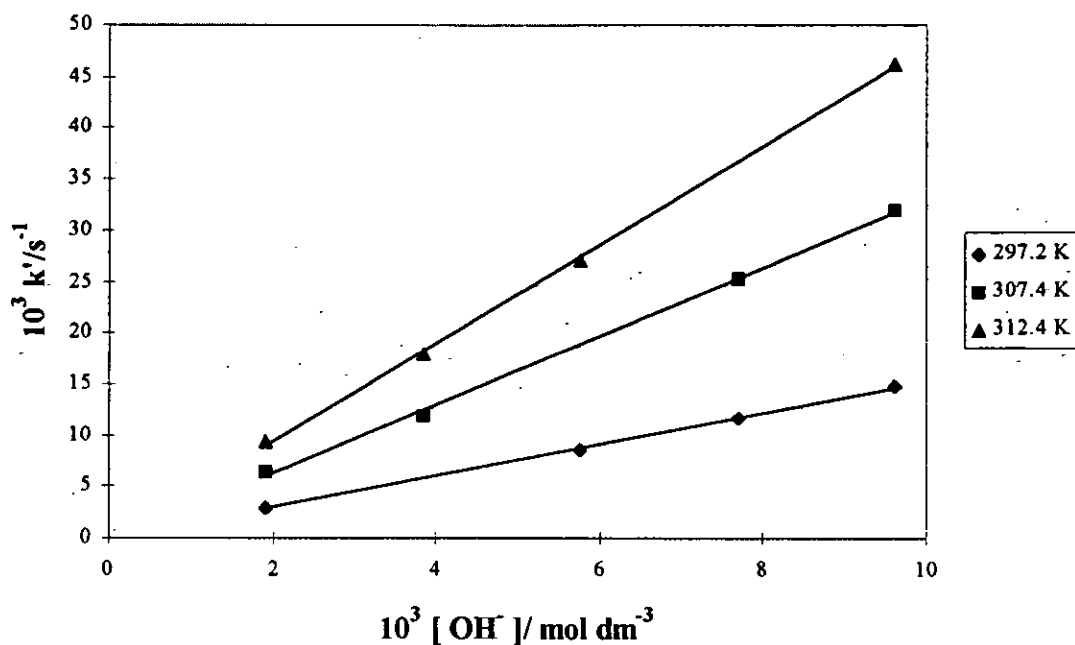


Figure 4: Kinetic plots for 4'-morpholino-4''-diethylaminotriphenylmethyl perchlorate

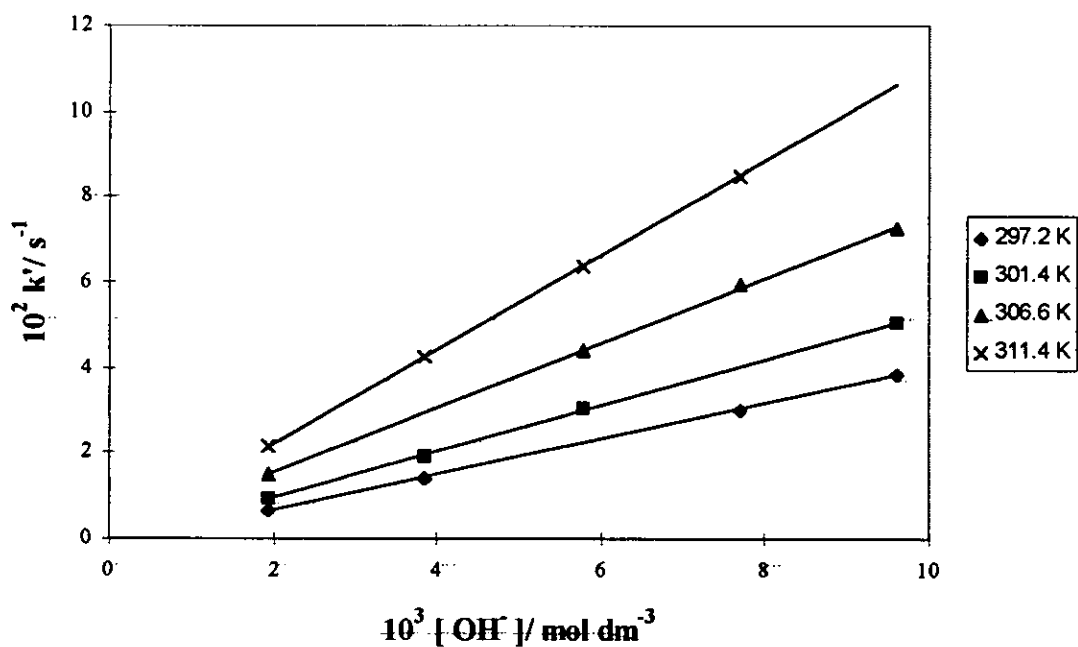


Figure 5: Kinetic plots for 4'-dimethylamino-4''-pyrrolidinotriphenylmethyl perchlorate

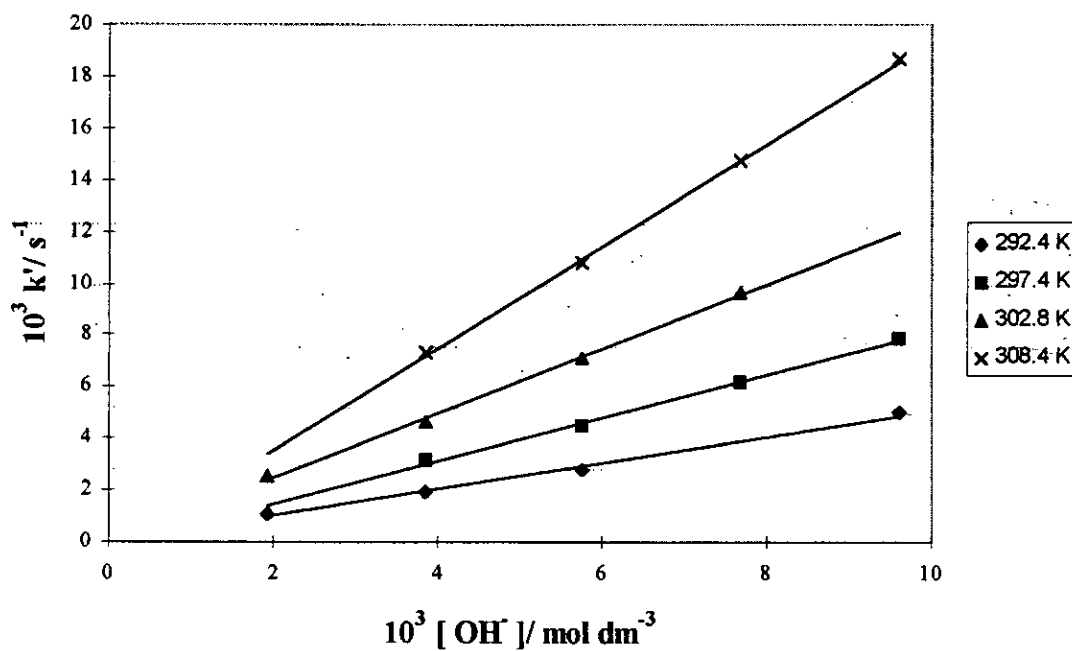


Figure 6: Kinetic plots for 4'-piperidino-4''-pyrrolidinotriphenylmethyl perchlorate

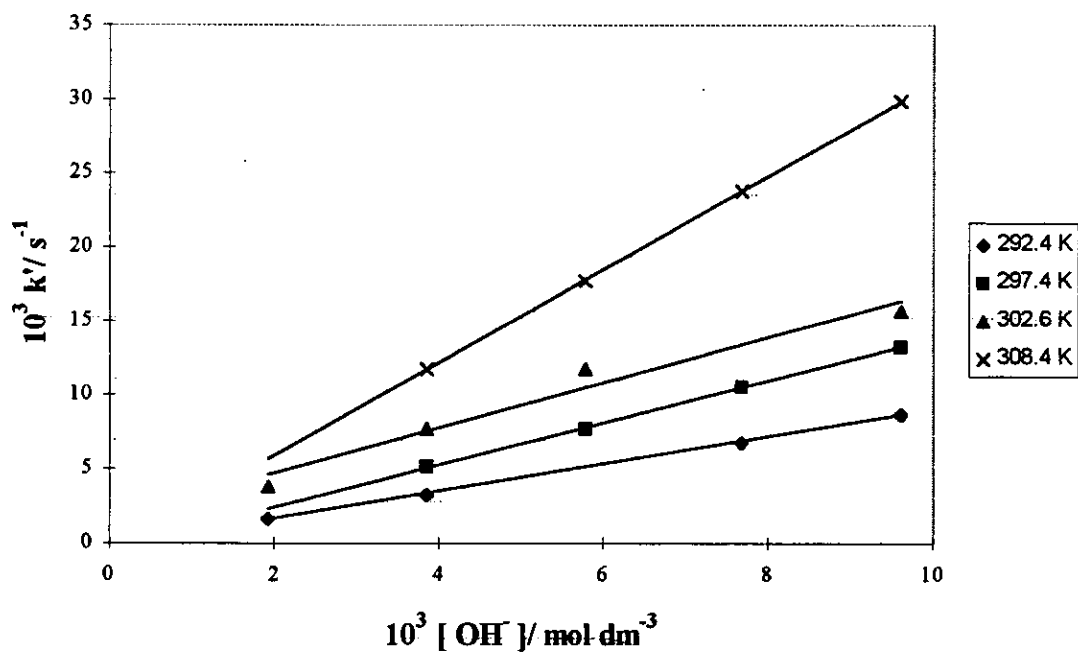


Figure 7: Kinetic plots for 4'-morpholino-4''-pyrrolidinotriphenylmethyl perchlorate

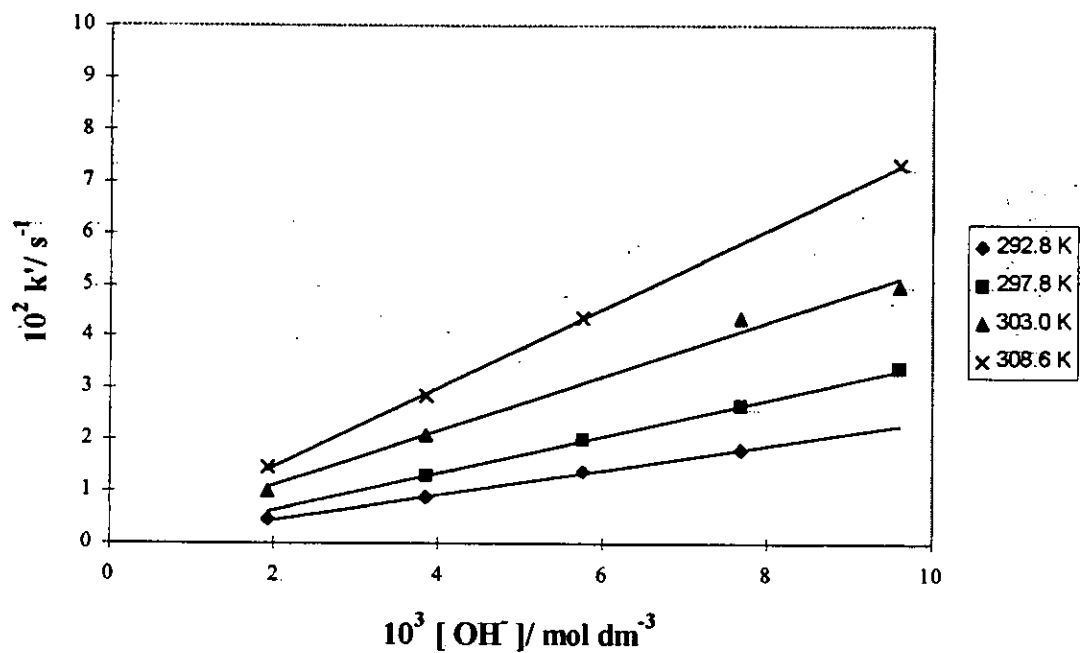


Figure 8: Kinetic plots for 4'-morpholino-4''-pyrrolidinotriphenylmethyl perchlorate

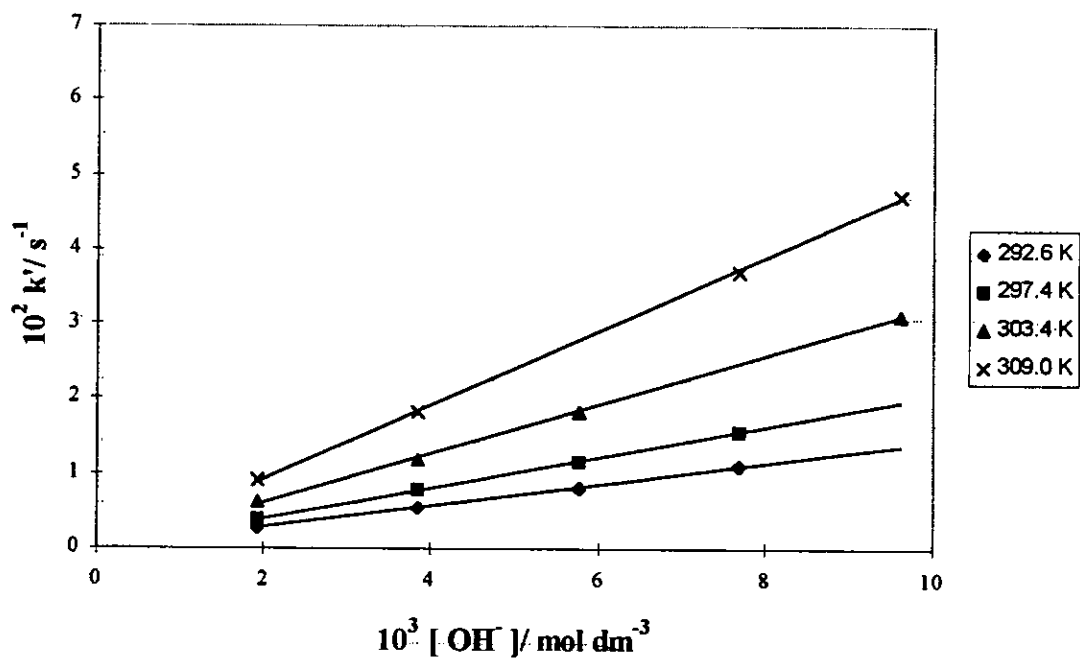


Figure 9: Kinetic plots for 4'-morpholino-4''-piperidinotriphenylmethyl perchlorate

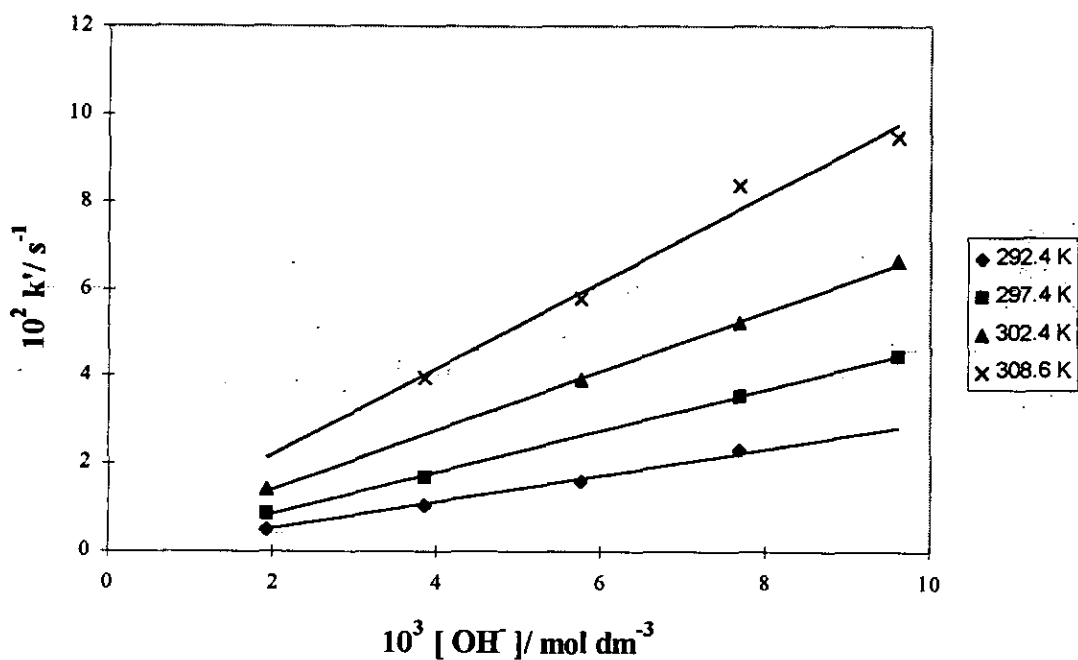


Figure 10: Kinetic plots for 4'-dimethylamino-4''-morpholinotriphenylmethyl perchlorate

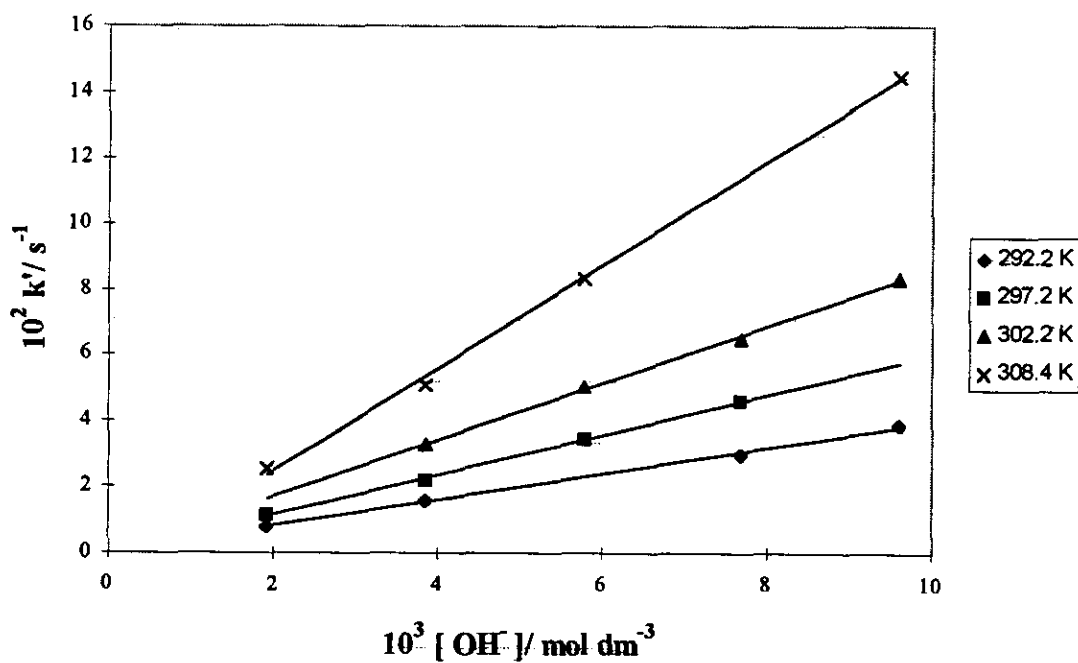


Figure 11: Kinetic plots for 4'-N-methylpiperazino-4''-diethylaminotriphenylmethyl perchlorate

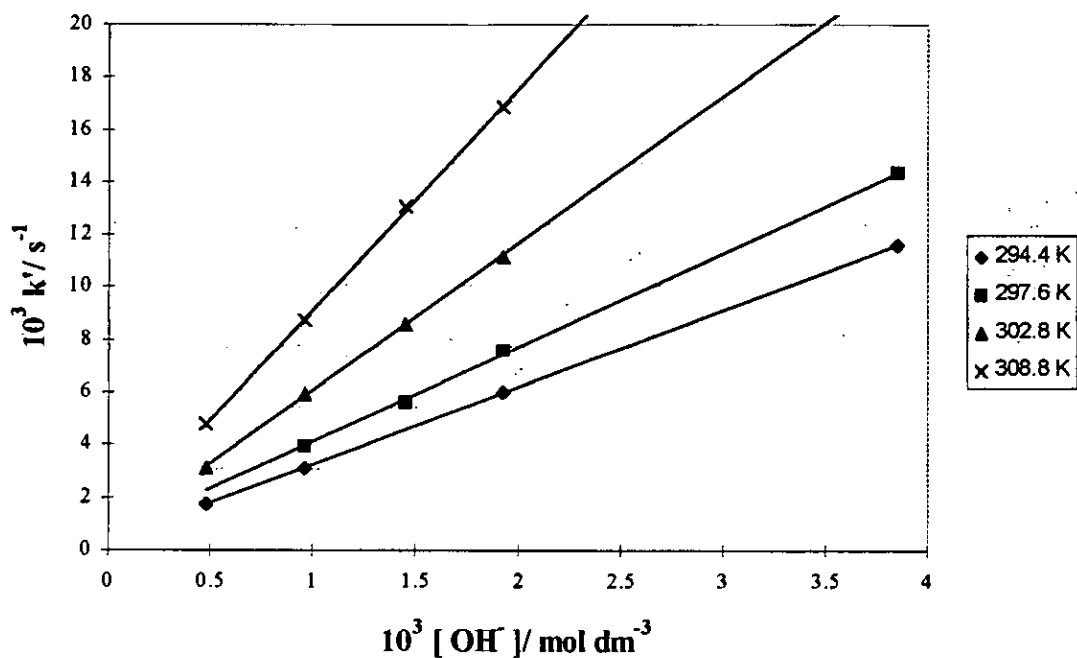


Figure 12: Kinetic plots for 4'-N-methylpiperazino-4''-dimethylaminotriphenylmethyl perchlorate

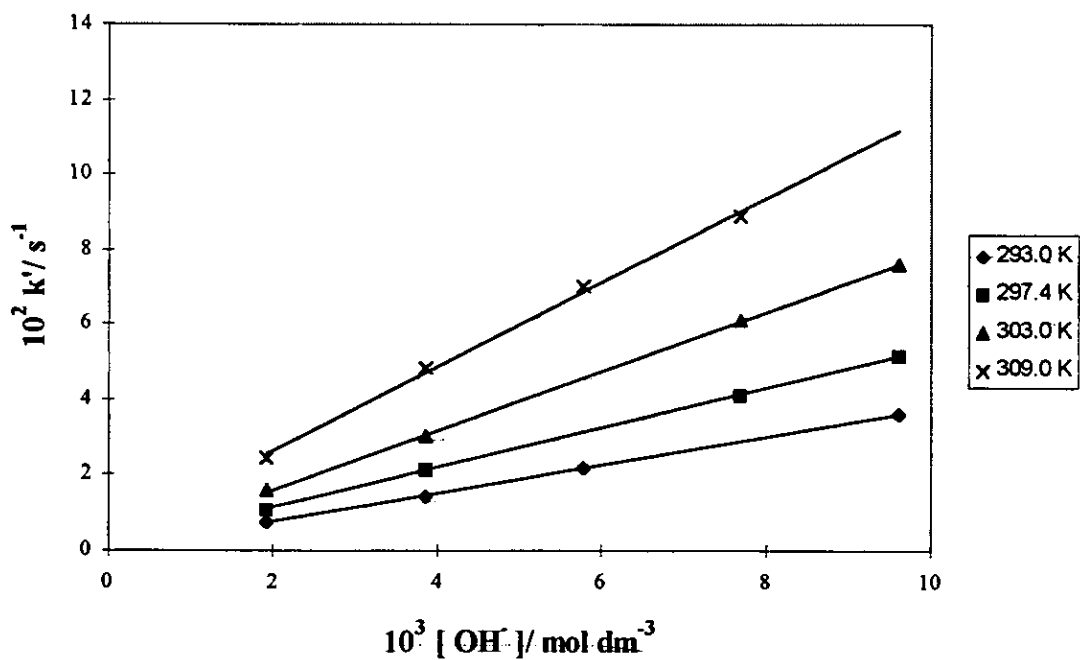


Figure 13: Kinetic plots for 4'-N-methylpiperazino-4''-pyrrolidinotriphenylmethyl perchlorate

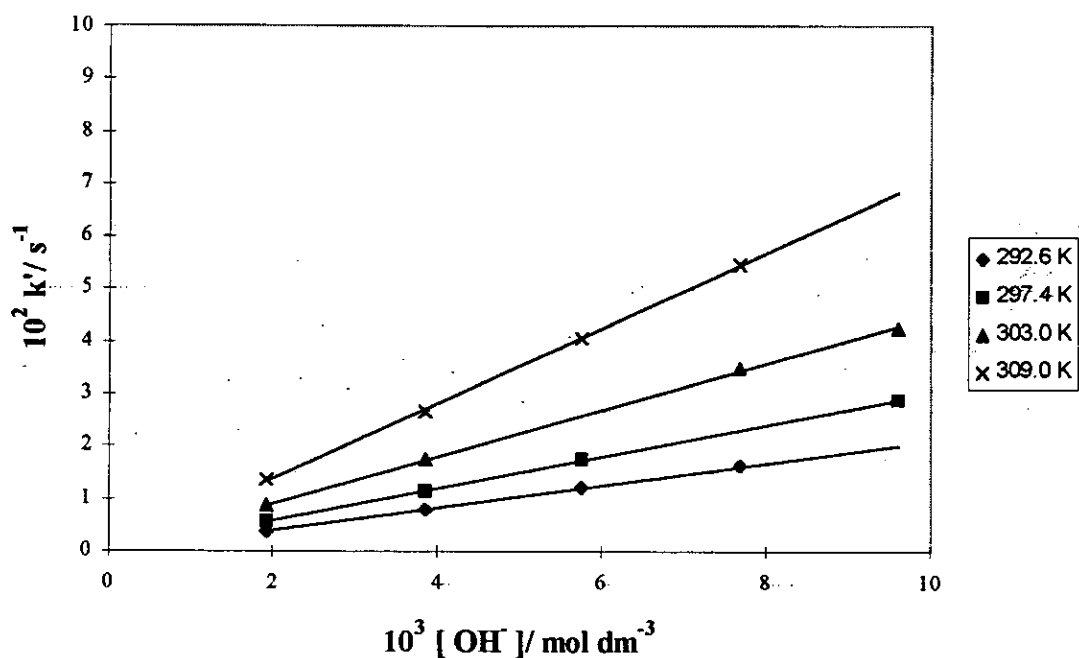


Figure 14: Kinetic plots for 4'-N-methylpiperazino-4''-piperidinotriphenylmethyl perchlorate

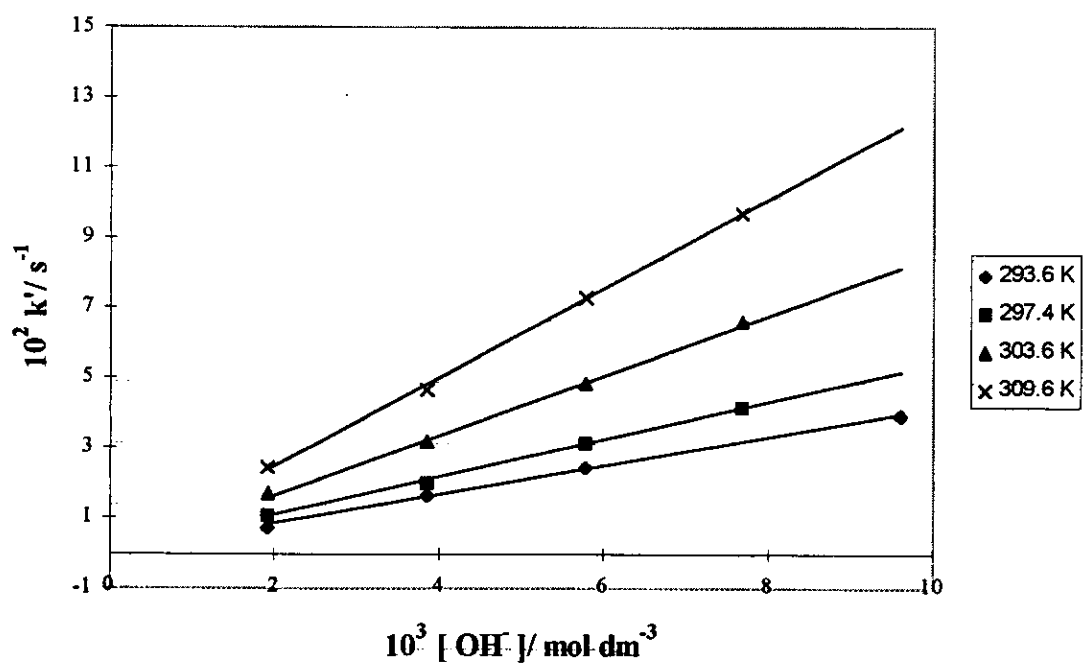


Figure 15: Kinetic plots for 4'-N-methylpiperazino-4''-morpholinotriphenylmethyl perchlorate

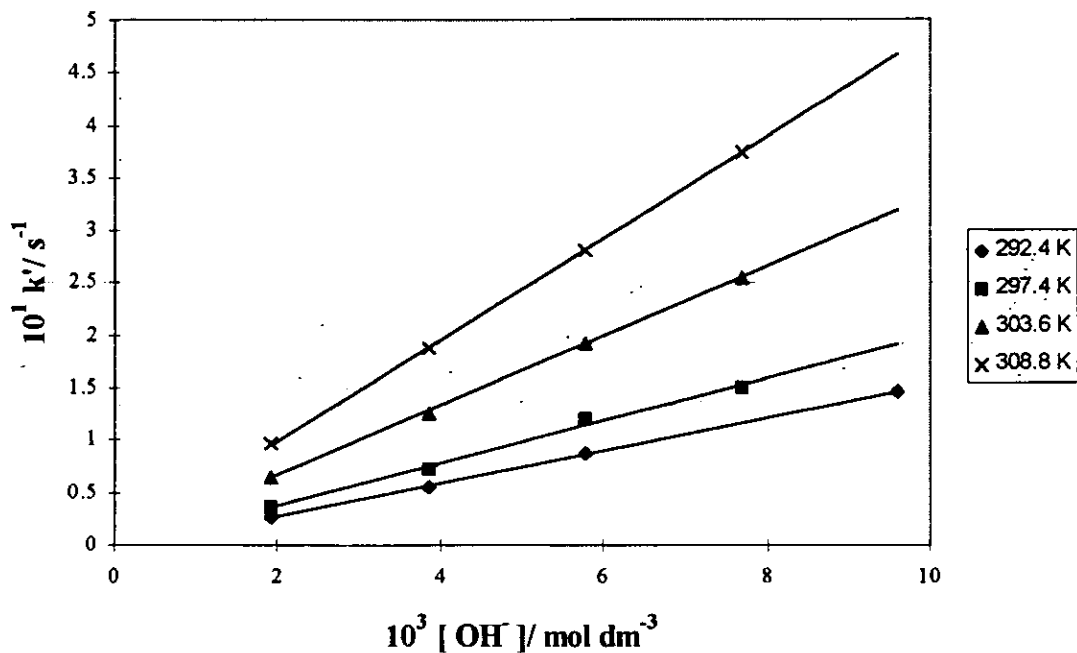
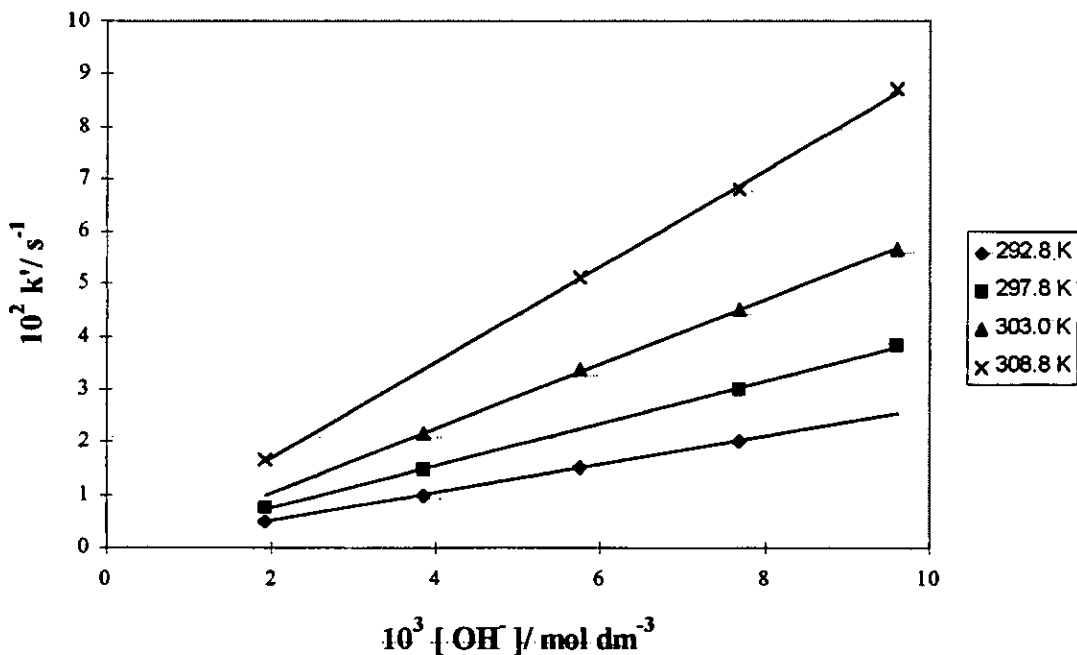


Figure 16: Kinetic plots for 4'-thiomorpholino-4''-dimethylaminotriphenylmethyl perchlorate



Appendix A3

Figure 1: Arrhenius plot for the 4'-dimethylamino-4''-diethylaminotriphenylmethyl cation

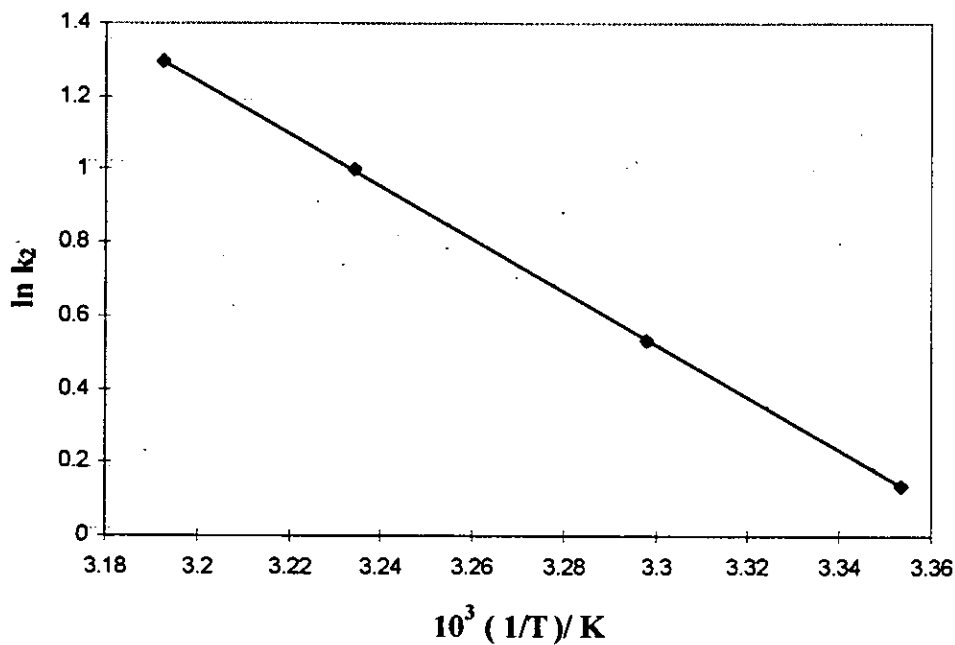


Figure 2: Arrhenius plot for the 4'-pyrrolidino-4''-diethylamino-triphenylmethyl cation

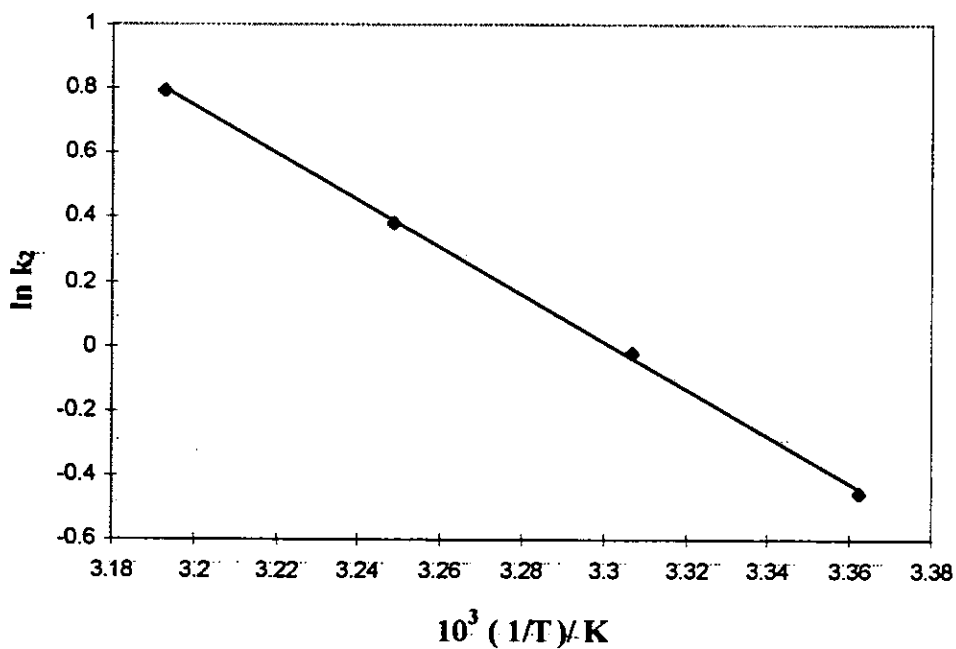


Figure 3: Arrhenius plot for the 4'-piperidino-4''-diethylamino-triphenylmethyl cation

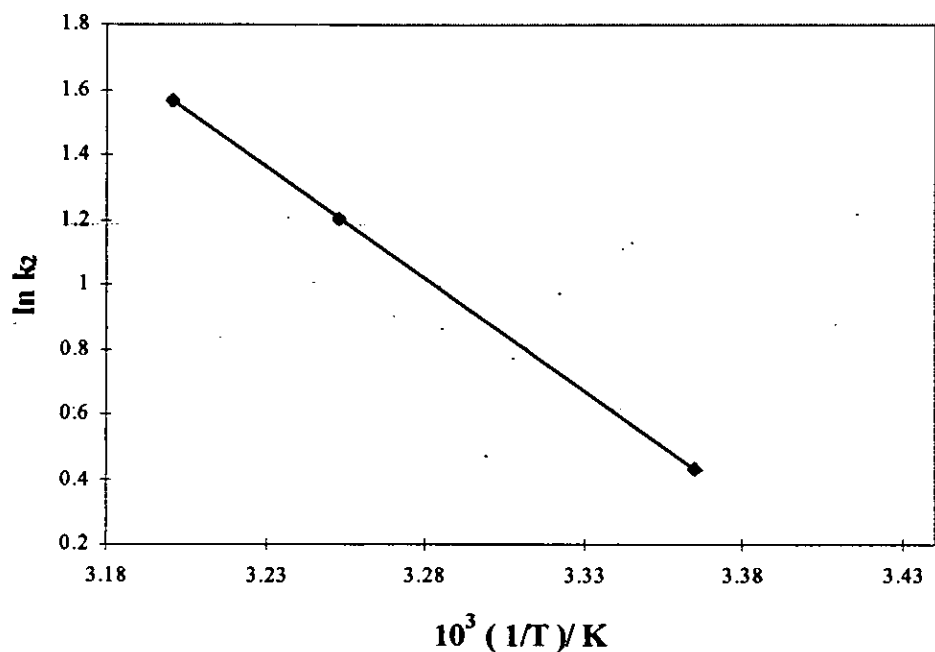


Figure 4: Arrhenius plot for the 4'-morpholino-4''-diethylamino-triphenylmethyl cation

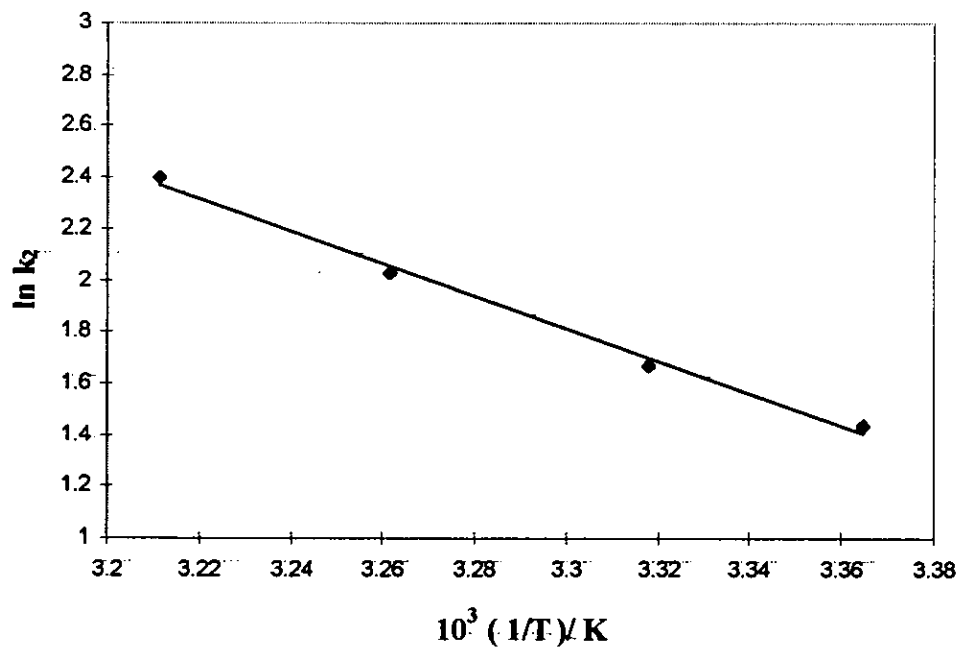


Figure 5: Arrhenius plot for the 4'-dimethylamino-4''-pyrrolidinotriphenylmethyl cation

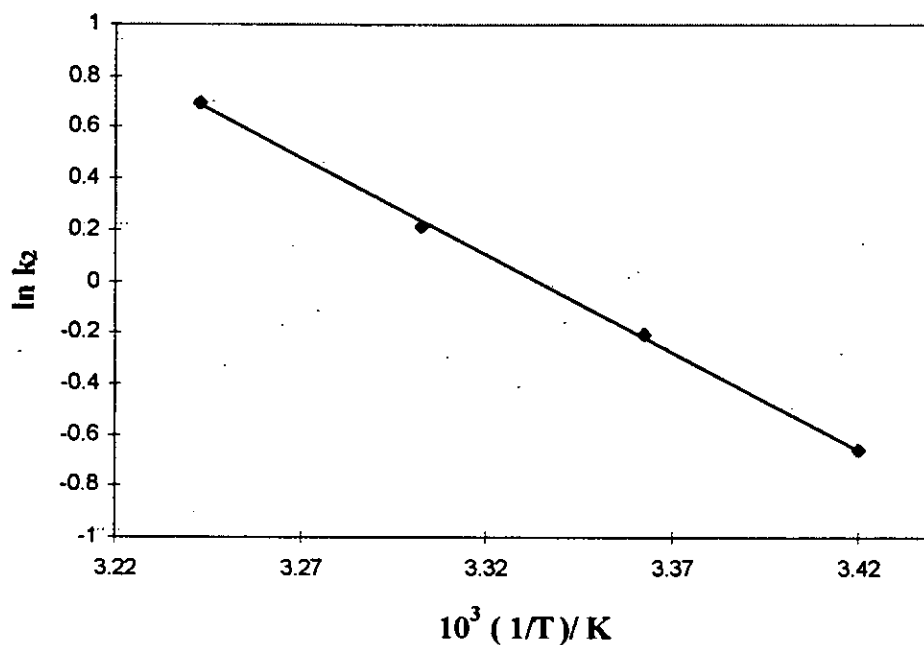


Figure 6: Arrhenius plot for the 4'-piperidino-4''-pyrrolidino-triphenylmethyl cation

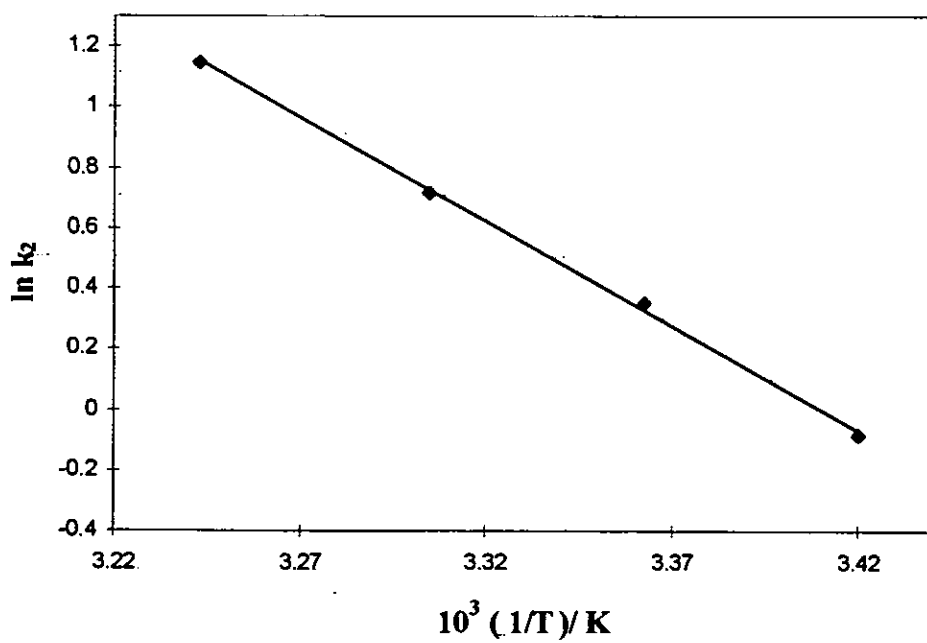


Figure 7: Arrhenius plot for the 4'-morpholino-4''-pyrrolidino-triphenylmethyl cation

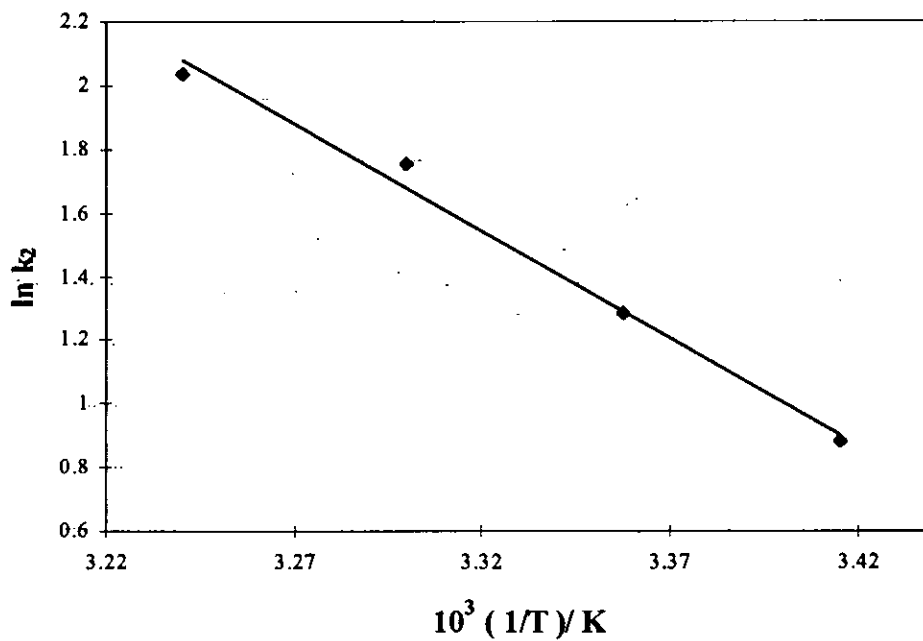


Figure 8: Arrhenius plot for the 4'-dimethylamino-4''-piperidino-triphenylmethyl cation

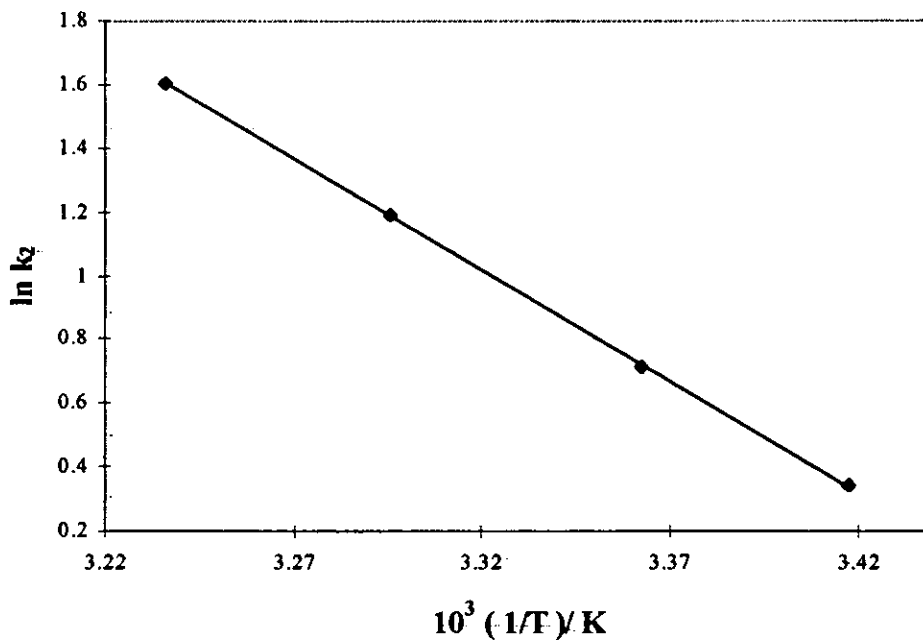


Figure 9: Arrhenius plot for the 4'-morpholino-4''-piperidino-triphenylmethyl cation

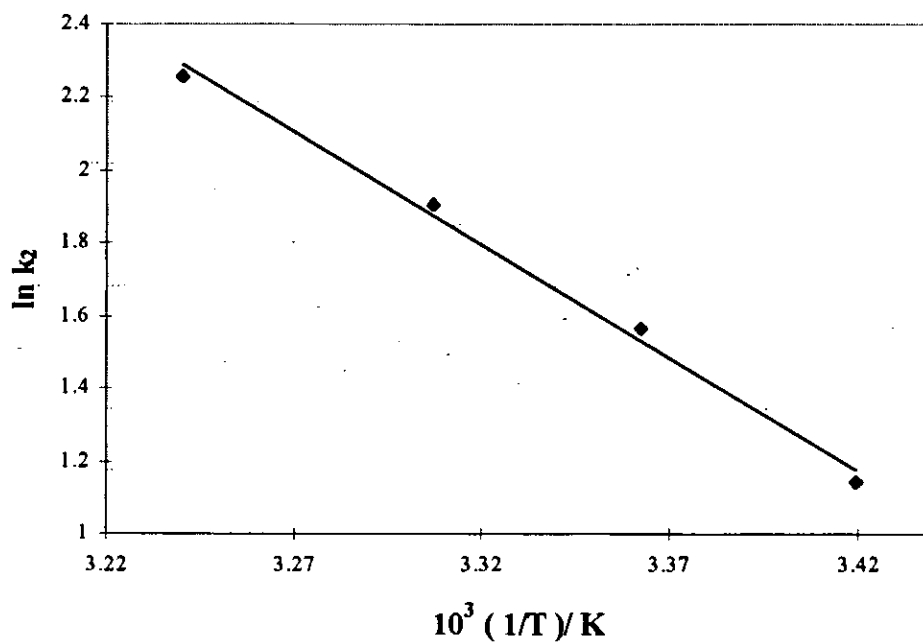


Figure 10: Arrhenius plot for the 4'-dimethylamino-4''-morpholinotriphenylmethyl cation

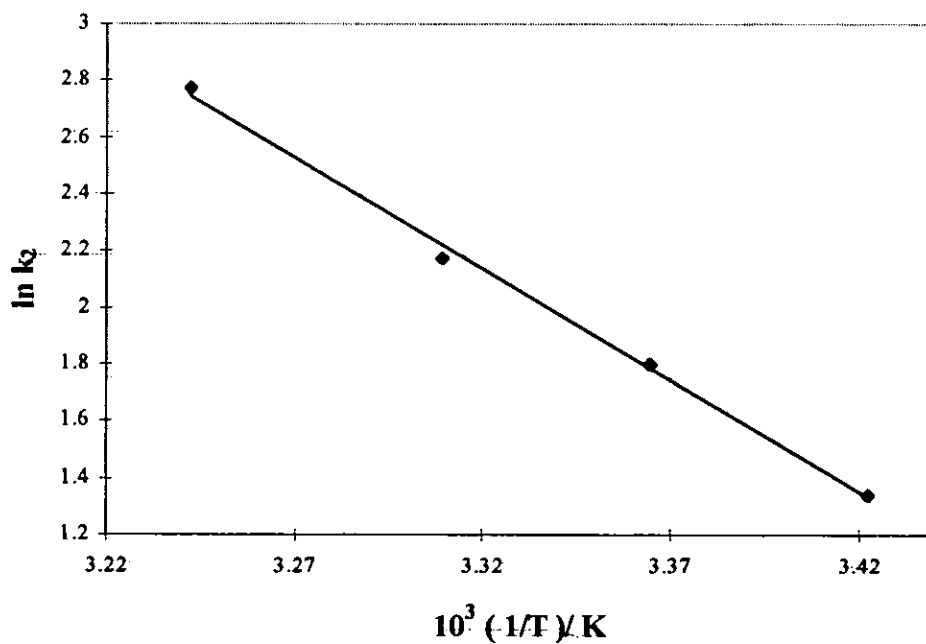


Figure 11: Arrhenius plot for the 4'-N-methylpiperazino-4''-diethylaminotriphenylmethyl cation

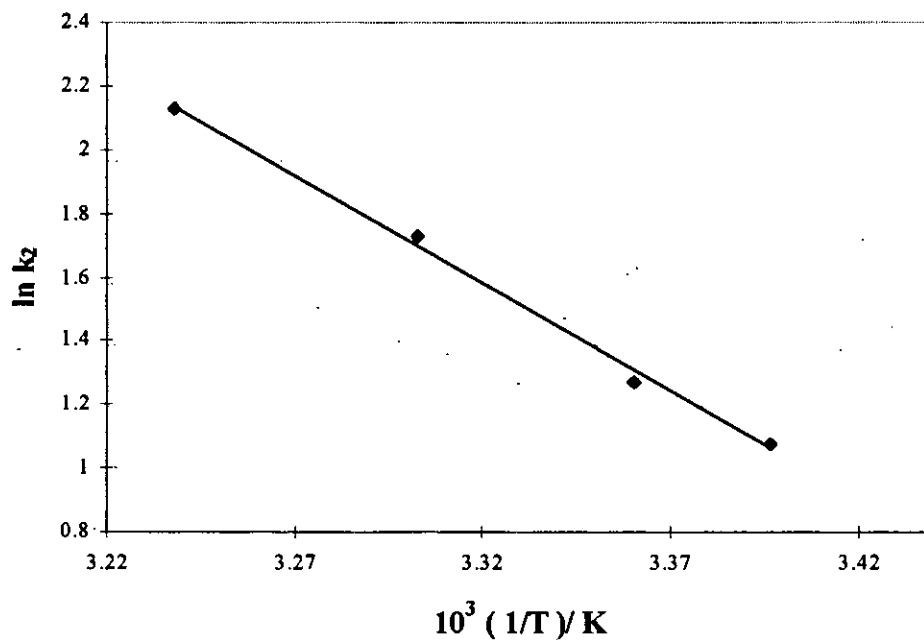


Figure 12: Arrhenius plot for the 4'-N-methylpiperazino-4''-dimethylaminotriphenylmethyl cation

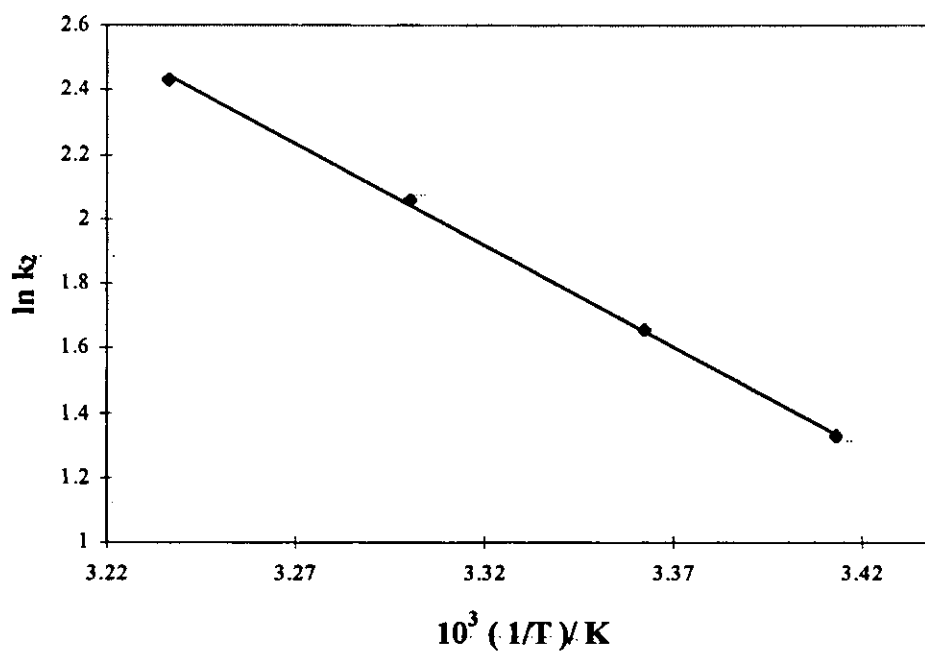


Figure 13: Arrhenius plot for the 4'-N-methylpiperazino-4''-pyrrolidinotriphenylmethyl cation

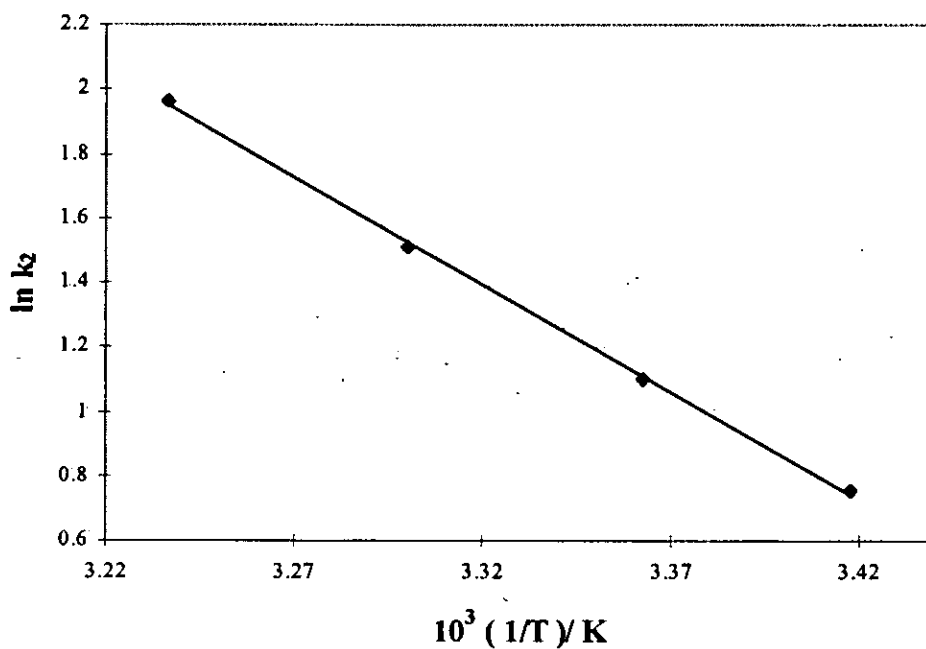


Figure 14: Arrhenius plot for the 4'-N-methylpiperazino-4''-pyrrolidinotriphenylmethyl cation

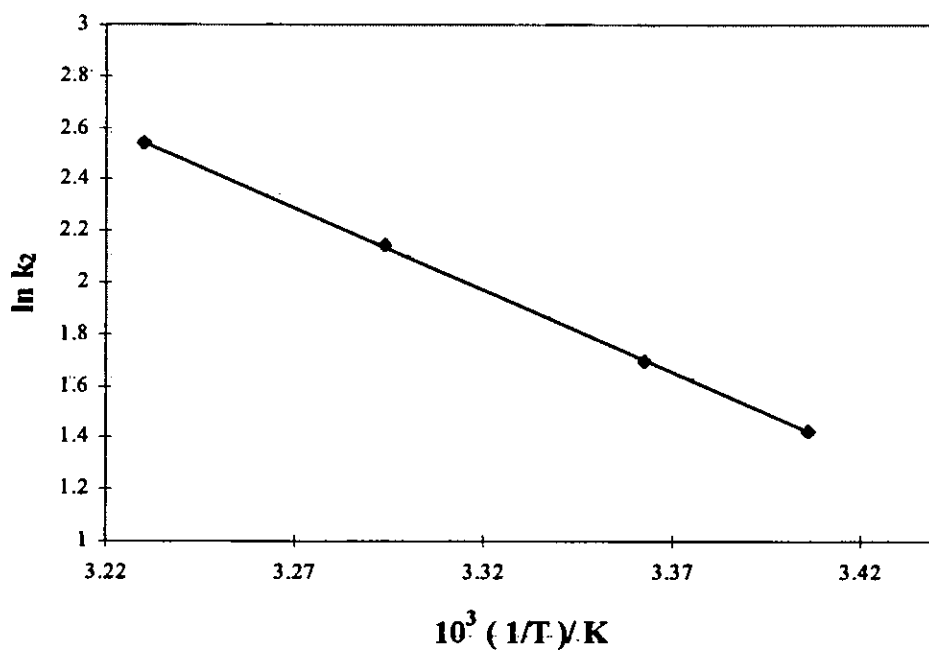


Figure 15: Arrhenius plot for the 4'-N-methylpiperazino-4''-morpholinotriphenylmethyl cation

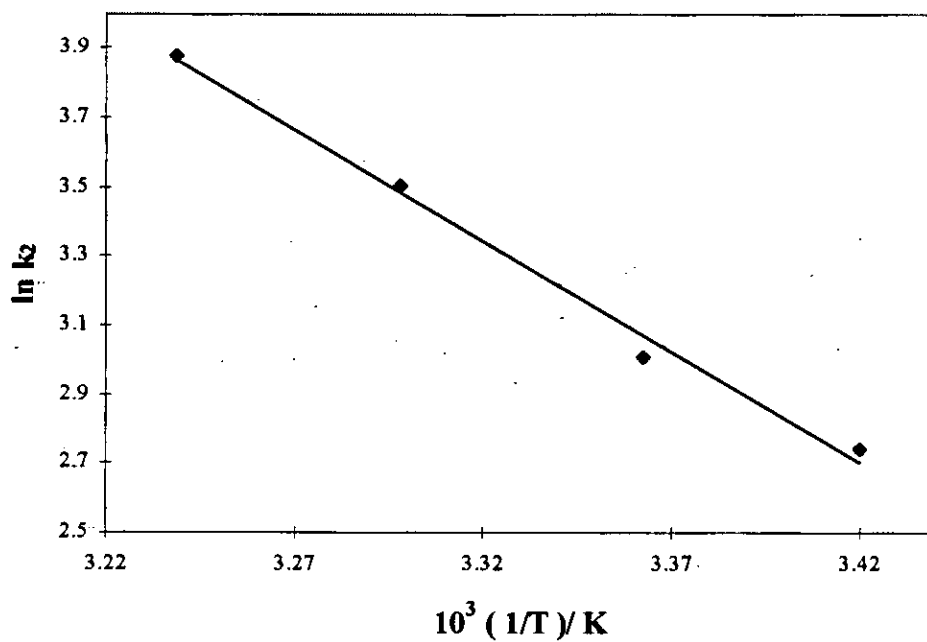
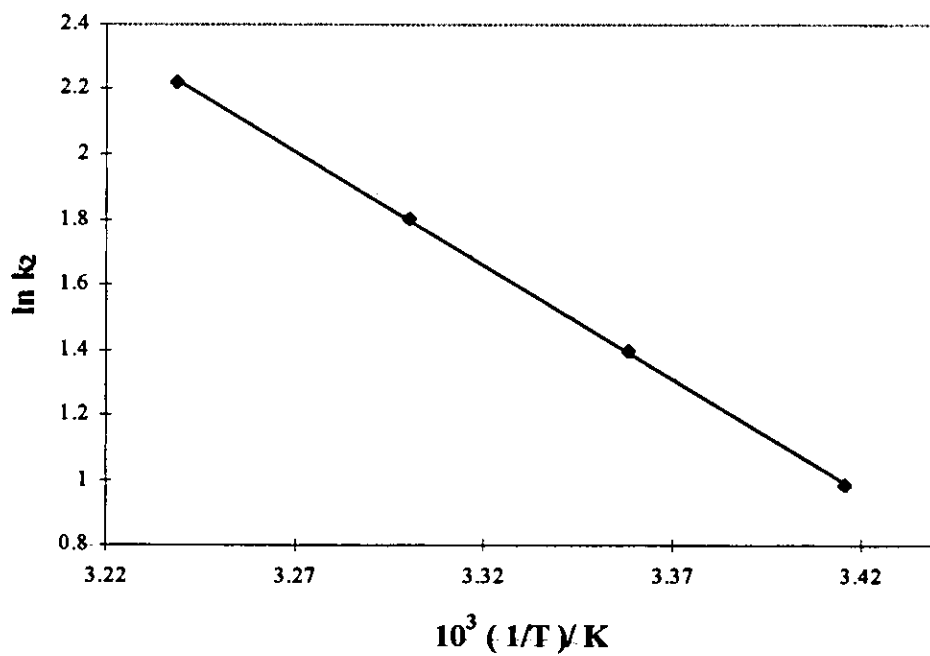


Figure 16: Arrhenius plot for the 4'-thiomorpholino-4''-dimethylaminotriphenylmethyl cation



Appendix A4

Figure 1: Kinetic plots for 4,4'-bis(dimethylamino)diphenylmethyl perchlorate

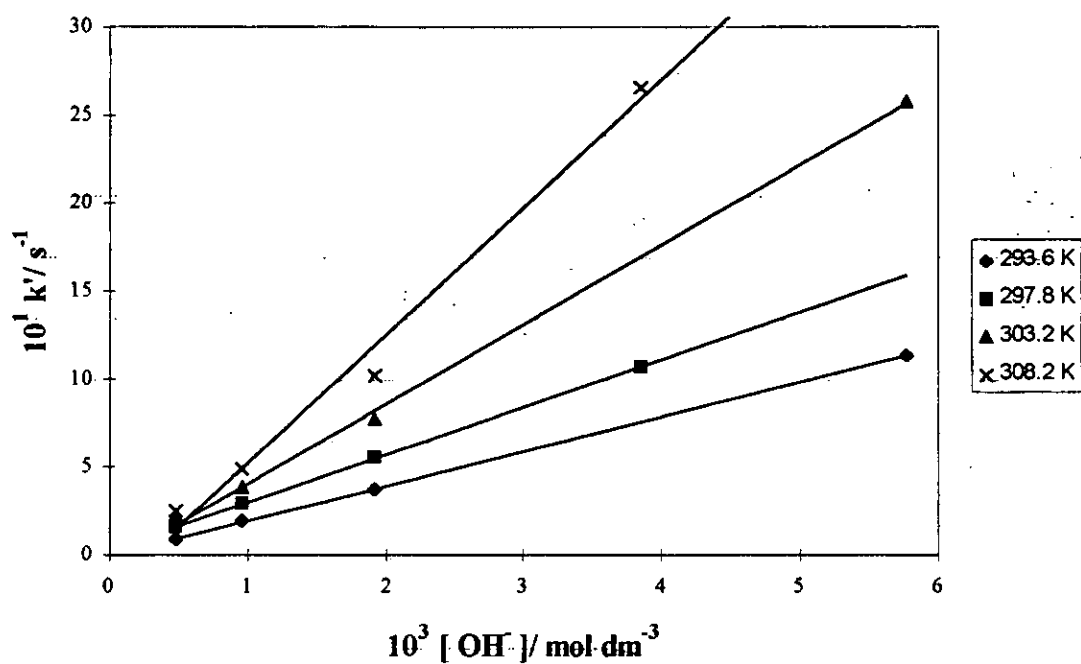


Figure 2: Kinetic plots for 4,4'-bis(diethylamino)diphenylmethyl perchlorate

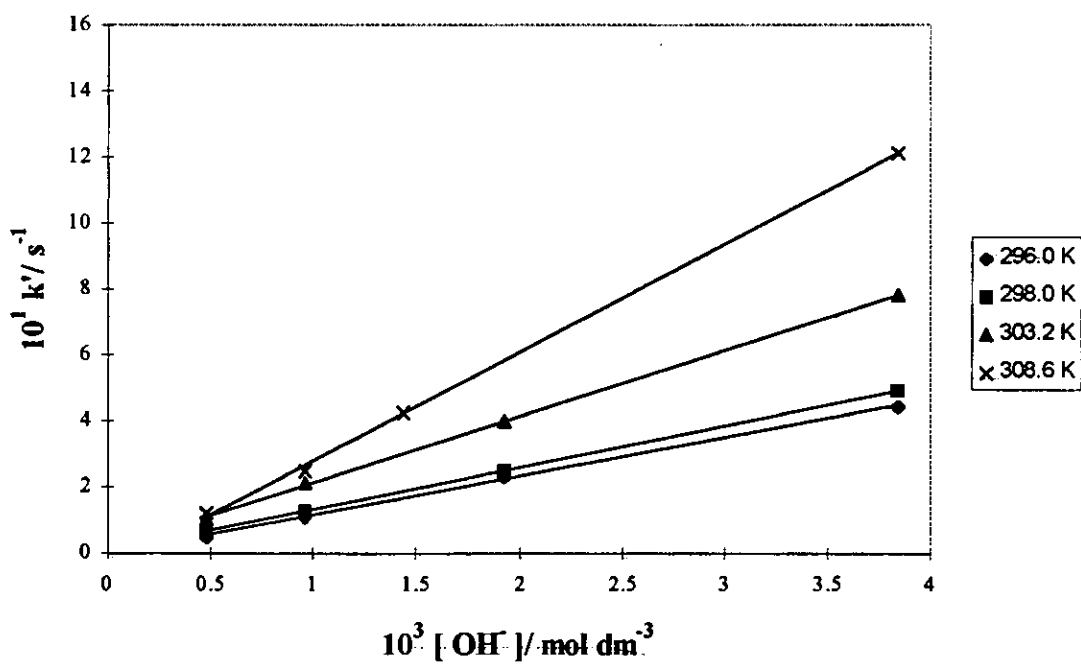
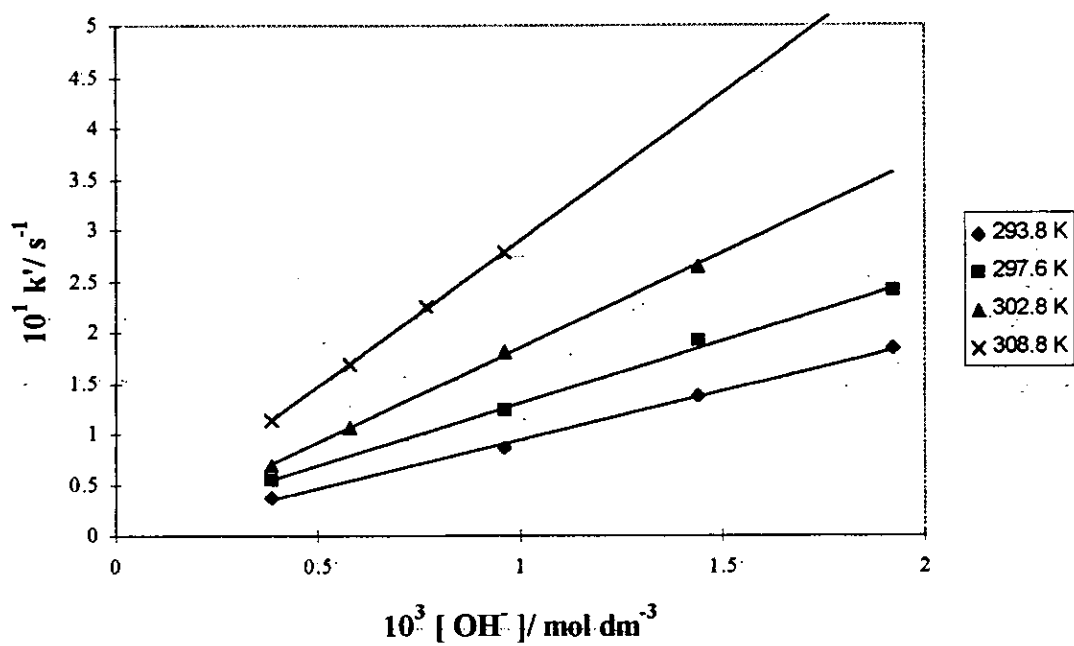


Figure 3: Kinetic plots for 4,4'-dipyrrolidinodiphenylmethyl perchlorate



Appendix A5

Figure 1: Arrhenius plot for the 4,4'-bis(dimethylamino)diphenylmethyl cation

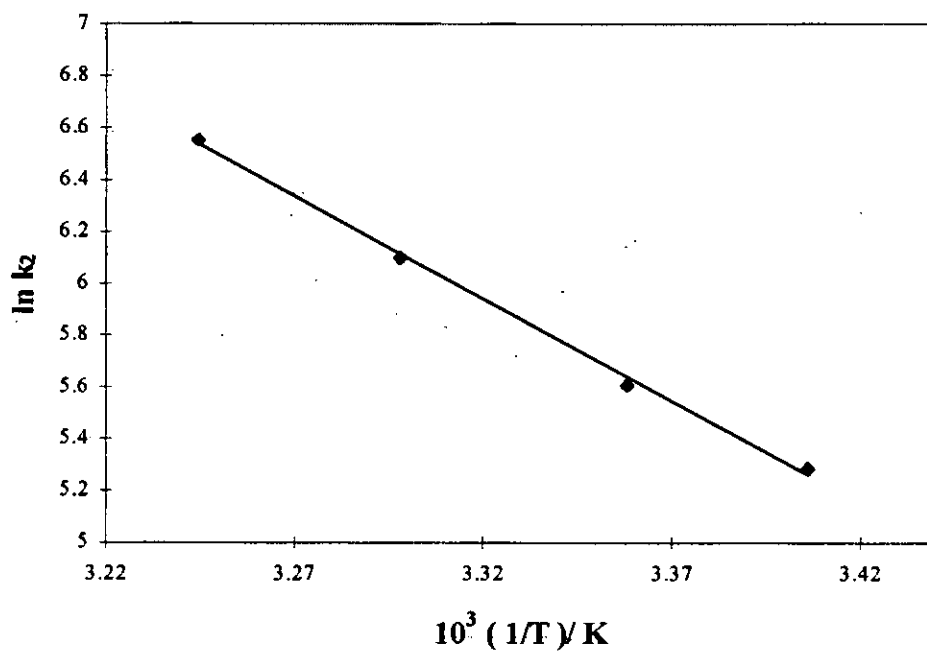


Figure 2: Arrhenius plot for the 4,4'-bis(diethylamino)diphenylmethyl cation

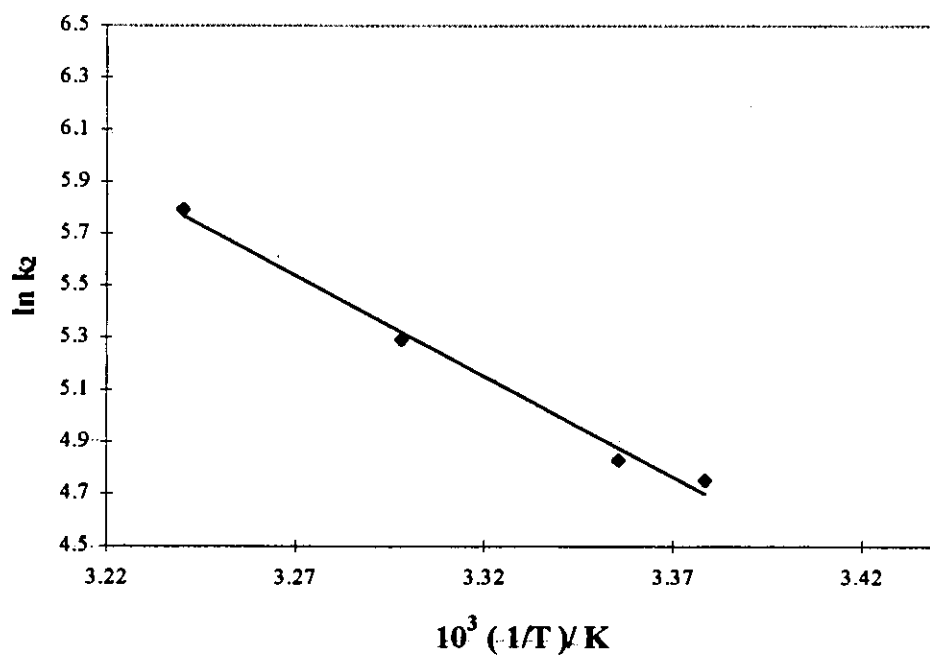
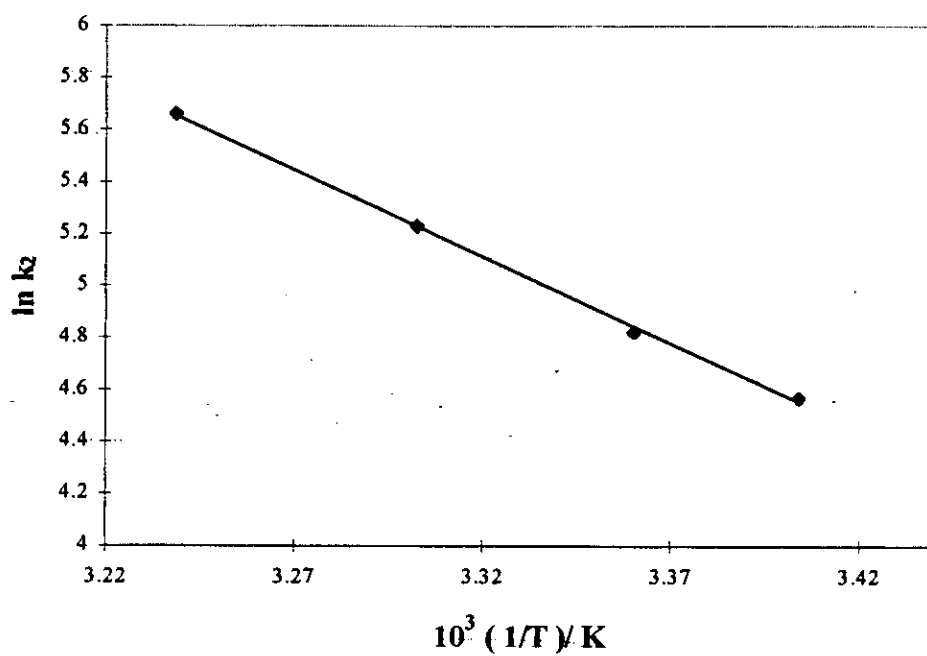


Figure 3: Arrhenius plot for the 4,4'-dipyrrolidinodiphenylmethyl cation



Appendix A6

Figure 1
Log k_2 against σ_p^+ for some unsymmetrical MGs containing dimethylamino at 288.2K (◆); 293.2K (■); 298.2K (▲); 303.2K (×) and 308.2K (✱)

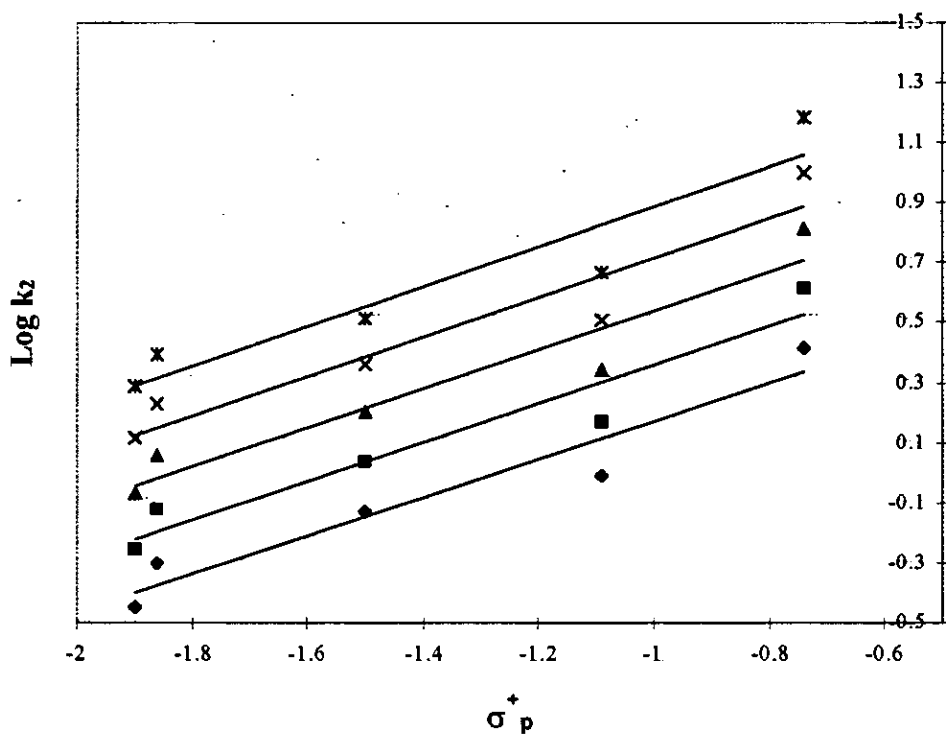


Figure 2
Log k_2 against σ_p^+ for some unsymmetrical MGs containing diethylamino at 288.2K (◆); 293.2K (■); 298.2K (▲); 303.2K (×) and 308.2K (*)

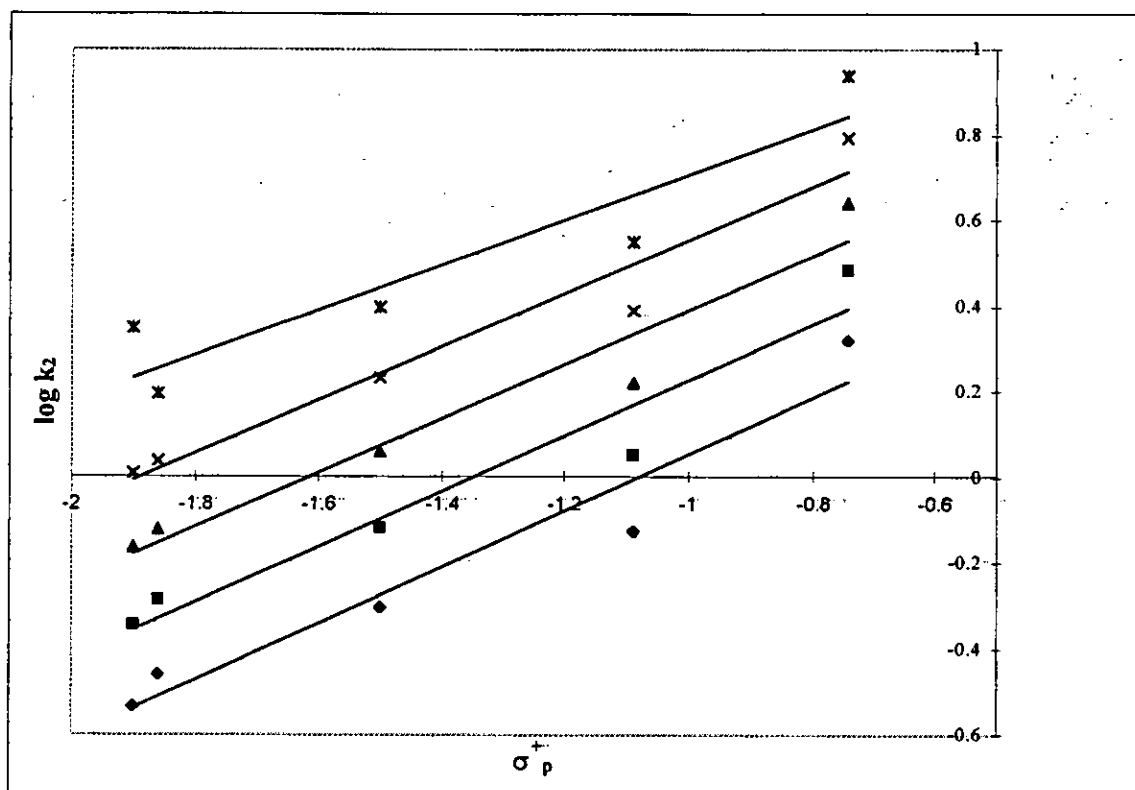


Figure 3
Log k_2 against σ_p^+ for some unsymmetrical MGs containing pyrrolidino at 288.2K (◆); 293.2K (■); 298.2K (▲); 303.2K (×) and 308.2K (✱)

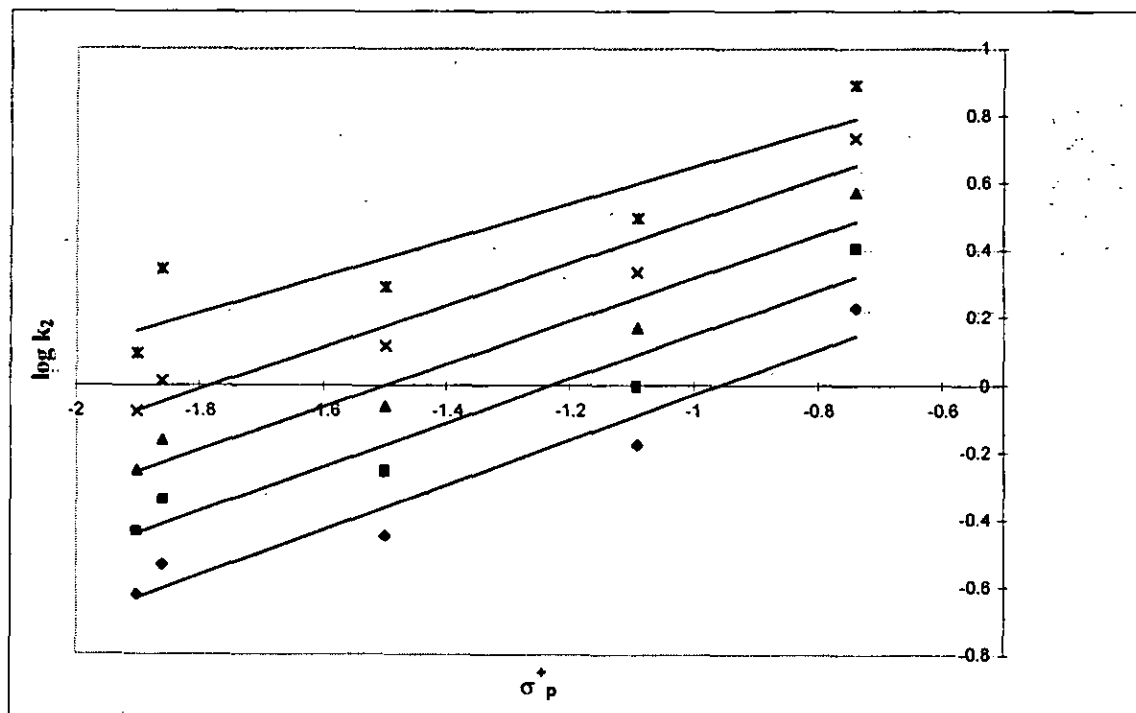


Figure 4
Log k_2 against σ_p^+ for some unsymmetrical MGs containing
piperidino at 288.2K (◆); 293.2K (■); 298.2K (▲);
303.2K (×) and 308.2K (*)

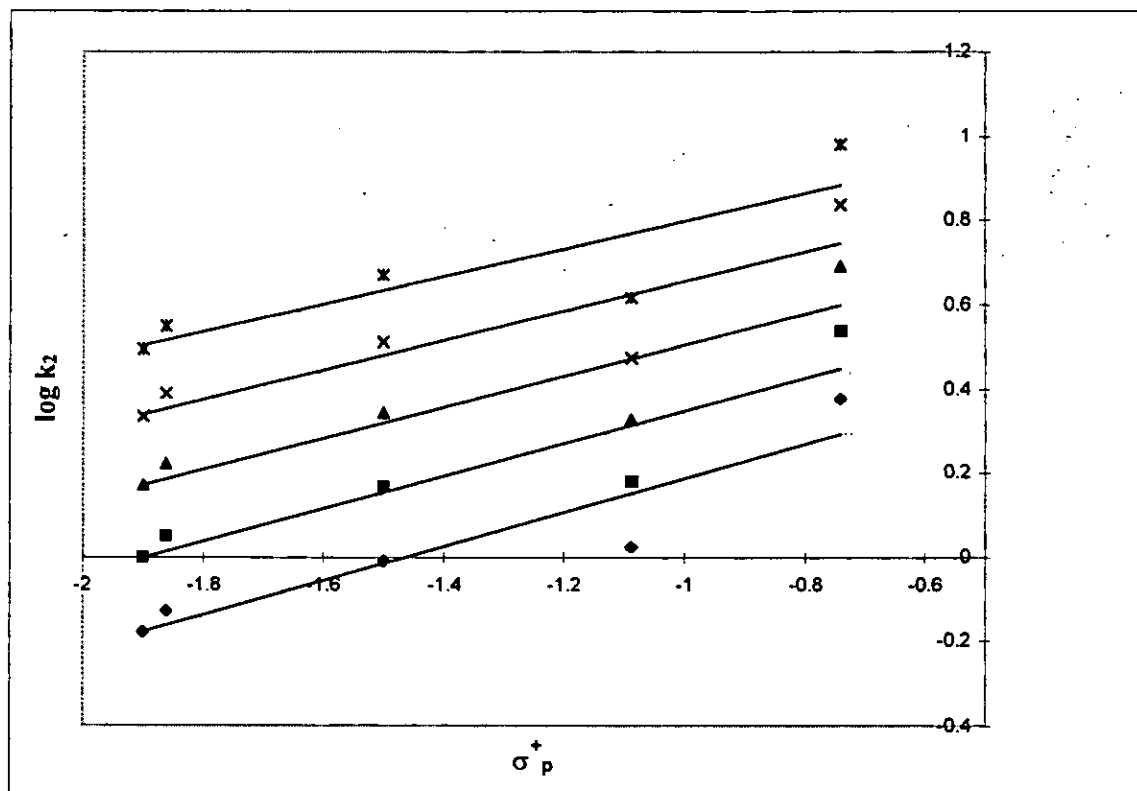


Figure 5
Log k_2 against σ_p^+ for some unsymmetrical MGs containing morpholino at 288.2K (◆); 293.2K (■); 298.2K (▲); 303.2K (×) and 308.2K (✱)

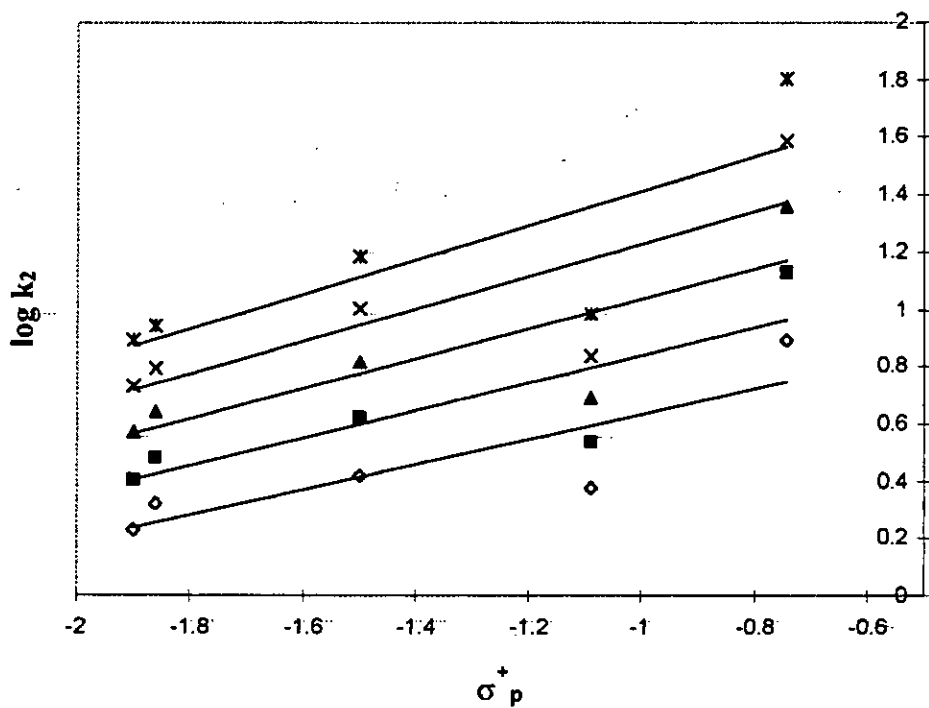


Figure 6
Log k_2 against σ_p^+ for some unsymmetrical MGs containing
***N*-methylpiperazino at 288.2K (◆); 293.2K (■); 298.2K (▲);**
303.2K (×) and 308.2K (*)

